



Rapid detection of immunotoxicity and
adverse reactions to new compounds using
3D skin equivalent models

Ana Patrícia Pimenta Martins Ribeiro

Submitted in partial fulfilment of the requirements for the degree of
Doctor of Philosophy

Haematological Sciences
Institute of Cellular Medicine
Newcastle University, UK

April 2020

Abstract

Safety testing procedures and risk assessment analysis of newly developed chemicals are mandatory to attest them as non-toxic for human handling. The European Union implemented several regulations enforcing safety testing and has recently banned the use of animals for toxicology studies for human safety.

From *in vitro* cell-based assays to reconstructed human epidermis (RHE) models, there are several non-animal alternatives for toxicology studies to determine human safety. Cell-based assays are not accurate enough to predict the toxic potential of chemicals as they are a two-dimensional (2D) representation of skin cells. Three-dimensional (3D) RHE models are better, as they allow for differentiation of skin epidermal layers (i.e. stratum corneum). Commercially available RHE models are now the gold standard for toxicity studies for human safety and some of these have been validated by the Organization for Economic Cooperation and Development (OECD) for skin irritation and corrosion testing (two major categories of skin toxicity).

The aim of this study was to develop an open source 3D epidermal skin culture based on Poumay's work. Using the Alvetex Strata scaffold, cell seeding was optimised using 1×10^6 keratinocytes for a 30 day culture period for best differentiation of the stratum corneum layer (confirmed by immunofluorescence staining of involucrin). Further optimization of vitamin C and calcium supplements did not seem to improve distribution of keratinocytes throughout the scaffold. Ultimately, the best results were achieved by the addition of a human-based collagen coat to the Alvetex Strata Scaffold, where development of stratum corneum was confirmed by collagen and involucrin staining. Moreover, development of the stratum basale layer was confirmed by cytokeratin 14 immunofluorescence.

Evaluation of the 3D epidermal skin culture was tested following OECD Testing Guideline (TG) 439 for skin irritation in 12 reference chemicals from the 20 reference chemicals list in TG 439. Results showed the 3D epidermal skin culture was able to distinguish non-irritant from irritant chemicals using 10 different keratinocyte donors. Comparative performance analysis with a monolayer (2D) keratinocyte culture, a commercial RHE model and a collagen-based RHE models were performed. Results showed similar outcomes between the different models, while the monolayer culture performed poorly in discriminating irritant from non-irritant chemicals. Overall, these results were indicative of the predictive capacity of the 3D epidermal skin culture for *in vitro* testing of skin irritation.

The second aim of this project was to use a skin explant assay, developed by Alcyomics, as a novel *in vitro* test for assessment of immunotoxicity caused by aggregation of monoclonal

antibodies (mAbs). mAbs are important therapeutics but their potential for aggregation has become a critical quality parameter that can turn into a potential health risk during the administration of mAb therapeutics to patients. While the extent of immunotoxicity in patient populations is uncertain, reports show that it can lead to immune responses via cell activation and cytokine release. Our results showed that aggregated mAbs caused adverse immune events by evidence of tissue damage, expression of cell death markers and overall increase of IFN- γ (pro-inflammatory cytokine). These results showed that the skin explant assay could be a promising tool for predicating immunotoxicity caused by mAb aggregation.

In conclusion, this study has provided further insight on the assessment of skin toxicity and immunotoxicity using *in vitro* skin assays.

Acknowledgements

Firstly, I would like to express my gratitude to my supervisors, Professor Anne Dickinson and Dr. Shaheda Ahmed for all the scientific support and guidance throughout my PhD.

I would also like to thank my project, BIORAPID (grant agreement No. 643056) from the European Union's Horizon 2020 research and innovation programme under the Marie Skłodowska-Curie actions. Not just for the funding but also for the opportunities it gave me - the training weeks, conferences and networking events that contributed to my scientific development. I would like to express my gratitude to Professor Jarka Glassey, the BIORAPID project supervisor for all the support. Special thanks to André Guerra and Arathi Kidzedath.

I would also like to thank all members of the Alcyomics team - Asif, Louis, Cindy, Lucy, Mahid, Moyassar and Florence for all the scientific feedback and help, either at the weekly meetings or in the lab. A special thanks to Asif for mentoring me during development of the epidermal model, sharing protocols with me and to Louis for all the emotional support during our PhDs.

Also, thank you to everybody at the Academic Haematology and ICM department who, directly or indirectly, helped me and worked with me.

Lastly, a big, warm, fat OBRIGADA to my family and friends who always supported and believed in me.

Author's declaration

I declare that, except where explicit reference is made to the contribution of others, this dissertation is the result of my own work and has not been submitted for any other degree at Newcastle University or any other institution.

Ana Ribeiro M.Sc.

July 2019

List of abbreviations

AF4-MALS	Asymmetric flow field-flow fractionation multi-angle light scattering
ALI	Air-Liquid Interface
AOP	Adverse Outcome Pathway
APC	Antigen presenting cell
ARE	Antioxidant response element
AUC	Analytical ultracentrifugation
Casp	Caspase
CLP	Classification, Labelling and Packaging
DAPI	4',6-diamidino-2-phenylindole
EU	European Union
EURL-ECVAM	European Union Reference Laboratory for alternatives to animal testing
FBS	Foetal Bovine Serum
GHS	Globally Harmonized System of Classification and Labelling
H&E	Hematoxylin and eosin
h-CLAT	Human cell line activation test
HRIPT	Human repeated insult patch test
HSP	Heat shock protein
ICCVAM	Interagency Co-ordinating Committee on the Validation of Alternative Methods
IFN-γ	Interferon gamma
IgG	Immunoglobulin G
IL	Interleukin
LLNA	local lymph node assay

LPS	Lipopolysaccharide
mAbs	Monoclonal antibodies
MTT	3-(4,5-Dimethylthiazol-2-yl)-2,5-diphenyltetrazolium bromide, Thiazolyl blue
MUSST	Myeloid U937 skin sensitization test
NUPPA	Newcastle University Protein and Proteome Analysis
OECD	Organization for Economic Cooperation and Development
OS-REp	Open source reconstructed epidermis
PBMC	Peripheral blood mononuclear cells
PBS	Phosphate buffered saline
QRA	Quantitative Risk assessment
QSAR	Quantitative Structure Activity Relationships
3Rs	Reduction, Replacement and Refinement
REACH	Registration, Evaluation, Authorisation and Restriction of Chemicals
RHE	Reconstructed human epidermis
RMSD	Root mean square deviation
RPMI	Roswell Park Memorial Institute (culture medium)
SDS	Sodium dodecyl sulfate
SI	Stimulation index
SEC-MALS	Size exclusion chromatography-multi angle light scattering
SV-AUC	Sedimentation velocity-Analytical ultracentrifugation
TEM	Transmission electron microscope
TEER	Transepithelial/transendothelial electrical resistance
TG	Testing guidelines
TG431	Testing guideline for skin corrosion

TG439	Testing guideline for skin irritation
TNF-α	Tumour necrosis factor alpha
UK	United Kingdom
VRM	Validated Reference Methods

List of tables and figures

Table 1. Characteristics of commercially available Reconstructed Human Epidermis (RHE) skin models.	33
Table 2. ECVAM-validated <i>in vitro</i> test methods for skin irritation testing according to OECD guidelines TG 439.	39
Table 3. ECVAM-validated <i>in vitro</i> test methods for skin corrosion testing according to OECD guidelines TG 431.	40
Table 4. Classification of corrosive and irritant substance under Globally Harmonised System (GHS) criteria.	41
Table 5. Minimum List of Reference Chemicals for Determination of Accuracy and Reliability Values for Similar or Modified RHE Skin Irritation TG 439.	43
Table 6. Test chemicals for the skin irritation test TG 439.	60
Table 7. Summary of antibodies used for immunofluorescent staining of the 3D epidermal skin culture.	64
Table 8. Summary of antibodies used for immunofluorescent staining of the skin explant samples.	68
Table 9. Specifications of the Alvetex scaffold membranes provided by Reprocell Europe Ltd	73
Table 10. Cell viability results for the 3D epidermal skin culture with the Alvetex Strata for skin irritation testing following TG 439.	129
Table 11. Cell viability results for the keratinocyte monolayer culture for skin irritation testing following TG 439.	134
Table 12. Cell viability results for the collagen-coated Transwell scaffold (Corning) for skin irritation testing following TG 439.	136
Table 13. OECD TG 439 results from different <i>in vitro</i> skin models.	138
Table 14. Comparison of the predictive capacity of each <i>in vitro</i> model for prediction of irritancy.	140
Table 15. Technical information of the testing compounds provided by FUJI.	146
Table 16. Quantification of aggregated content of heat-stressed mAb samples by analytical ultra-centrifugation.	153

Figure 1. Structure of epidermis..	20
Figure 2. Histological comparison between human skin and a commercially available RHE model.....	31
Figure 3. Schematic representation of an Adverse Outcome Pathway (AOP)..	35
Figure 4. Schematic representation of the development of a 3D reconstructed human epidermis.....	45
Figure 5. Alcyomics <i>in vitro</i> skin explant assay.....	49
Figure 6. Structure of the IgG antibody.....	51
Figure 7. 3D epidermal skin culture using the Alvetex Scaffold in donor 1 and 2..	74
Figure 8. 3D epidermal skin culture using the Alvetex Scaffold in donor 3 and 4..	75
Figure 9. 3D epidermal skin culture using the Alvetex Strata for 14 days in ALI at different keratinocyte concentrations in donor 1 and 2..	77
Figure 10. 3D epidermal skin culture using the Alvetex Strata for 14 days in ALI at different keratinocyte concentrations in donor 3, 4 and 5..	78
Figure 11. 3D epidermal skin culture using the Alvetex Strata for 21 days in ALI at different keratinocyte concentrations in donor 1 and 2..	80
Figure 12. 3D epidermal skin culture using the Alvetex Strata for 21 days in ALI at different keratinocyte concentrations in donor 3, 4 and 5..	81
Figure 13. 3D epidermal skin culture using the Alvetex Strata for 30 days in ALI at different keratinocyte concentrations in donor 1 and 2..	83
Figure 14. 3D epidermal skin culture using the Alvetex Strata for 30 days in ALI at different keratinocyte concentrations in donor 3, 4 and 5..	84
Figure 15. Viability of keratinocyte monoculture with vitamin C.....	86
Figure 16. Experimental layout for testing high concentrations of vitamin C.....	87
Figure 17. Vitamin C optimization in donor 1 and 2.....	88
Figure 18. Vitamin C optimization in donor 3 and 4.....	89
Figure 19. Histological detection of collagen in the 3D skin epidermal models formed using the Alvetex Strata.....	91
Figure 20. Immunofluorescence staining of involucrin for vitamin C optimization..	92
Figure 21. Immunofluorescence staining of Cytokeratin 14 for vitamin C optimization.....	94
Figure 22. Viability for different concentrations of CaCl ₂ (calcium - 1.5, 2 and 3mM) was tested on a keratinocyte monoculture.....	98
Figure 23. Calcium optimization for donor 1 and 2.....	100
Figure 24. Calcium optimization for donor 3 and 4.....	101
Figure 25. Histological detection of collagen in the 3D skin epidermal models formed using the Alvetex Strata.	102
Figure 26. Immunofluorescence staining of involucrin for calcium optimization..	103
Figure 27. Immunofluorescence staining of cytokeratin 14 for calcium optimization.....	104
Figure 28. Development of a 3D epidermal skin model using the Corning® Transwell®-COL collagen coated scaffold.....	108
Figure 29. Histological detection of collagen in the 3D epidermal skin models formed using the Corning® Transwell®-COL collagen coated scaffold..	109
Figure 30. Immunofluorescence staining of involucrin for the 3D epidermal skin models formed using the Corning® Transwell®-COL collagen coated scaffold..	110

Figure 31. 3D epidermal skin culture using the Alvetex Strata coated with human collagen for 3 and 7 days..	112
Figure 32. 3D epidermal skin culture using the Alvetex Strata coated with human collagen for 14 and 19 days.	113
Figure 33. 3D epidermal skin culture using the Alvetex Strata coated with human collagen for 21 and 30 days..	114
Figure 34. Histological detection of collagen in the 3D epidermal skin models formed using the Alvetex Strata coated with human collagen.....	115
Figure 35. Immunofluorescence staining of involucrin for collagen coated 3D skin models.	117
Figure 36. Comparison between the different 3D epidermal skin models used to real human skin.....	122
Figure 37. TG 439 Skin irritation testing of the 3D epidermal skin cultures using the Alvetex Scaffold.....	125
Figure 38. TG 439 Skin irritation testing of the 3D epidermal skin cultures using the Alvetex Strata.	126
Figure 39. <i>In vitro</i> testing of TG 439 skin irritation using the 3D epidermal skin culture with Alvetex Strata.....	130
Figure 40. <i>In vitro</i> testing of TG 439 skin irritation using the EpiDerm™ RHE model (MatTek)..	132
Figure 41. <i>In vitro</i> testing of TG 439 skin irritation using a keratinocyte monolayer culture..	135
Figure 42. <i>In vitro</i> testing of TG 439 skin irritation using a collagen-based Transwell scaffold (Corning).....	137
Figure 43. T cell proliferation following exposure to mAb samples.	147
Figure 44. Grading score for assessment of skin damage using the Skimune® skin explant assay.....	148
Figure 45. Skimune® Mab result with testing of biopharmaceutical compounds..	149
Figure 46. Size distribution of the heat-stressed aggregated samples of Rituximab..	154
Figure 47. Size distribution of the heat-stressed aggregated samples of Herceptin..	155
Figure 48. Visual characterization of two heat-stressed mAb samples by TEM.....	157
Figure 49. Skin explant assay results from exposure to heat stressed mAb samples.	160
Figure 50. Histopathological damage from exposure to heat stressed mAb samples.....	161
Figure 51. T cell proliferation responses following exposure to heat stressed mAb samples..	162
Figure 52. Pro-inflammatory cytokine profile at 1µg/mL.	163
Figure 53. Pro-inflammatory cytokine profile at 10µg/mL..	164
Figure 54. Cell death caused by mAb aggregation..	166

Table of contents

Abstract.....	3
Acknowledgements.....	5
Author's declaration.....	6
List of abbreviations	7
List of tables and figures.....	11
Table of contents.....	15
CHAPTER 1	19
1. Introduction and scientific aims	20
1.1. The human skin structure	20
1.2. Assessment of skin sensitization	21
1.3. Evolution of allergic sensitization assessment.....	22
1.3.1. Animal-based experimental approaches	22
1.3.2. Mathematical models for evaluation of skin sensitization	25
1.3.3. Legislation on safety testing	26
1.3.4. The golden 3Rs for animal alternatives	27
1.3.5. Alternative non-animal approaches using skin models	28
1.4. Animal-free toxicity test methods for regulatory decision-making	34
1.5. Validation of alternative skin equivalent 3D methods	37
1.6. Validated 3D skin models for regulatory skin toxicity	38
1.7. Testing Guidelines for skin toxicity testing	40
1.8. Development of a novel reconstructed human epidermis culture	44
1.9. Limitations of RHE models for skin sensitization	46
1.10. Alcyomics.....	48
1.10.1. A novel skin explant assay for assessment of adverse immune reactions	48
1.10.2. Immunotoxicity of monoclonal antibodies	50
1.11. Aims.....	55
CHAPTER 2	57
2. Materials & Methods	58
Part I – Development of a 3D skin culture model for skin irritation testing.....	58
2.1. Isolation of primary keratinocytes for 3D culture	58
2.2. Monolayer culture of keratinocytes.....	58

2.3.	Assembly of the 3D skin culture	59
2.4.	Skin irritation testing following Testing Guideline 439.....	59
2.5.	Cell viability of the test chemicals	60
2.6.	Calculation of cell viability	60
2.7.	Statistical analysis	61
2.8.	Collagen-coated scaffolds	61
2.9.	Commercially available alternatives for skin irritation testing	62
2.10.	Histological and immunofluorescence analysis of the 3D skin culture.....	62
Part II – Assessment of immunotoxicity of aggregated mAbs using an <i>in vitro</i> skin explant assay		65
2.11.	Human and blood samples.....	65
2.12.	Skin explant assay for immunotoxicity of aggregated mAbs.....	65
2.13.	T cell proliferation	66
2.14.	Cytokine release assay	66
2.15.	Immunofluorescence	67
2.16.	Heat stress protocol for aggregation of monoclonal antibodies	68
2.16.1.	Degradation of mAb samples.....	68
2.16.2.	Protein analysis of heat stressed mAb samples.....	69
2.17.	Statistical analysis.....	69
CHAPTER 3		71
3.	Development of an open source 3D epidermal skin culture.....	72
3.1.	Aim.....	72
3.2.	Results	72
3.2.1.	Optimization of the standard Alvetex scaffold.....	73
3.2.2.	Optimization of Vitamin C	85
3.2.3.	Optimization of CaCl ₂	97
3.2.4.	Optimization of collagen coated scaffold	106
3.3.	Reproducibility of the 3D epidermal skin cultures	119
3.4.	Discussion of the results.....	119
CHAPTER 4		123
4.	Assessment of skin irritation testing using a 3D epidermal skin culture.....	124
4.1.	Aim.....	124
4.2.	Results	124
4.2.1.	Skin irritation testing using the standard Alvetex scaffold.....	125

4.2.2.	Skin irritation testing using Alvetex Strata.....	126
4.2.3.	Skin irritation testing using EpiDerm™ (MatTek).....	131
4.2.4.	Skin irritation testing using a keratinocyte monolayer culture.....	133
4.2.5.	Skin irritation testing using a collagen-based scaffold.....	136
4.3.	Performance analysis of the models for TG 439.....	138
4.4.	Discussion of the results.....	140
CHAPTER 5	144
5.	Immunotoxicity by aggregated monoclonal antibodies.....	145
5.1.	Aim.....	145
5.2.	Results	145
5.2.1.	Skimune® for assessment of immunotoxicity to mAbs (native form).....	145
5.2.2.	Skimune® for assessment of immunotoxicity to aggregated mAbs	150
5.2.2.1.	Protein analysis of the stressed mAb samples	151
5.2.2.2.	Visual characterization of the aggregates	156
5.2.2.3.	Aggregated mAb samples induce immune activation	158
5.3.	Discussion of the results.....	167
CHAPTER 6	172
6.	Concluding remarks.....	173
CHAPTER 7	180
7.	Appendices	181
	Appendix A – Publications	181
	Appendix B – Personal development	183
	Appendix C – Ethics agreement.....	185
CHAPTER 8	188
8.	References	189

CHAPTER 1

Introduction and scientific aims

1. Introduction and scientific aims

1.1. The human skin structure

The human skin is a major organ of the human body. It is actively involved in the defense against exogenous damaging substances or microorganisms. Because of its physiological properties which create a complex web of interacting structures, the skin is a protective shield from the exterior environment and helps maintain the homeostasis of the body (Bouwstra & Ponc, 2006; Naish & Syndercombe Court, 2014). It is composed of three layers – epidermis, dermis and hypodermis. The epidermis, the outermost layer of human skin consists of different strata (layers) constructing an epidermal barrier, the first impermeable barrier of protection against the exterior. This epidermal barrier consists of multiple layers of keratinocytes, under different stages of differentiation. The basal layer of the epidermis (stratum basale) consists of undifferentiated keratinocytes, while the outermost layer (stratum corneum) is composed of terminally differentiated keratinocytes that have migrated from the stratum basale (Figure 1) (Eckert & Rorke, 1989; Presland & Dale, 2000). While keratinocytes represent most of the cells present in the epidermis, there are also specific immune cells present, such as dendritic cells or Langerhans cells. Keratinocytes are in close contact with Langerhans cells to form an immune barrier against the outside environment (Janeway, Travers, Walport, & Shlomchik, 2001; Naish & Syndercombe Court, 2014).

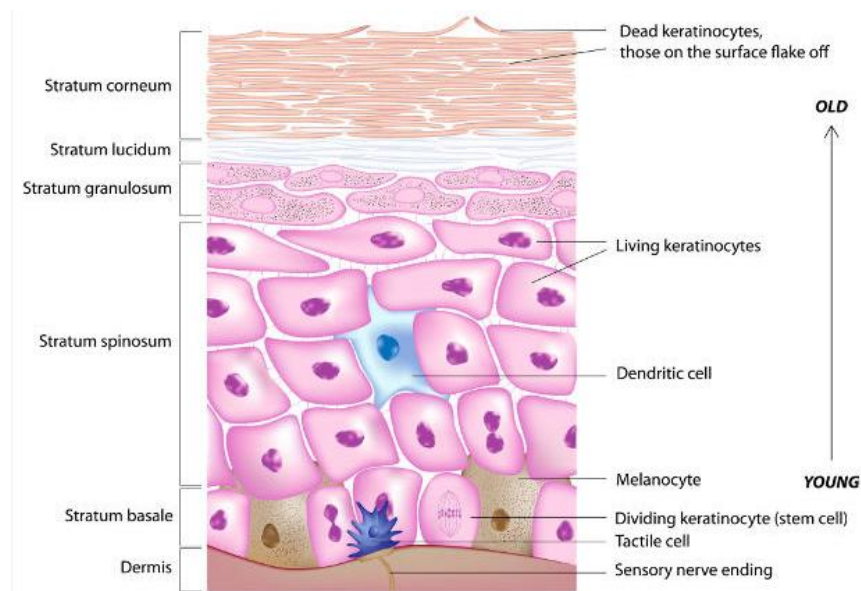


Figure 1. Structure of epidermis. The human skin is composed of different layers – epidermis, dermis and hypodermis. The epidermis is the outermost layer, representing the first immune barrier against the outside environment and it is subdivided in specific strata with different immune cell types. Skin cells (keratinocytes) regenerate from the bottom to the top layers, meaning that the upper layers (stratum corneum) are usually composed of dead keratinocytes (Naish & Syndercombe Court, 2014).

1.2. Assessment of skin sensitization

Nowadays, skin sensitization has become a pressing issue, since exposure to allergenic compounds present in commercial products like cosmetics and other skin products can trigger skin allergic sensitization, an inflammatory reaction of the skin. The contact of these exogenous compounds with human skin can trigger an immune reaction by interaction with antigen-presenting cells (APC, as the case of dendritic cells), leading to T cell activation (Bouwstra & Ponc, 2006; Louis-dit-sully et al., 2014). The interesting aspect of this allergic sensitization is that it is intrinsically dependent on the host's immune features (immunobiological system) and in some cases its predisposition (genetic background) to develop sensitization against a certain antigen. As so, it is very important to understand the immune mechanism behind allergic sensitization and how the exposure to allergens and the immune cells involved in the process of skin inflammation takes place.

The pathway by which skin sensitization takes place involves allergen exposure, antigen recognition by dendritic cells as Langerhans cells and consequent T cell activation. This molecular response causes an inflammatory response (cytokine release, vasodilation and transepidermal water loss) followed by the onset of symptoms (swelling, oedema and/or erythema) (Louis-dit-sully et al., 2014). The epithelium is the most important skin layer involved in the skin sensitization process, since it is the first physical layer of protection. More specifically, within the stratum corneum, desmosomes and free lipids (as cholesterol esters and free fatty acids) surround any dead keratinocytes. This arrangement of dead cells and free lipids makes the epithelium an effective barrier against exogenous allergenic compounds (Imokawa, Kuno, & Kawai, 1991; Schurer & Elias, 1991). Skin sensitization occurs due to penetration of the stratum corneum and it is dependent on the concentration and time of exposure of the allergen against the barrier capacity of the stratum corneum.

Topical allergen exposure causes priming of the immune system by recruitment of dendritic cells, T cell activation and cytokine production. Initially, dendritic cells interact with the allergen by internalizing it and presenting it to responsive T cells, triggering them to activate and proliferate (Louis-dit-sully et al., 2014). Considering the diversity of T cell receptors present in the T cell repertoire, only naïve T cells with affinity to the allergen antigen receptor will undergo clonal expansion. This is called antigen-specific T cell proliferation.

1.3. Evolution of allergic sensitization assessment

As an effort to reduce the occurrence of skin sensitization, legislation on commercialization of chemicals has been implemented. All products commercially available are thoroughly screened for the presence of possible sensitizers before entering the market to assure no risk of sensitization to humans. Many of the chemical compounds present in these new products are missing valuable safety information, hence the need to always perform a risk assessment for sensitization. The experimental approach of sensitization started with animal testing in the 1940s, mainly in guinea pigs and rabbits (Chase, 1941; Landsteiner & Chase, 1941) and it is still a standard approach in some countries such as the United States of America, Japan and China. However, a general concern for the use of animals in safety tests has led to a conceptual change and increase in alternative methods for testing compound safety, more specifically in Europe.

1.3.1. Animal-based experimental approaches

One of the first experimental approaches for sensitization was the Draize test, established in the 1940s (Draize, Woodard, & Calvery, 1944). This approach is performed using guinea pigs or rabbits, where the testing product is topically applied onto the animal skin and evaluated during a period of time for visible skin damage symptoms (inflammation, swelling, erythema or oedema). This experimental approach was largely replaced in the 1980s by the mouse local lymph node assay (LLNA), a more quantitative and manageable approach (I Kimber, Mitchell, & Griffin, 1986; I Kimber & Weisenberger, 1989). LLNA was accepted by different regulation committees regarding validation of alternative methods to animal testing (i.e. Interagency Co-ordinating Committee on the Validation of Alternative Methods, ICCVAM) as an improvement to Draize guinea pig testing, since it reduced the number of animals required in the assessment of skin sensitization (minimum of 8 guinea pigs compared to a minimum of 4 mice) (Dean et al., 2001a, 2001b). LLNA is one of the few animal experimental approaches validated for skin sensitization, corrosion and irritation testing which is still currently used in countries like the United States of America (Dean et al., 2001a, 2001b; OECD, 2010).

LLNA relies on the principle of antigen-specific T cell proliferation. It measures the ability of an exogenous compound to cause skin sensitization according to its ability to induce lymph node cell proliferation (T cell proliferation within the lymph node) after topical exposure to the compound (Frank Gerberick, Ryan, Dearman, & Kimber, 2007). The output response of

lymphocyte proliferation is measured by incorporation of ^3H -thymidine into the DNA of newly formed lymph node T cells. The test compound is topically exposed to mice ears daily for three days and on the fifth day following initial exposure, mice are intravenously injected with a dose of radiolabelled thymidine. Animal sacrifice is then required for excision of the draining lymph nodes for assessment of T cell proliferation (Frank Gerberick et al., 2007; Ian Kimber & Dearman, 2010). The outcome of T cell proliferation is measured with regards to the vehicle control, as an index of stimulation. To be considered a sensitizer (compound that causes skin sensitization), the effect of exposure to the compound is measured by following the EC3 value rule (Frank Gerberick et al., 2007). This means a three-fold increase of T cell proliferation when compared to the vehicle control should be observed. As the LLNA can give a quantitative measure of sensitization, it can be used as an estimation of relative potency. This is based on the hypothesis that T cell proliferation is dependent not just on the incidence of skin sensitization but rather on its extent (as a causal quantitative effect). Thus, LLNA is used for assessment of skin sensitization and relative potency effect and it is currently considered the gold-standard approach for risk assessment of new compounds. However, recent findings have raised concerns for this method as a valid *in vivo* reference tool for assessment of chemical sensitization, as results showed that sensitization endpoint was not specific enough and could exclude known human sensitizers as they did not reach the sensitization threshold in the LLNA method (i.e. nickel chloride). Therefore, this recent report calls for a careful review of the *in vivo* reference data using LLNA method, possibly to be replaced by a more suitable assessment method (Kolle, Hill, Raabe, Landsiedel, & Curren, 2019).

Alternatively, there is also a human-based predictive assay for skin sensitization – the human repeated insult patch test (HRIPT). This assay is been used for the last few decades as a confirmatory test for skin sensitization (Marzulli & Mamach, 1974; Stotts, 1980). Briefly, this assay consists of two phases – an induction phase (exposure to the test sensitizer) and a challenge phase (exposure to a different area to challenge sensitization). During the induction phase, the test sensitizer is applied to the torso back area of the human volunteer in the form of a patch for a 24-hour period. The skin responses are read after 48 hours, to check for occurrence of skin allergies. This process is repeated for the next 15 days as a “repeat insult”, as the name of the assay suggests. After a rest period of at least 15 days, a challenge exposure is again performed in the torso back area tested during the induction phase and in a new area (naïve area), using the same method of a patch test for 24 hours. Occurrence of skin allergies are checked for the subsequent days. While there can be some variations to this protocol (type of

patch, duration of exposure, grading of skin allergies), the human repeat insult patch test is still widely acknowledged for assessment of skin sensitization (McNamee et al., 2008).

Direct predictive comparisons between LLNA and the HRIPT methods have shown a good correlation of the sensitization threshold. From a dataset of 57 chemicals, 46 were correctly identified as sensitizers in both LLNA and HRIPT methods, with a correlation of $r = 0.77$ (Schneider & Akkan, 2004). From a different dataset of 26 skin-sensitizing chemicals, correlation between LLNA and HRIPT methods was reported as $r = 0.90$ (David A. Basketter et al., 2005).

Even though there are several studies reporting a significant correlation between animal models and human testing (Marzulli & Maibach, 1975; Schneider & Akkan, 2004), there are many others indicating that this relationship is not so linear (Frankild, Volund, Wahlberg, & Andersen, 2000; Nixon, Tyson, & Wertz, 1975; Phillips, Steinberg, Maibach, & Akers, 1972). While results may show that rabbits and mice are suitable animal models to assess skin sensitization because they report similar visible effects of skin damage by swelling, erythema or oedema, it is imperative to recall that these results are based on a non-human model. Thus, interspecies variability has a major effect in the assessment of skin sensitization and all data should be extrapolated with caution.

The TGN1412 clinical trial (an immunomodulatory drug also known as CD28 super-agonist monoclonal antibody) is one of the most unfortunate examples of this hazardous correlation between animal models and human test trials (Attarwala, 2010). All preliminary safety studies of TGN1412 as potential immunomodulatory drug were performed in rodents and primates and was unable to predict that, when tested in man it would lead to a pro-inflammatory cytokine storm and ultimately to multiple organ failure. As a result, during phase I clinical trials, six healthy volunteers developed multiple organ failure. Investigations concluded that the results from animal testing were misrepresentative since the animal model lacked expression of CD28, a cell receptor that binds to memory CD4⁺ T cells and induces a pro-inflammatory cytokine cascade in humans (Stebbings, Eastwood, Poole, & Thorpe, 2013). Because of this difference in the response between the test species and humans, it was impossible to predict any adverse effects. Ultimately, the preclinical safety testing that led to this human trial was not suitable or not properly representative of the human condition to which it was targeted. This type of occurrence strengthens the need for more appropriate preclinical safety testing.

1.3.2. Mathematical models for evaluation of skin sensitization

The LLNA method was developed as a tool to assess the sensitization potential of chemicals. An output of a stimulation index of 3 or higher would characterize the test chemical as a sensitizer. As use of LLNA increased for characterization of a larger range of sensitizers, cross-comparison of the stimulation indexes between the guinea pig and LLNA methods showed consistent results. For example, chemicals regarded as weak sensitizers in the guinea pig test would also present a low stimulation index in the LLNA test, while strong sensitizers would have a much higher stimulation index in the LLNA test (D. A. Basketter et al., 2000; Ian Kimber & Basketter, 1997). From these observations it was questioned whether LLNA could be used not only for identification of skin sensitizers, but also to calculate their potency via calculation of the concentration required to produce a positive 3-fold sensitization reaction. If possible, assessment of potency could then be used as a Quantitative Risk Assessment (QRA) tool for skin sensitization.

QRA is a new *in silico* approach for assessment of skin sensitizers (Felter, Robinson, Basketter, & Gerberick, 2002; Felter, Ryan, Basketter, Gilmour, & Gerberick, 2003). It focuses on extrapolation of sensitization data from animal studies, as the LLNA method, for prediction of potency threshold of skin sensitization in humans using the HRIPT method. While the HRIPT method is not actually performed, the extrapolated threshold from LLNA data is used to lower the sensitization threshold considering several factors (as human variability, chemical exposure time and concentration). From this, an acceptable exposure level (upper limit threshold) is defined for a sensitizing chemical and compared to its consumer exposure level (if such sensitizing chemical was commercially marketed). If the consumer exposure level is higher than the acceptable exposure level, this becomes a safety issue as the marketed product has a higher exposure threshold than what is regarded as safe. If the acceptable exposure level is higher than the consumer exposure level, then the likelihood of sensitization occurrence is low and there is no imminent safe risk. QRA approach is very helpful for occupational health risk assessments as it does not normally require any human testing. However, in cases of uncertainty during the risk assessment analysis, safety testing using HRIPT might contribute to the elimination or minimization of uncertainty.

Alternatively, another potential *in silico* approach for characterization of skin sensitization is the use of quantitative structure-activity relationships (QSAR) regression models. The foundation for QSAR use started from the hypothesis of a possible quantitative correlation between the physicochemical properties of a chemical and its ability to be a skin sensitizer. For instance, how can the physicochemical properties as a set of predictors variables correlate to the potency of skin sensitization (response variable). This is because sensitizer chemicals that penetrate the skin will incur in covalent modifications of skin proteins and disrupt the cellular mechanisms, leading to an event of sensitization. The mechanism of action of chemicals into skin has been investigated for years (Landsteiner & Chase, 1939; Mayer, 1954) but it was only in 1982 that the physicochemical parameters of sensitizers were combined with a mathematical model to generate a quantitative structure-activity relationship (QSAR) (D. W. Roberts & Williams, 1982). Integration of QSAR models with LLNA data has also been shown (David A. Basketter, Roberts, Cronin, & Scholes, 1992), as well as prediction of skin sensitization according to chemical reactivity domain (Aptula, Patlewicz, & Roberts, 2005; David W. Roberts, Aptula, & Patlewicz, 2006). As the QSAR tool are improving and are evaluated against existing skin sensitization databases, it allows for better identification of sensitizing chemicals (either commercialized chemicals or those in development phase) without resorting to animal studies. There are in fact some computer-based predictive systems – Derek, TOPKAT and TOPS-MODE as *in silico* QSAR tools developed for prediction frameworks for skin sensitization (Kumar, Tangadpalliwar, Desai, Singh, & Jere, 2016) or even ocular irritation (Bhatarai, Wilson, Parks, Carney, & Spencer, 2016).

1.3.3. Legislation on safety testing

The European Union (EU) is the major driving force in the implementation of legislation for safety testing, as the case of the Registration, Evaluation, Authorisation and Restriction of Chemicals (REACH) legislative action in 2006 (European Commission, 2006) and the Cosmetics Regulation action in 2009 (European Commission, 2009). REACH action addresses the impact chemical production and usage might have on human and environmental health, making risk assessment of all new compounds as mandatory. One of the key aspects of this action is the recommendation of alternative approaches to animal testing, either by predictive *in silico* modelling methods or by *in vitro* assays. The Cosmetics Action aimed to eliminate animal testing for cosmetics products, by establishing a 10-year prohibition phase of animal testing. This cosmetic ban was fully regulated and put into action from 11th March 2013,

marking the end of animal suffering for cosmetics purposes (European Commission, 2009). Together, these two legislative actions have dramatically changed the numbers of experimental animals used in cosmetic testing (European Commission, 2007, 2013). Moreover, assessment of sensitization by using animal models presents a major ethical dilemma associated with unnecessary discomfort and pain to which animals are subjected. Animal welfare supporters forced the cosmetic industry to look for safe and non-animal alternatives. The most famous case is perhaps the multimillion-dollar investment done by L'Oréal, a giant cosmetics brand, in 1997. To be ahead of the animal testing problem, L'Oréal acquired Episkin, a biotechnology company that developed *in vitro* animal alternatives, i.e. 3D skin tissues for testing of adverse outcomes. And in 2011, L'Oréal opened its Predictive Evaluation Centre in Lyon, France. This allowed L'Oréal to use the lab-produced 3D skin tissues to test the efficacy of ingredients and tolerance of L'Oréal products before they were commercially ready. This in-house testing is a very smart strategic move as it results in cost-effective safety testing of all L'Oréal products with no animal suffering and good public outreach.

But a lot still had to be done regarding animal use for scientific purposes. In 2011, the European Union Reference Laboratory for alternatives to animal testing (EURL-ECVAM) was officially created as a scientific research validation hub in Europe. Its key role was to validate methods that reduce, refine or replace (known as the golden 3Rs) animal use for safety testing and efficacy of chemicals and other compounds designed for human use. Research labs developing alternative methods to use of animal models can submit their work to EURL-ECVAM for validation which, if approved, could become a benchmark method for non-animal safety testing worldwide.

1.3.4. The golden 3Rs for animal alternatives

Economical and ethical regulations have opened a need for more reliable alternative methods that could replace, reduce and refine animal experimentation. This concept was first introduced in 1959 by Russel and Burch as the golden 3Rs – reduce, refine and replace (Russel & Burch, 1959). In it, Russel and Burch defined the “reduction” concept as alternative methods that would provide the same information using less animals, like developing better experimental designs with relevant statistical support. The “refinement” concept would appeal for minimal pain and suffering throughout animal experimentation, encouraging any condition that would improve the animal well-being (i.e. anaesthetics, bigger cages, sacrifice before terminal pain). Lastly, and the most praised concept, the “replacement” concept would call for

animal-free alternative methods as *in silico* models or *in vitro* cell-based assays to assess human safety. In fact, the “golden 3Rs” can be achieved in the same alternative method, as an *in vitro* cell-based assay would replace the need of animal experimentation or reduce the number of animals required if the *in vitro* assay is used as a screening test during the pipeline development (Michael Balls, 2005). The “golden 3Rs” were officially included in Directive 86/609/EEC, as an attempt to regulate animal experimentation for scientific purposes across the European Union (European Commission, 1986). This directive was the first official document to demand priority of a scientifically reliable alternative method over animal experimental studies for scientific purposes (“Replacement and Reduction” concepts). However, this directive is no longer in force and was replaced by Directive 2010/63/EU, stating protection of animals used for scientific purposes as mandatory (focusing on the “Refinement” concept) (European Commission, 2010).

1.3.5. Alternative non-animal approaches using skin models

In response to the increasing EU legislations banning animal testing, several animal-alternative models of reconstructed human skin have been developed and commercialized as replacements of the established animal models for sensitization testing. Human *in vitro* skin assays present a more genuine feedback in mimicking *in vivo* immunological responses since 1) they are based in a human test condition; 2) are more reflective of the tissue microenvironment where cells reside and 3) are more predictive of the *in vivo* behavior of the cells.

It all started in 1975 with the ground-breaking work of Rheinwald and Green, pioneers of cell tissue techniques regarding reconstructed human epidermis (RHE) models. It was the first report on successful *in vitro* culturing of human keratinocytes (Rheinwald & Green, 1975). Using 3T3 fibroblasts as feeder layer, they were able to generate multiple colonies of keratinocytes from a single keratinocyte cell. This discovery was of immense importance, since it allowed for isolation and culture of larger quantities of keratinocytes in a monolayer culture.

For many years following Rheinwald and Green’s pivotal work, monolayer culture of keratinocytes was the conventional technique for skin metabolism, skin disease (as burn wound or psoriasis) and skin toxicity studies (as cell death and/or cell viability upon chemical exposure).

It rapidly became a standard protocol due to its reproducibility and consistency. From this, several *in vitro* two-dimensional (2D) monolayer cell-based assays were developed to assess skin sensitization.

One of the many *in vitro* cell-based assays developed for skin sensitization is the KeratinoSens™ assay. This test assay uses an immortalized cell line from human keratinocytes transfected with a luciferase report gene plasmid under the control of the antioxidant response element (ARE). It is an ARE-Nrf2 luciferase method because it detects activation of the Keap-1/Nrf2 signaling pathway, the regulator of cellular responses to oxidative and electrophilic stress. It allows for quantitative measurement of sensitization by light signalling of the luciferase gene induction (Emter, Ellis, & Natsch, 2010). It is widely used for assessment of skin sensitization to chemicals (Belot, Sim, Longmore, Roscoe, & Treasure, 2017; Natsch, Emter, Gfeller, Haupt, & Ellis, 2015; Settivari et al., 2015), as it has a reported 77% predictive capacity (79% sensitivity and 72% specificity) in a testing set of 145 chemicals (Natsch et al., 2013). This assay was formally validated by ECVAM in 2015 and a detailed protocol can be found in Testing Guideline 442D – “*in vitro* Skin Sensitisation: ARE-Nrf2 Luciferase Test Method” (OECD, 2015b).

The human cell line activation (h-CLAT) assay is another assay which is commonly used for assessment of skin sensitization. It measures dendritic cell activation by expression of CD86 and CD54 cell surface markers on THP-1 cells, a human monocytic leukaemia cell line. Increased expression of CD86 and CD54 markers upon exposure to the test chemical indicates activation of dendritic cells and T cell priming, confirming the test chemical as sensitizer (as opposed to a non-sensitizer that will not elicit expression of CD86 and CD54) (Sakaguchi et al., 2006). Co-expression of CD86 and CD54 has an overall accuracy of 89% in prediction of sensitizers (Sakaguchi et al., 2006). This assay was formally validated by ECVAM in 2018 and a detailed protocol can be found in Testing Guideline 442E – “*in vitro* skin sensitisation assays addressing the key event on activation of dendritic cells on the adverse outcome pathway for skin sensitisation” (OECD, 2018)

Formerly known as MUSST (myeloid U937 skin sensitization test), U-SENS™ is also an *in vitro* test for the assessment of skin sensitization. It is similar to h-CLAT test and measures the CD68 marker for dendritic cell activation, but it is performed using a myeloid U-937 cell line instead (Ade, Martinozzi-teissier, Pallardy, & Rousset, 2006; Piroird et al., 2015). This assay was formally validated by ECVAM in 2018 and a detailed protocol can be found in Testing Guideline 442E – “*in vitro* skin sensitisation assays addressing the key event on activation of dendritic cells on the adverse outcome pathway for skin sensitisation” (OECD, 2018). The reported predictive capacity of this assay is of 71%, with a 71% sensitivity and 70% specificity and this assay (Natsch et al., 2013).

However, growing concerns for the predictive capacity of these 2D test assays have questioned their feasibility and relevance to human safety. Monolayer 2D skin cultures do not resemble real human skin because they do not present stratified epidermal layers, and this is considered a crucial feature for an accurate *in vitro* model of skin. Considering that monolayer cultures grow in submerged conditions on a flat surface (bottom of a plastic well plate), this does not provide favourable conditions for keratinocytes to differentiate into the different stratum of real skin (Klicks, Molitor, Ertongur-fauth, & Hafner, 2017; Vollmers et al., 2012). In fact, 2D culture conditions may actually alter cell morphology or even gene expression (Hewitt et al., 2013). These concerns have triggered a change in the cell culture realm, with the focus changing from monolayer cell cultures to multilayer three-dimensional (3D) models. This resulted in the development of new *in vitro* RHE models, that are more physiologically similar to real human skin as they present a multi-layered cell organization with different stages of cell differentiation, mimicking the different skin layers of human skin. The establishment of RHE models have opened a world of new possibilities regarding skin studies such as cell-cell interactions, cell differentiation, skin barrier functionality, skin metabolism and even wound healing studies (Klicks et al., 2017).

Overall, these reconstructed skin models can either be epidermal equivalents (where the multi-layered keratinocytes grow on a synthetic scaffold) or full-skin equivalents (in which the multi-layered keratinocytes representing the epidermis grow on top of a fibroblast matrix representing the dermis). Nevertheless, both versions of the skin equivalent models present a stratum corneum layer due to the air-liquid interface (ALI), mimicking a typical human epidermal barrier. One of the very first 3D model of skin was described in 1976 (Freeman, Igel, Herrman, & Kleinfeld, 1976), where pig skin was used as a “collagen bed” for the expansion and differentiation of human keratinocytes. This was later optimized by the use of a collagen matrix as base layer to culture keratinocytes to an air-liquid interface (Lillie, MacCallum, & Jepsen, 1980). From this primordial 3D model of skin, many more models have emerged over the years becoming more applicable and easier to access.

Nowadays, there are many commercially available RHE models available as end-point products for assessment of skin testing. While all skin reconstructed models are based on a multi-layered keratinocyte approach, they differ in the origin of the keratinocyte cells provided (usually from abdominal or foreskin as surgical waste), in the specifications of the membrane (either coated with collagen from an animal source or polycarbonate), the insert size and its application for testing purposes. The most commonly used RHE model for skin irritation and skin corrosion *in vitro* testing is the EpiDerm™ model from MatTek

(<https://www.mattek.com/products/epiderm/>). This is a ready-to-use RHE model consisting of human-derived epidermal keratinocytes from foreskin or abdomen region, cultured on a collagen coated scaffold with an insert size of 0.6 to 4cm² depending on cell culture requirements. This RHE is phenotypically similar to human skin, as it also presents a multi-layered epidermal region, with a stratum corneum, stratum spinosum and stratum basale regions (Figure 2).

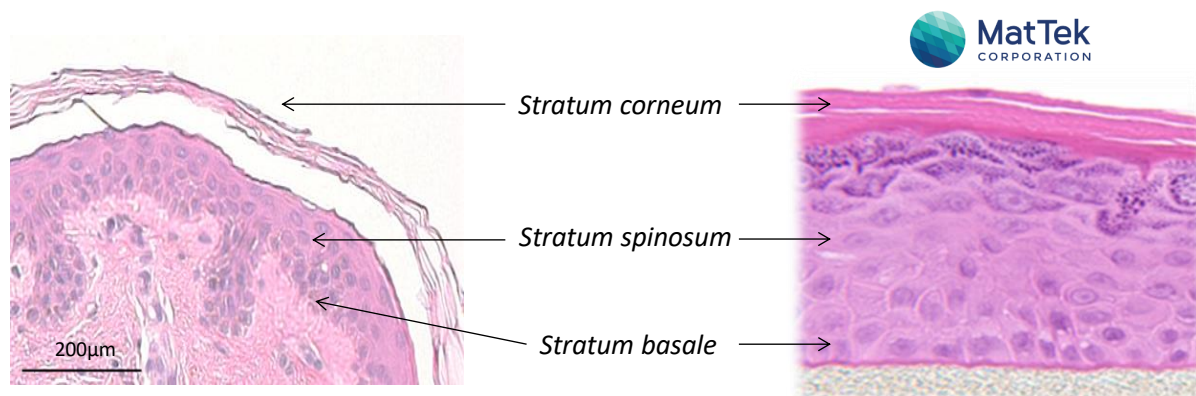


Figure 2. Histological comparison between human skin and a commercially available RHE model. The commercially available RHE model from MatTek, EpiDerm™ shows histological similarity with human skin, with presence of the different epidermal layers – stratum corneum, stratum spinosum and stratum basale.

The marketing point of this RHE model is the fact that is validated by ECVAM for different *in vitro* testing purposes – skin irritation (Hartung, 2007) and skin corrosion (ECVAM, 2000) as described further in section 1.6. Thus, this RHE is the leading RHE in the market for toxicology studies. Moreover, the continuous R&D investment from MatTek in this RHE model will eventually result in its ECVAM validation for further applications like phototoxicity or drug absorption studies.

As mentioned before, a cosmetic company (L'Oréal) bought EpiSkin to acquire its 3D skin models for in house toxicology testing of its products. L'Oréal is also selling its 3D skin model as a ready-to-use assay for toxicology testing to cosmetics, pharmaceutical and chemical manufacturers (<http://www.episkin.com>). There are two commercially available RHE models being sold by L'Oréal/Episkin – the EpiSkin™ and the Skin Ethic™. The EpiSkin™ model consists of keratinocytes from the abdomen region cultured in a collagen-coated scaffold and can be used for skin irritation, corrosion, UV exposure and permeability studies. The Skin Ethic™ can also be used for the same applications but instead of a collagen-coated scaffold, keratinocytes are cultured in a polycarbonate scaffold. Both RHE models have ECVAM

validation for skin irritation (ECVAM, 2009c; Hartung, 2007) which increases their marketing value. L'Oréal/Episkin is also currently working on expanding their ECVAM validation portfolio for phototoxicity and absorption studies.

Smaller scale companies like Cell Systems® GmbH also have a commercially available RHE model, the epiCS (previously known as EST1000®). Information regarding this RHE model is not very much known as there is no specifications about the origin of keratinocytes used for this RHE model. It is known, however, that keratinocytes are grown in a polycarbonate scaffold with an insert size of 0.6cm². This RHE model can be used for skin corrosion and irritation studies, as well as phototoxicity and absorption studies. Full details of all RHE models mentioned above are described in Table 1.

Table 1. Characteristics of commercially available Reconstructed Human Epidermis (RHE) skin models. RHE models differ in the origin of cells, the scaffold specifications and its application purpose.

Reconstructed human epidermis (RHE) models	Company	Origin of cells	Membrane specifications	Insert size (cm²)	Application of model	Company website
EpiDerm™	MatTek	Foreskin/abdomen	Collagen coated	0.6 - 4	Skin corrosion, irritation, phototoxicity and absorption	https://www.mattek.com/products/epiderm/
EpiSkin™	L'Oréal	Abdomen	Collagen coated	0.38 and 1.07	Skin corrosion, irritation, UV exposure and permeability	https://www.episkin.com/Episkin
SkinEthic™	EpiSkin	Foreskin/abdomen	polycarbonate	0.5 and 4	Skin corrosion, irritation, UV exposure and permeability	https://www.episkin.com/RHPE
epiCS (previously EST1000®)	Cell Systems® GmbH	Not specified	polycarbonate	0.6	Skin corrosion, irritation, phototoxicity and absorption	https://cellsystems.de/cells-and-media/c/epics
StratiCELL® Reconstituted Human Epidermis (RHE/001)	StratiCELL	Not specified	Serum-free polycarbonate	Not specified	Skin corrosion, irritation phototoxicity and genotoxicity	https://straticell.com/in-vitro-skin-models/
LabCyte EPI-MODEL	Japan Tissue Engineering Co., Ltd.,	Not specified	polycarbonate	Not specified	Skin corrosion and irritation	http://www.jppte.co.jp/english/business/LabCyte/LabCyte.html
Healthy Leiden epidermal skin model (LEM)	biomimiq	Not specified	polycarbonate	Not specified	Skin corrosion, irritation, toxicity and infection	http://www.biomimiq.nl/Healthy%20Skin%20Models

These RHE models are widely available as “ready-to-use” products with guaranteed quality control performance and reproducibility. Such high standards of good manufacturing practice and its predictive capacity have enabled some of these RHE to be validated by EURL-ECVAM criteria for testing of skin toxicity for irritation and corrosion purposes. This validation “endorsement” represents a great marketing value, since the validated RHE model can then be considered a benchmark RHE model for skin testing. While these commercially available reconstructed models of human epidermis are trademark protected (by their “know-how” and cell culture requirements), there are some open source protocols for the development of reconstructed human epidermis models (Groeber et al., 2016; Jung et al., 2014; Pedrosa et al., 2017; Roger et al., 2019).

1.4. Animal-free toxicity test methods for regulatory decision-making

Rheinwald and Green’s work was the starting point for investigating skin toxicity, with years of further development and improvement of new *in vitro* animal-alternative assays for assessment of topical toxicity to chemicals. Governmental organizations have become involved in this issue, making sure that experimental protocols and guidelines regarding assessment of toxicity are openly accessed and followed in a standardized fashion. The Organization for Economic Cooperation and Development (OECD) is an intergovernmental economic organization founded in 1961 with the goal of worldwide economic and trade improvement. It provides a platform for good practices, policy recommendations or general guidelines that will promote growth and stability regarding economic, environmental and social issues.

The need for a change regarding animal-based toxicity approach was the priority for both the regulatory and governmental authorities as the OECD, enforcing the use of mechanistic pathway-based data (molecular/cellular level), incorporating computational *in silico* methods and animal-free *in vitro* assays from human data (National Research Council, 2007). But because there was a risk of insufficient knowledge regarding how pathway-based toxicity methods would result in toxic adverse outcomes at the organism level, a new regulatory framework was developed to collect, evaluate and establish link elements between the different levels of biological organization. In 2012, OECD launched a new program for the development of adverse outcomes with regulatory relevance, called Adverse Outcome Pathway (AOP) (OECD, 2012b). It is a structural representation of critical toxicological events that could ultimately lead to an unexpected adverse outcome. AOPs have a broad range since they are a linear progression covering from molecular scale events up to organism responses (Figure 3). An AOP starts with a molecular event of toxic consequences that is followed by causally related

key events of increased toxicity, ultimately leading to an adverse outcome of regulatory importance. The adverse outcome can occur at the organism or population level and result in organ toxicity, reduced survival, impaired growth and/or reproduction development.

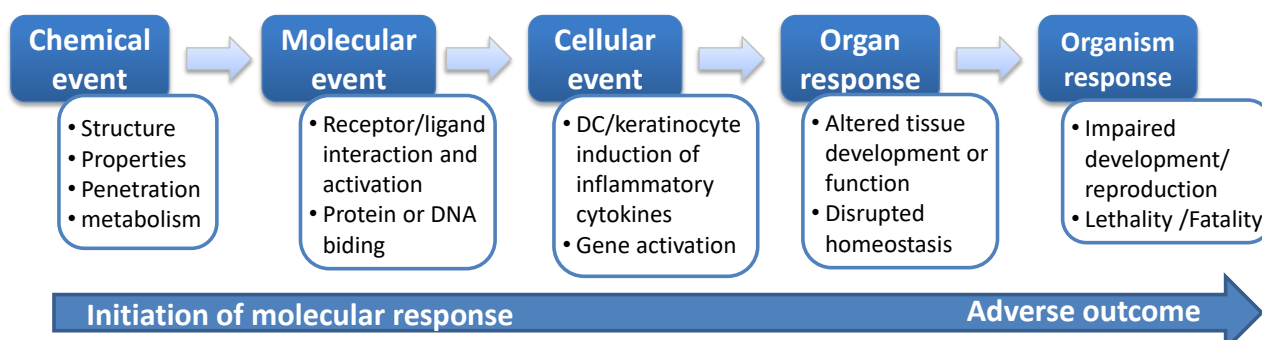


Figure 3. Schematic representation of an Adverse Outcome Pathway (AOP). AOPs are a conceptual map for toxicity pathways from both the chemical and the body response, ranging from molecular events to adverse effects from the organism response.

AOPS are tools of great relevance for risk assessment of new products or assays involving human safety, as in the case of skin toxicity (Vinken, 2013). In fact, OECD guidelines highly recommend elaboration of AOPs for any newly developed product or method related to human safety during risk assessment. This is because AOPs allow to shape the available knowledge on a specific substance from *in silico* and *in vitro* assays approaches into a framework, identifying possible information gaps in its toxicity profile and ultimately mapping the sequence of events leading to an adverse outcome. Therefore, an AOP is crucial to improve the predictive capacity of these *in silico* and *in vitro* assays approaches, highlighting the importance for animal-free toxicity testing approaches.

OECD has released the OECD's AOP Knowledge Base tools – the AOP Portal, the AOP Wiki and the Effectopedia, a web-based platform that aims to collect all available information on how chemicals induce adverse outcomes into an AOP “encyclopaedia”. The AOP Portal (<https://aopkb.oecd.org/>) is the main focus of this AOP Knowledge Base, and it works as a user-friendly search engine for AOP key events and data input. It is an important search tool for all OECD endorsed AOPs.

The AOP Wiki is the most commonly used tool as it allows for development of new AOPs or editing of existing AOPs with new relevant data. It is in this tool that users can search for

published research on network pathways of toxicity or information of newly developed chemicals (<https://aopwiki.org/>).

Finally, Effectopedia focuses on improving of the predicative capacity of *in silico* and *in vitro* tools using the AOP data input from the AOP Wiki. This AOP “encyclopaedia” allows the user to input test data into an interface template and generate quantitative relationships between pathway elements and key events for adverse outcomes. The user-friendly model template makes it simple to upload data in a standardized manner and compare against relevant information provided by other users in the database. This will not only allow to share and improve AOP information but also improve the interface model’s predictive capacity for *in vitro* toxicity tools (<https://www.effectopedia.org/>).

The first AOP officially endorsed by the OECD related to skin sensitization, named “Skin Sensitization Initiated by Covalent Binding to Proteins” (reference: ENV/JM/MONO(2012)10/PART1) (European Commission, 2012). This AOP describes four key events that lead to skin sensitization by covalent binding of chemical substances to proteins. The first key event is at the molecular level, where the chemical interacts with the skin proteins by covalently binding to lysine residues. This is considered the site of action. The second key event is at the cellular level, the keratinocytes. This level is described as an inflammatory response with gene expression for cell signalling pathways. The third key event refers to activation of dendritic cells, with expression of cell activation markers and cytokine release. Lastly, the fourth key event concerns T cell proliferation, measured in the murine Local Lymph Node Assay (at organism level). This AOP includes 3 levels of biological organization – molecular, cellular and organism events that leads to skin sensitization as an adverse outcome. More AOPs have since been endorsed and published by the OECD and can be found in the OECD “Series on Adverse Outcome Pathways” section of the OECD online library (<https://www.oecd-ilibrary.org/environment/oecd-series-on-adverse-outcome-pathways.com>).

Overall, AOPs are very important risk assessment tools as they bring together existent knowledge into a predictive platform, allowing to prioritize risk assessment (by improved and updated knowledge by users) and refine predictive tools. AOPs can also be included in the development of QRA and QSAR tools as they contribute with a hierarchical order of adverse events. This will refine the predictive capacity of QSAR tools for the different biological levels (molecular, cellular, organ, organism).

AOPs have raised the standards for assessment of toxicology, since it requires a more detailed planning and toxicity impact of any newly developed product or assay for toxicology purposes. Alongside AOP’s guidelines, OECD has also provided several testing guidelines

(TG) as standardized protocols for assessment of skin toxicity (OECD, 2013, 2014, 2015a). These TGs have become imperative for the commercialization of RHE and its testing purposes and are now widely followed for validation and commercialization purposes. As so, AOPs have been implemented in all marketing strategies and TGs have become the standard for research development of new *in vitro* assays for skin toxicity. These two perspectives are crucial for any *in vitro* assay seeking OECD approval.

1.5. Validation of alternative skin equivalent 3D methods

Formal validation of an alternative method should only occur if that alternative method is to be used for regulatory purposes – i.e. a regulatory toxicity *in vitro* test for human safety or production and handling of chemicals (M. Balls & Fentem, 1999). If the alternative method is only to be used for fundamental research, in-house product development or product safety purposes, it does not require formal EURL-ECVAM validation.

Any alternative *in vitro* skin model seeking formal EURL-ECVAM validation for regulatory toxicology needs to prove comparable reliability, reproducibility and scientific relevance to the conventional animal test (Michael Balls et al., 1995; CPMP, 1997; Liebsch & Spielmann, 2002).

Reliability is defined as reproducibility of the *in vitro* assay results for intra- and inter-laboratory conditions over time (Michael Balls et al., 1995). Scientific relevance is defined by the scientific usefulness and added value of a specific alternative method for a scientific purpose (Michael Balls et al., 1995; CPMP, 1997). These two parameters are deeply linked, as an alternative method that shows reliable results, but no added value, is as irrelevant as an alternative method with a relevant scientific scope but showing unreliable results.

The reliability and scientific relevance of any alternative *in vitro* test should be investigated using substances with known *in vivo* toxicity effects as suitable reference standards (M. Balls & Fentem, 1999; Michael Balls et al., 1990). Such reference standards should i) be easily obtained in a chemically pure and stable form, ii) should cover the complete *in vivo* toxicity spectrum (from low to high toxicity level) and iii) correlate with known reproducible *in vivo* toxicity data (preferably human data).

There are five main processes that an *in vitro* alternative method needs to go through for EURL-ECVAM validation: test development, pre-validation, formal validation, independent assessment and regulatory acceptance (M. Balls & Fentem, 1999; Michael Balls et al., 1995; Hartung et al., 2004).

Firstly, test development of an *in vitro* alternative model involves definition of its scientific purpose and its target organ (i.e. skin, eye, liver), as well as the type of assessment it delivers (toxic, potency, hazard or risk assessment) and the chemical spectrum (range of chemicals possible to test in the model). A detailed protocol should also be included to allow for inter-laboratorial transferability.

Secondly, a pre-validation test is mandatory before formal validation as this step will focus on any necessary protocol optimization or standardization, risk assessment and identification of critical steps regarding test design and procedure and initial inter-laboratorial transferability strategy.

Only after pre-validation, can validation by inter-laboratorial blind performance take place. A blind inter-laboratorial test validation is crucial to show the *in vitro* alternative model's reliability and relevance. This performance analysis can include a "training set" with the coded chemical test range. Data analysis and assessment of outcome results of the blind inter-laboratorial test validation are then published and submitted for independent assessment.

The published results from the inter-laboratorial test validation are reviewed by independent panels, at either national or international level. The independent panel can include governmental bodies, industry associations or societies and it should be representative of the toxicological, industrial and animal welfare communities. However, all members of the panel should be independent to any alternative model being revised. If the independent panel agrees that the *in vitro* alternative method meets the criteria for test development and validation, the validated *in vitro* alternative method is then submitted to the EURL-ECVAM office for consideration for regulatory acceptance (OECD, 2005).

Currently, not many alternative models going through this process have been validated, despite years of exhaustive research and validation efforts. Failure to achieve validation can be caused by insufficient *in vivo* data or *in vivo* data from animal studies that does not have relevant comparison to human studies. Additionally, design of experiments lacking proper statistical analysis or protocol transferability is sufficient to delay validation (M. Balls & Fentem, 1999).

1.6. Validated 3D skin models for regulatory skin toxicity

Currently, only a few *in vitro* assays have been approved by OECD for regulatory skin toxicity in the different classification groups of topical toxicity. This is not because the currently available RHE models are not good enough to be validated, but rather because the validation process can be lengthy and expensive (as described in the section before).

According to OECD guidelines, there are different categories of topical toxicity – irritation (eye and skin), corrosion (skin), phototoxicity and sensitization (skin). This study will only focus on skin irritation. The difference between skin irritation and skin corrosion relies in the severity and irreversibility of the damage caused by the testing chemical. Corrosion refers to irreversible damage of the skin (visible necrosis through the epidermis layer), while irritation refers to reversible damage to the skin following application of test chemical (itching and/or rash symptoms).

OECD has released two very important testing guidelines for assessment of irritation and corrosion. Testing Guideline 439 (TG 439) refers to testing of chemicals for *in vitro* skin irritation in reconstructed human epidermis test models and it should be used to determine the skin irritancy of chemicals (OECD, 2013). Testing Guideline 431 (TG 431) refers to testing of chemicals for *in vitro* skin corrosion in reconstructed human epidermis test models and it use allows identification of non-corrosive and corrosive substances (OECD, 2014).

Current regulatory requirements as the “Classification, Labelling and Packaging (CLP) regulation 1272/2008” (European Commission, 2008) demand detailed information regarding the irritation or corrosion potential of a new chemical, as part of the AOP and risk assessment regarding its handling, transport or storage. Therefore, all new chemicals have to be tested for topical toxicity using the OECD testing guidelines for irritation chemicals - TG 439 (OECD, 2013), or corrosion chemicals - TG 431 (OECD, 2014).

Currently, the accepted testing methods for skin irritation and corrosion include both *in vivo* animal testing (Draize rabbit test, TG 404 (OECD, 2015a)) and *in vitro* test methods (based on RHE models). To date, EURL-ECVAM has only validated three of the currently available RHE models for skin irritation (Table 2) and four for skin corrosion testing (Table 3).

Table 2. ECVAM-validated *in vitro* test methods for skin irritation testing according to OECD guidelines TG 439.

Skin irritation model	Validation study type	Date of validation	Reference	Reference of current SOP ¹ for testing method
EpiDerm™	TG 439 – skin irritation	2009	(Hartung, 2007)	(MatTek, 2008)
EpiSkin™		2007	(Hartung, 2007)	(EpiSkin, 2009)
SkinEthic™ RHE		2009	(ECVAM, 2009d)	(SkinEthics, 2009)

¹ Standard operating procedure

Table 3. ECVAM-validated *in vitro* test methods for skin corrosion testing according to OECD guidelines TG 431.

Skin corrosion model	Validation study type	Date of validation	Reference	Reference of current SOP ¹ for testing method
EpiDerm™	TG 431 – skin corrosion	2000	(ECVAM, 2000)	(MatTek, 2012)
EpiSkin™		1998	(ECVAM, 1998)	(EPISKIN, 2013)
SkinEthic™ RHE		2006	(Kandárová et al., 2006)	(SkinEthic, 2012)
epiCS		2009	(ECVAM, 2009a)	(EpiCS, 2012)

¹ Standard operating procedure

1.7. Testing Guidelines for skin toxicity testing

Presently, the only regulatory accepted method for evaluation of skin irritation is Testing Guideline 439 (OECD, 2013). TG 439 defines skin irritation as reversible skin damage caused by application of a test chemical for up to 4 hours as defined by the Globally Harmonised System (GHS) of Classification and Labelling of chemicals (REF) (UN, 2009). According to GHS guidelines, there are several criteria that need to be met for a substance to be classified as corrosive (Category 1) or irritant (Category 2) (Table 4).

Table 4. Classification of corrosive and irritant substance under Globally Harmonised System (GHS) criteria. A substance is classified as corrosive (category 1) or irritant (category 2) according to performance criteria from *in vivo* or *in vitro* results.

Category	Classification Criteria
Category 1 Corrosive	<ul style="list-style-type: none"> - Human experience showing irreversible damage to the skin; - Structure or mode of action similar to a substance already classified as corrosive; - pH extremes of ≤ 2 and ≥ 11.5 including acid/alkali reserve capacity; - Positive results in a valid and accepted <i>in vitro</i> skin corrosion test; - Animal experience or test data that indicates that the substance causes irreversible damage to the skin following exposure of up to 4 hours.
Category 2 Irritant	<ul style="list-style-type: none"> - Human experience or data showing reversible damage to the skin following exposure of up to 4 hours; - Structure or mode of action similar to a substance already classified as irritant; - Positive results in a valid and accepted <i>in vitro</i> skin irritation test; - Animal experience or test data that indicates that the substance causes reversible damage to the skin following exposure of up to 4 hours.

However, many commercially available chemical products are still labelled as “no GHS category”. This means that the toxicity test results for that chemical were not substantial enough to classify it as irritant or corrosive (UN, 2009). Therefore, these chemicals might still be hazardous by lack of relevant *in vivo* or *in vitro* scientific data.

TG 439 provides a detailed protocol for identification of irritant chemicals from GHS category 2 using an *in vitro* RHE model with similar physiological properties to human epidermis. For EURL-ECVAM validation, any *in vitro* alternative model needs to demonstrate reliability and accuracy performance by determination of irritancy of 20 reference chemicals (Table 5).

Performance results from the proposed *in vitro* alternative model (i.e. reliability and accuracy) need to be comparable or better than the Validated Reference Methods (VRM). Currently, the 3 accepted VRMs are the 3 RHE models validated by EURL-ECVAM: EpiSkin™, EpiDerm™ SIT (EPI-200) and SkinEthic™ RHE. These RHE models are considered VRMs because they were used to define the Performance Standards of TG 439

(ECVAM, 2009b). Performance Standards of TG 439 include viability, reproducibility, quality control and predictive capacity (sensitivity and specificity).

In order to facilitate TG 439 validation, EURL-ECVAM guidelines determined that the list of reference chemicals include chemicals that are commercially available and representative of the full range of Draize irritancy scores (from non-irritant to strong irritant); have a well-defined chemical structure; and they are not associated with an extremely toxic profile (e.g. carcinogenic or toxic to the reproductive system) and they are not associated with prohibitive disposal costs (ECVAM, 2009b). Therefore, Table 5 includes chemicals ranging from low irritation potential (*in vivo* Draize score of 0) to high irritation potential (*in vivo* Draize score of 3), chemicals lacking GHS *in vivo* data (non-classified chemicals) and irritant chemicals with GHS category 2 (classified chemicals).

Regarding protocol guidelines, TG 439 skin irritation assessment with RHE models measures the initial events of cell death (keratinocytes) upon chemical exposure by cell viability, focusing only on damage to the stratum corneum. Quantification of cell viability is performed by direct MTT ([3-(4,5- Dimethylthiazol-2-yl)-2,5-diphenyltetrazolium bromide, Thiazolyl blue; CAS number 298-93-1] dye reduction. Threshold for irritancy is defined as a reduction in cell viability greater than 50%.

TG 431 skin corrosion assessment with RHE models measures the ability of the chemical to penetrate the stratum corneum and become cytotoxic to the skin layers below. Cell viability is also measured by reduction of MTT viability dye. Threshold for corrosion is defined as a reduction in cell viability greater than 50% (threshold differs according to the RHE used but explanation of threshold can be found in TG 431).

Not considering specific features inherent to each *in vitro* model, TG 439 (skin irritation) and TG 431 (skin corrosion) have similar protocols. Both guidelines are based in direct topical exposure of a well characterized chemical according to GHS standards for a short time period. This is followed by a washing step (to mimic a real human response after chemical exposure) and assessment of toxicity is assessed after an incubation period by defining the cell viability by MTT reduction. However, specific protocol parameters should be followed for each RHE requirements including volume of testing chemical, chemical application time, medium volume during post-incubation and acceptance limits. All specifications are listed in each Testing Guideline.

Table 5. Minimum List of Reference Chemicals for Determination of Accuracy and Reliability Values for Similar or Modified RHE Skin Irritation TG 439.

Chemical	CAS number	Physical state	<i>In vivo</i> score	VRM* Cat. Based on <i>in vitro</i>	GHS Cat. Based on <i>in vivo</i> results
Non-classified chemicals					
1-bromo-4-chlorobutane	6940-78-9	Liquid	0	Cat. 2	No cat.
diethyl phthalate	84-66-2	Liquid	0	No cat.	No cat.
Naphthalene acetic acid	86-87-3	Solid	0	No cat.	No cat.
Allyl phenoxy-acetate	7493-74-5	Liquid	0.3	No cat.	No cat.
Isopropanol	67-63-0	Liquid	0.3	No cat.	No cat.
4-methyl-thio-benzaldehyde	3446-89-7	Liquid	1	Cat. 2	No cat.
Methyl stearate	112-61-8	Solid	1	No cat.	No cat.
Heptyl butyrate	5870-93-9	Liquid	2	No cat.	No cat.
Hexyl salicylate	6259-76-3	Liquid	2	No cat.	No cat.
Cinnamaldehyde	104-55-2	Liquid	2	Cat. 2	No cat.
Classified chemicals					
1-decanol	112.30-1	Liquid	2.3	Cat. 2	Cat. 2
Cyclamen aldehyde	103-95-7	Liquid	2.3	Cat. 2	Cat. 2
1-bromohexane	111-25-1	Liquid	2.7	Cat. 2	Cat. 2
2-chloromethyl-3,5-dimethyl-4-methoxypyridine HCl	86604-75-3	Solid	2.7	Cat. 2	Cat. 2
di-n-propyl disulphide	629-19-6	Liquid	3	No cat.	Cat. 2
Potassium hydroxide (5% aq.)	1310-58-3	Liquid	3	Cat. 2	Cat. 2
Benzenethiol, 5-(1,1-dimethylethyl)-2-methyl	7340-90-1	Liquid	3.3	Cat. 2	Cat. 2
1-methyl-3-phenyl-1-piperazine	5271-27-2	Solid	3.3	Cat. 2	Cat. 2
Heptanal	111-71-7	Liquid	3.4	Cat. 2	Cat. 2
Tetrachloroethylene	127-18-4	Liquid	4	Cat. 2	Cat. 2

* Validated Reference methods

1.8. Development of a novel reconstructed human epidermis culture

The EURL-ECVAM validated models mentioned above present two similar features - first, their protocol is patent protected to protect the “know-how” involved in their production; secondly, most of these RHE models are not entirely animal-free as they rely on animal-based collagen-coated scaffolds for differentiation of keratinocytes.

The protected protocol specifications for production of these RHEs is proportionally correlated with their financial cost. Additionally, the costs involved in shipment of the models and possible customs fees impose a heavy monetary burden for research purposes. It could be argued that standardized and quality controlled RHE models for testing purposes are worth such investment, but the constant purchase necessity of these RHE models can easily make a cheaper alternative more appealing. Some research labs worldwide are focusing on open source reconstructed epidermis (OS-REp) models to combat the purchase of commercial RHE models for research purposes. As the main advantage to use open source RHE models is the monetary cost, since in house development of an RHE model is cheaper than the commercialisation of one. However, it also means that quality control and standardization of the RHE model is not guaranteed as it is not limited by strict Good Laboratory Practises (GLP) and Good Manufacturing Practices (GMP). Therefore, research labs using open source RHE need to be make sure they have an optimized protocol that will always provide consistent RHE models over time for different users. This is key for a good performance of the RHE model. Therefore, it is crucial to have excellent cell culturing techniques and adequate laboratory training, as well as a good source of primary cells. Moreover, it also means lengthy development times as cell culturing is required for open sources RHE, while commercially available RHE models are ready to use. Consequently, open source RHE models can be more advantageous from a financial perspective but adequate laboratory practices need to be put in place to guarantee standardized quality and performance of the RHE model.

The concept for open source was first introduced in the informatics world around 1980s, with LINUX (Linus Torvald's Uniplexed Information and Computing System) as the first open source software. Later, the first open access platform relevant for the scientific field started with the introduction of open access repositories (as PUBMED) and open access journals (as the Public Library of Science, PLOS One Online Journal). These open access platforms changed the way the user can access information freely for non-commercial purposes. Bringing the concept of open access into the skin toxicity domain allows for easy access to protocols and guidelines on how to develop in-house RHE models for toxicity testing. This was done by the

pioneering work of Yves Poumay (Y Poumay et al., 2004), published in 2004 and it is, presently, the foundation for some OS-REp protocols currently published (Mewes et al., 2016; Pedrosa et al., 2017). This work aimed to develop an open source 3D epidermal skin culture that could fulfil the quality standards of RHE models for toxicity studies.

Poumay's work (Y Poumay et al., 2004) describes a free access protocol for establishment of a reconstructed epidermal model, using human epidermal keratinocytes (Figure 4). Primary keratinocytes isolated from a skin explant were seeded onto a polystyrene scaffold and left submerged in culture medium for a maximum period of 24 hours. Afterwards, culture medium was replaced but the volume of the new medium added was now reduced in order to only reach the scaffold, leaving the keratinocyte layer exposed to the air to encourage keratinocyte differentiation into the different epidermal layers. This concept was described as the Air-Liquid Interface (ALI), in which the keratinocytes grow in between a liquid and air phase (Pruniéras, Régnier, & Woodley, 1983). ALI resembles the real skin microenvironment as the top layer (stratum corneum) also grows in between a liquid and air phase. The 3D RHE model was left in the ALI phase for 14 to 19 days, to allow differentiation of the keratinocytes into the different skin layers – organized layers of stratum basale, stratum spinosum and stratum corneum that can resemble real human epidermis.

This current thesis aimed to replicate Poumay's work, using an open source protocol with some modifications (Chapter 3) to assess skin irritation by following OECD guidelines (Chapter 4).

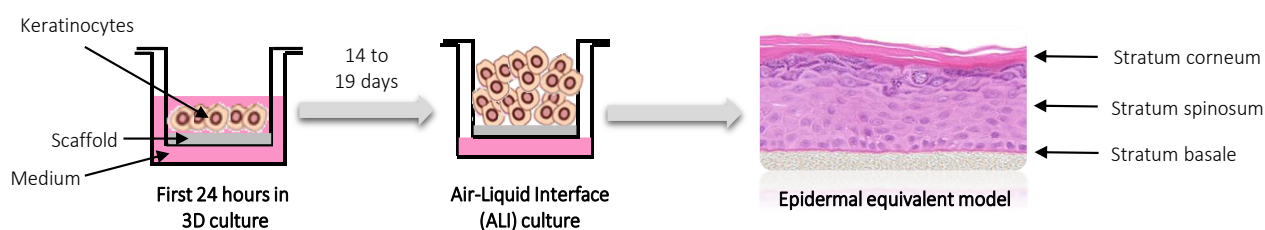


Figure 4. Schematic representation of the development of a 3D reconstructed human epidermis. Primary keratinocytes are seeded onto a polystyrene scaffold and left submerged for an initial period of 24 hours. Afterwards, scaffold is raised into air-liquid interface (ALI) for 14 to 19 days. The final 3D reconstructed epidermis presents typical features of human skin, with formation of stratum basale, stratum spinosum and stratum corneum.

The fact that the commercially available RHE models are not entirely animal-free, can be seen as a disadvantage for the culture and differentiation of skin cells. While not significant for the output of the skin irritation assay, it is still an important feature as it depreciates the concept of creating animal-free RHE models for safety testing in humans. Therefore, this thesis aimed to develop an open source 3D skin culture model using no animal collagen for the assessment of *in vitro* skin irritation following TG 439 (Chapter 4). Following the work originally developed by Poumay et al. (2004), the open source 3D skin culture model was developed using a porous scaffold containing no animal-based collagen or polycarbonate – the Alvetex® scaffold membranes.

1.9. Limitations of RHE models for skin sensitization

The global development and acceptance of *in vitro* assays for skin sensitization over *in vivo* models was greatly empowered by regulatory bodies seeking to end animal suffering. Rapidly, these *in vitro* assays fulfilled all legal requirements to halt animal testing for skin toxicity purposes. Among the many advantages of using *in vitro* assays over *in vivo* models, is the fact that *in vitro* assays are usually faster (no need for animal breeding and/or sacrifice) and more standardized than *in vivo* animal models (Liebsch & Spielmann, 2002; Zucco, De Angelis, Testai, & Stamatii, 2004).

In vitro assays also usually require smaller amounts of the test substance than *in vivo* models, which could be important during discovery and development phase if substance availability is low. Moreover, the use of *in vitro* assays during a substance development phase could result in better and earlier screening of safe substances for human consumption (Zucco et al., 2004). Additionally, it would stop the need for data extrapolation from *in vivo* animal models (Worth & Balls, 2001).

But while the *in vitro* assays are a major step forward regarding safe alternative approaches to animal testing, full safe prediction of skin sensitization with these models is not yet realistic as they are not fully equivalent to *in vivo* human skin. The major drawback of these models is the fact that they only focus on the molecular and cellular stages of the AOP hierarchy, leaving out the organ and organism stages. This disadvantage is major as any adverse outcomes in the organ and organism stages would not be predicted by the *in vitro* assays, jeopardizing human safety. Moreover, these *in vitro* assays also lack sufficient skin barrier function (SCCS - Scientific Committee on Consumer Safety, 2010) and generally present a higher permeability rate (Schäfer-korting et al., 2008; Schmook, Meingassner, & Billich, 2001; Schreiber et al.,

2005). This could be seen as an advantage, by increasing the sensitivity threshold of the model but it can also lead to an overrated prediction of sensitization due to the higher rate of permeability.

Considerable efforts have been made to increase the complexity of *in vitro* models to mimic real *in vivo* human skin. However, to build more physiologically relevant human skin models, other skin components such as pigmentation, immunity, innervation and vascularization which are involved in the sensitization process would need to be incorporated, which remains a serious challenge (Abaci, Guo, Doucet, Jackow, & Christiano, 2017). Consequently, these models are less suitable for testing the efficacy of biopharmaceutical or cosmetic products, in which important inflammatory responses (cell activation, cell damage, cytokine release) are important output parameters. Therefore, screening of biopharmaceuticals and cosmetics is more often performed in cell-based assays than in *in vitro* 3D models

An alternative to the RHE models for skin sensitization assays (and without resorting to *in vivo* animal models) is *ex vivo* human skin samples. These *ex vivo* skin explants are usually obtained from plastic surgery as disposable tissue. Due to the increase of abdominoplasty procedures and breast augmentation surgery, it has become easier to gain access to disposable human skin samples. *Ex vivo* human skin is considered the best surrogate for *in vivo* human skin, since it holds normal skin barrier function, presents a mature stratum corneum and comprises innervation and vascularization (Franz, Lehman, & Raney, 2009).

There is an array of companies that specialize in providing normal and diseased human skin tissue samples for testing purposes, such as Tissue Solutions (UK), GenoSkin (France), SeraLab (Spain) or BioPredict (USA). But the difficulty remains in being able to replicate the *in vivo* microenvironment with the tissue and the immune cells, and the cause-consequence relationship they have *in vivo*. Alcyomics Ltd (www.alcyomics.com) is one of few companies that can replicate this *in vivo* niche, by providing a model which uses autologous (from the same individual) tissue and immune cells for *in vitro* safety testing on in-house *ex vivo* skin models.

Therefore, this work aimed to use the Alcyomics *ex vivo* skin model, Skimmune®, to evaluate immunotoxicity by aggregated monoclonal antibodies (Chapter 5). Compared to the open source 3D skin culture model, the *ex vivo* skin model comprises of skin tissue and immune cells (i.e Dendritic Cells and T cells) so the measurement of immunotoxicity is more appropriate using this *in vitro* skin model.

1.10. Alcyomics

Alcyomics is a UK based Newcastle University spin out company founded by Professor Anne Dickinson in 2007. It provides a human *in vitro* pre-clinical safety service for testing novel compounds (biopharmaceuticals, cosmetics, chemical) before human administration. The technology available at Alcyomics is a suitable alternative to animal testing, because it can accurately predict the likelihood of adverse immune events in a human perspective (Ahmed et al., 2016, 2019).

1.10.1. A novel skin explant assay for assessment of adverse immune reactions

Alcyomics developed a novel human *in vitro* skin explant assay (patent EP2524227) for assessment of adverse immune reactions. Originally developed for graft-versus-host disease (Dickinson et al., 1998; Sviland & Dickinson, 1999; Vogelsang et al., 1985), a systemic post-transplant complication, it was further modified and patented as an autologous skin explant model for predicting adverse immune reactions to chemicals (Ahmed et al., 2016). The initial step of this assay consisted of priming of dendritic cells with the test chemical and consequent T cell activation. Afterwards, these primed cells were co-cultured with a skin biopsy from the same donor (hence an autologous system) to see if the test compound induced tissue damage (Figure 5). The output of this skin explant assay is *in situ* histopathological characterization of the skin damage according to Lerner's grading system (Lerner et al., 1974).

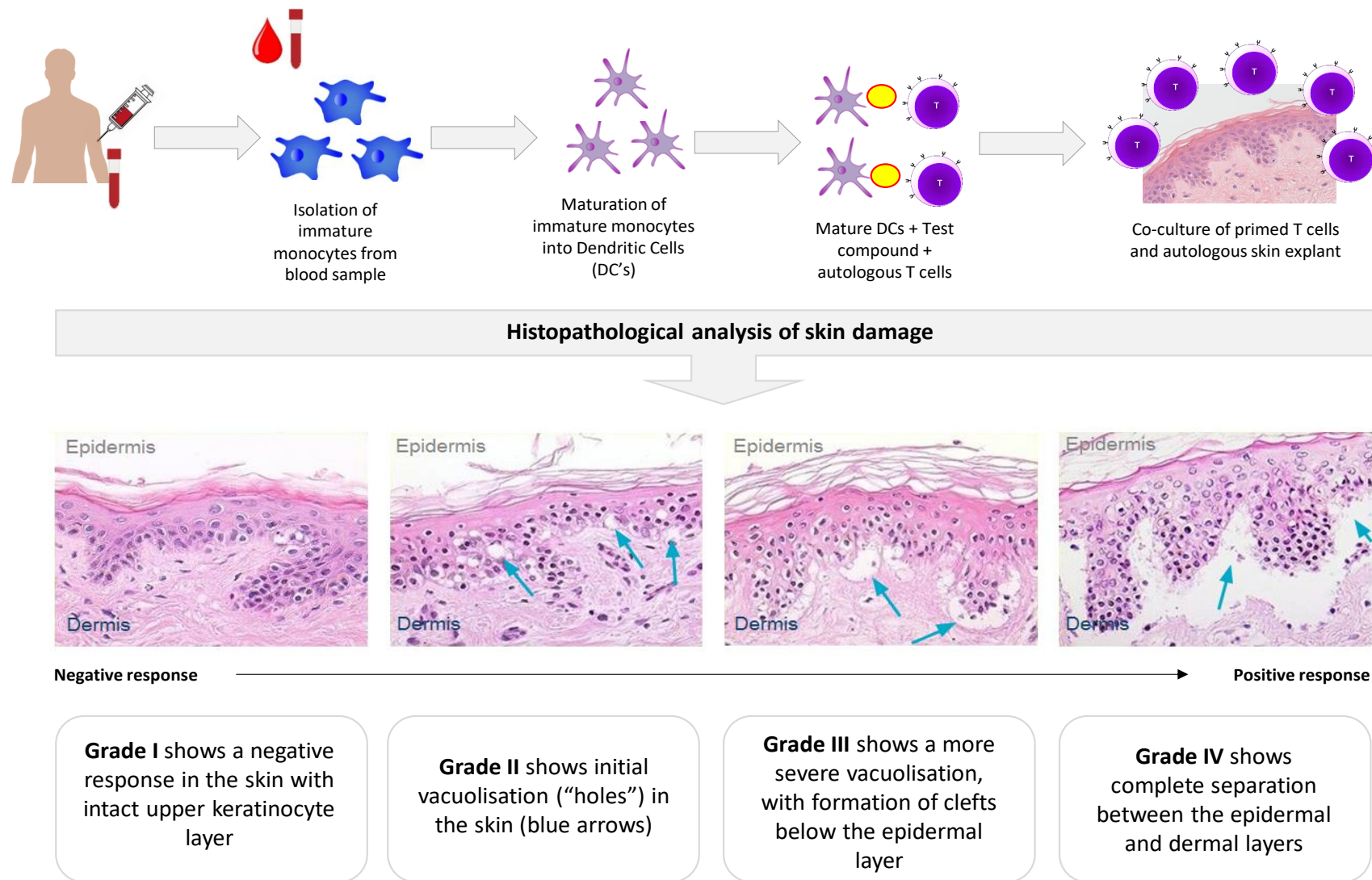


Figure 5. Alcyomics *in vitro* skin explant assay. This autologous assay consists on isolation of monocytes from a blood sample. Monocytes are matured into Dendritic Cells (DCs) and incubated with test compound and autologous T cells. Primed T cells are co-cultured with autologous skin biopsy. Histopathological assessment of damage is done according to a scoring grade (I-IV).

The assay has since been further modified for assessment of immune reactions to monoclonal antibodies (Ahmed et al., 2019). The skin and immune cell microenvironment should be considered as a “surrogate” microenvironment for the *in vivo* response, allowing assessment of systemic immune activation. Therefore, it can be used as a first-line tool to predict adverse immune reactions (hypersensitivity and immunotoxicity) to biopharmaceuticals and cosmetic products, assessment of dose-responses to compounds or for comparative studies with other biomolecules. Moreover, it can be used during the different stages of a product development pipeline, either in the initial stages of product screening (i.e. product optimization) as well as the preclinical stage testing. Overall, this *in vitro* skin explant assay is a cost- and time-efficient *in vitro* screening tool for assessment of immunotoxicity.

1.10.2. *Immunotoxicity of monoclonal antibodies*

Monoclonal antibodies (mAbs) are a major class of biological drugs, representing a multi-million dollar revenue stream each year in the biopharmaceutical market (EvaluatePharma, 2014). The increased commercial interest around mAbs for therapeutic use relies in the fact that mAbs are designed to be very target specific (and therefore more efficient) and are also well tolerated by the human body (meaning lower changes of rejection/side effects) (Carter, 2001; Reichert & Valge-Archer, 2007) than small molecule drugs.

Orthoclone OKT3 was the first commercial mAb to be introduced onto the market, in 1986 (Starzl & Fung, 1986). It was approved for the prevention of kidney transplant rejection. From that year on, mAb products have rapidly risen as lead products in the biopharmaceutical market. There are more than 20 commercially available mAbs approved for a range of therapies – ranging from use in oncology, immunological disorders, neurodegenerative pathologies, cardiology and also as diagnostic tools (EvaluatePharma, 2014). The drive behind mAb development is fuelled by the increased need of cost-effective therapies, by the increased success rates of newly developed mAb and lastly, by the emerging realm of *in silico* protein engineering tools (as proteomics and genomics).

Most of the commercially available antibodies are Immunoglobulin G (IgG) structure type (Figure 6) as this isoform accounts for almost 75% of all immunoglobulins found in the human blood (Roitt & Delves, 1998). An IgG antibody is a large molecule, weighting around 150kD. It is composed of two different polypeptide chains – a double heavy chain (50kD) and a double light chain (25kD). There are two major components in an IgG mAb – the Fc fragment and the Fab fragment. While the Fab fraction binds to the antigen receptor, the Fc fragment is

responsible for the immune response, stimulating activation of different immune cells (macrophages, neutrophils, NK cells...) (Janeway et al., 2001).

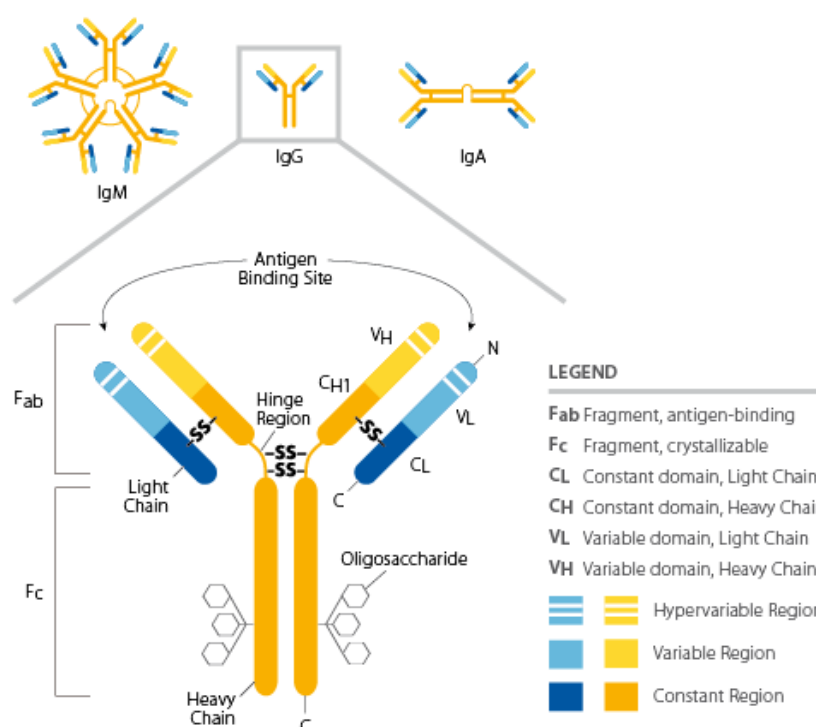


Figure 6. Structure of the IgG antibody. The IgG antibody is composed of two heavy chains (50kD) and two light chains (25kD) that are bonded by disulphide bridges. The antibody can be divided in two major fragments from its hinge region – the Fab fragment (upper part) and the Fc fragment (lower part). (<http://www.ebioscience.com/knowledge-center/antigen/immunoglobulin/structure.htm>)

However, large-scale production of mAbs is a challenging process that demands a complex industrial process. Filtration of IgG samples during its manufacturing process is quite common, in order to remove all large aggregates. However, residual small-size aggregates (below the 0.22µm membrane filter limit) can surpass the filter and remain in the IgG solution. These residual aggregate species can aggregate into large aggregates during manufacturing, shipping and storage stages if exposed to specific stress factors.

Temperature is one such critical parameter since thermal changes can affect the conformational structure and stability of the IgG molecule (Vermeer & Norde, 2000). This imposes a serious production failure cost as it can lead to an irreversible aggregation status of the batch. At higher temperatures, the disulphide bridges binding the polypeptide chains of the antibody can start to weaken and even unbind by denaturation (Luo et al., 2011). This leads to an unfolding of the overall structure, leading to an unstable conformational state (Joubert, Luo, Nashed-Samuel, Wypych, & Narhi, 2011; Menzen & Friess, 2014; Vermeer, Bremer, & Norde,

1998; Vermeer & Norde, 2000). pH can also induce antibody aggregation via protein instability (Buchner, Renner, Lilie, Hinz, & Jaenicke, 1991; Joubert et al., 2011; Talley & Alexov, 2010). Acid-induced changes can promote loss of native structure, by means of secondary structure refolding (Kent, Schroeder, & Sharma, 2018). More specifically, Vermeer *et al.* showed that while the Fab fragment is very sensitive to heat stress, the Fc region is more sensitive to pH (acidic conditions) (Vermeer & Norde, 2000). A recent study has also shown that interaction between pH and temperature as critical parameters for aggregation increased occurrence of aggregation in 3 mAbs, as mAbs were subjected to rapid thawing cycles with a pH variation from 3 to 7 (Kent et al., 2018).

Physical or mechanical stress can also potentiate antibody aggregation such as stirring during manufacture (Kiese, Pappenberg, Freiss, & Mahler, 2008), storage, shipping or shaking during administration of the antibody (Peters, Capelle, Arvinte, & van de Garde, 2013). Protein aggregation is a consequence of denaturation conditions (such as temperature, pH and stirring), driven by free non-specific hydrophobic interactions of unfolded antibody molecules. Commercially available mAbs are formulated to be very stable endpoint products but exposure to these stress factors can compromise mAb stability.

Taking into account the size of protein aggregates, their characterization becomes quite complex. Affinity chromatography methods for separation of larger aggregates can be very difficult as aggregates will constrain or even block the chromatography columns (Evans, 2015). Therefore, multi-technique analysis or combination approaches would provide more information. New analytical techniques like analytical ultracentrifugation (AUC) (Wafer, Kloczewiak, & Luo, 2016), size exclusion chromatography-multi angle light scattering (SEC-MALS) (Ye, 2006), and asymmetric flow field-flow fractionation multi-angle light scattering (AF4-MALS) (Fraunhofer & Winter, 2004) are the current most reliable methods for quantifying low levels of aggregates. AUC allows for the quantitative description of protein aggregation and formulation of large supramolecular complexes based on their sedimentation properties (Berkowitz, 2006). Sedimentation velocity (SV)-AUC is a hydrodynamic approach, which provides details of particle mass and shape and is particularly useful for studying multicomponent irreversible and reversible mixtures of species (Cole, Lary, Moody, & Laue, 2008).

Considering the panoply of protein-based therapeutics, there is concern that protein aggregation can be one potential cause of immunogenicity in humans. However, little is known about mAb aggregation following patient administration. While there is a significant chance that mAb preparations alone will cause some degree of immunotoxicity (Baert et al., 2003;

West, Zelinkova, Wolbink, Kuipers, & Rs, 2008), mAb aggregation can exponentially increase the likelihood of causing an adverse immune event.

Previous reports have shown that detection of aggregated mAb samples can be found in human biological fluids such as serum (Filipe et al., 2011; Filipe, Poole, Oladunjoye, Braeckmans, & Jiskoot, 2012) and plasma (Filipe et al., 2011). Furthermore, aggregated mAbs have been shown to give rise to *in vitro* cell proliferation via activation of dendritic cells (Rombach-Riegraf et al., 2014) and T cells (Ahmadi, Bryson, Cloake, Welch, Filipe, Romeijn, Hawe, Jiskoot, Baker, et al., 2015; Joubert et al., 2012, 2016). These *in vitro* results are derived from cell-based assays that mimic the normal immune response (e.g. dendritic cells and T cells), from cell activation and proliferation to cytokine secretion. *In vivo* response to mAb aggregation from animal-based studies show that heat-aggregated IgG aggregates lead to cell activation (Bessa et al., 2015; St. Clair et al., 2017).

So far, previous studies focusing on assessing the immunotoxic profile of aggregated mAbs were either cell-based or performed in animal models (mice and primates). The lack of human-based *in vitro* assays makes it difficult to truly understand mAb immunotoxicity as a potential threat to humans. This project intends to contribute with valuable insights by using a novel *in vitro* skin explant assay for assessment of immunotoxicity of aggregated monoclonal antibodies (Chapter 5).

Overall, and while many efforts have been done for development of *in vitro* safety testing methods as replacement for animal studies, there is still a long road to go for development of the most suitable *in vitro* method that can truly mimic the *in vivo* microenvironment of the human skin. From epidermal models to *ex vivo* skin models, there has been a massive progress for optimization, commercialization and validation of a panoply of different *in vitro* skin models. Further efforts to combine these *in vitro* skin models with *in silico* approaches have raised the legislative standards for risk assessment analyses and adverse pathway frameworks.

Currently, there are several commercially available *in vitro* skin models in the form of Reconstructed Human Epidermis models or full-thickness skin models for assessment of different magnitudes of sensitization – irritation, corrosion, immunotoxicity. From patented to open source models, it is possible to choose different methods as screening test method. However, much needs to be taken into consideration regarding these models like origin of cells, reproducibility, commercial cost, applications, use of animal components, standardization of protocols... And while issues like skin irritation have been a priority for regulatory authorities, immunotoxicity as a secondary form of sensitization still lacks proper attention due to its

novelty. Increased concerns for immunotoxicity in the context of aggregated monoclonal antibodies has driven researchers to develop more accurate *in vitro* assays for detection of immunotoxicity by immune cell activation and/or proliferation.

Therefore, this project was developed to bring a new insight into the issues mentioned above following a general research hypothesis: How can we improve assessment of sensitization using *in vitro* test methods, in a more accurate and human relevant manner? Two parallel approaches were formulated to try answering this research hypothesis:

- Is it possible to develop an open source *in vitro* epidermal model that can compete with the commercially available ones for assessment of skin irritation? Can this optimized *in vitro* epidermal model be free of animal components, reproducible and demonstrate accurate identification of irritants vs non-irritant chemicals in the context of safety testing regulations?
- Considering immunotoxicity as a form of sensitization, is it possible to assess immunotoxicity using a human-based *in vitro* assay for the effect of aggregated monoclonal antibodies?

Several small tasks and aims were outlined to answer these research hypotheses as described in the next section (section 1.11).

1.11. Aims

This project is divided in two segments of assessment of skin toxicity and sensitization for human safety. The initial emphasis of this PhD project was to develop an open source 3D epidermal skin culture of human epidermis for the assessment of skin irritation testing (OECD TG 439) in accordance with the Globally Harmonized System (GHS) of Classification and Labelling Category 2. For this, several tasks were performed using the 3D epidermal skin culture, namely:

- ▽ Establishment of a 3D epidermal skin culture by optimization of cell density, nutrient requirements and other specifications;
- ▽ Optimization of keratinocyte differentiation and phenotype using collagen-coated and non-collagen-coated scaffolds;
- ▽ Assessment of skin irritation testing following OECD TG 439 protocol using the optimized 3D skin culture;
- ▽ Comparison of skin irritation testing between the 3D skin culture, monolayer keratinocyte culture and commercially available RHE models.

The second focus of this project was regarding sensitization and prediction of adverse immune events. Therefore, an *in vitro* skin explant assay was used to assess immunotoxicity by aggregated monoclonal antibodies. Additional assays such as T cell proliferation and cytokine release were also used for further assessment of immunotoxicity by aggregated monoclonal antibodies. Similar to the previous aim, several tasks were performed using the *ex vivo* skin explant, as following:

- ▽ Assessment of immune activation by aggregated and non-aggregated monoclonal antibodies by the *ex vivo* skin explant assay;
- ▽ Assessment of immune activation of aggregated and non-aggregated monoclonal antibodies by T cell activation and pro-inflammatory cytokine activation.

CHAPTER 2

General Materials and methods

2. Materials & Methods

Part I – Development of a 3D skin culture model for skin irritation testing

2.1. Isolation of primary keratinocytes for 3D culture

All skin samples were obtained from healthy donors after informed consent. Keratinocytes were isolated from skin explant biopsies, either taken from the abdominal region (by a 4mm punch biopsy) or foreskin region (surgically removed). Use of skin biopsies was approved by the Local Research Ethics Committee. Skin biopsies were collected and kept in *ex-vivo* medium (X-Vivo™ 15, Lonza) and processed on the same day. The skin explant biopsy was subjected to enzymatic digestion with dispase (Sigma) to allow separation of the epidermis from the dermis. After enzymatic incubation for at least 18 hours at 4°C, the epidermis was separated from the dermis with the use of forceps. The epidermal layer was incubated with Trypsin (Sigma) for 5 minutes at 37°C to improve the dissociation process. The trypsin was neutralized with an equal volume of Epilife® medium (Life Technologies GmbH) and the epidermis was transferred into a cell culture flask (T25 cm² area) for seeding of keratinocytes in Epilife® medium. The Epilife® medium was supplemented with 1% Human Keratinocyte Growth Supplement (HKGS) (Life Technologies GmbH), 1% penicillin/streptomycin solution (Sigma) and 1% amphotericin B (Life Technologies GmbH). This was considered passage 0. Keratinocytes were cultured at 37°C with 5% CO₂ in an incubator. Medium exchange was required every two days, with addition of fresh 20 mL Epilife® medium. Keratinocytes were subcultured to passage 1 after reaching 80% confluency. The flask was washed with phosphate-buffered saline (PBS, Sigma), detached by incubating for 5 minutes with trypsin, centrifuged and resuspended in Epilife® medium. After determination of the cell number, the keratinocytes were seeded at a concentration of 5x10⁵ cells/flask into a 175 cm² culture flask. Passage 2 and 3 were performed following the same protocol.

2.2. Monolayer culture of keratinocytes

Keratinocytes were seeded at passage 3 at 5x10³ cells/well in flat-bottom 96-well plate using Epilife® medium and left to adhere for at least 24 hours before addition of the testing chemical.

2.3. Assembly of the 3D skin culture

Keratinocytes were seeded in Alvetex Strata scaffolds (from Reprocell Europe, polystyrene, 15µm pore size, 24mm outer insert diameter, 20mm membrane area) at passage 3 and kept submerged in Epilife® medium enriched with CaCl₂ (1.5mM concentration, Sigma) for 24 hours. Medium was afterwards aspirated, from both the bottom of the well and the inside of the insert and replaced with 4mL fresh Epilife® enriched with HKGS (1%), CaCl₂ (1.5mM) and vitamin C (100µg/mL, Sigma) reaching to just the bottom of the insert. This was considered the beginning of the Air Liquid Interface (ALI) for the 3D skin culture model. The model was cultured under these conditions for 30 days, with medium being replaced every two days. Different cell concentrations (1x10⁶, 1.5x10⁶ and 2x10⁶ cells/scaffold) and ALI times (14, 21 and 30 days) were tested.

2.4. Skin irritation testing following Testing Guideline 439

Skin irritation testing was conducted according to the Testing Guideline (TG) 439 defined by EURL-ECVAM (OECD, 2013). From the List of Reference Chemicals in TG 439, 12 chemicals were chosen to be tested in both the monolayer cell culture and the RHE model (the chemicals tested are shown in Table 6). Tests were performed in triplicate for all donors. Chemicals were tested with stock concentration, no further dilution performed as defined by OECD TG 439. Negative and positive controls were also used, PBS being defined as the negative control and 5% aqueous SDS solution as the positive control.

For the monolayer keratinocyte culture, 30µL of each testing chemical was added to the Epilife® medium and left to incubate for 24 hours. Medium was then discarded, and the cells washed with PBS before addition of fresh medium for the cell viability assay. Chemical testing was performed using keratinocytes from 10 healthy donors.

For the 3D skin culture, the models were transferred to a new plate containing Epilife® medium prior to the chemical testing. As stated on TG 439, 30µL of each testing chemical was dispensed directly on top on the 3D skin culture, covering the entire surface of the scaffold and left to incubate for 35 minutes. After topical exposure, all 3D skin culture models were rinsed with PBS (both outside and inside the insert), transferred to a new plate containing fresh Epilife® medium and maintained in the incubator for a further 42 hours. Chemical testing was performed in the 3D skin culture models formed by keratinocytes from 10 healthy donors.

Table 6. Test chemicals for the skin irritation test TG 439. For each chemical, Chemical Abstract Service (CAS) number is listed, as well as physical state, *in vivo* score based on Draize irritancy score and *in vivo* category according to Globally Harmonized System (GHS).

Chemical	CAS number	Physical state	<i>In vivo</i> score	GHS category <i>in vivo</i>
1-bromo-4-chlorobutane	6940-78-9	Liquid	0	No cat.
Allyl phenoxy-acetate	7493-74-5	Liquid	0.3	No cat.
Isopropanol	67-63-0	Liquid	0.3	No cat.
4-methyl-thio-benzaldehyde	3446-89-7	Liquid	1	No cat.
Heptyl butyrate	5870-93-9	Liquid	1.7	No cat.
Hexyl salicylate	6259-76-3	Liquid	2	No cat.
1-decanol	112-30-1	Liquid	2.3	Cat. 2
1-bromohexane	111-25-1	Liquid	2.7	Cat. 2
di-n-propyl disulphide	629-19-6	Liquid	3	Cat. 2
Heptanal	111-71-7	Liquid	3.4	Cat. 2
Tetrachloroethylene	127-18-4	Liquid	4	Cat. 2

2.5. Cell viability of the test chemicals

Cell viability assay for each chemical was performed according to TG 439, using the 3-(4,5-Dimethylthiazol-2-yl)-2,5-Diphenyltetrazolium Bromide (MTT) assay. 3D skin culture models were incubated with 300µL of MTT solution (1mg/mL, Sigma) at 37°C for 3 hours protected from light to allow formation of formazan crystals. After this incubation period, MTT was removed and the models washed with PBS. Formazan crystals were extracted by incubation with 2mL isopropanol (Sigma) for 1 hour with constant low speed shaking on a plate shaker. Afterwards, 200µL in triplicate of the extraction solution from each chemical was transferred to a 96-well plate and the Optical Density (OD) was measured at 575nm using a plate reader (Thermo).

2.6. Calculation of cell viability

The OD mean for the triplicates of each testing chemical was calculated. For each chemical, the relative cell viability was calculated in comparison to the negative control, by the following equation:

$$\% \text{ cell viability} = \left(\frac{OD_{\text{testing chemical}}}{OD_{\text{negative control}}} \right) \times 100$$

According to the Performance Standards from TG 439, for a chemical to be considered an irritant, it should cause a reduction in viability greater than 50%. Therefore, the threshold for irritancy will be defined in this study as 50% viability. Performance Standards also apply to the test controls, in which the positive control should cause a cell viability no higher than 10% (compared to the negative control).

2.7. Statistical analysis

Average mean of each chemical was analysed by one-way analysis of variance (ANOVA) and significant mean differences were determined by Dunnett posthoc test, by comparison between all chemical conditions to the negative control. A Chi-Square (χ^2) test of independence was carried out to determine if classification of irritants and non-irritants by each *in vitro* method was accurate (comparison of observed versus expected). A two-way ANOVA was performed to determine difference of performance between each *in vitro* model with chemicals (non-irritant and irritant) and *in vitro* models as independent variables.

All statistical tests were carried out using Prism GraphPad software (version 5). Statistical differences were considered significant if p value <0.05.

2.8. Collagen-coated scaffolds

Two types of collagen-coated scaffolds were used as “direct” comparison to the 3D skin culture model. The first scaffold was a Corning transwell® insert previously coated with type I and III collagen (Transwell®-COL scaffolds, Corning, 0.4µm pore size, 24mm outer insert diameter).

The second scaffold was the Alvetex Strata (from REPROCELL, UK) coated with human collagen (Sigma, recombinant). The collagen solution was prepared in a 1:1 dilution with ethanol absolute and applied to the scaffold. Overnight incubation in a laminar flow hood was required to allow the scaffold to dry completely. Prior to the seeding of keratinocytes, scaffolds were washed with PBS to remove any excess collagen-Ethanol solution.

In both conditions, keratinocytes were seeded and submerged in enriched Epilife® for 24 hours before starting ALI. Different times for the ALI were tested – 14, 19 and 21 days for Transwell®-COL scaffolds and 3,7, 14, 19, 21 and 30 days for Alvetex Strata coated with human collagen. This optimization was performed using keratinocytes from five different healthy donors.

2.9. Commercially available alternatives for skin irritation testing

A commercially available RHE model was bought from MatTek (EpiDerm™ 24-well model, USA) for an in-house comparative study with the 3D skin culture model. Upon receipt of the EpiDerm™ models, the models were transferred to a new 24-well plate containing fresh Epilife® medium and left to incubate overnight at 37°C and 5% CO₂. Skin irritation testing was performed using the same chemicals as the monolayer culture and the 3D skin culture models (see Table 6), following the manufacturer's protocol (MatTek, 2004). 30µL of test chemical were dispensed on top of the models and left to incubate for 1 hour (35 minutes in the incubator and 25 minutes at room temperature). The models were then rinsed with PBS and transferred to a new 6-well plate with 0.9mL Epilife® medium and incubate for 42 hours with medium exchange every 24 hours. MTT viability test was performed after those 42 hours, transferring the models to a new 6-well plate containing 300µL of MTT solution at 1 mg/mL.

2.10. Histological and immunofluorescence analysis of the 3D skin culture

3D skin culture models were fixed in 4% formaldehyde for at least 24 hours before disassembling of the scaffold and embedding in paraffin. Tissue sections (4µm thick) were prepared for histological staining (Hematoxylin and Eosin - H&E and collagen) and immunofluorescence (involucrin for the stratum corneum and cytokeratin 14 for the stratum basale).

Collagen and immunofluorescence staining were performed in paraffin embedded 3D epidermal skin models. Therefore, 4µm sections of the 3D epidermal skin models were cut in a microtome, incubated overnight in a benchtop oven at 37°C and for 1 hour at 60°C before rehydrated. Rehydration was achieved by washing slides containing sections of the 3D epidermal skin models for 3 minutes in Xylene, 100% ethanol, 95% ethanol, 70% ethanol and distilled water, blotting excess in between each wash. After staining, all slides were dehydrated again by submerging in distilled water, 70% ethanol, 95% ethanol, 100% ethanol and xylene for 3 minutes and covered with a glass cover slip glued with DPX synthetic resin (mixture of distyrene, a plasticizer (tricresyl phosphate), and xylene, Sigma). Slides were left to dry overnight before taken for imaging on microscope.

Collagen staining was performed using the picro-sirius red stain kit (Abcam), following the manufacturer's instructions. 1 drop of picro-sirius red solution was added to each slide, making sure it covered the whole sample. Slides were left to incubate for one hour at room temperature

in the dark and washed afterwards with acidified water (distilled water with 5% acetic acid) twice. Slides were blotted and dehydrated as mentioned above. Imaging was performed using a Zeiss AxioImager at 10x zoom. Images were not modified or manipulated at any point.

Immunofluorescence labelling of the epidermal differentiation markers - stratum corneum (involucrin) and basal layer (cytokeratin 14) was performed using anti-involucrin (ab68 from Abcam) and anti-cytokeratin 14 (ab7800 from Abcam) antibodies with in-house optimized protocol. Alexa Fluor 488 and 647 (Life technologies) were used as species-specific secondary antibodies, at a concentration of 1 μ g/mL (see Table 7 for summary of all antibodies used). After rehydration of the slides, antigen retrieval was performed with 10mM citrate buffer (pH=6) in a microwave for 5 minutes twice. Slides were then washed in 5mM TBS (pH=7.6) for 5 minutes and prepped for permeabilization step. 0.2% Triton-X (in PBS) was added to all slides and left to incubate for 10 minutes at room temperature. Slides were then washed with TBS. A blocking step with 100 μ L of 10% Goat Serum solution diluted in PBS (Sigma) was added to all slides and left to incubate for 30 minutes at room temperature. A washing step with TBS was performed to remove all traces of the goat serum. All slides were incubated with anti-involucrin (1mg/ml diluted with 10% goat serum solution at 1:400) and anti-cytokeratin 14 (1mg/ml diluted with 10% goat serum solution at 1:250) primary antibodies (Abcam) for 1 hour. Null primary slides were coated with 10% goat serum solution instead for background unspecific binding from the secondary antibody. After incubation, sections were washed twice in TBS for 5 minutes. Slides were then incubated with the secondary antibody (AF488 for involucrin and AF647 for cytokeratin 14). A mix solution was prepared containing both secondary antibodies diluted at 1:200 in the 10% goat serum solution. 100 μ L of the mix solution was added to all slides and slides were incubated for 2 hours at room temperature in a moist chamber in the dark. After the 2-hour incubation period, slides were washed twice in TBS for 5 minutes and dehydrate as mentioned before. Slides were covered with Fluoroshield Mounting Medium with DAPI (ab104139 from Abcam) and left overnight at 4°C. Microscopy images of histopathological skin damage were taken using a Zeiss AxioImager with Apotome (wide field fluorescence) at 10x zoom. Images were not modified or manipulated at any point.

Table 7. Summary of antibodies used for immunofluorescent staining of the 3D epidermal skin culture.

Antibody name	Company	Concentration	Dilution	Application/Target
Anti-Involucrin antibody [SY5] (ab68)	Abcam	1mg/mL	1:400	Involucrin – stratum corneum (primary antibody)
Anti-Cytokeratin 14 antibody [LL002] (ab7800)	Abcam	1mg/mL	1:400	Cytokeratin 14 – basal layer (primary antibody)
Goat Serum (G9023-5ML)	Sigma	-	1:10	Blocking solution
Anti-Mouse IgG Alexa Fluor 488 (A-11001)	Life Technologies	2 mg/mL	1:200	Secondary Antibody for Anti-involucrin
Anti-Mouse IgG, Alexa Fluor 647 (A-21235)	Life Technologies	2 mg/mL	1:200	Secondary Antibody for Anti-Cytokeratin 14
Mounting Medium with DAPI - Aqueous, Fluoroshield (ab104139)	Abcam	20mL	1:1	Mounting medium designed to preserve fluorescence when imaging tissue samples

Part II – Assessment of immunotoxicity of aggregated mAbs using an in vitro skin explant assay

2.11. Human and blood samples

All blood and skin samples were obtained from healthy volunteers after informed consent. Each volunteer donated 60mL of peripheral blood and two 4mm skin biopsies. 55mL of peripheral blood was used to isolate peripheral blood mononuclear cells (PBMCs) by density-gradient centrifugation (15 minutes at 2500rpm) with LymphoprepTM medium (Sigma). PBMCs were collected by aspiration and washed with PBS before counted with Trypan blue solution for cell concentration correctness. The remaining 5mL of peripheral blood were used to purification of serum. The blood collection tube was centrifuged at 2500rpm for 5 minutes and serum was collected from the top layer into a 1.5mL Eppendorf tube. Heat inactivation of serum was performed by incubating the Eppendorf tube with the serum sample for 30 minutes at 56°C in a waterbath. Serum sample was then frozen down at -80°C until used.

Skin biopsies (abdominal area) were collected fresh with a 4mm punch biopsy and transferred to *ex vivo* X-VivoTM medium (Lonza) until used. Before processing, skin biopsies were washed in PBS (Sigma) and was trimmed of excess fat. The skin was dissected into small sections for the skin explant test.

2.12. Skin explant assay for immunotoxicity of aggregated mAbs

The skin explant assay was performed as previously described (Ahmed et al., 2016) with small modifications. Small sections of the skin biopsy were incubated in autologous medium – Roswell Park Memorial Institute (RPMI) culture medium (Sigma) supplemented with 1% penicillin/streptomycin solution (Sigma), 1% L-glutamine supplement (Sigma) and 20% of the donor's heat-inactivated serum (instead of Foetal Bovine Serum, FBS). To perform the skin explant assay for immunotoxicity of aggregated mAbs, PBMCs from the same donor were added to the skin explant incubated in autologous medium at a concentration of 1×10^6 cells/well, as well as the non-aggregated or aggregated (heat stressed) mAb samples at 1 µg/mL and 10 µg/mL for 3 days. Therefore, skin explants were collected after the 3 days incubation period and fixed in formalin for at least 24 hours, preparing the skin explants for a hematoxylin and eosin (H&E) staining. IgG1 (Biorad) was used as negative control for immunotoxicity at 1µg/mL and included in all assays. OKT3 (eBioscience) was used as positive control for immunotoxicity at 1µg/mL and included in all assays.

The endpoint of this skin explant assay was the histopathological analysis of damage caused by exposure to the mAb sample. This output was based on a scoring scale (grades I to IV) according to the severity of the skin tissue damage observed (Lerner et al., 1974). Grade I was considered negative, with an intact upper keratinocyte layer; grade II showed vacuolisation of the epidermis; grade III showed severe damage of the epidermal layer, with cleft formation and initial separation of the epidermal and dermal layers and grade IV showed further damage, with complete separation of the epidermal and dermal layers.

Imaging of the histopathological skin damage was performed using a Zeiss AxioImager with Apotome (wide field fluorescence) at 10x zoom. Images were not modified or manipulated at any point.

2.13. *T cell proliferation*

PBMCs were incubated with the mAb samples at 1 µg/ml or 10 µg/mL (cell concentration of 1×10^6 cells/well) for 3 days. IgG1 (Biorad) at 1 µg/mL was used as a negative control for T cell proliferation. OKT3 (eBioscience) at 1 µg/mL was used as a positive control for T cell proliferation. After the incubation period, supernatants were collected for cytokine analysis. T cell proliferation was assessed by tritiated thymidine ($[^3\text{H}]$ -Thymidine) uptake by adding 3.7Mbq to each well at a 1:10 dilution and left for an 16-hour period incubation. Cells were harvested onto a filtermat and counted using a β -scintillation counter (PerkinElmer).

2.14. *Cytokine release assay*

Multiplex cytokine analysis was performed using both the skin explant assay and the T cell proliferation cell culture supernatants using MSD Multi-Spot Proinflammatory panel 1 V-Plex kit (Meso Scale Diagnostics) following the manufacturer's instructions. The biomarkers included in this panel were IFN- γ , IL-1 β , IL-2, IL-4, IL-6, IL-8, IL-10, IL-12p70, IL-13 and TNF- α . All diluents and read buffers were included in the kit and prepared according to manufacturer's instructions. Supernatant samples were diluted 1:10 with diluent 2 (from the kit) and 50µL of each sample were transferred to the MSD plate. MSD plate was washed 3 times with wash buffer (included in the kit) and 25µL of detection antibody solution was added to all wells. MSD plate was sealed and left to incubate for 2 hours at room temperature in a shaking plate at low speed. Afterwards, MSD plate was washed with wash buffer three times

and 150 μ L of read buffer (included in the kit) was added to all wells. Calibrator diluents were also prepared for a standard curve by 4-fold serial dilutions of calibrator 1 (included in the kit) 5 times and included in the same MSD plate containing the samples. The MSD plate was then read on an MSD plate reader. Average calculation of concentration of each biomarker was calculated by the MSD plate reader software (in pg/mL) for each sample and adjusted for the standard curve.

2.15. *Immunofluorescence*

Cell death labelling was performed by staining with Anti-Hsp70 (Heat-Shock protein 70) (1mg/ml) and Anti-Caspase 3 (casp3) (1mg/ml) antibodies (Abcam) with in-house optimized protocol. Alexa Fluor 488 (A488, Life Technologies) was used as the secondary antibody, at a concentration of 1 μ g/mL (see Table 8 for summary of all antibodies used). After rehydration of the slides (same protocol as described in section 2.10), antigen retrieval was performed with 10mM citrate buffer (pH=6) in a microwave for 5 minutes twice. Slides were then washed in 5mM TBS (pH=7.6) for 5 minutes and prepped for permeabilization step. 0.2% Triton-X (in PBS) was added to all slides and left to incubate for 10 minutes at room temperature. Slides were then washed with TBS. A blocking step with 100 μ L of 10% Goat Serum solution diluted in PBS (Sigma) was added to all slides and left to incubate for 30 minutes at room temperature. Washing with TBS was performed to remove all traces of the goat serum. All slides were incubated with anti-HSP70 (1mg/ml diluted with 10% goat serum solution at 1:20) and anti-Caspase3 (1mg/ml diluted with 10% goat serum solution at 1:20) primary antibodies (Abcam) for 1 hour. Null primary slides were coated with 10% goat serum solution instead for background unspecific binding from the secondary antibody. After incubation, sections were washed twice in TBS for 5 minutes. Slides were then incubated with the secondary antibody (AF488 diluted at 1:200 with the 10% goat serum solution). 100 μ L of the secondary antibody solution was added to all slides and slides were incubated for 2 hours at room temperature in a moist chamber in the dark. After the 2-hour incubation period, slides were washed twice in TBS for 5 minutes and dehydrate as mentioned before. Slides were covered with Fluoroshield Mounting Medium with DAPI (ab104139 from Abcam) and left overnight at 4°C. Imaging of the immunofluorescence staining was performed using a Zeiss AxioImager with Apotome (wide field fluorescence) at 10x zoom. Images were not modified or manipulated at any point.

Table 8. Summary of antibodies used for immunofluorescent staining of the skin explant samples.

Antibody name	Company	Concentration	Dilution	Application/Target
Anti-Hsp70 antibody [5A5] (ab2787)	Abcam	1mg/mL	1:20	Heat Shock Protein 70 (cell death)
Anti-Caspase-3 antibody (ab4051)	Abcam	1mg/mL	1:20	Caspase 3 (cell death)
Goat Serum (G9023-5ML)	Sigma	-	1:10	Blocking solution
Anti-Mouse IgG Alexa Fluor 488 (A-11001)	Life Technologies	2 mg/mL	1:200	Secondary Antibody for Anti-involucrin
Anti-Mouse IgG, Alexa Fluor 647 (A-21235)	Life Technologies	2 mg/mL	1:200	Secondary Antibody for Anti-Cytokeratin 14
Mounting Medium with DAPI - Aqueous, Fluoroshield (ab104139)	Abcam	20mL	1:1	Mounting medium designed to preserve fluorescence when imaging tissue samples

2.16. Heat stress protocol for aggregation of monoclonal antibodies

2.16.1. Degradation of mAb samples

Herceptin (Trastuzumab) and Rituximab (Mabthera) monoclonal antibodies (IgG1 class) were commercially bought from the Newcastle Hospital Pharmacy. Herceptin was bought as a 600mg/5L solution for injection in a vial, while Rituximab was bought as a 100mg/10L concentrate for solution for infusion. Upon purchase, both mAbs were prepared and diluted to multiple 1mL aliquots of 1 mg/mL stock concentration. Aliquots were used to expose the two mAbs to a heat stress protocol by exposure to different heat conditions: 4°C (fridge), 37°C (incubator) and 40°C (water bath) for the following time points: 0, 3, 6, 12, 24 and 48 hours. A positive control for aggregation was also prepared for each mAb, by leaving

the samples at 65°C for one hour in an acidic buffer (pH=3). Samples were stored immediately after the heat stress protocol at 4°C until further analysis.

2.16.2. *Protein analysis of heat stressed mAb samples*

Protein content of the heat stressed mAb samples was quantified by sedimentation velocity-analytic ultra-centrifugation (SV-AUC). Sedimentation analysis was carried out using a ProteomeLab XL-I analytical centrifuge (Beckman Coulter, Palo Alto, USA). The following conditions were used in all centrifugation runs: 40.000-rpm angular velocity, 20°C rotor temperature and 280-nm absorbance scanned. Absorbance and interference data were collected for each experiment with a minimum of 65 scans. Protein quantification (percentage of monomers, dimers and heavier species) was calculated using SEDNTERP software. Sedimentation velocity profiles were treated using size-distribution models and refined with Bayesian statistics. This quantification was carried out in the Newcastle University Protein and Proteome Analysis (NUPPA) facilities as a service.

Protein characterization was analysed by Transmission Electron Microscopy (TEM). 10µL of the mAb stressed samples were deposited on carbon coated TEM grids, after which the grids were stained with uranyl acetate (10µL at 150mg/ml) for negative staining. The grid was air-dried and the excessive staining was removed from the grid specimens by paper blotting. The grids were then analysed under acceleration voltage of 100 kV under a Philips CM100 Transmission Electron Microscope. This characterization was carried out in the Electron Microscopy Research Unit of Newcastle University.

2.17. *Statistical analysis*

The T cell proliferation assay endpoint was a log(2) fold-increase Stimulation Index (SI) in response to exposure to the test compound. This cut-off value was defined previously in similar studies (Rombach-Riegraf et al., 2014). SI were measured by the ratio between the test conditions (mAb exposure) and the untreated control (no mAb exposure). Statistical analysis was carried out using repeated measures one-way ANOVA.

For the skin explant test, statistical analysis was performed to 1) compare the mAb concentration (1 and 10 µg/mL) in the same donor by a repeated measures two-way ANOVA with a Bonferroni correction (post-test) and 2) to see the effect of the different mAb temperature

conditions in the same donor by a one-way repeated measures ANOVA with a Bonferroni post-test.

Statistical analysis of the cytokine levels was carried out using repeated measures one-way ANOVA.

All statistical tests were carried out using Prism GraphPad software (version 5). Statistical differences were considered significant if p value <0.05 . Statistical significance was reported as following: * $p<0.05$, ** $p<0.01$, *** $p<0.001$, **** $p<0.0001$.

CHAPTER 3

Development of an open source 3D epidermal skin culture

3. Development of an open source 3D epidermal skin culture

3.1. Aim

Reconstructed human epidermis (RHE) models are gaining relevance for *in vitro* screening of chemical compounds that seek regulatory approval before commercialization. Several RHE models are already available as commercial kits for toxicology testing and some are, in fact, validated by EURL-ECVAM standards for use in irritation and corrosion testing of chemicals.

However, the high cost of these models can rapidly become a financial burden for scientific research. Consequently, research labs are trying to develop their own open source RHE model from open source protocols. Therefore, the aim of this chapter was to develop a 3D epidermal skin culture based on the previous work by Poumay et. al (2004) using the Alvetex Scaffold membranes.


3.2. Results

To achieve an optimized protocol for the 3D epidermal skin culture, several optimization features were performed.

Origin of the skin cells was from a primary keratinocyte culture, isolated from excess foreskin or abdomen explants of healthy volunteers undergoing surgery. Information regarding the healthy volunteers was not provided (i.e. age), other than confirmation of no infections or co-morbidities that could impair quality of the skin explant provided. Keratinocyte cells were isolated as described in section 2.1, starting with isolation of cells, bulking for 80% confluency and seeding into the skin model scaffold at passage 3. This is a standard protocol that did not required optimization.

The first optimization step was the scaffold used. The Alvetex Scaffold (standard scaffold) and the Alvetex Strata (new scaffold) (Reprocell Europe Ltd.) were used since they are collagen and animal-free scaffolds (Table 9). Both scaffold membranes present similar features (membrane constitution, height and diameter) but were designed for different applications. Alvetex Scaffold membrane was designed for 3D culture of cells within the scaffold (average void size of 42 μm), while Alvetex Strata membrane was designed to support the growth of cells on the surface of the membrane (average void size of 15 μm). This design feature proved to be crucial for the adhesion and differentiation of keratinocytes as shown in the following results.

Table 9. Specifications of the Alvetex scaffold membranes provided by Reprocell Europe Ltd. Two scaffold membranes were used for the 3D epidermal skin culture – the Alvetex Scaffold and the Alvetex Strata. Both scaffold membranes present similar specifications, except in the void size.

	alvetex scaffold	alvetex strata
Scaffold material	Polystyrene	Polystyrene
Height	13mm	13mm
Bottom diameter	13mm	13mm
Void size	42µm	15µm
Company website	https://www.reprocell.com/what-is-alvetex-i70	

3.2.1. Optimization of the Alvetex Scaffold

The initial protocol was designed using the Alvetex Scaffold, using 1×10^6 cells per scaffold during a 30 days period of ALI. The culturing conditions were based on previous reports by Poumay et. al (2004) and (Mewes et al., 2016) that reported a seeding density of around 5×10^5 keratinocytes/cm² membrane area as a general rule for optimized cell seeding. Considering that both Alvetex membranes have a membrane area of around 1.2cm², seeding 1×10^6 keratinocytes at passage 3 into the Alvetex scaffold membranes was considered appropriate.

The finalised 3D epidermal skin culture can be observed in a total of 4 donors in Figure 7 (donor 1 and 2) and Figure 8 (donor 3 and 4). Incomplete differentiation and organization of the keratinocytes can be observed in the H&E images (indicated by the black arrows), as they are scattered and not evenly adhering to the scaffold. This is especially evident in donor 4, where there is barely any keratinocytes adherent to the scaffold. Immunofluorescent staining of involucrin and cytokeratin 14 showed no positive staining for both markers, indicating that the few keratinocytes adherent to the scaffold did not differentiate into the different skin layers.

Additionally, an excessive infiltration of the keratinocytes into the scaffold can be observed in the second donor. Overall, the results from the Alvetex Scaffold using 4 donors showed poor keratinocyte adhesion and no further differentiation into different skin layers. The general disorganization of the keratinocytes was also confirmed by lack of clear expression of protein markers involucrin and cytokeratin 14. Immunofluorescence staining results also highlighted infiltration of keratinocytes into the scaffold rather than on top of it.

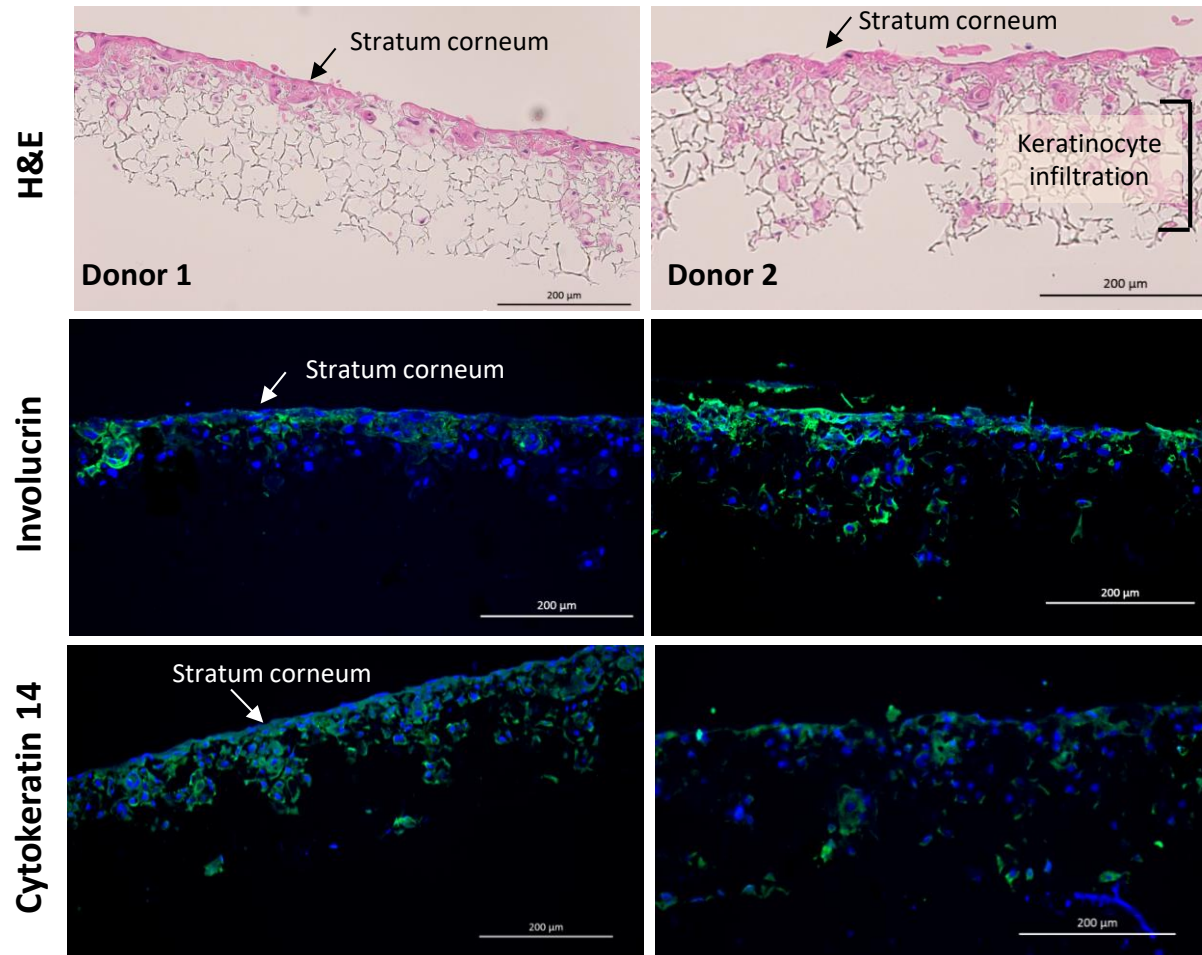


Figure 7. 3D epidermal skin culture using the Alvetex Scaffold in donor 1 and 2. Experiment was performed using 1×10^6 cells/scaffold (passage 3) during 30 days at ALI. Incomplete differentiation and organization of keratinocytes was observed. Involucrin staining was observed as positive bright green with DAPI (blue staining) for co-localization of cells. Cytokeratin 14 staining was observed as positive bright green with DAPI (blue staining) for co-localization of cells. Scale bar of 200 μ m is representative and similar in all testing conditions.

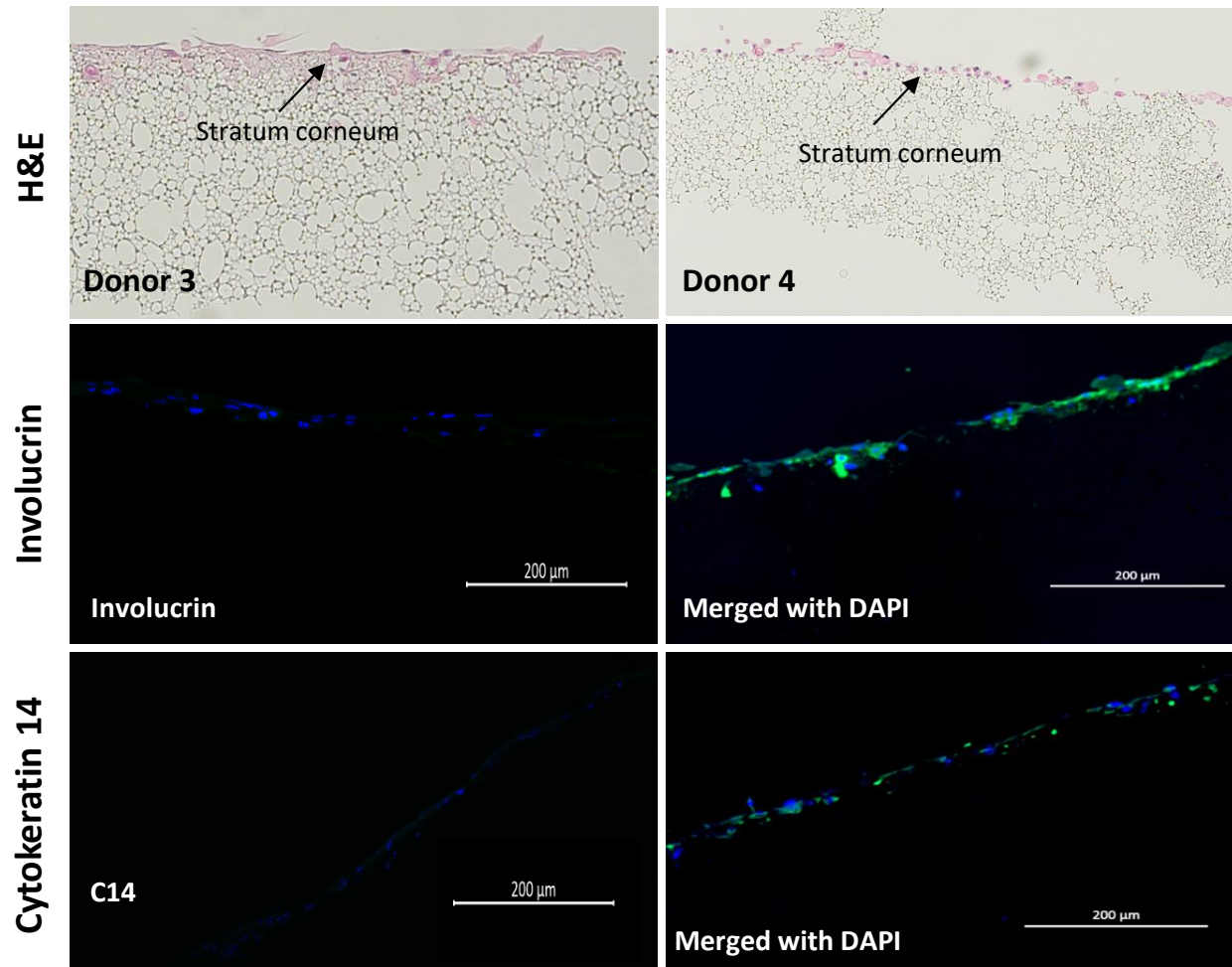


Figure 8. 3D epidermal skin culture using the Alvetex Scaffold in donor 3 and 4. Experiment was performed using 1×10^6 cells/scaffold (passage 3) during 30 days at ALI. Incomplete differentiation and organization of keratinocytes was observed. Involucrin staining was observed as positive bright green with DAPI (blue staining) for co-localization of cells. Cytokeratin 14 staining was observed as positive bright green with DAPI (blue staining) for co-localization of cells. Scale bar of 200μm is representative and similar in all testing conditions.

Results from the involucrin immunofluorescent staining showed that keratinocytes seemed to form only a very thin stratum corneum layer, meaning one out of possible two scenarios: 1) there was not enough keratinocytes seeded to form proper epidermal layers; 2) there was enough keratinocytes seeded onto the scaffold, but they did not adhere properly. Considering that 1×10^6 keratinocytes were seeded onto each scaffold, it would seem unlikely that that quantity would not be enough to form an even epidermal layer. This together with the fact that some keratinocyte infiltration could be observed, suggested that this scaffold was not appropriate since its pore size was too large. This would enable keratinocytes to migrate through the scaffold rather than layering on the top and differentiating into stratum corneum.

Therefore, it was decided to change to the Alvetex Strata as this scaffold has a smaller pore size ($15\mu\text{m}$), which could therefore prevent keratinocyte infiltration into the scaffold. However, since it is a smaller pore size, different numbers of seeded keratinocytes were tested to see if it would be possible to reduce the required number of keratinocytes. Keratinocytes were tested at 0.5, 1 and 2×10^6 cells/scaffold for different incubation times at ALI (14, 21 and 30 days) in 5 donors, to see if this scaffold could reduce the number of cells needed and the time required to develop the model.

Incubating for 14 days at ALI culture (Figure 9 and Figure 10), H&E results from five donors showed poor distribution of the keratinocytes, with several gaps throughout the scaffold membrane. An even epidermal layer is almost non-existent at the lowest concentration of keratinocytes, 0.5×10^6 keratinocytes/scaffold in all the donors. Also, there was almost no consistent epidermal layer regardless of the concentration of keratinocytes seeded, indicating that the poor distribution of the keratinocytes was maybe due to a short ALI culture time. Overall, results showed that 14 days at ALI culture was insufficient for proper epidermal differentiation using the Alvetex Strata.

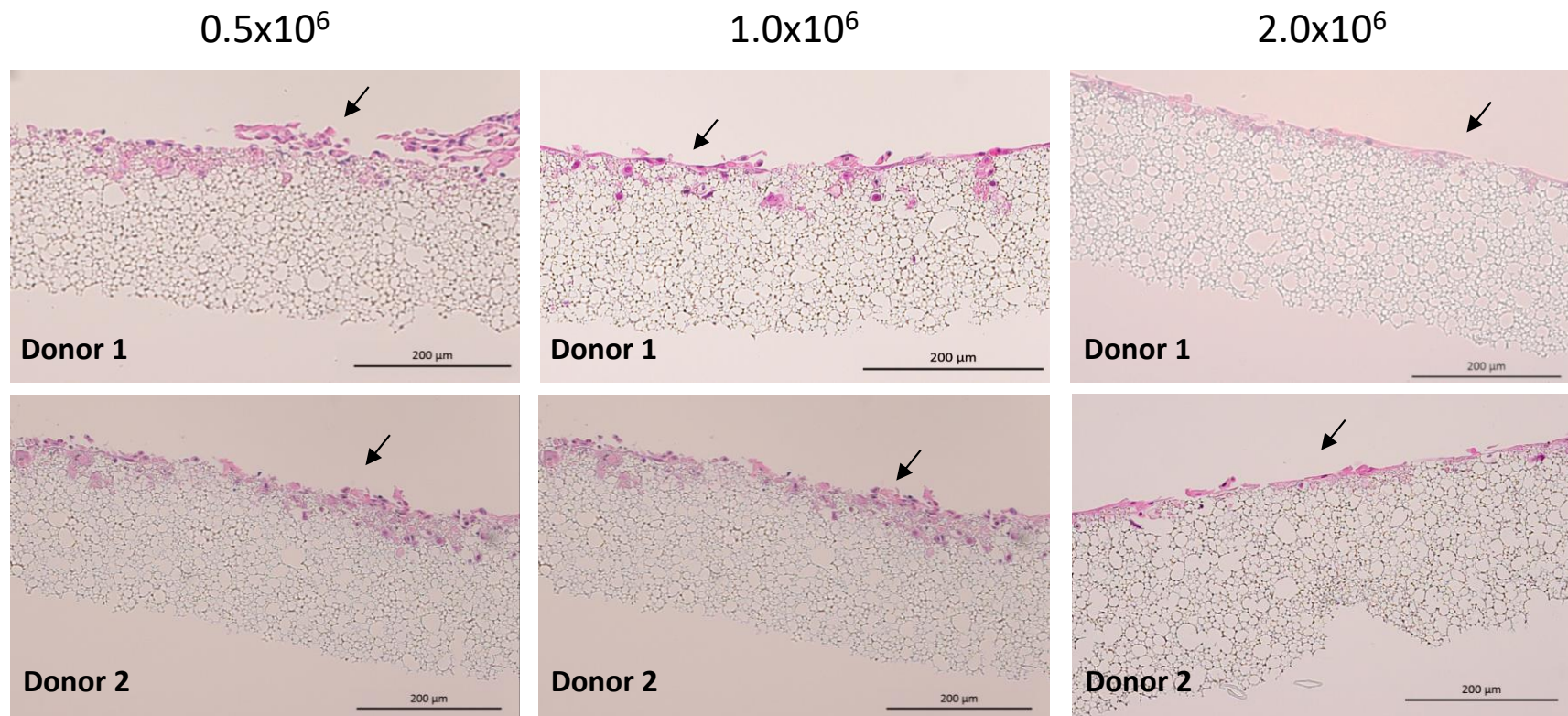


Figure 9. 3D epidermal skin culture using the Alvetex Strata for 14 days in ALI at different keratinocyte concentrations in donor 1 and 2. Experiments were performed using different keratinocyte numbers – 0.5, 1 and 2×10^6 cells/scaffold during 14 days at ALI (passage 3). Incomplete differentiation and organization of keratinocytes could be observed (black arrows). Scale bar of 200 μm is representative and similar in all testing conditions.

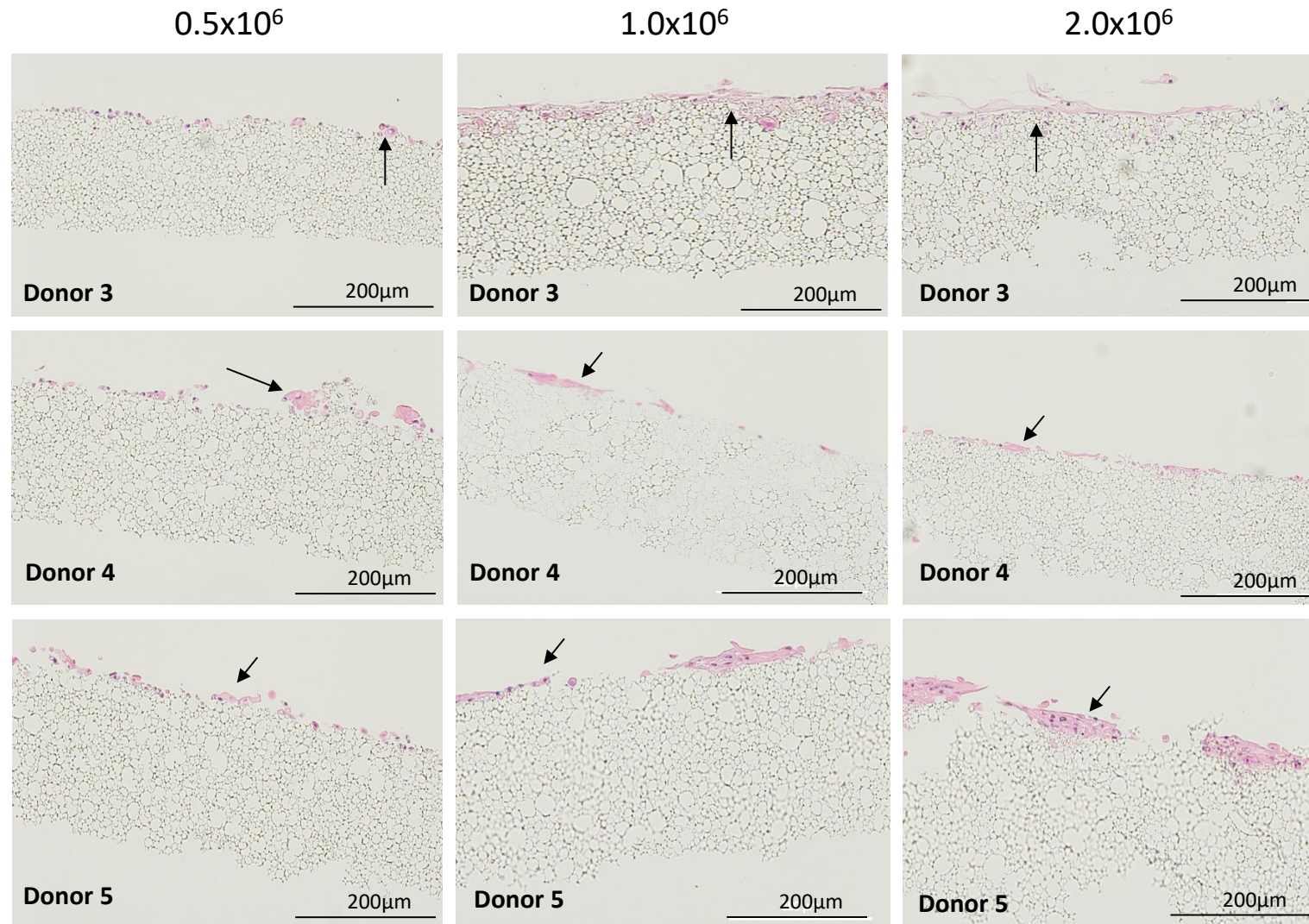


Figure 10. 3D epidermal skin culture using the Alvetex Strata for 14 days in ALI at different keratinocyte concentrations in donor 3, 4 and 5. Experiments were performed using different keratinocyte numbers – 0.5, 1 and 2x10⁶ cells/scaffold during 14 days at ALI (passage 3). Incomplete differentiation and organization of keratinocytes could be observed (black arrows). Scale bar of 200μm is representative and similar in all testing conditions.

At 21 days under ALI conditions, a more consistent epidermal layer was observed (Figure 11 and Figure 12). Seeding 0.5×10^6 cells/scaffold seemed to be insufficient, since only a thin epidermal layer was developed in all donors. Seeding at 1×10^6 and 2×10^6 keratinocytes per scaffold resulted in a better distribution of the keratinocytes across the scaffold. However, there was still some gaps present in the 3D epidermal skin models cultured with 1×10^6 keratinocytes, as visible in donors 2, 4 and 5.

In general, the 3D epidermal skin models cultured with 2×10^6 keratinocytes showed a more even epidermal layer. Moreover, the 3D epidermal skin models seem to present formation of the stratum corneum, especially visible in donor 2. Presence of gaps was only observed in the 3D epidermal skin model from donor 3.

Overall, the 3D epidermal skin models cultured at 21 days in ALI seemed to be an improvement from the 3D epidermal skin models cultured at 14 days, as it presented a more even distribution of the keratinocytes with formation of the stratum corneum in 4 donors at 2×10^6 keratinocytes/scaffold. However, 21 days was still not enough time to allow for proper epidermal differentiation in all donors.

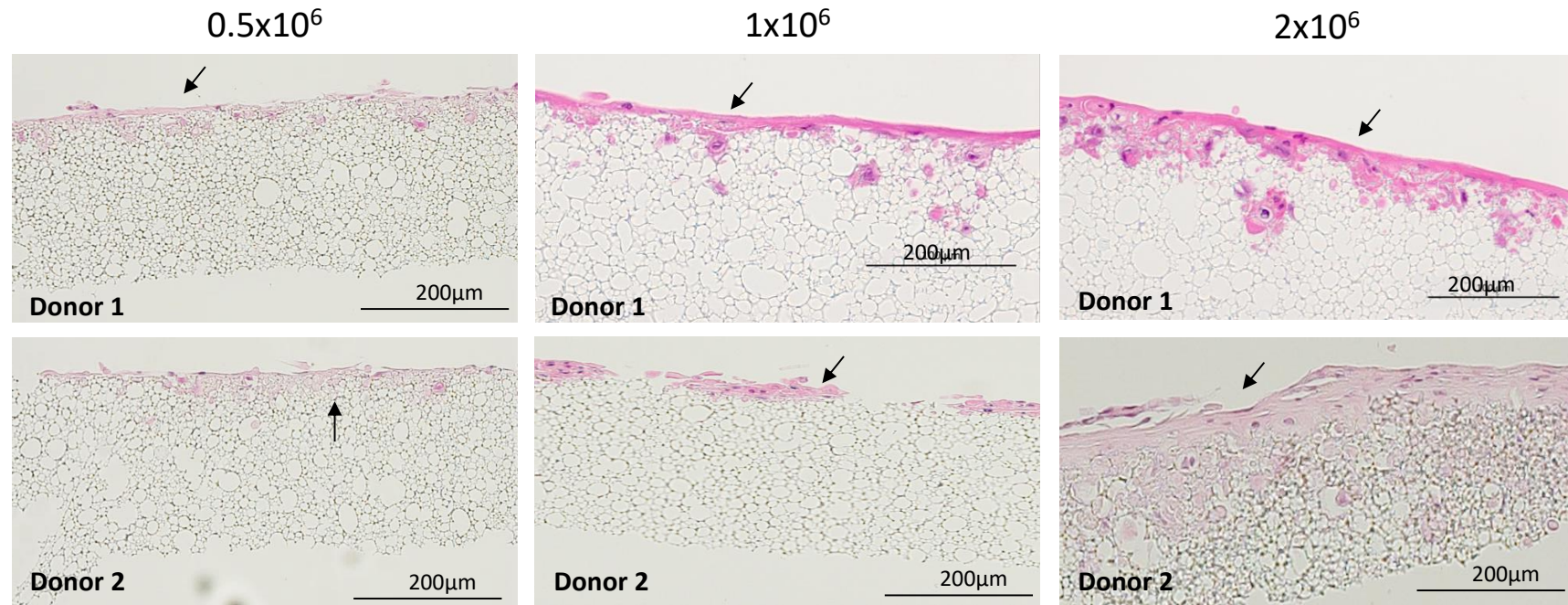


Figure 11. 3D epidermal skin culture using the Alvetex Strata for 21 days in ALI at different keratinocyte concentrations in donor 1 and 2. Experiments were performed using different keratinocyte concentrations – 0.5, 1 and 2×10^6 cells/scaffold during 21 days at ALI (passage 3). Incomplete differentiation and organization of keratinocytes could be observed (black arrows). Scale bar of 200µm is representative and similar in all testing conditions.

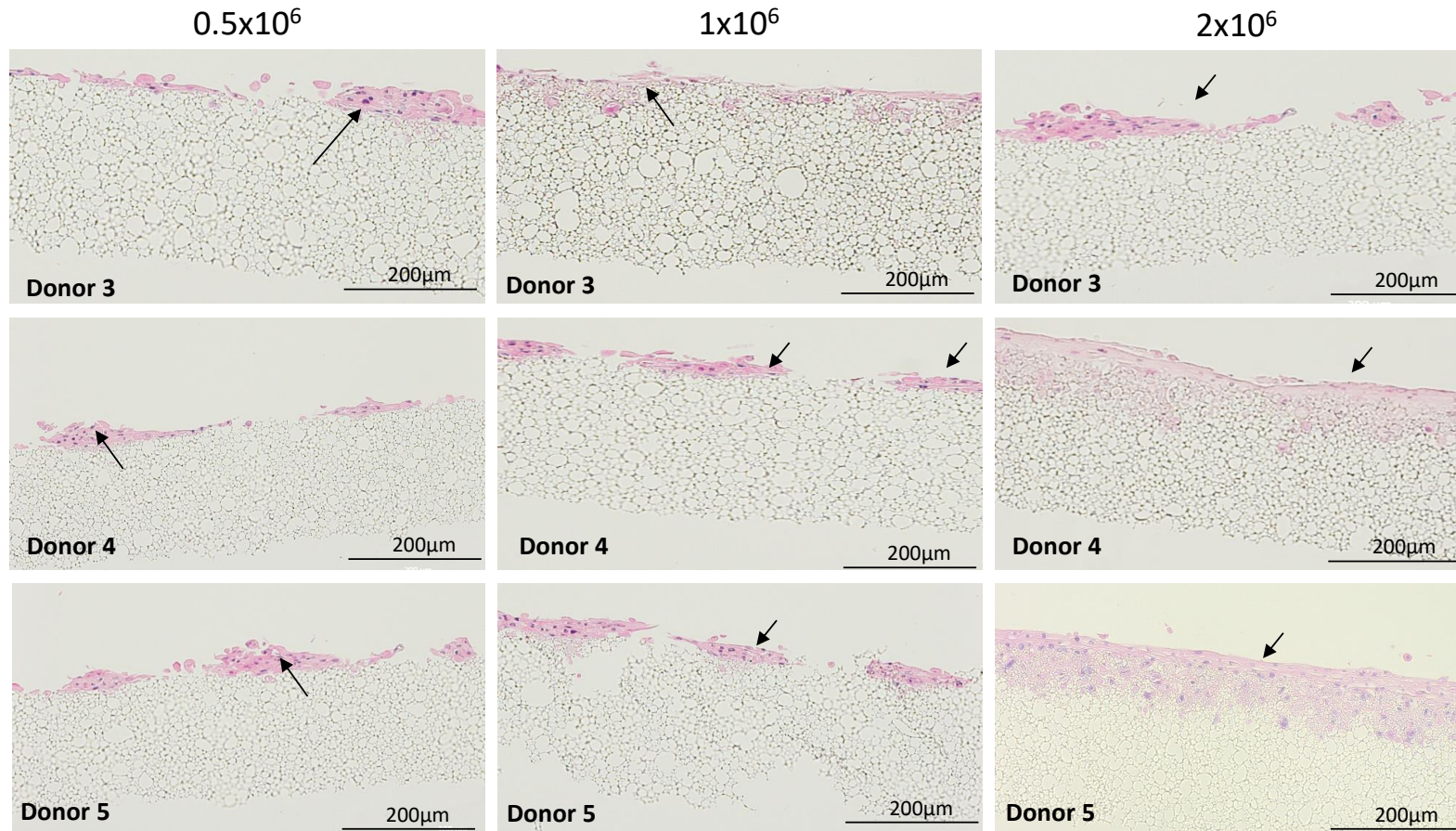


Figure 12. 3D epidermal skin culture using the Alvetex Strata for 21 days in ALI at different keratinocyte concentrations in donor 3, 4 and 5. Experiments were performed using different keratinocyte concentrations – 0.5, 1 and 2x10⁶ cells/scaffold during 21 days at ALI (passage 3). Incomplete differentiation and organization of keratinocytes could be observed (black arrows). Scale bar of 200µm is representative and similar in all testing conditions.

H&E results from 30 days under ALI conditions showed the best developed 3D epidermal skin culture (Figure 13 and Figure 14). However, seeding at 0.5×10^6 cells/scaffold still seemed to be insufficient as it showed poor distribution of the keratinocytes with several gaps in the epidermal layer. Comparing the results using 1×10^6 and 2×10^6 keratinocytes/scaffold, a more even distribution of the keratinocytes was observed, with a more complete epidermal layer on both conditions. All donors presented a well distributed epidermal layer with no gaps throughout the scaffold. Beginning of differentiation into stratum corneum was observed indicating that keratinocytes were fully organized and adherent to the scaffold. This observation together with the fact that 2×10^6 keratinocytes/scaffold required a challenging amount of tissue culture conditions to bulk the keratinocytes, 1×10^6 keratinocytes/scaffold was used in all further experiments.

As cell optimization results showed that the best conditions for development of the 3D epidermal skin models was seeding of 1×10^6 keratinocytes/scaffold, further optimization was then performed with regards to the nutrients required for keratinocyte differentiation – vitamin C and calcium.

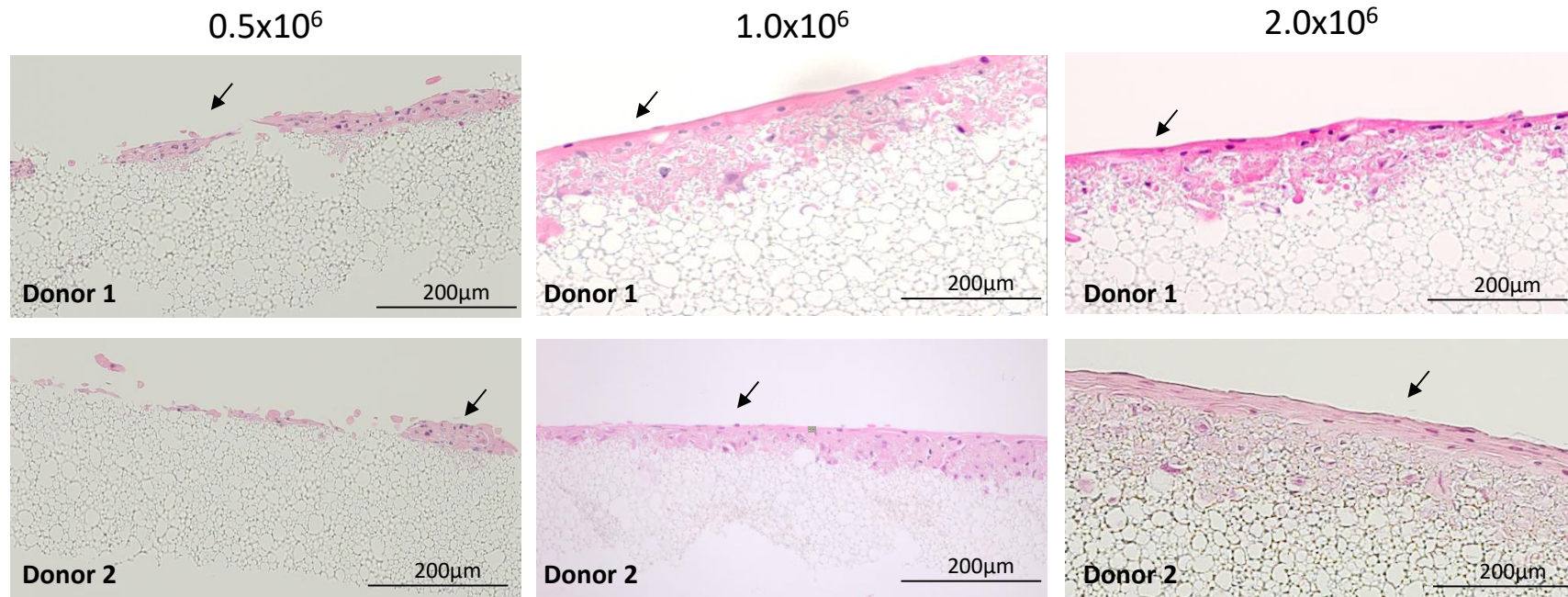


Figure 13. 3D epidermal skin culture using the Alvetex Strata for 30 days in ALI at different keratinocyte concentrations in donor 1 and 2. Experiments were performed using different keratinocyte concentrations – 0.5, 1 and 2×10^6 cells/scaffold during 30 days at ALI (passage 3). Differentiation and organization of keratinocytes could be observed (black arrows).

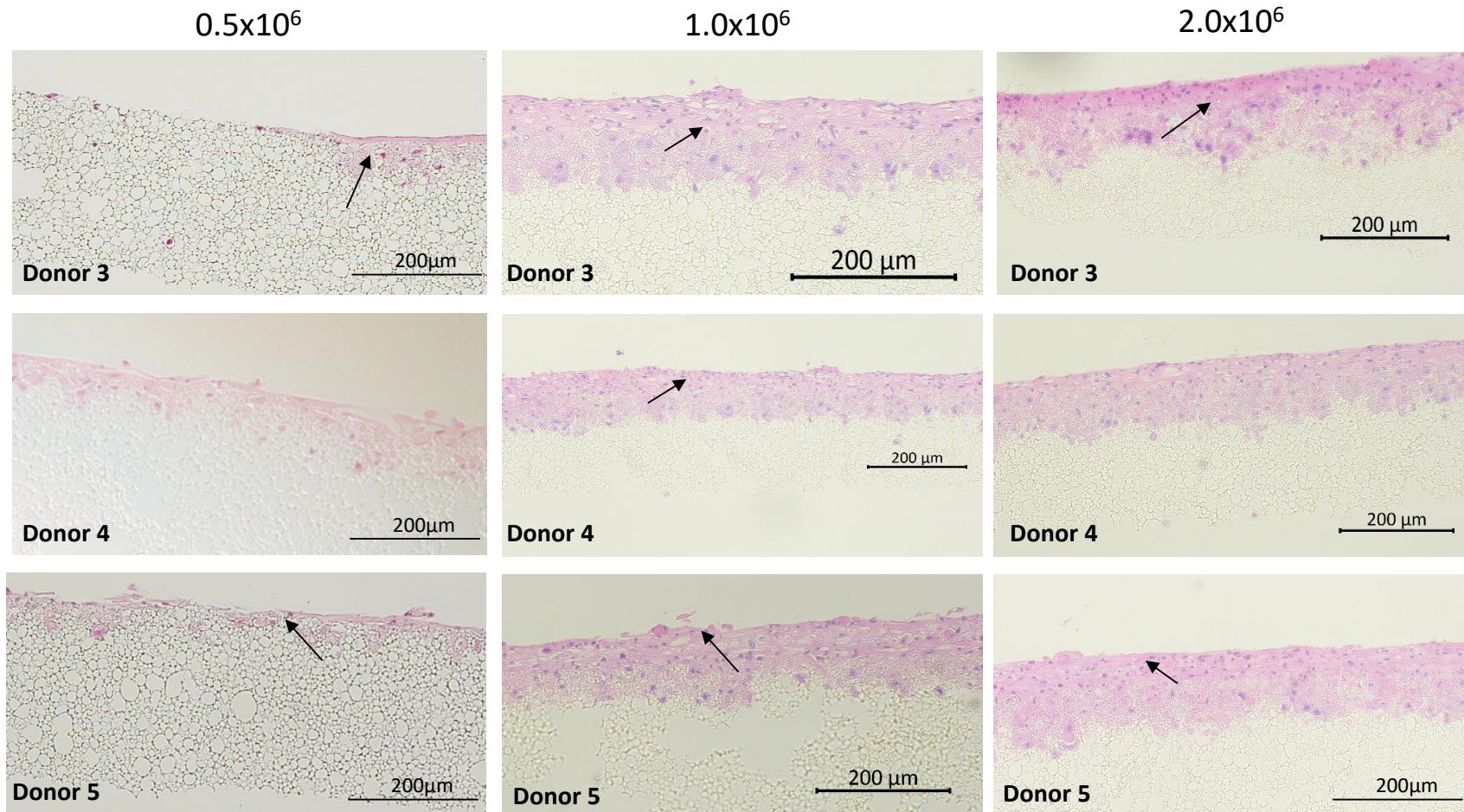


Figure 14. 3D epidermal skin culture using the Alvetex Strata for 30 days in ALI at different keratinocyte concentrations in donor 3, 4 and 5. Experiments were performed using different keratinocyte concentrations – 0.5, 1 and 2×10^6 cells/scaffold during 30 days at ALI (passage 3). Differentiation and organization of keratinocytes could be observed (black arrows). Scale bar of 200µm similar in all testing conditions.

3.2.2. Optimization of Vitamin C

Vitamin C is essential for cell differentiation and it is known to enhance the general morphology of the skin layers, by improving the differentiation of keratinocytes into stratum corneum (Pasonen-Seppanen et al., 2001) and by helping the formation of dermal-epidermal junction (Marionnet et al., 2006). Considering the previous results from the optimization of the scaffold and cell concentration, it was decided to investigate if increased vitamin C concentration during the culturing of the 3D epidermal skin cultures would improve the differentiation process of the keratinocyte, help the development of the stratum corneum and the general organization of the basal layer.

The initial concentration of vitamin C used was 1.5mM solution, defined as the optimal concentration from previous studies (Groeber et al., 2016; Mewes et al., 2016; Y Poumay et al., 2004). However, considering that nutrients optimal concentrations are always dependent on scaffold specifications, it was decided to test the optimal concentration of Vitamin C for the Alvetex Strata Scaffold. Therefore, 3 concentrations of vitamin C were tested in a keratinocyte monoculture - 1.5mM, 2mM and 3mM. Comparison of cell viability of the different concentrations of vitamin C to the baseline condition (no vitamin C) showed no significant decrease in cell viability (1.5mM= 96.46%; 2mM= 106.3%; 3mM=115.6%), especially for the higher concentration of vitamin C (3mM) indicating that the increase of vitamin C was non-toxic to the keratinocytes (Figure 15). On the contrary, increasing the concentration of vitamin C seemed to promote proliferation of cells as cell viability at 3mM is above 100%. Compared to the baseline condition, the positive control for cell death, CuSO₄, caused a statistically significant reduction of cell viability greater than 80% (viability of 11.5%).

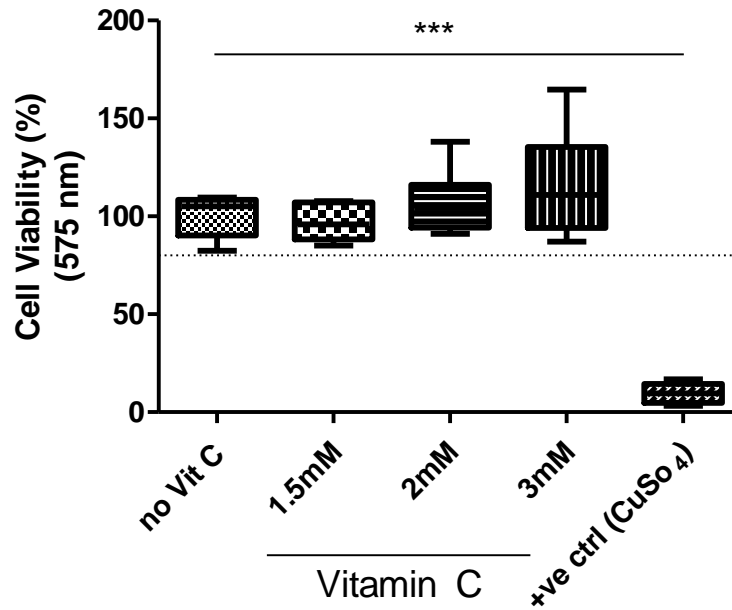


Figure 15. Viability of keratinocyte monoculture with vitamin C. Viability for different concentrations of Vitamin C (1.5, 2 and 3mM) were tested in a keratinocyte monoculture. Medium in the absence of vitamin C was used as a negative control. CuSO₄ was used to assess cell death. Results are expressed as mean and standard deviation of three independent experiments. *** p < 0.001. Dotted line represents the 80% viability threshold.

An experimental plan was designed to understand the impact of high vitamin C concentrations on the formation of skin layers (Figure 16). Considering the previous results, keratinocytes were seeded at 1×10^6 /cells/scaffold in all conditions. The variable condition of the layout was, therefore, the concentration of vitamin C which was tested at 1.5, 2 and 3mM. An extra variable was also tested, the time of ALI culture (21 *versus* 30 days in ALI), to see if increased vitamin C required a shorter ALI period. Thus, it would mean faster development of the 3D epidermal skin culture.

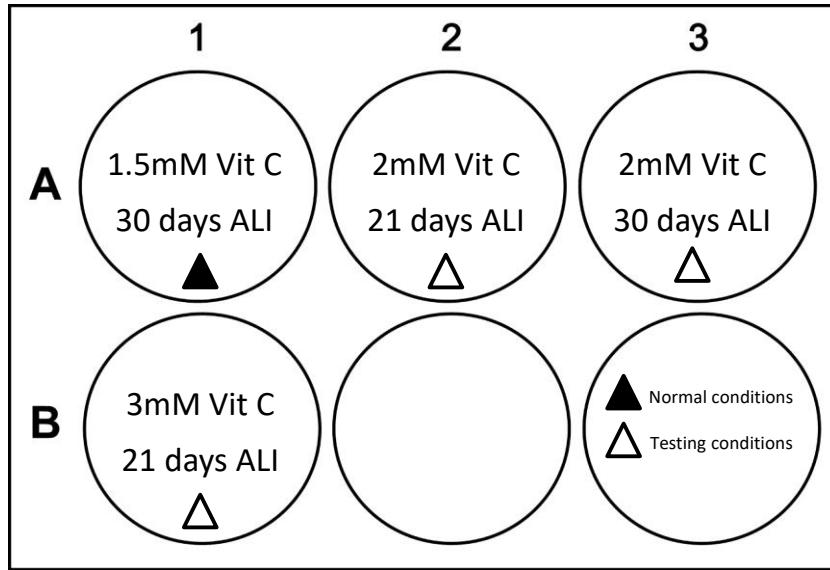


Figure 16. Experimental layout for testing high concentrations of vitamin C. Different concentrations of vitamin C (1.5, 2 and 3mM) were tested at different ALI times to assess overall keratinocyte differentiation into epidermal layers. 1.5mM vitamin C at 30 days ALI was the current established protocol (▲), while testing conditions were labelled as △.

The results from the H&E staining of the 3D epidermal skin cultures (Figure 17 and Figure 18) showed improved organization of the keratinocytes and much better developed epidermal layers than the initial models developed with the Alvetex Strata (Figure 13). Overall, the 3D epidermal skin cultures (Figure 17) showed an even distribution of the keratinocytes throughout the scaffold with no unpopulated areas, demonstrating the successful adhesion of the keratinocytes onto the scaffold. Additionally, keratinocytes seemed to only populate the top part of the scaffold, instead of migrating all the way through the scaffold, possibly indicating formation of the basal epidermal layer. Supporting this hypothesis is the presence of nuclear keratinocyte cells (deep purple) in the basal layer region across all donors but especially visible in donors 3 and 4.

However, increased concentration of vitamin C did not seem to promote improved differentiation of stratum corneum any more than the normal concentration of 1.5mM. In fact, the 3D epidermal skin culture at normal concentration (1.5mM) seemed to present a more fully developed epidermal layer than the 3D skin culture at 3mM. Formation of the epidermal layers was also confirmed by immunofluorescence staining.

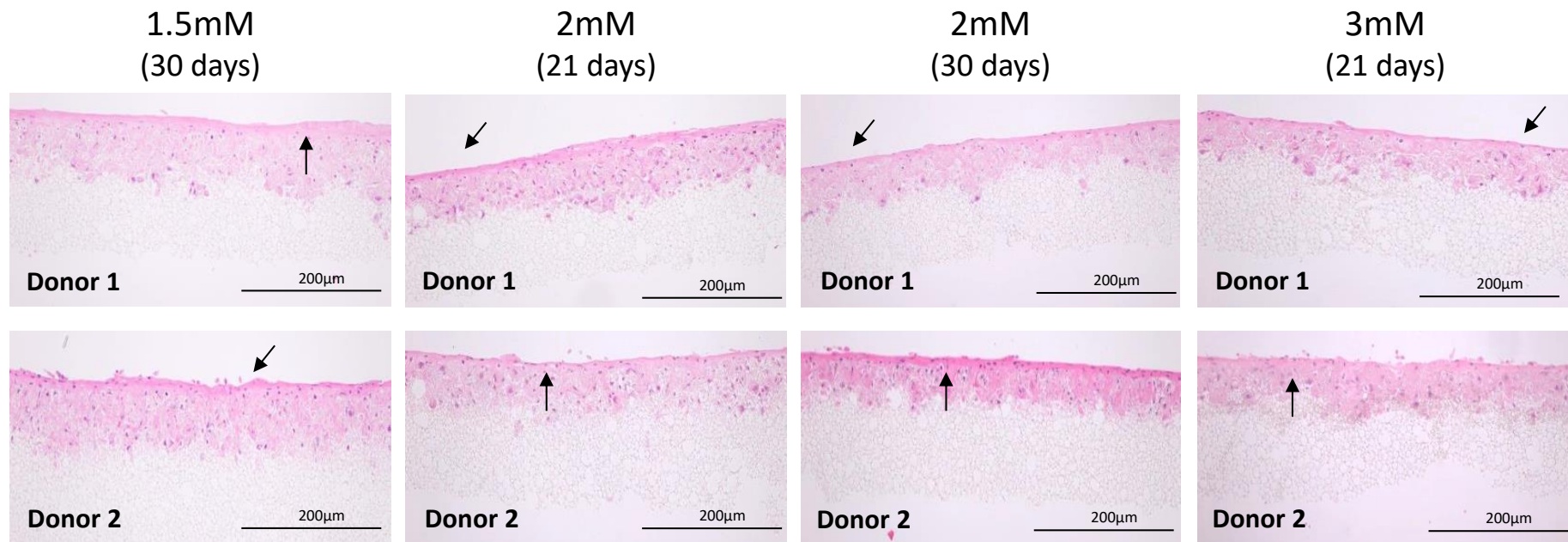


Figure 17. Vitamin C optimization in donor 1 and 2. Different concentrations of vitamin C (1.5, 2 and 3mM) were tested at different ALI times to improve overall keratinocyte differentiation into epidermal layers (black arrow). Scale bar of 200μm representative and similar in all testing conditions.

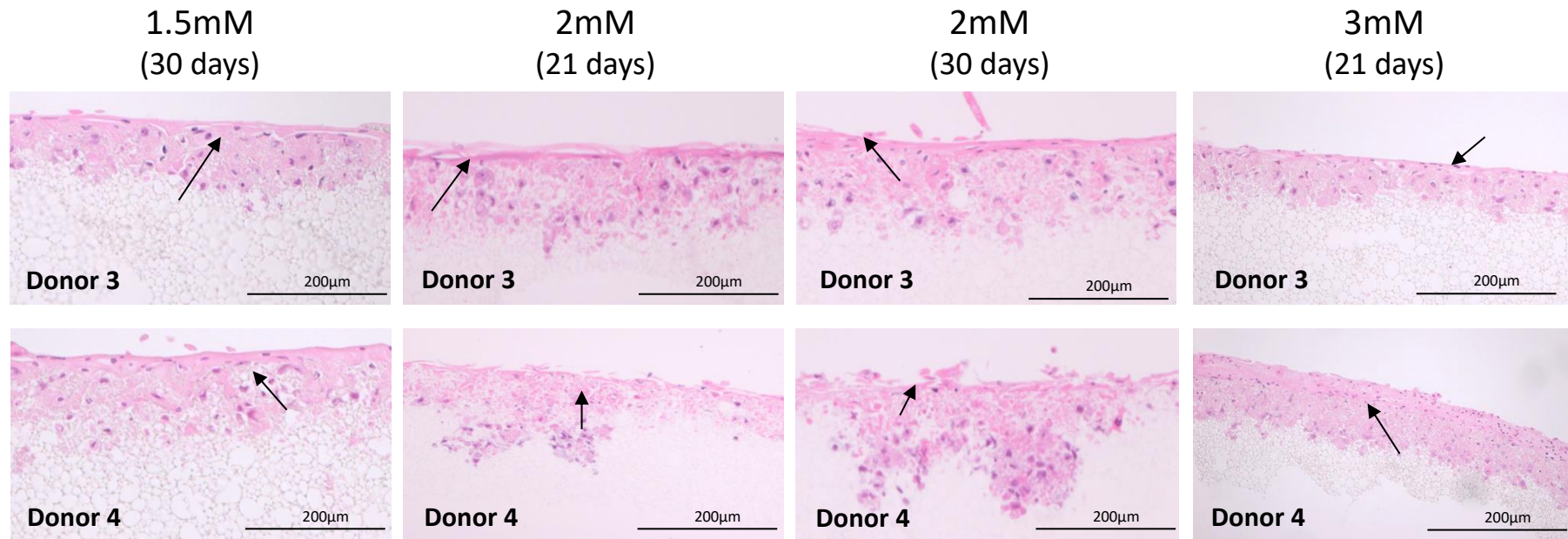


Figure 18. Vitamin C optimization in donor 3 and 4. Different concentrations of vitamin C (1.5, 2 and 3mM) were tested at different ALI times to improve overall keratinocyte differentiation into epidermal layers (black arrow). Scale bar of 200µm representative and similar in all testing conditions.

To confirm that the seeded keratinocytes were able to structurally organize themselves into the different skin layers (stratum corneum and stratum basale), two immunostaining analyses were performed in addition to the H&E staining – picro Sirius red staining for presence of collagen and immunofluorescence staining for presence of involucrin and cytokeratin 14 (skin protein markers).

Histological detection of collagen using Picro Sirius Red staining was performed for all testing concentrations of vitamin C. Positive staining for collagen is considered as a bright red colour in the stratum corneum area. Therefore, presence of collagen in the 3D skin epidermal cultures formed using the Alvetex Strata indicate formation of the stratum corneum layer. The results from the Picro Sirius Red Staining showed, in fact, positive detection of collagen in all concentrations of vitamin C (Figure 19, representative image of donor 2). Some background staining is also possible to observe within the scaffold, most likely resulting from the infiltrated keratinocytes. Nevertheless, the clear positive red staining can be found mainly in the stratum corneum layer, confirming its presence.

Further differentiation of the different skin strata was confirmed by immunofluorescence staining - stratum corneum was characterized using involucrin antibody, while presence of stratum basale was confirmed using cytokeratin 14 antibody. Immunofluorescence results for stratum corneum with involucrin (Figure 20, representative image of donor 2) showed positive staining (bright pink) for involucrin, confirming the presence of stratum corneum. Staining also confirmed a thicker stratum corneum layer at 1.5mM for 30 days (normal condition). 21 days in ALI did not appear to be long enough to form a full layer of stratum corneum, even at a higher concentration of vitamin C (i.e. 2 and 3mM at 21 days).

Regarding formation of the stratum basale, positive staining for cytokeratin 14 (bright green) could also be observed (Figure 21, representative image of donor 2). This confirmed the presence of an organized stratum basale layer that could not be clearly defined in the H&E pictures (Figure 17).

Overall, these immunostaining analyses have helped confirm the presence of stratum corneum and stratum basale layers in 3D the skin epidermal cultures formed using the Alvetex Strata. Moreover, they have shown that optimal concentration of vitamin C would be of 1.5mM, since this concentration allowed for formation of the stratum corneum (positive staining for involucrin) with secretion of collagen (positive staining for collagen) and formation of stratum basale (positive staining for cytokeratin 14).

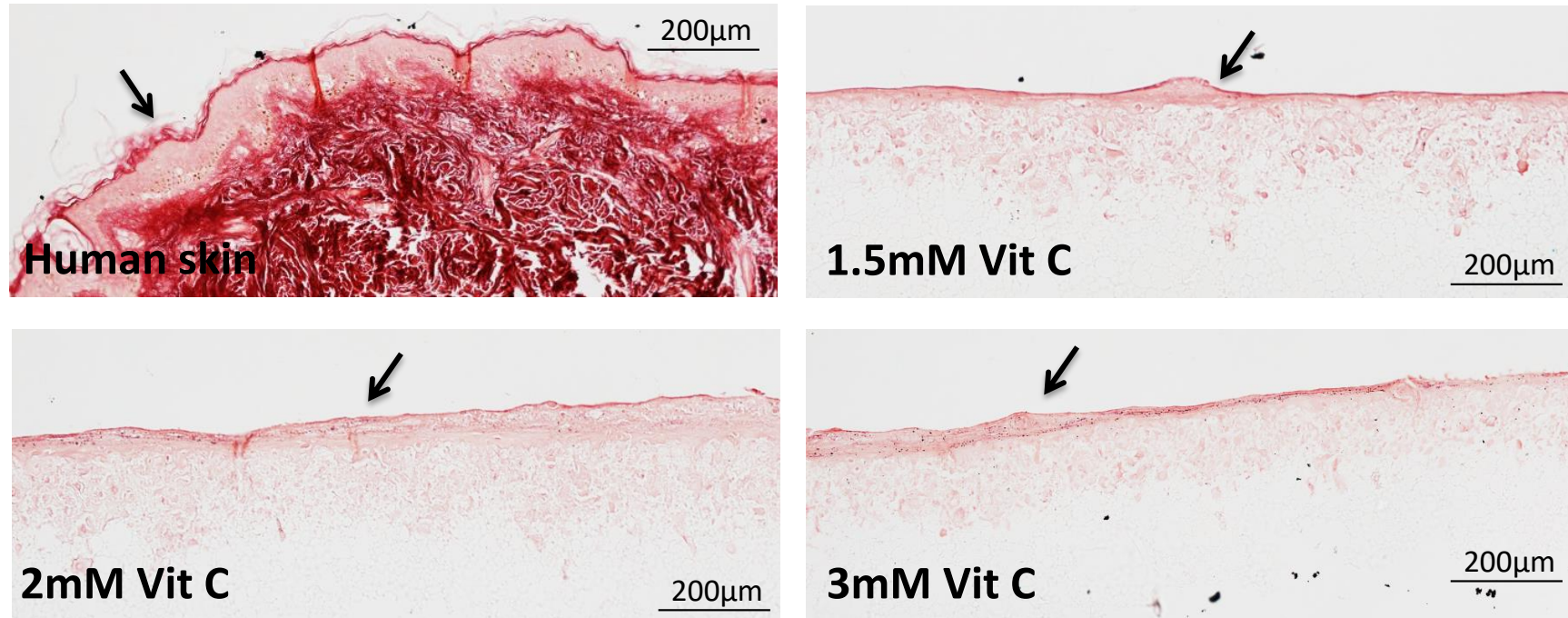


Figure 19. Histological detection of collagen in the 3D skin epidermal models formed using the Alvetex Strata. Histological detection of collagen was performed using Picro Sirius Red staining for all testing concentrations of vitamin C. Human skin was used as a positive control for presence of collagen - bright red colour in the stratum corneum region (indicated by the black arrow). Scale bar of 200µm is representative and similar in all testing conditions.

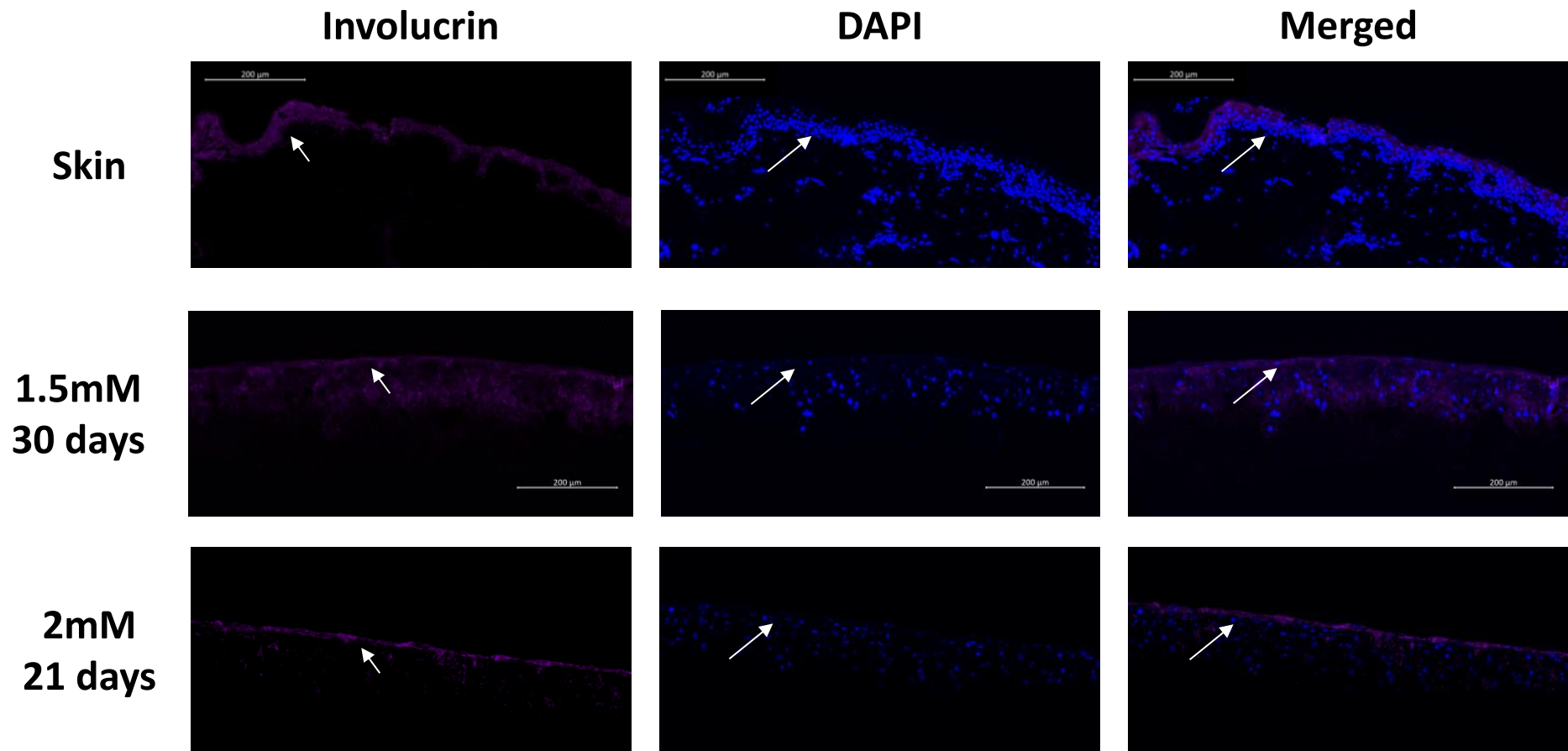


Figure 20. Immunofluorescence staining of involucrin for vitamin C optimization. Positive staining for involucrin (protein marker for epidermal differentiation of stratum corneum) was observed (bright pink) in the different concentrations of vitamin C (1.5, 2 and 3mM) (indicated by the white arrow). Human skin was used as positive control for staining of involucrin. Individual DAPI staining and merged staining (involucrin and DAPI) showed co-localization of epidermal cells. Scale bar of 200μm is representative and similar in all testing conditions.

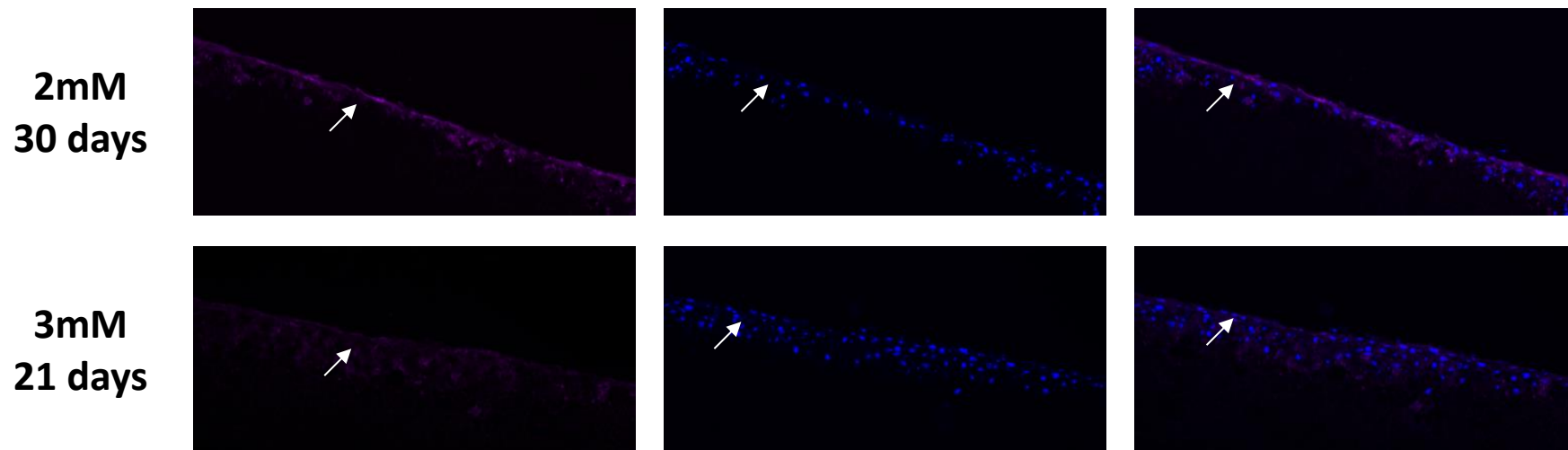


Figure 20 (continuation). Immunofluorescence staining of involucrin for vitamin C optimization. Positive staining for involucrin (protein marker for epidermal differentiation of stratum corneum) was observed (bright pink) in the different concentrations of vitamin C (1.5, 2 and 3mM) (indicated by the white arrow). Individual DAPI staining and merged staining (involucrin and DAPI) showed co-localization of epidermal cells. Scale bar of 200 μ m is representative and similar in all testing conditions.

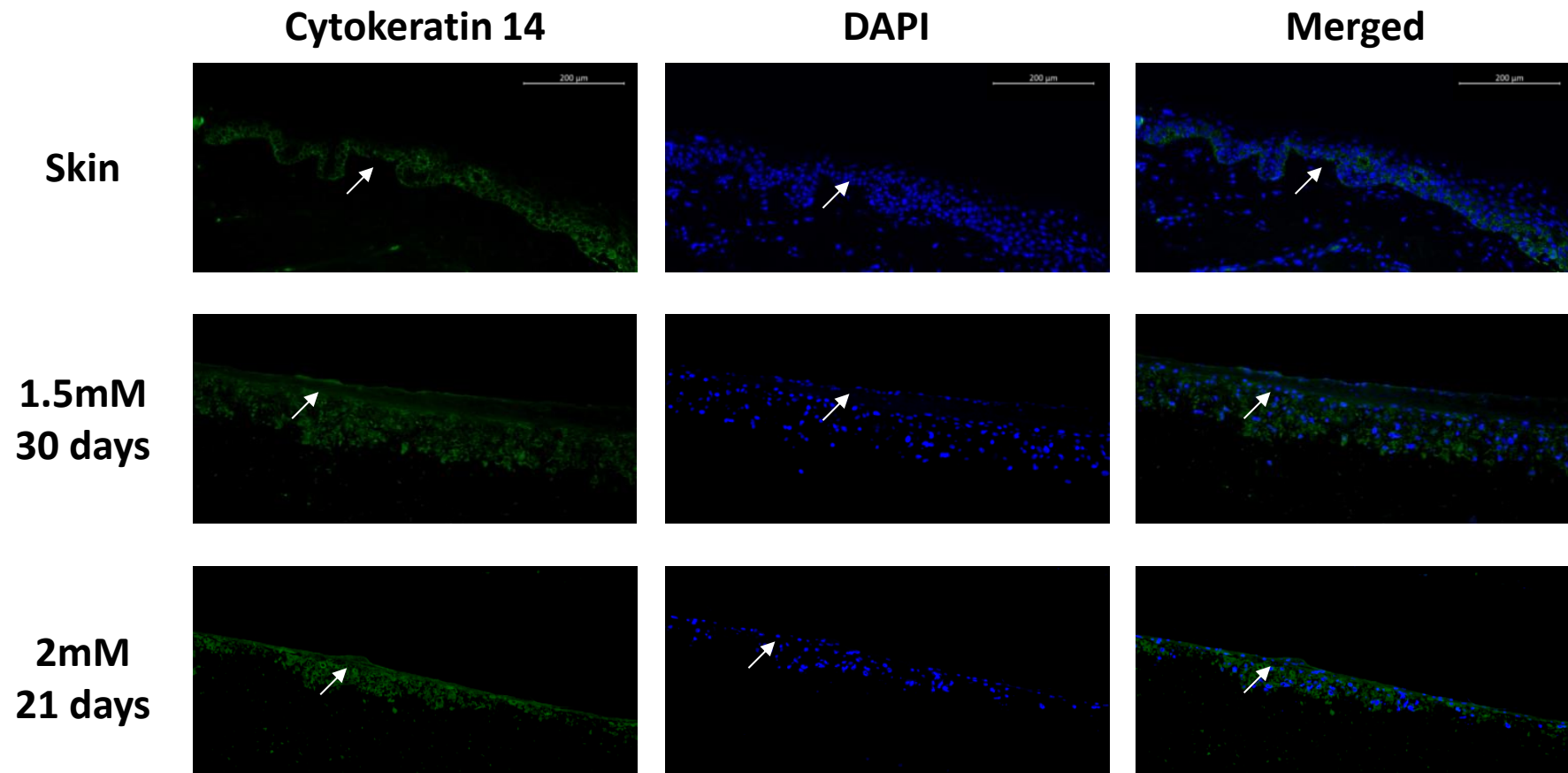
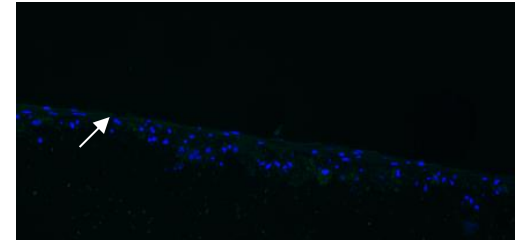
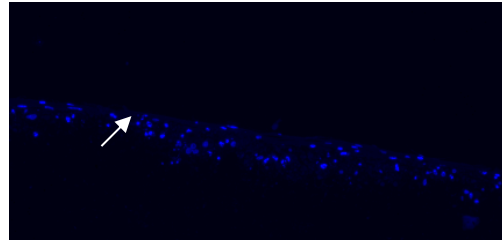
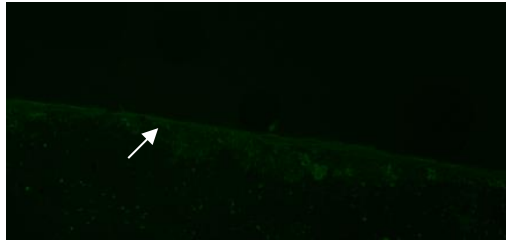


Figure 21. Immunofluorescence staining of Cytokeratin 14 for vitamin C optimization. Positive staining for cytokeratin 14 (protein marker for epidermal differentiation of stratum basale) was observed (bright green) in the different concentrations of vitamin C (1.5, 2 and 3mM) (indicated by the white arrow). Human skin was used as positive control for staining of involucrin. Individual DAPI staining and merged staining (cytokeratin 14 and DAPI) showed co-localization of epidermal cells. Scale bar of 200μm is representative and similar in all testing conditions.

**2mM
30 days**



**3mM
21 days**

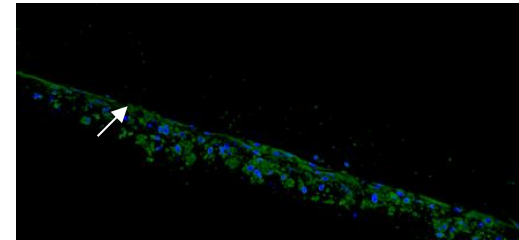
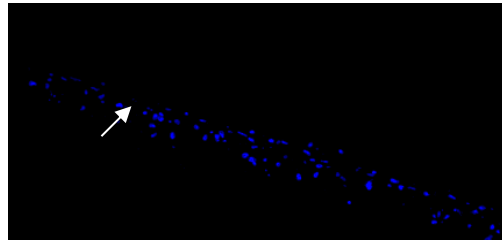
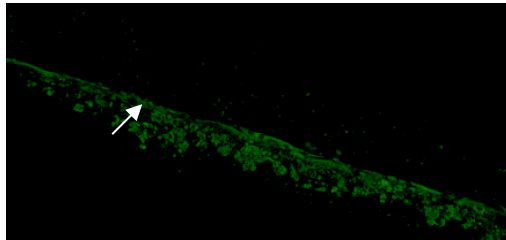


Figure 21 (continuation). Immunofluorescence staining of Cytokeratin 14 for vitamin C optimization. Positive staining for cytokeratin 14 (protein marker for epidermal differentiation of stratum basale) was observed (bright green) in the different concentrations of vitamin C (1.5, 2 and 3mM) (indicated by the white arrow). Individual DAPI staining and merged staining (cytokeratin 14 and DAPI) showed co-localization of epidermal cells. Scale bar of 200 μ m is representative and similar in all testing conditions.

Overall, the results from the vitamin C optimization study showed that although increased concentrations of vitamin C (2 and 3mM) helped with better distribution of the keratinocytes across the scaffold top, it did not seem to improve development of the epidermal layers better than what was observed under normal conditions (1.5mM). Stratum corneum differentiation seemed, in fact, to be better at 1.5mM as higher concentrations of vitamin C only seemed to promote general proliferation of cells in a unorganized manner.

In regard to culturing the 3D epidermal skin cultures at 21 or 30 days in ALI, the epidermal constructs left for 30 days in ALI appeared to present thicker layers of stratum corneum. The extra 10 days from the 21 days test conditions appeared to have allowed keratinocytes to evenly populate the scaffold and not present gaps in between keratinocytes throughout the scaffold. Also, it appears that these extra 10 days allowed keratinocytes to better differentiate into the stratum corneum and stratum basale layers.

Parallel to the optimization of vitamin C, optimization of calcium was also performed.

3.2.3. Optimization of CaCl_2

Optimal calcium concentration for 3D skin cultures has been reported between 1mM (Hennings et al., 1980), 1.5mM (Mewes et al., 2016; Pedrosa et al., 2017) and 2mM (Manaves et al., 2004). In fact, high concentrations of calcium (between 1.5 to 2mM) are believed to promote terminal differentiation of cultured keratinocytes than low calcium concentrations (less than 1mM) as it inhibits expression of integrin, transmembrane receptors responsible for cell adhesion. High calcium concentrations will downplay integrin binding, ensuring differentiating keratinocytes will migrate from the basal layer to upper epidermal layers (Hennings et al., 1980; Hodivala & Watt, 1994; Pillai, Bikle, Mancianti, Cline, & Hincenbergs, 1990).

As stated before, optimal nutrient concentration is always dependent on scaffold and cell seeding specifications. Considering that the Alvetex Strata has a membrane area twice as big as the scaffolds used in other experiments and that it requires a cell seeding density of 1×10^6 keratinocytes/scaffold, it was decided to test 1.5mM of calcium as an initial standard concentration. Higher calcium concentrations were also tested, at 2 and 3mM, to understand if a high calcium microenvironment would improve development of the 3D epidermal skin culture.

Preliminary viability assay determined that the highest concentration of calcium (3mM) was cytotoxic as it presented a cell viability of 73.47%, that is below the 80% viability threshold (Figure 22) and was therefore excluded from the optimization. The 2mM concentration showed a small reduction of cell viability compared to the normal 1.5mM concentration (1.5mM= 107.2%; 2mM= 82.24%) but because it was not statistically significant, it was not excluded from the optimization experiment. As expected, the positive control for cell death, CuSO_4 , caused a statistically significant reduction of 80% cell viability.

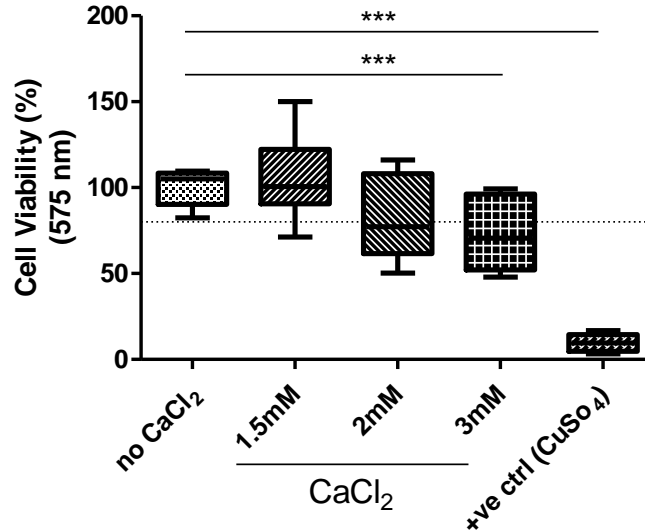


Figure 22. Viability for different concentrations of CaCl₂ (calcium - 1.5, 2 and 3mM) was tested on a keratinocyte monoculture. Medium in the absence of calcium was used as a negative control. CuSO₄ was used to assess cell death. Results are expressed as mean and standard deviation of three independent experiments. *** p < 0.001. Dotted line represents the 80% viability threshold

As performed for Vitamin C optimization, the time of ALI culture for the higher concentration of calcium was also tested. Once again, it was important to understand if a higher concentration of calcium at a shorter ALI period would result in a faster development of the 3D epidermal skin culture. Therefore, the high concentration of 2mM calcium was tested at both 21 and 30 days at ALI culture time in five donors.

H&E results comparing the different concentration of calcium and time of ALI showed that 2mM (high calcium) condition did not improve the overall organization of the epidermal layer than the standard 1.5mM calcium concentration (Figure 23 and Figure 24). Looking with more detail at the 3D skin culture with 2mM of calcium for 21 days, it is possible to see a general disorganization of the keratinocytes, with visible gaps throughout the scaffold. No proper formation of stratum corneum could be observed and this was confirmed by the involucrin immunofluorescence staining (Figure 26). Compared to the standard concentration of 1.5mM, the 3D skin cultures at 2mM for 30 days did not showed further improvement of the stratum corneum.

As mentioned before in section 3.2.2, H&E staining was complemented with two immunostaining analyses – picro Sirius red staining for presence of collagen and immunofluorescence staining for presence of involucrin and cytokeratin 14 (protein markers).

Histological detection of collagen showed positive staining in the stratum corneum layer, once again indicating proper formation of this layer in the 3D epidermal skin cultures formed

using the Alvetex Strata (Figure 25, representative image of donor 3). Some background staining is also possible to observe within the scaffold, especially for the 2mM and 3mM conditions. This is most likely resulting from the infiltrated keratinocytes. Nevertheless, the clear positive red staining can be found mainly in the stratum corneum layer, confirming its presence.

Development of the epidermal layers was also confirmed by immunofluorescence staining of involucrin (Figure 26, representative image of donor 3) and cytokeratin 14 (Figure 27, representative image of donor 3). However, it seems that the positive staining of the stratum corneum and stratum basale layers is not as pronounced as previously seen for the vitamin C optimization. Additionally, there is a lot of background staining within the scaffold region in all calcium concentrations for both involucrin and cytokeratin 14 staining. This could be due to unspecific binding of the antibodies to the scaffold mesh or the difficulty to wash them off due to the scaffold pore size.

The information collected from all these immunostaining analyses has helped confirm that 1.5mM of calcium provides the best conditions for formation of stratum corneum and stratum basale in the 3D skin epidermal cultures formed using the Alvetex Strata.

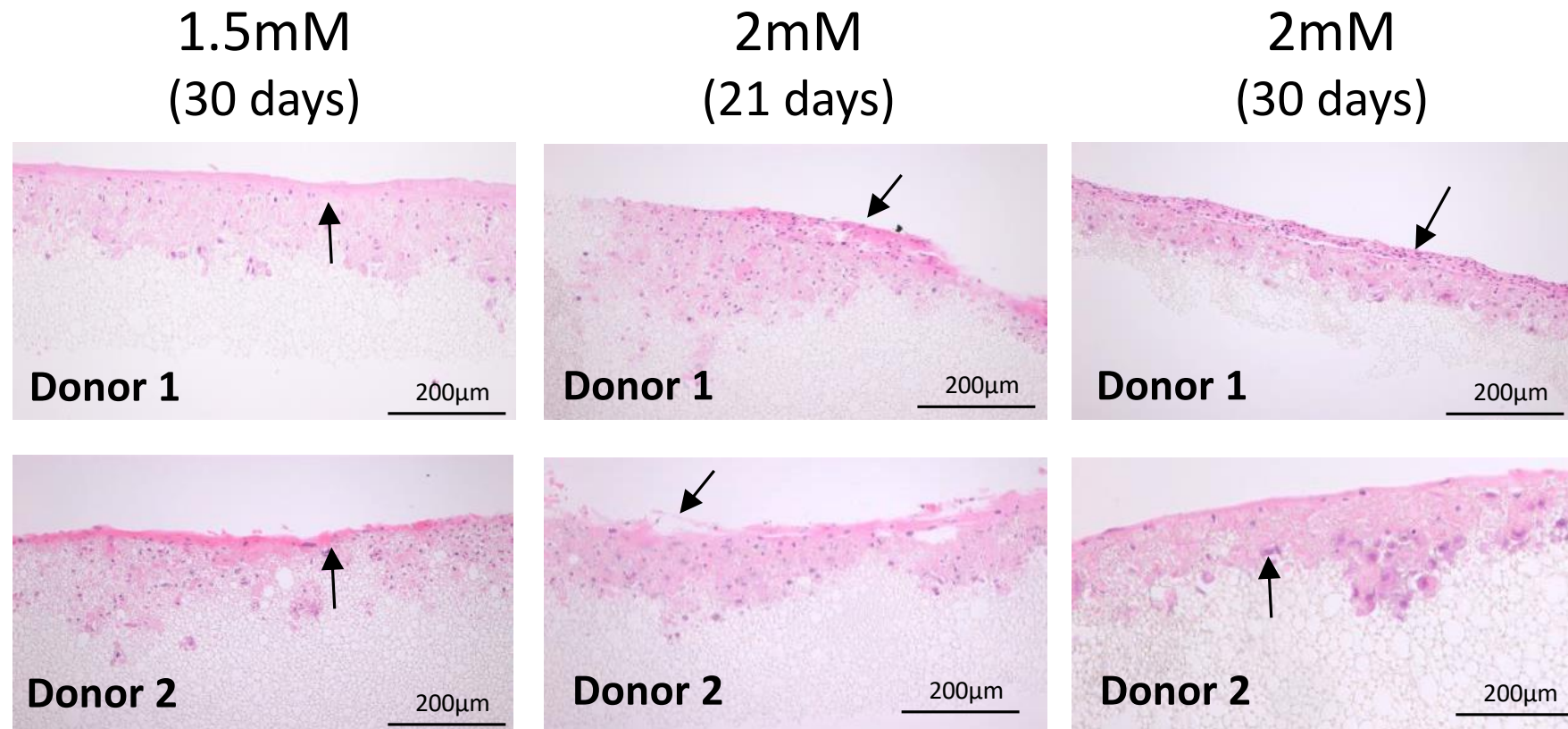


Figure 23. Calcium optimization for donor 1 and 2. A standard (1.5mM) and high (2mM) concentration of calcium were tested at different ALI times (21 and 30 days) using the Alvetex Strata to improve overall keratinocyte differentiation into epidermal layers (black arrows). Scale bar of 200μm representative and similar in all testing conditions.

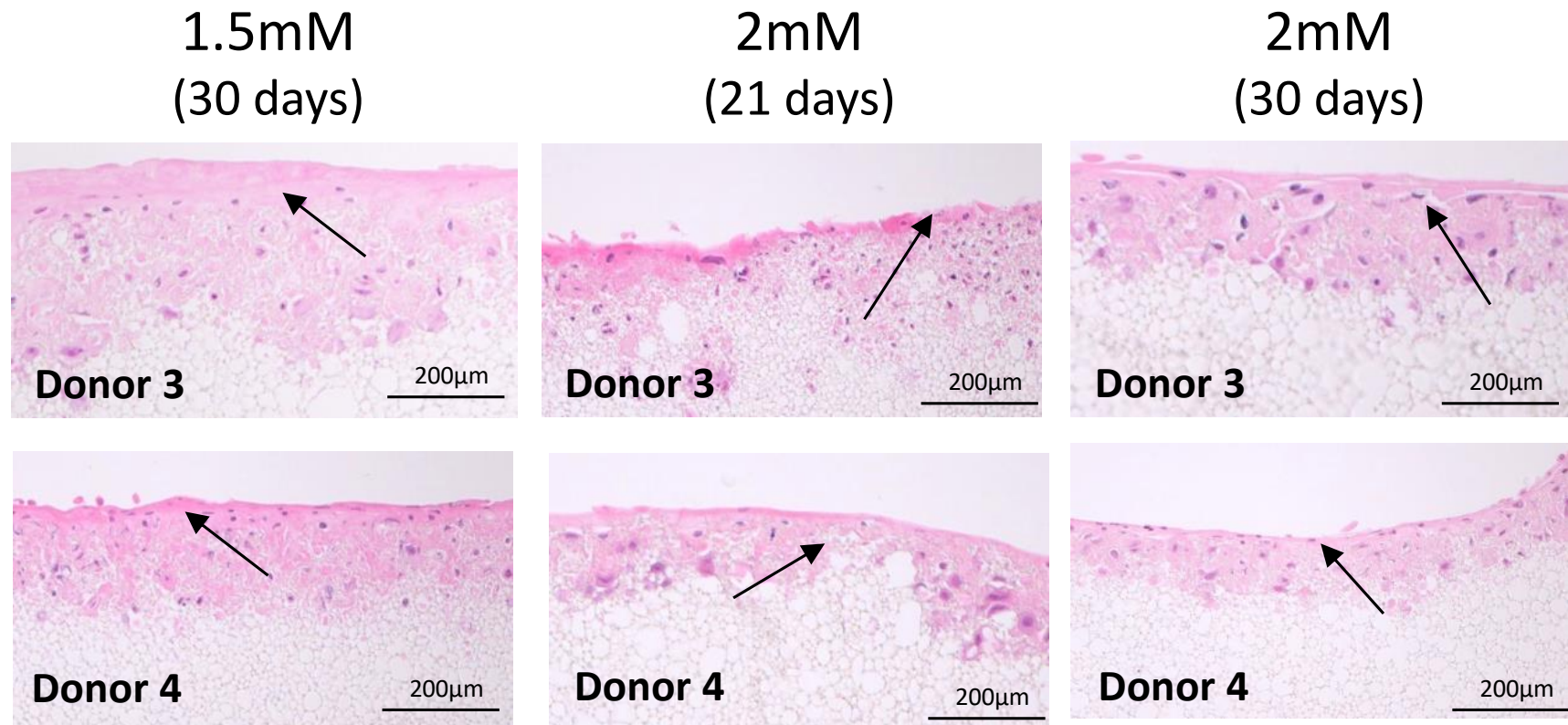


Figure 24. Calcium optimization for donor 3 and 4. A standard (1.5mM) and high (2mM) concentration of calcium were tested at different ALI times (21 and 30 days) using the Alvetex Strata to improve overall keratinocyte differentiation into epidermal layers (black arrows). Scale bar of 200μm representative and similar in all testing conditions.

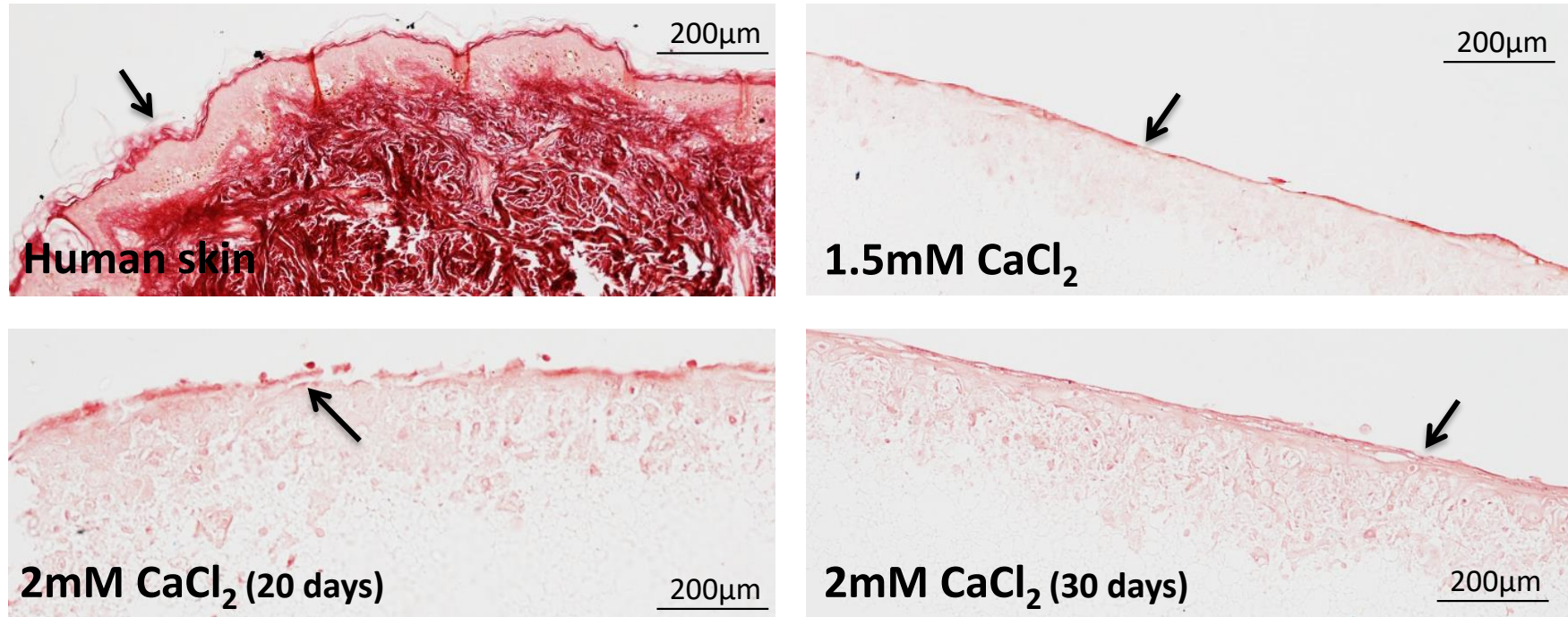


Figure 25. Histological detection of collagen in the 3D skin epidermal models formed using the Alvetex Strata. Histological detection of collagen was performed using Picro Sirius Red staining for all testing concentrations of Calcium (CaCl_2). Human skin was used as a positive control for presence of collagen - bright red colour in the stratum corneum region (indicated by the black arrow). Scale bar of 200µm representative and similar in all testing conditions.

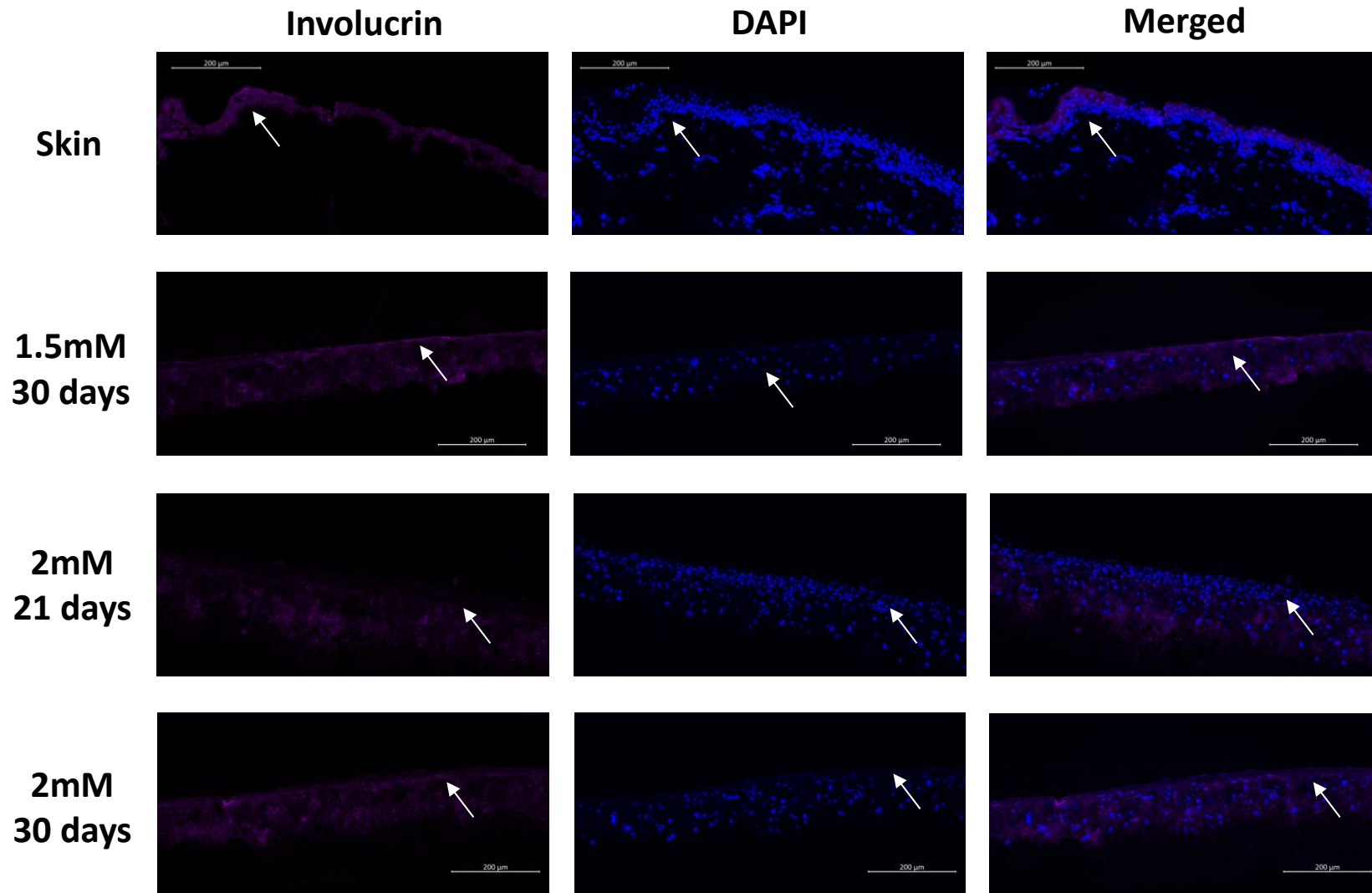


Figure 26. Immunofluorescence staining of involucrin for calcium optimization. Positive staining for involucrin (protein marker for epidermal differentiation of stratum corneum) was observed (bright pink) at the different concentrations of calcium (1.5 and 2mM) for 21 and 30 days at ALI culture (indicated by the white arrow). Human skin was used as positive control for staining of involucrin. Individual DAPI staining and merged staining (involucrin and DAPI) showed co-localization of epidermal cells. Scale bar of 200μm is representative and similar in all conditions.

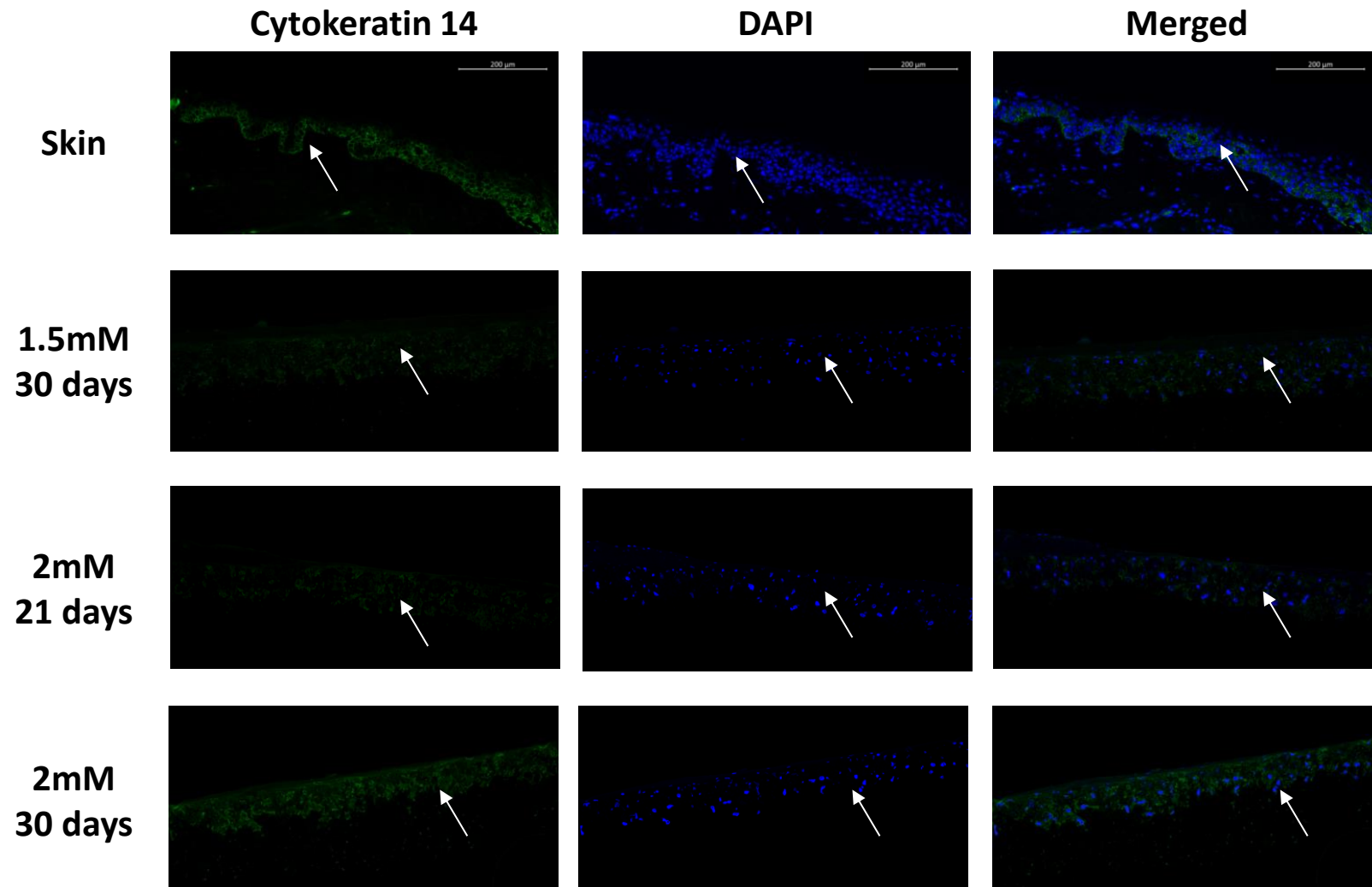


Figure 27. Immunofluorescence staining of cytokeratin 14 for calcium optimization. Positive staining for cytokeratin 14 (protein marker for epidermal differentiation of stratum basale) was observed (bright green) at the different concentrations of calcium (1.5 and 2mM) for 21 and 30 days at ALI culture (indicated by the white arrow). Human skin was used as positive control for staining of involucrin. Individual DAPI staining and merged staining (cytokeratin 14 and DAPI) showed co-localization of epidermal cells. Scale bar of 200μm is representative and similar in all conditions.

As mentioned above, increased concentrations of calcium did not seem to improve the development of the epidermal layers any further than the normal concentration of 1.5mM. 21 days of ALI was, again, not sufficient to allow a consistent distribution of the keratinocytes throughout the scaffold. The results indicate no reduction of ALI time would be possible as 30 days at ALI was the optimal time frame. Considering that results from the 2mM concentration showed a (non-significant) cell viability reduction and no improvement in differentiation of the epidermal layers, it was decided to continue with the normal 1.5mM concentration of calcium for the development of the 3D epidermal skin cultures.

Ultimately, results showed that optimized conditions for development of 3D epidermal skin cultures using the Alvetex Strata were 1×10^6 keratinocytes per scaffold, cultured for 30 days in ALI with culture medium enriched with 1.5mM vitamin C and 1.5mM calcium.

3.2.4. Optimization of collagen coated scaffold

A comparative analysis with a different scaffold was performed to evaluate performance of the Alvetex Strata. The scaffold chosen was the Corning® Transwell®-COL collagen coated (rat tail purified collagen) scaffold as this scaffold is currently used in many protocols for development of 3D skin models. Protocol for adhesion of cells was similar to the Alvetex scaffold, but the collagen-coated scaffold was tested for 14, 19 and 21 days following guidelines in the literature (Jung et al., 2014; Pedrosa et al., 2017; Y Poumay et al., 2004). Keratinocyte culture medium was enriched with 1.5mM vitamin C and calcium, defined as optimal conditions from the results of sections 3.2.2 and 3.2.3.

Results from the H&E staining of 3 donors showed good formation of stratum corneum, with typical “wave shape” stratification of dead keratinocytes (Figure 28). However, it was also possible to observe the stratum corneum formed was very thin, especially for the 3D skin models formed at 14 and 19 days and almost no basal keratinocytes are present. From the three timepoints, 21 days seemed to present a more consistent stratum corneum, considering donor 2 as the best sample.

Histological detection of collagen was also performed to confirm formation of the stratum corneum (Figure 29, representative image of donor 2). When compared to human skin and to the commercially bought epidermal model, EpiDerm™ from MatTek, the 3D skin models formed using the Corning® Transwell®-COL collagen coated scaffold did not show a strong positive collagen staining throughout the entire stratum corneum layer. Nevertheless, collagen staining was visible in the stratum corneum (as red staining), suggesting proper organization of the seeded keratinocytes into a stratum corneum layer.

Further characterization of the stratum corneum by immunofluorescence staining showed positive staining for involucrin, the protein marker for detection of stratum corneum (Figure 30, representative image of donor 2). Confirming the H&E results, involucrin staining was stronger at 21 days, suggesting that this timepoint would allow for a better developed stratum corneum layer.

Overall, the 3D epidermal skin models formed showed even distribution of the keratinocytes and no migration into the scaffold (as opposed to the models using the Alvetex Strata). Considering all results from the H&E, Picro Red Sirius and immunofluorescence stainings, the 3D epidermal skin models formed for 21 days at ALI seemed to present the best formation of the stratum corneum. Therefore, 21 days at ALI results indicate that this

incubation time provides better epidermal development when using the Corning® Transwell®-COL collagen coated scaffold.

CORNING

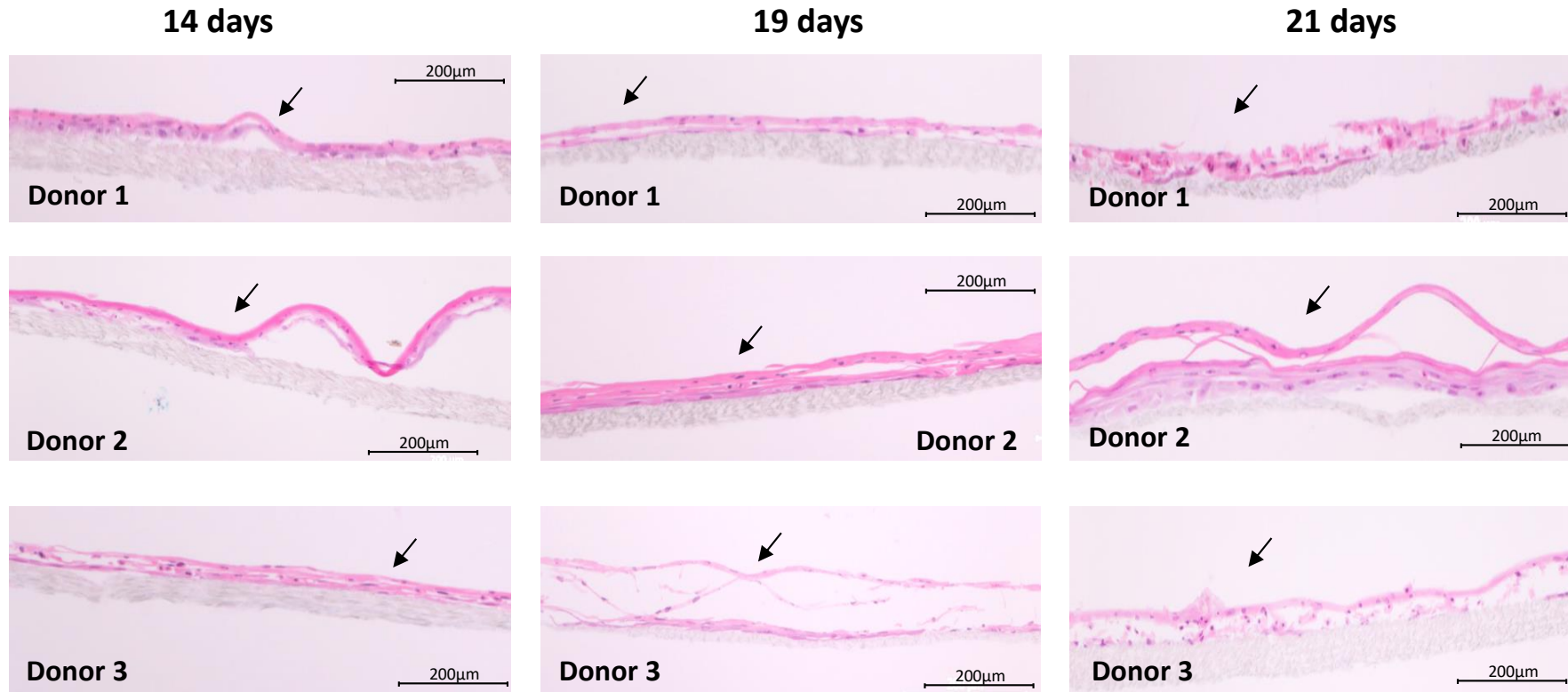


Figure 28. Development of a 3D epidermal skin model using the Corning® Transwell®-COL collagen coated scaffold. Different times of ALI were tested with this animal-based collagen coated scaffold – 14, 19 and 21 days. Organization of keratinocytes into an epidermal layer can be observed (black arrows). Scale bar of 200µm is similar in all testing conditions.

CORNING

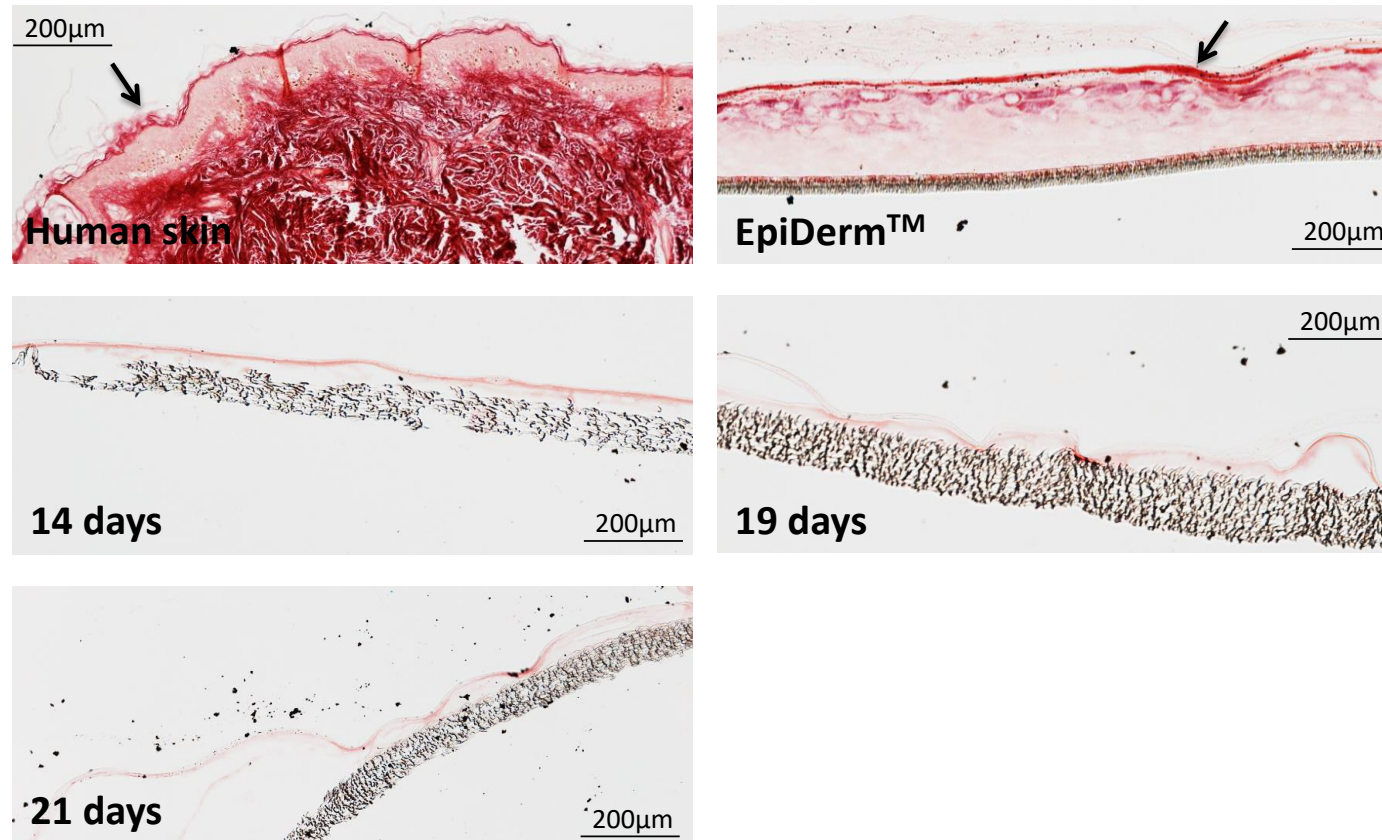


Figure 29. Histological detection of collagen in the 3D epidermal skin models formed using the Corning® Transwell®-COL collagen coated scaffold. Histological detection of collagen was performed using Picro Sirius Red staining for all ALI culture timepoints – 14, 19 and 21 days. Human skin and EpiDerm™ (commercially bough epidermal model from MatTek) were used as a positive control for presence of collagen - bright red colour in the stratum corneum region (indicated by the black arrow). Scale bar of 200µm is similar in all testing conditions.

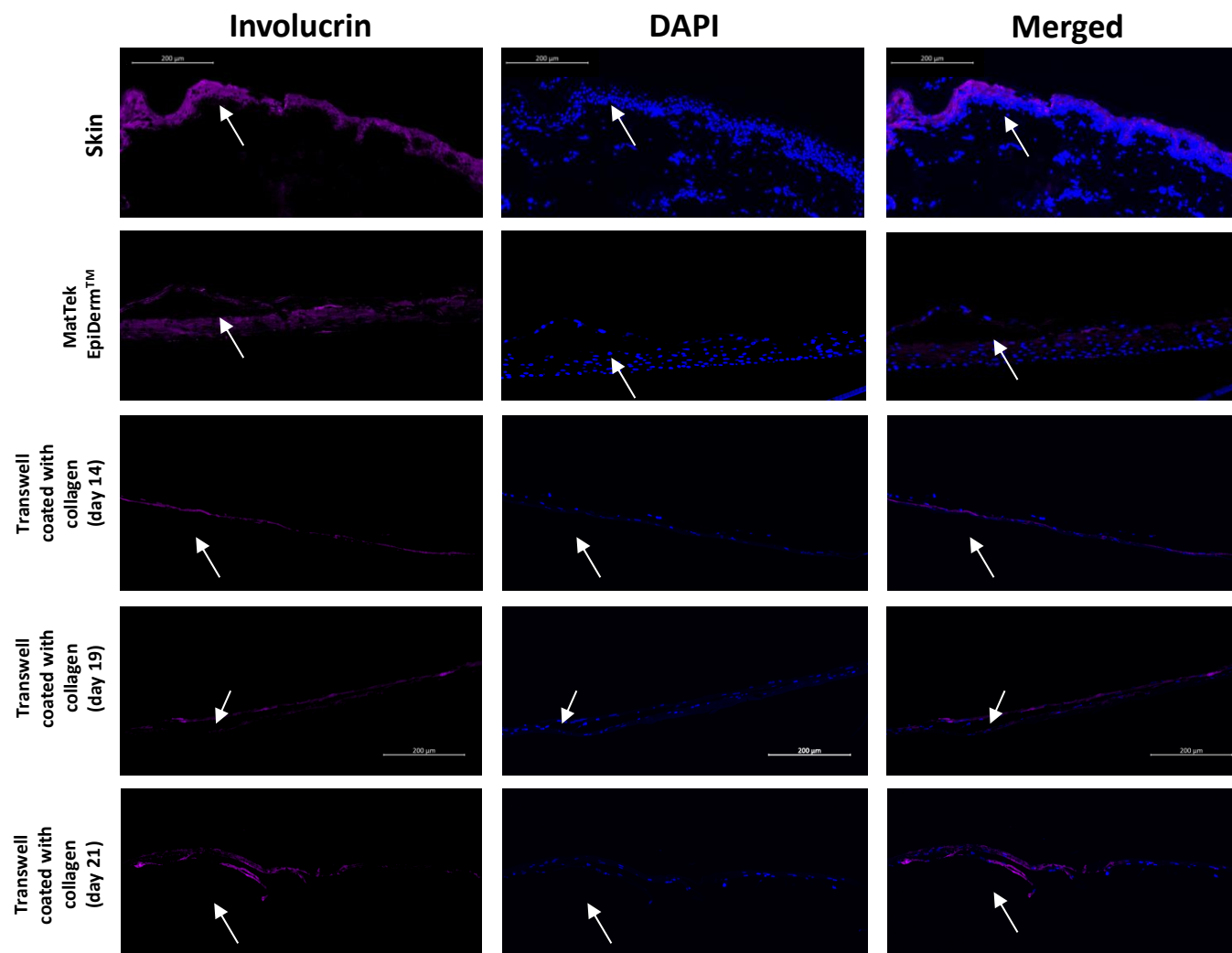


Figure 30. Immunofluorescence staining of involucrin for the 3D epidermal skin models formed using the Corning® Transwell®-COL collagen coated scaffold. Positive staining for involucrin (protein marker for epidermal differentiation of stratum corneum) was observed (bright pink) in the different timepoints of ALI (14, 19 and 21 days) (indicated by the white arrow). Human skin and EpiDerm™ (commercially bought epidermal model from MatTek) were used as a positive control for staining of involucrin. Individual DAPI staining and merged staining (involucrin and DAPI) showed co-localization of epidermal cells. Scale bar of 200μm is representative and similar in all testing conditions.

As previously mentioned, the focus of this task was to develop a comparative performance analysis between a commercially made collagen-coated scaffold and the Alvetex Strata with added coated collagen. Because the use of the Alvetex Strata required optimization of ALI culture time, it was decided to also test the use of the Alvetex Strata Scaffold with added coated collagen for different ALI culture times. So, more timepoints were added to the previous ones tested with the Corning® Transwell®-COL collagen coated scaffold – day 3, day 7 and day 30. This way, it was possible to recreate a continuous “timeline” of keratinocyte differentiation into the different skin layers to better understand the cellular organization of keratinocytes into stratum corneum and stratum basale. Additionally, it was important to assess if the use of a collagen layer onto the Alvetex Strata would help prevent infiltration of keratinocytes into the scaffold. As previously mentioned, keratinocyte culture medium was enriched with 1.5mM vitamin C and calcium, defined as optimal conditions from the results of sections 3.2.2 and 3.2.3.

Results from the H&E staining using collagen showed general good adhesion to the scaffold membrane with an even distribution of the keratinocytes through the scaffold (Figure 32). The day 3 timepoint was clearly not enough as ALI culture time, since there are barely any keratinocytes attached to the scaffold. Increasing the ALI culture time to 7 days seemed to improve adhesion of keratinocytes and its consequent proliferation, but this timepoint is still not enough for proper development of the 3D epidermal skin culture models. These conclusions are also supported by the fact that there is no collagen present in the stratum corneum of any of the 3D epidermal skin models formed at 3 and 7 days of ALI culture time (Figure 34).

The 3D epidermal skin models formed at 14 days of ALI culture time seemed to provide enough time for a reasonably formed stratum corneum layer, especially in donor 1, where a characteristic “wave” shaped stratum corneum. Donor 2 and 3 present a very thin stratum corneum layer that is confirmed by positive staining for collagen in Figure 34. The three remaining timepoints – 19, 21 and 30 days of ALI culture time did not seem to improve any further the formation of the stratum corneum layer. It is possible to observe a characteristic “wave” shaped stratum corneum in donors 1 and 2 at the 30 days timepoint in ALI with positive collagen secretion (Figure 34) but not as evident as the stratum corneum formed in the 3D epidermal skin model from donor 1 at 14 days of ALI. Therefore, these results might suggest that 14 days of ALI culture time might be enough to provide good formation of the stratum corneum layer in the 3D epidermal skin models formed with Alvetex Strata coated with human collagen.

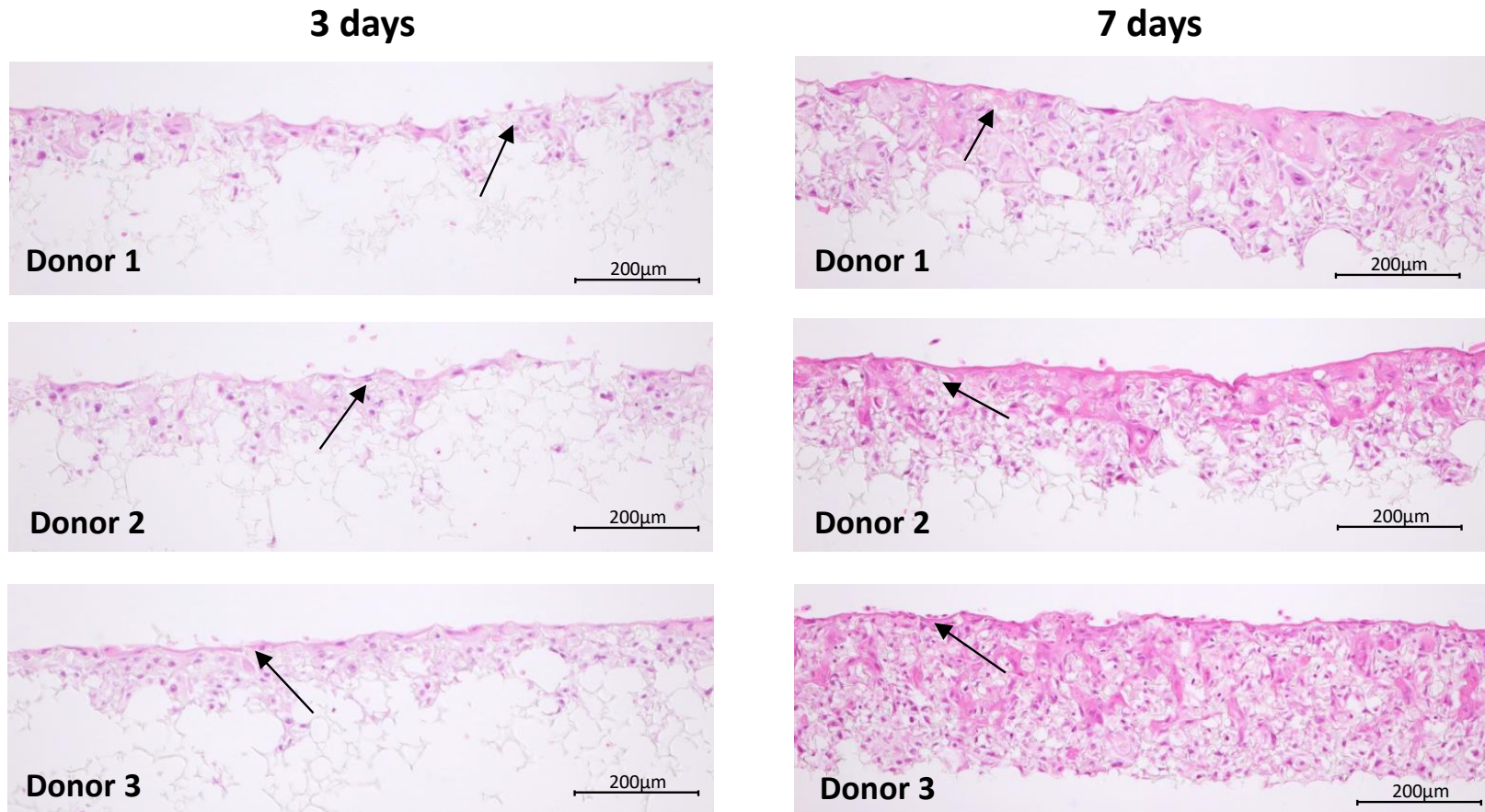


Figure 31. 3D epidermal skin culture using the Alvetex Strata coated with human collagen for 3 and 7 days. The Alvetex Strata was coated with human collagen to improve the cellular organization of the stratum corneum and prevent further keratinocyte infiltration into the scaffold. The culturing time for keratinocytes was tested at 3 and 7 days of ALI culture time in three donors. Organization of keratinocytes into an epidermal layer can be observed (black arrows). Scale bar of 200µm is similar in all testing conditions.

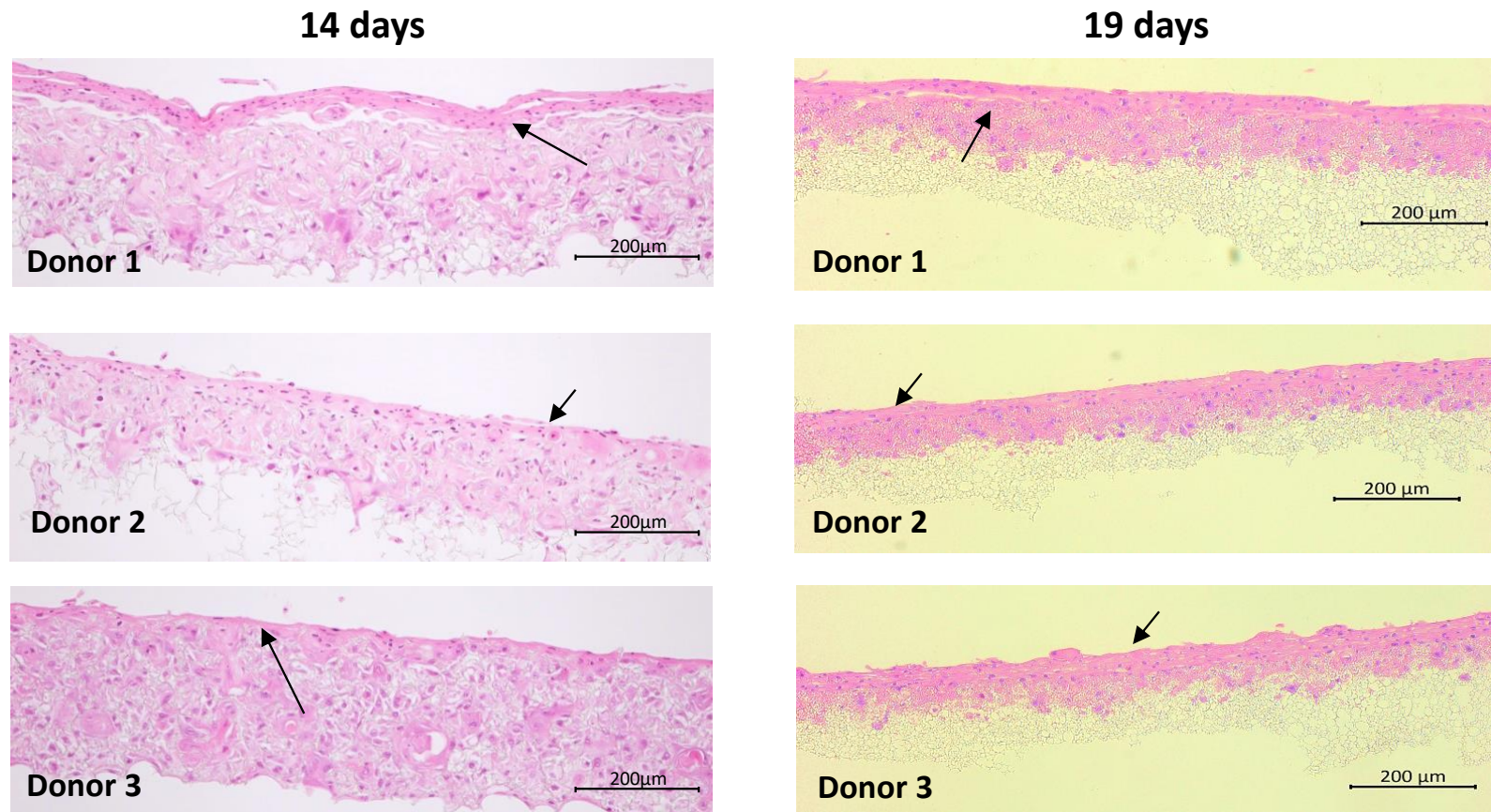


Figure 32. 3D epidermal skin culture using the Alvetex Strata coated with human collagen for 14 and 19 days. The Alvetex Strata was coated with human collagen to improve the cellular organization of the stratum corneum and prevent further keratinocyte infiltration into the scaffold. The culturing time for keratinocytes was tested at 14 and 19 days of ALI culture time in three donors. Organization of keratinocytes into an epidermal layer can be observed (black arrows). Scale bar of 200μm is similar in all testing conditions.

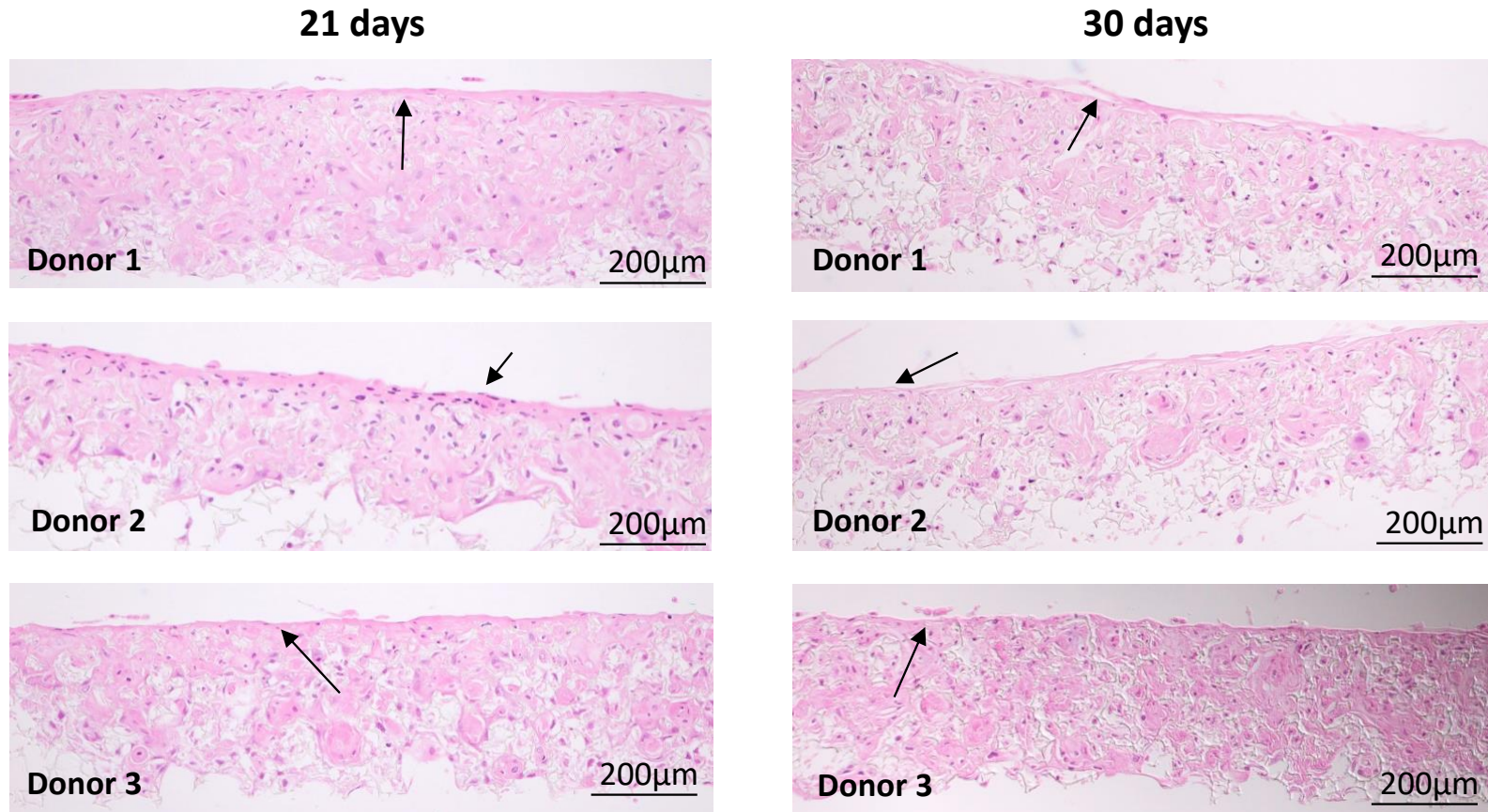


Figure 33. 3D epidermal skin culture using the Alvetex Strata coated with human collagen for 21 and 30 days. The Alvetex Strata was coated with human collagen to improve the cellular organization of the stratum corneum and prevent further keratinocyte infiltration into the scaffold. The culturing time for keratinocytes was tested at 21 and 30 days of ALI culture time in three donors. Organization of keratinocytes into an epidermal layer can be observed (black arrows). Scale bar of 200µm is similar in all testing conditions.

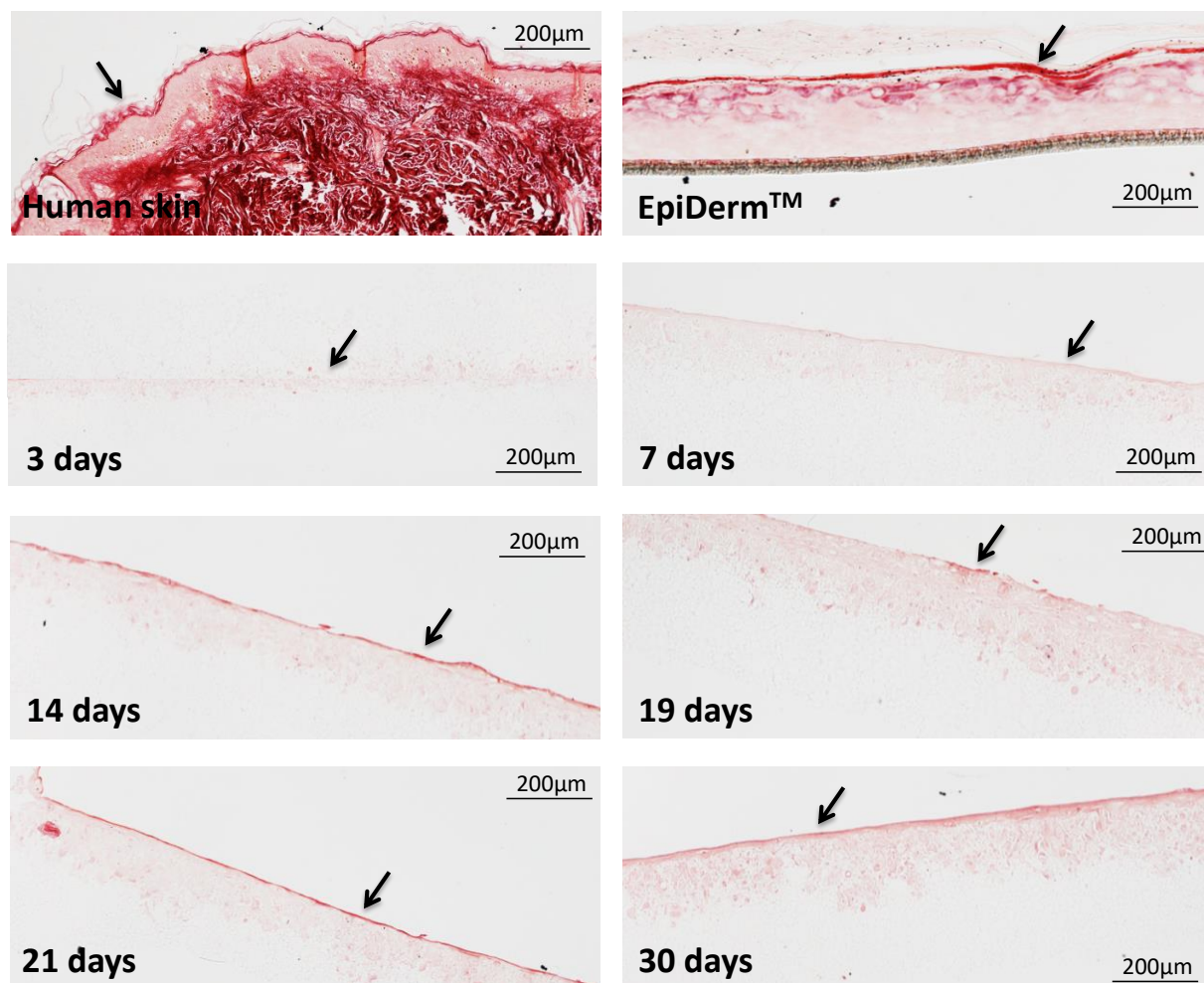


Figure 34. Histological detection of collagen in the 3D epidermal skin models formed using the Alvetex Strata coated with human collagen. Histological detection of collagen was performed using Picro Sirius Red staining for all ALI culture timepoints – 3, 7, 14, 19, 21 and 30 days. Human skin and EpiDerm™ (commercially bough epidermal model from MatTek) were used as a positive control for presence of collagen - bright red colour in the stratum corneum region (indicated by the black arrow). Scale bar of 200µm is similar in all testing conditions.

It was expected that addition of collagen would prevent keratinocyte fallout into the scaffold as the scaffold pores would be filled with collagen fibres, forming a collagen matrix so keratinocytes could differentiate on top of the scaffold. Compared to the 3D skin cultures made without collagen coating, the collagen coating did seem to increase keratinocyte infiltration into the scaffold. H&E results showed that the 3D epidermal skin models formed using the collagen coated scaffold are much more populated with keratinocytes, being almost impossible to see unoccupied scaffold. However, it did not seem to inhibit formation of stratum corneum, as it can be seen in donors 1 and 2 at 14 and 30 days of ALI with consequent collagen detection.

Further characterization of the stratum corneum formation was performed by immunofluorescence staining of involucrin (Figure 35, representative image of donor 1). Expression of involucrin was consistent throughout the different timepoints of ALI and even similar to the involucrin staining expressed in human skin and in the commercially available RHE model (MatTek EpiDermTM). Therefore, the results from the immunofluorescence staining have helped confirm the presence of stratum corneum in the 3D epidermal skin models formed using the Alvetex Strata coated with collagen.

Altogether, the results from the collagen optimization have shown that it is possible to develop 3D epidermal skin models using the Alvetex Strata coated with collagen, as it will allow for proper formation of the stratum corneum with collagen formation and involucrin expression. The output 3D model from the Alvetex Strata is also similar to the ones from commercially available models, as in the case of the EpiDermTM (from MatTek) and the Corning® Transwell®-COL collagen coated scaffold.

Considering the different timepoints, results have shown that there is not much difference between the standard 14 days of ALI and longer time periods (21 or 30 days), so perhaps 14 days would be more beneficial from a cost/time perspective.

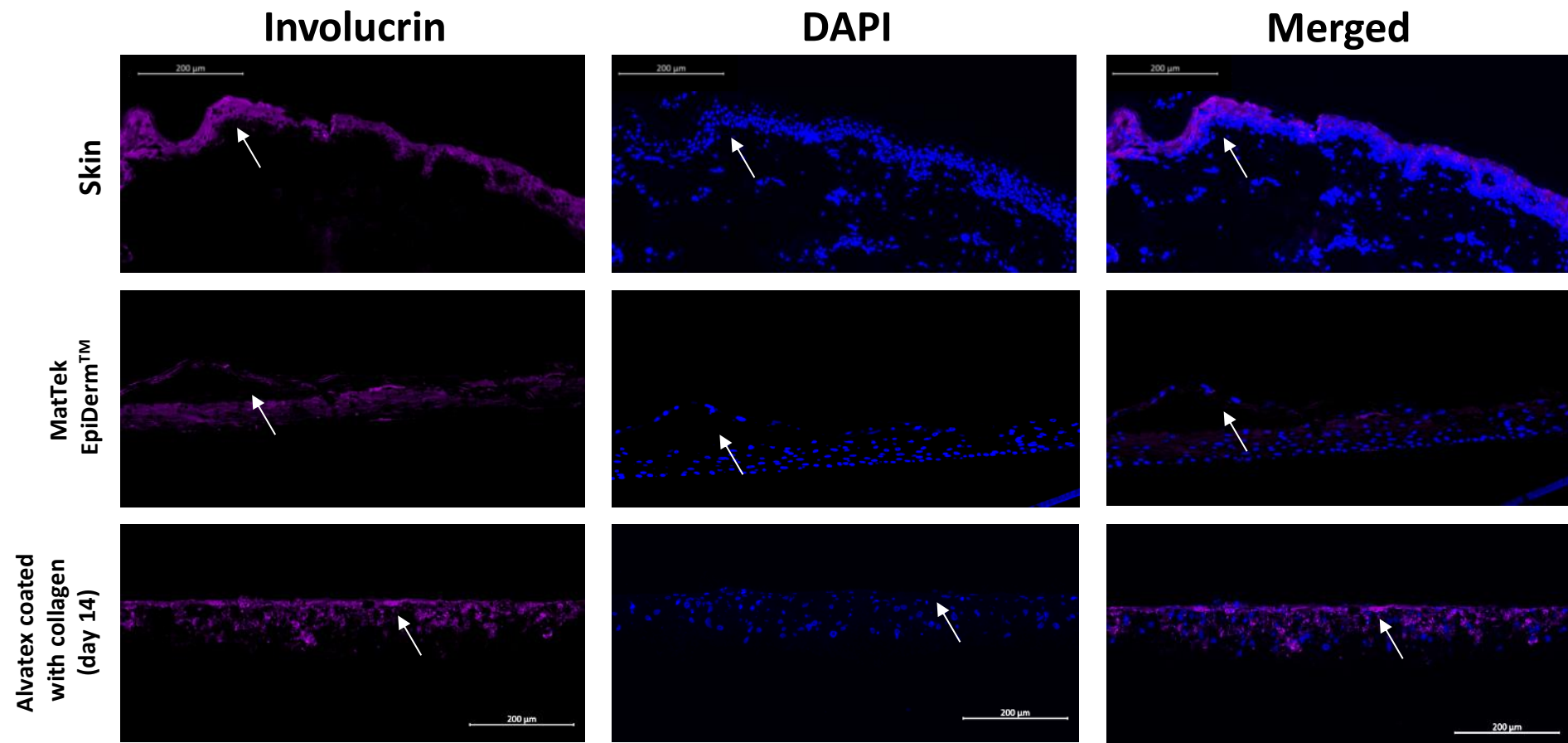


Figure 35. Immunofluorescence staining of involucrin for collagen coated 3D skin models. Positive staining for involucrin (protein marker for epidermal differentiation of stratum corneum) was observed (bright pink) in the 3D epidermal skin models formed using Alvetex Strata coated with collagen (day 14, 19, 21 and 30) (indicated by the white arrow). Human skin and EpiDermTM (commercially bough epidermal model from MatTek) were used as a positive control for staining of involucrin.

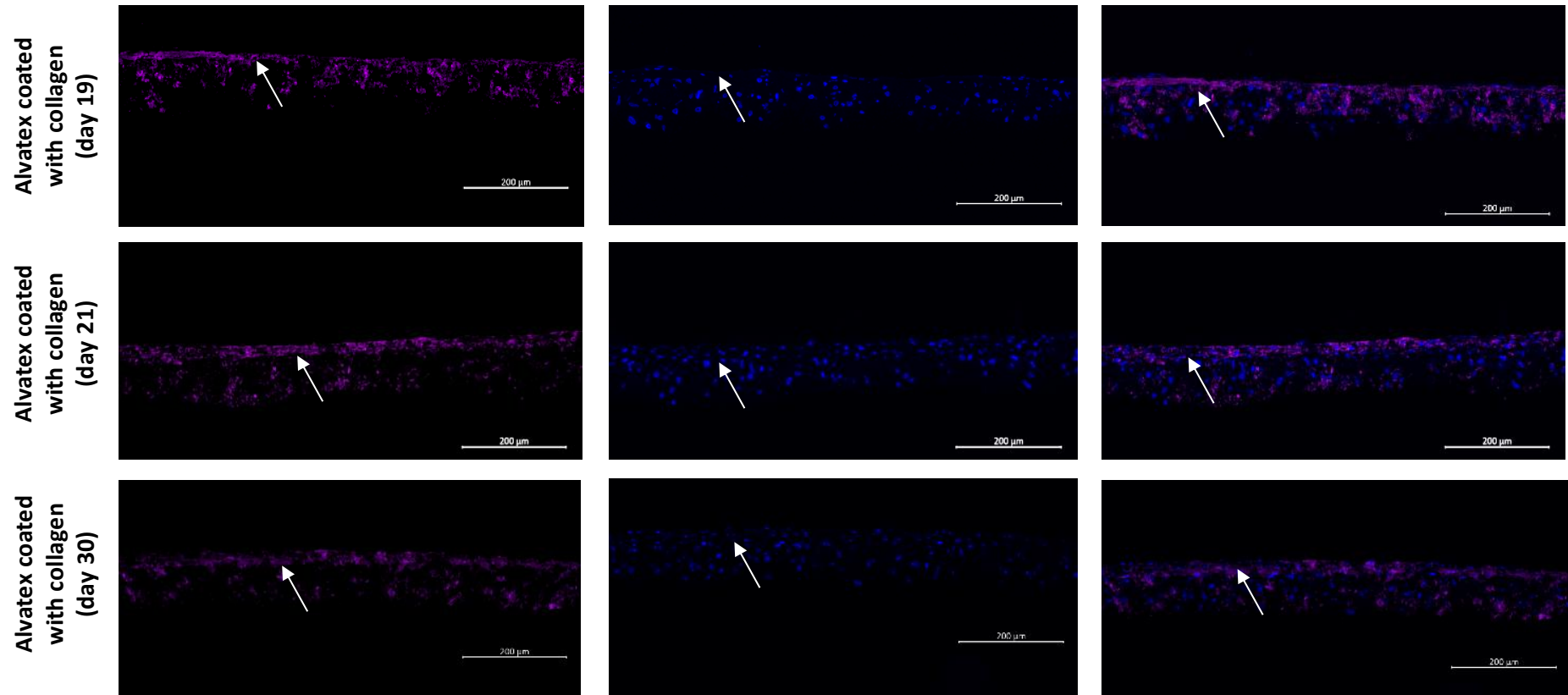


Figure 35 (continuation). Immunofluorescence staining of involucrin for collagen coated 3D skin models. Positive staining for involucrin (protein marker for epidermal differentiation of stratum corneum) was observed (bright pink) in the 3D epidermal skin models formed using Alvetex Strata coated with collagen (day 14, 19, 21 and 30) (indicated by the white arrow). Human skin and EpidermTM (commercially bought epidermal model from MatTek) were used as a positive control for staining of involucrin. Scale bar of 200μm is similar in all testing conditions.

3.3. Reproducibility of the 3D epidermal skin cultures

In addition to the optimization process of the 3D epidermal skin cultures, it is also important to consider its reproducibility and variability between donors. All 3D epidermal skin cultures were constructed by the same operator following the same protocol, but minor technical variations could still influence the reproducibility of the 3D epidermal skin cultures. As keratinocytes are centrifuged to remove any trace of culturing medium before seeding, resuspension of the keratinocytes was sometimes difficult due to cell clumping. Therefore, and while taking this into account, there could have been some minor differences in the pipetting volume of the keratinocytes into the scaffold. Moreover, cell clumping could also have resulted in an uneven adhesion of the keratinocytes into the scaffold.

Additionally, it is also important to consider donor variability. Although keratinocytes were isolated, cultured and seeded at the same passage number and corrected for cell concentration of 1×10^6 keratinocytes/scaffold, it could still result in a not similar growth and differentiation of the keratinocytes into the epidermal layer.

However, and considering all these limitations, the 3D epidermal skin cultures developed showed an overall consistency and resemblance across all donors. Slight observed differences in different donors were discussed throughout the previous sections of optimization.

Further reproducibility studies on the development of the 3D epidermal skin cultures should include development of these models by a different operator to better evaluate transferability of the protocol and culture technique.

3.4. Discussion of the results

Optimization of the 3D epidermal skin culture was carried out considering several aspects – cell number, culture period, vitamin C concentration, calcium concentration and scaffold properties. Results from all cell culturing conditions in this chapter suggest that the optimized protocol for development of the 3D epidermal skin models would be seeding 1×10^6 keratinocytes in a collagen-coated Alvetex Strata membrane for 14 days of ALI.

Cell number is a very important feature because it will determine the maximum number of 3D skin cultures that can be constructed from one donor. A larger number of cells per scaffold would require laborious cell culture, bulking of cells at low passage numbers and large volumes

of culture medium which could be very challenging. This could increase the likelihood of infections or stress resulting in unwanted differentiation of the keratinocytes while still in the culture flask or the keratinocytes reducing their proliferative capacity. The use of 1×10^6 cells per scaffold showed good cell adhesion, consistent distribution through the scaffold and proper differentiation of the epidermal layers without encumbering lengthy cell culture work, it was used as the optimal cell number required for development of the 3D epidermal skin cultures.

Optimizing the duration time of culture is important to reduce the turnover of the 3D cultures for *in vitro* testing studies. Previous protocols for the development of 3D skin models have used 14, 19 and 21 days of ALI, for good formation of the stratum corneum and stratum basale layers. However, results using the Alvetex Strata showed that 21 days of ALI was not sufficient to guarantee reasonable differentiation of the epidermal layers. This was a crucial feature to guarantee quality standards of the 3D skin culture and incomplete formation of the stratum corneum could compromise the results of the test they would be used for. The optimal time of 30 days of ALI was used for development of the 3D epidermal skin cultures as it showed the best results of epidermis formation.

Optimization of vitamin C and calcium showed some improvements in the distribution of the keratinocytes in the 3D epidermal skin culture compared to normal concentrations. The importance of calcium addition in keratinocyte cultures has been controversial. Calcium was identified as vital for growth and differentiation of keratinocytes in culture in the early 1980s by direct relationship of extracellular calcium concentration and differentiation markers of mouse keratinocytes (Hennings et al., 1980). This association was immediately considered fundamental for keratinocyte culture and calcium was from this point forward an inarguable requirement for epidermal differentiation (Elsholz, Harteneck, Muller, & Friedland, 2014; Pillai et al., 1990). However, it is important to highlight that such findings were related to mouse keratinocytes and more recent studies using human keratinocytes have actually disputed the fundamental role of calcium in keratinocyte differentiation. In 1984, conditions such as cell density were shown to be more relevant to keratinocyte differentiation than calcium concentration (Wille, Pittelkow, Shipley, & Scott, 1984). Further reports showing how cell concentration affects the expression levels of differentiation markers cytokeratin 1 and 10 (Drozdoff & Pledger, 1993; Yves Poumay & Pittelkow, 1995) corroborate the notion that calcium stimulus on keratinocyte differentiation is not significant. In fact, some authors claim these findings are irrelevant (Yves Poumay & Coquette, 2007), and others went as far as stating that calcium relevance in keratinocyte differentiation is overestimated (Kolly, Suter, & Mu, 2005). While no consensus has yet been agreed regarding calcium requirement in 3D culture

of keratinocytes, the results observed in this chapter showed that normal concentration of calcium (1.5mM) was sufficient to guarantee good keratinocyte differentiation.

With regard to using a collagen base in the scaffold, results from the Corning® Transwell®-COL scaffolds showed good stratification of the stratum corneum but almost no evidence of stratum basale. That together with the fact that the Corning® Transwell®-COL scaffolds use animal-based collagen is discouraging for the development of a 3D animal-free skin equivalent model. The Alvetex Strata coated with human collagen could possibly be the best optimized 3D epidermal skin model, as it showed good formation of the stratum corneum with formation of collagen. Moreover, it allowed for development of the 3D epidermal skin models in the shortest ALI time – 14 days.

Overall, the aim of this project was to develop an open source 3D epidermal skin culture with relevant epidermal stratification. The results showed that this was achieved using the Alvetex Strata membrane using 1×10^6 keratinocytes per scaffold for 30 days ALI culture, enriched with 1.5mM vitamin C and calcium concentrations. H&E results showed stratification of the epidermal layers, stratum corneum and stratum basale and this was also confirmed by expression of the protein markers involucrin and cytokeratin 14. While presence of the stratum basale was not phenotypically well defined in the H&E pictures (Figure 17), positive staining for cytokeratin 14 confirmed its presence (Figure 21). This indicated that while keratinocytes might not resemble a typical stratum basale layer with round shaped keratinocytes, the basal cells were still present in the 3D skin epidermal cultures developed. The fact that keratinocytes of the stratum basale did not present a well-defined round shape could be attributed to the scaffold properties. It is a porous scaffold, acting as a “sponge” so the keratinocytes can adhere and be in contact with the culture medium from below. So, the lack of a proper scaffold bottom structure could inhibit the phenotypic development of the stratum basale.

All the phenotypic characteristics mentioned above are of crucial important for development of *in vitro* skin models. Because the major drive force for development and commercialization of an *in vitro* alternative skin models needs to be its close resemblance to the *in vivo* human skin microenvironment, so any safety testing or screening will provide a relevant readout for human purposes. Considering that three *in vitro* 3D models were used in this chapter, phenotypic comparison of the different skin layers from each model is expected (Figure 36).

Starting from the outer epidermal layer, formation of the stratum corneum is visible in all three *in vitro* skin models, with its characteristic “wave shape”. This layer is consistently the

most well-defined layer across the three *in vitro* skin models. As for the inner layers, the stratum spinosum and the stratum basale, phenotypic resemblance to human skin is not so evident. The cells from the stratum spinosum present a large purple tone nuclei that is possible to observe in all *in vitro* 3D models. There is just a visible difference in the consistency and thickness of this layer across the *in vitro* 3D models, since the stratum spinosum is much more defined in the EpiDerm™ RHE model. The same observations are valid for the stratum basale, which should be composed of a single layer of “square-shaped” keratinocytes in the bottom of the epidermis. Nevertheless, immunofluorescence staining using cytokeratin 14 indicated presence of stratum basale in both the 3D epidermal skin culture using the Alvetex Strata coated with human collagen and in the 3D skin model using the Corning® Transwell®-COL scaffold.

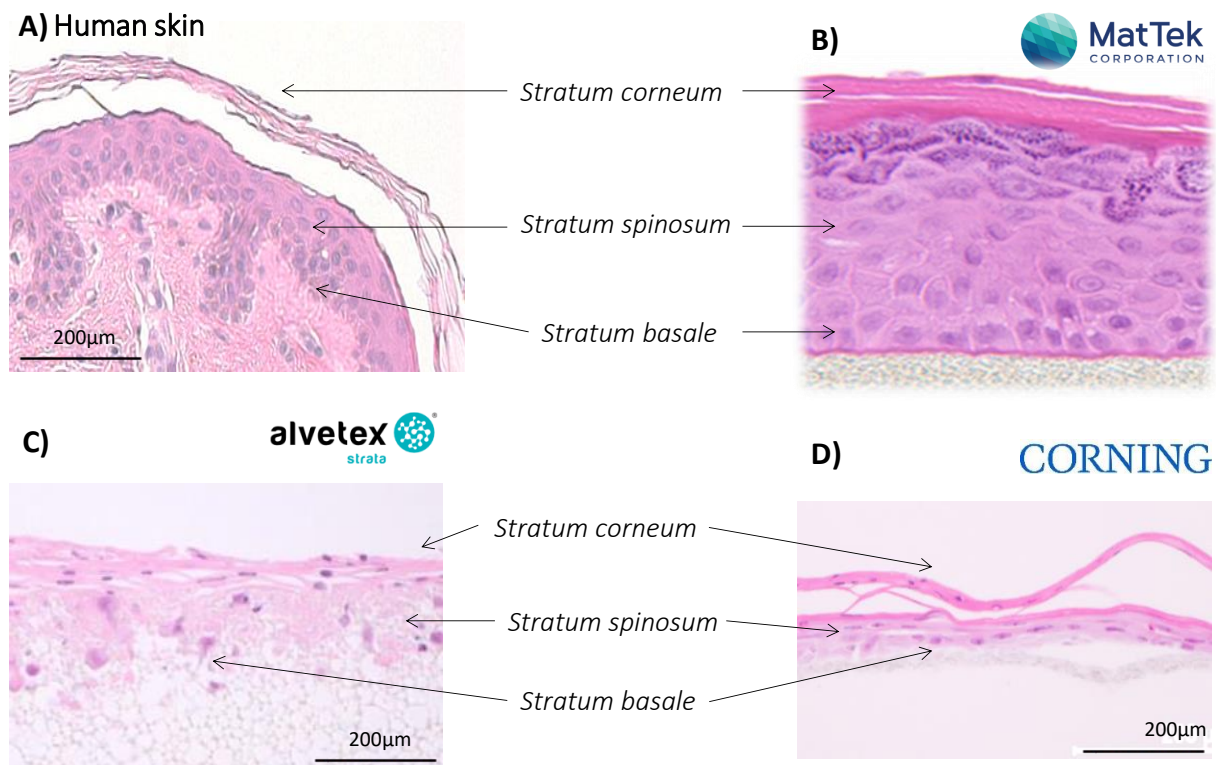


Figure 36. Comparison between the different 3D epidermal skin models used to real human skin. Phenotypic comparison of the different epidermal skin layers – stratum corneum, stratum spinosum and stratum basale – between A) human skin, B) the EpiDerm™ RHE model (from MatTek), C) the 3D epidermal skin culture using the Alvetex Strata coated with human collagen and D) the 3D skin model using the Corning® Transwell®-COL scaffold.

Ultimately, optimization results from this chapter showed that the D epidermal skin culture developed using the Alvetex Strata coated with collagen is phenotypically relevant to human skin.

CHAPTER 4

Assessment of skin irritation testing using a 3D epidermal skin culture

4. Assessment of skin irritation testing using a 3D epidermal skin culture

4.1. Aim

OECD performance standards for 3D epidermal models can be found in the form of Testing Guidelines. In fact, the use of 3D epidermal models following the appropriate Testing Guidelines is mandatory for official EURL-ECVAM validation of the RHE models.

Testing Guideline (TG) 439 refers to skin irritation testing using reconstructed skin models. It contains a detailed protocol for assessment of skin irritation by determination of cell viability. Skin irritants differ from non-irritants by causing a reduction in cell viability of more than 50%. ECVAM used this Testing Guideline to validate 3 commercially available 3D epidermal skin models for assessment of skin irritation - EpiDerm™, EpiSkin™ and SkinEthic RHE (Table 2).

Morphology of the 3D epidermal models is a very important quality control parameter as described in OECD TG 439. In fact, morphology of the *in vitro* skin explant can impact the assessment of skin irritation testing described in OECD TG 439. Parameters like incorrect organization of the keratinocytes throughout the epidermal layer or background interference from the scaffold should be carefully considered as they can hamper the damage caused by the chemical exposure and ultimately affect the readout from the skin irritation testing, by not correctly identifying a non-irritant or irritant chemical.

Therefore, it was imperative to complement optimization of the 3D epidermal model using two Alvetex scaffold membranes (chapter 3) with the assessment of the skin irritation testing (chapter 4). All the histological results concerning morphology of the developed 3D epidermal skin culture are described in Chapter 3 and results showed that the Alvetex Strata was the best scaffold to use. Consequently, the aim of this chapter was to evaluate the 3D epidermal skin culture developed using the Alvetex Strata for its ability to assess skin irritation, by distinguish between non-irritant and irritant chemicals.

4.2. Results

The 3D epidermal skin cultures were tested using a skin irritation testing assay following the OECD Testing Guideline 439. Briefly, the 3D epidermal skin model was exposed to a non-irritant or irritant chemical for 30 minutes, followed by a washing step to mimic a real-life scenario. Damage to the skin cells was assessed by keratinocyte cell death using a MTT

viability test. The readout from the MTT test directly indicates skin irritancy, if cell viability falls below a 50% viability threshold upon exposure to the testing chemical.

4.2.1. Skin irritation testing using the Alvetex Scaffold

Results from Chapter 3 showed that the standard Alvetex Scaffold did not allow for complete epidermal formation. However, preliminary skin irritation testing was performed using this model as a 3D culture model to evaluate the scaffold performance in the same 4 donors. Only negative and positive controls were tested – PBS and 5% SDS in aqueous solution, respectively, as stated in TG 439. An additional positive control was used as test chemical, Triton-X 1% (Figure 37).

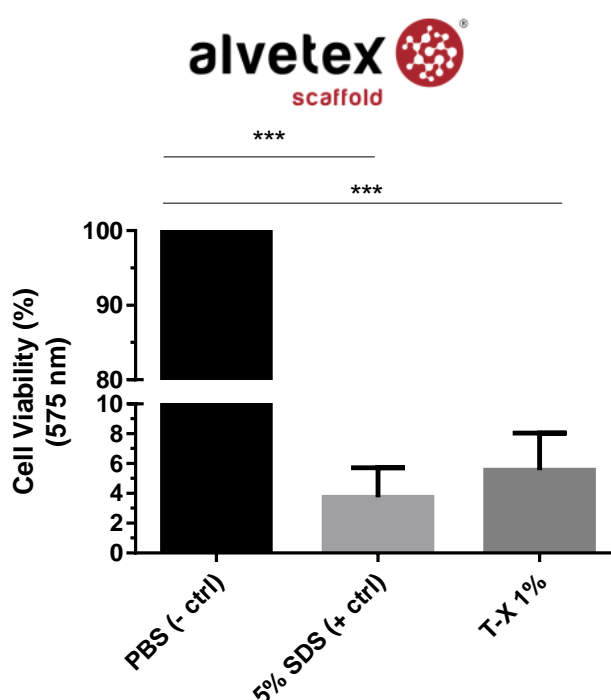


Figure 37. TG 439 Skin irritation testing of the 3D epidermal skin cultures using the Alvetex Scaffold. PBS and 5% SDS in aqueous solution were used as negative and positive control respectively, following the TG 439 protocol. Triton-X (T-X) 1% was used as additional test condition. Results are expressed as mean and standard deviation of three independent experiments measured at 575nm. *** $p < 0.001$

While histological results from Chapter 3 showed that the Alvetex Scaffold did not allow for complete epidermal differentiation, it still performed well in the skin irritation testing. Compared to the negative control (PBS), 5% SDS (positive control) caused a significant reduction in cell viability of more than 90%. Triton-X 1% also achieved similar results (showing a cell viability of 5.9%), showing that the 3D epidermal skin culture using the Alvetex Scaffold could correctly identify irritants (5% SDS and T-X 1%) from non-irritants (PBS).

4.2.2. Skin irritation testing using Alvetex Strata

Skin irritation testing was also performed in the 3D skin epidermal cultures using the Alvetex Strata. Preliminary irritation testing was performed in the same conditions as the Alvetex Scaffold membrane for the 3 timepoints tested - 14, 21 and 30 days of ALI (Figure 38) in the same 5 donors used for the construction of the 3D epidermal skin model.

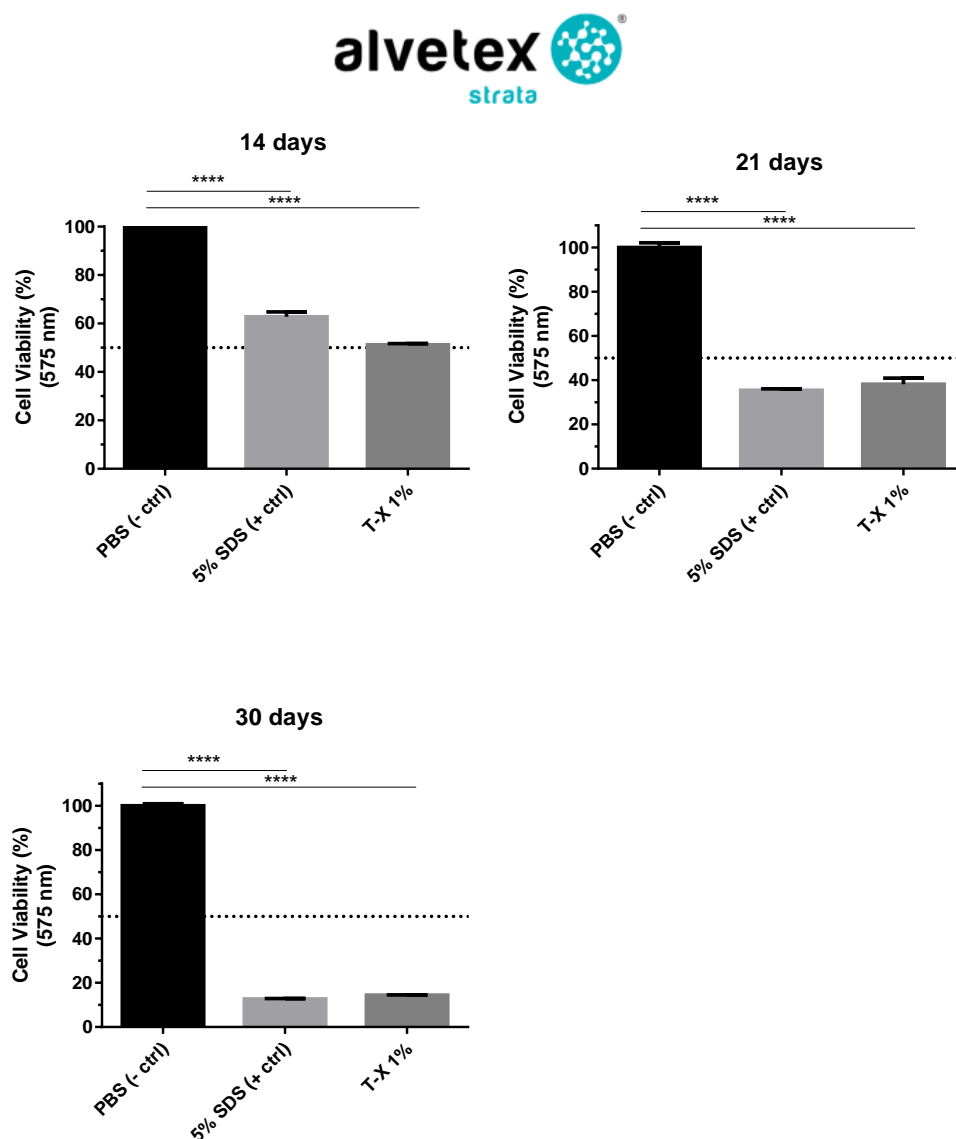


Figure 38. TG 439 Skin irritation testing of the 3D epidermal skin cultures using the Alvetex Strata. Irritation testing was performed in all 3 optimization timepoints for ALI – 14, 21 and 30 days. PBS and 5% SDS in aqueous solution were used as negative and positive control respectively, following TG 431. Triton-X (T-X) 1% was used as additional test condition. Dotted line represents the 50% viability threshold. Results are expressed as mean and standard deviation of three independent experiments measured at 575nm. **** p < 0.0001

Results showed that 3D epidermal skin cultures cultured for 14 days at ALI failed to accurately distinguish the irritant controls (5% SDS and TX-1%) from the non-irritant control (PBS). While the reduction in cell viability caused by the positive controls was significantly different from the negative control ($p < 0.0001$), it still failed to reach the 50% viability threshold established by the TG 439.

The viability results from the 3D epidermal skin cultures cultured for 21 and 30 days at ALI showed significant reduction in cell viability by the positive controls below the 50% viability threshold ($p < 0.0001$). At 21 days, the 3D epidermal skin models showed a cell viability of 35% for 5% SDS solution and a 38% viability for T-X 1% solution. At 30 days, the 3D epidermal skin models showed a cell viability of 12% for the 5% SDS solution and a 14% viability for the T-X 1% solution. These preliminary results showed that the optimized 3D epidermal skin cultures performed well according to OECD TG 439 standards. Considering the histological results from Chapter 3, only the 3D epidermal skin cultures cultured for 30 days at ALI were considered for further skin irritation testing. Therefore, a more detailed evaluation of the 3D epidermal skin culture model was performed using 12 chemicals (6 irritant and 6 non-irritant) from the Validated Reference Methods List of test chemicals (Table 6), each chemical tested in 10 independent tests.

Viability results for each tested chemical were calculated in comparison to the negative control, PBS and are given in Table 10, as well as the mean value of the 10 independent donors in which chemicals were tested. Cell viability of the positive control, 5% SDS in aqueous solution, was of $22.25 \pm 0.86\%$ ($p < 0.001$) when compared to the 100% viability of the negative control. These results showed the stability and consistency of the 3D epidermal cultures in culture across different donors, which was also a quality control parameter of the OECD TG 439. An extra positive control was also tested in all donors, Triton X-1%. This chemical is used as positive control for acute eye irritancy, as specified in OECD TG 405 (OECD, 2012a). Results from the 3D epidermal skin culture showed that the optimized model could also classify TX-1% as an irritant, since it caused an average viability of only $36.79 \pm 2.23\%$ ($p < 0.001$).

Regarding the non-irritant chemicals tested, the 3D epidermal skin culture was able to correctly classify 4 out of the 6 chemicals tested as non-irritants since the viability was above the 50% threshold—allyl phenoxy-acetate ($62.70 \pm 3.56\%$; $p < 0.001$), isopropanol ($78.81 \pm 2.35\%$), heptyl butyrate ($71.09 \pm 2.50\%$; $p < 0.001$) and hexyl salicylate ($72.73 \pm 3.44\%$).

1-bromo-4-chlorobutane ($44.03 \pm 2.19\%$; $p < 0.001$) and 4-methyl-thio-benzaldehyde ($45.07 \pm 3.03\%$; $p < 0.001$) showed viability below the 50% viability threshold, indicating them as false positives for irritancy. However, if considering the specifications of these chemicals

mentioned on Table 6, both chemicals are classified as non-irritant in *in vivo* assays with no GHS category. This means that there is not enough *in vivo* data to support classification of these chemicals as irritants, so they are classified as non-irritants. It could be argued that these chemicals are in fact irritants and that the 3D epidermal skin culture is sensitive enough to determine their irritancy. However, further validation is required to confirm this hypothesis.

Regarding the irritant chemicals tested, all 6 irritants were correctly categorised by the 3D epidermal skin culture showing a viability below 50%: 1-decanol ($36.48 \pm 1.80\%$; $p < 0.001$), 1-bromohexane ($35.19 \pm 4.08\%$; $p < 0.001$), di-n-propyl disulphide ($37.16 \pm 1.19\%$; $p < 0.001$), heptanal ($32.06 \pm 1.04\%$; $p < 0.001$), tetrachloroethylene ($36.98 \pm 2.51\%$; $p < 0.001$).

Table 10. Cell viability results for the 3D epidermal skin culture with the Alvetex Strata for skin irritation testing following TG 439. 6 non-irritant (■) and irritant (□) chemicals from TG 439 for skin irritation were tested in the 3D epidermal skin culture in 10 donors with 30µL of the testing chemical dispensed directly on top of the skin model cells. Cell viability is reported as percentage of viability for each chemical is calculated in comparison to the negative control (PBS). For each donor, chemical test was performed in triplicate and viability is reported as average of 10 independent tests with standard deviation (SD).

Chemical	% Cell viability ± Standard Deviation (SD)										
	Donor 1	Donor 2	Donor 3	Donor 4	Donor 5	Donor 6	Donor 7	Donor 8	Donor 9	Donor 10	Total 10 donors
PBS (- ctrl) ■	100.10±0.75	100.00±2.71	100.00±6.56	100.00±11.42	100.00±2.28	100.00±0.67	100.00±0.37	100.00±1.57	100.00±0.30	100.00±0.31	100.01±2.49
1-bromo-4-chlorobutane ■	36.15±0.65	48.09±0.89	26.43±1.70	60.11±10.78	50.85±5.55	20.93±0.24	93.51±1.03	33.89±0.18	35.20±0.41	35.15±0.44	44.03±2.19
allyl phenoxy-acetate ■	63.34±12.42	46.50±1.40	81.43±3.79	71.45±5.05	94.98±1.23	76.03±0.05	76.03±0.05	36.92±1.16	41.32±5.35	39.01±5.13	62.70±3.56
Isopropanol ■	90.89±1.61	44.77±0.49	82.38±0.93	76.15±1.40	75.96±2.62	55.67±0.24	94.36±1.76	89.75±6.87	93.02±4.26	85.14±3.36	78.81±2.35
4-methyl-thio-benzaldehyde ■	35.27±1.20	45.93±1.42	21.62±1.64	84.66±8.33	50.85±5.76	52.42±5.34	52.42±5.34	36.25±0.97	35.62±0.09	35.67±0.19	45.07±3.03
heptyl butyrate ■	69.36±2.93	50.68±2.82	73.52±2.20	85.37±5.34	90.49±9.56	53.20±0.41	84.11±0.88	66.63±0.51	68.86±0.24	68.71±0.09	71.09±2.50
hexyl salicylate ■	69.35±2.10	97.62±4.37	70.82±1.73	77.22±10.99	89.53±12.53	32.09±0.23	88.96±1.73	68.22±0.09	66.70±0.34	66.84±0.24	72.73±3.44
5% SDS (+ ctrl) □	32.99±0.44	19.39±0.14	24.97±0.72	36.79±1.17	44.23±4.27	18.23±0.12	10.43±0.04	9.71±0.51	12.43±0.09	13.37±1.14	22.25±0.86
1-decanol □	33.14±1.63	42.11±1.45	23.17±1.10	78.10±4.72	45.51±0.55	45.95±6.05	43.51±1.78	18.17±0.46	17.54±0.11	17.59±0.12	36.48±1.80
1-bromohexane □	46.29±2.10	53.21±2.14	25.38±2.54	55.67±16.39	58.33±15.30	24.68±0.00	30.03±0.53	15.67±0.19	17.31±0.09	25.34±1.54	35.19±4.08
di-n-propyl disulphide □	30.57±0.86	59.12±1.63	26.78±1.47	53.01±4.012	43.91±0.88	39.78±1.25	40.15±1.03	19.01±0.24	29.60±0.09	29.64±0.45	37.16±1.19
Heptanal □	34.39±0.63	45.06±1.21	22.74±1.40	13.21±0.67	56.62±3.30	41.16±0.16	28.13±0.39	20.19±0.65	29.50±0.44	29.60±1.58	32.06±1.04
Tetrachloro Ethylene □	47.32±2.36	59.48±3.56	29.38±1.03	55.32±12.31	50.64±3.13	28.13±0.39	27.65±0.52	19.57±0.81	26.13±0.18	26.17±0.79	36.98±2.51
TX-1% □	34.83±1.11	22.28±0.76	23.12±1.41	47.70±7.71	48.93±1.08	14.66±0.08	57.57±0.37	39.04±3.24	44.54±2.25	35.25±4.25	36.79±2.23

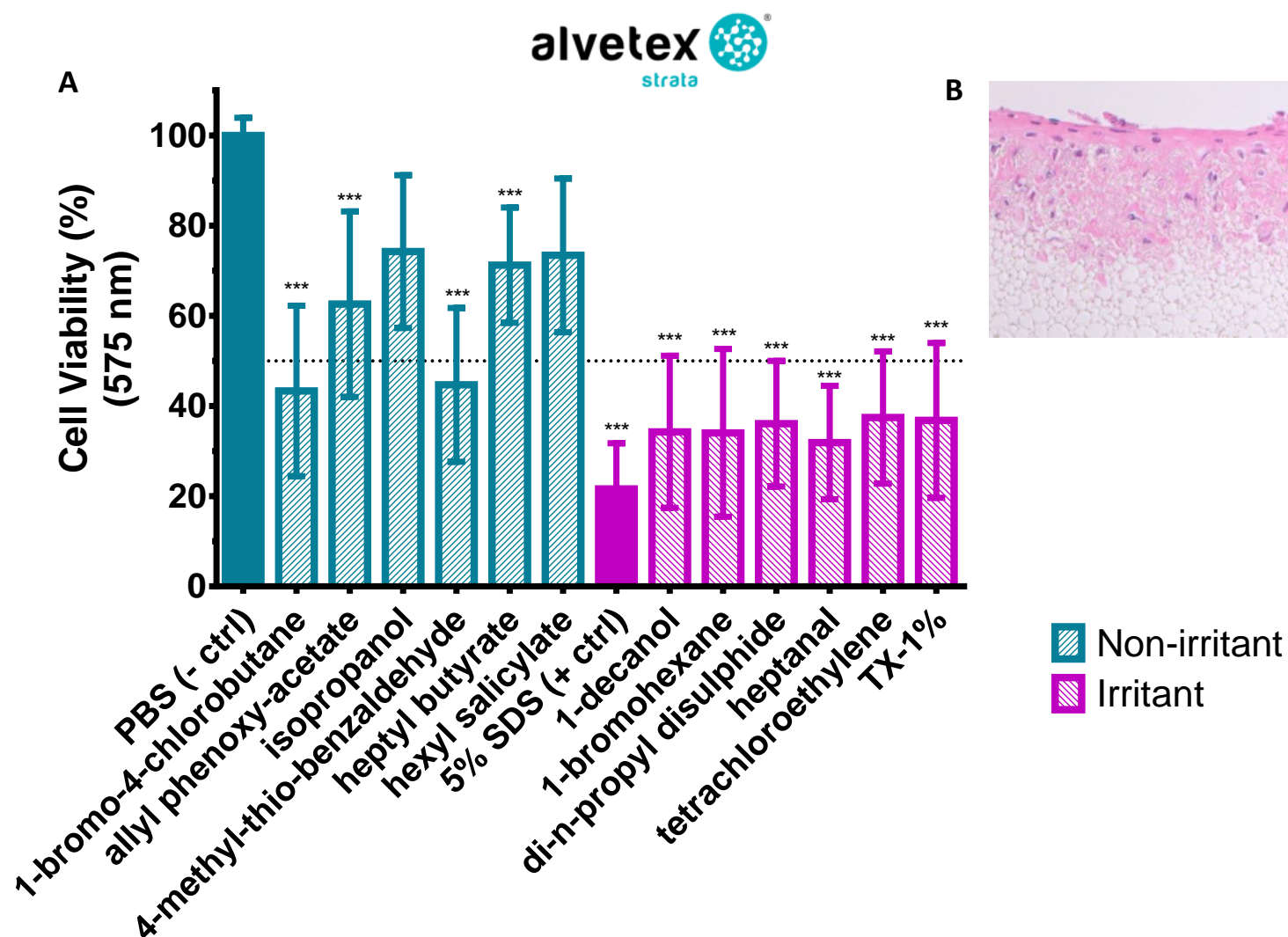


Figure 39. *In vitro* testing of TG 439 skin irritation using the 3D epidermal skin culture with Alvetex Strata. A. *In vitro* performance testing of the 3D epidermal skin culture using six non-irritants (blue stripped columns) and six irritants (pink stripped columns). Results are expressed as mean and standard deviation of ten independent experiments. *** $p < 0.001$ when compared to the negative control (- ctrl), PBS (blue filled column). Positive control (+ ctrl) as 5% SDS in aqueous solution (pink filled column). Dotted line represents the 50% viability threshold. **B.** Representative image of the 3D epidermal skin culture with Alvetex Strata (donor 5).

Altogether, these results substantiate the performance of the optimized 3D epidermal skin culture for skin irritation testing. Furthermore, a skin irritation testing comparative analysis was performed using a commercially available RHE model (EpiDermTM, MatTek), a keratinocyte monolayer culture and a 3D skin model using a collagen-based scaffold (Corning).

4.2.3. Skin irritation testing using EpiDermTM (MatTek)

A commercially available 24-well plate RHE model was obtained from MatTek (EpiDermTM). This RHE model consists of differentiated human-derived keratinocytes cultured in inserts at ALI (culture time of ALI is not specified). The origin of keratinocytes is also not specified, and therefore it was not known if all 24 model wells consisted of keratinocytes from the same donor or a pool of keratinocyte donors. We therefore considered all 24 well models of the EpiDermTM model as from one single keratinocyte donor. Therefore, the three replicates for each condition of skin irritation testing are not independent replicates.

Results from the skin irritation testing using the EpiDermTM RHE model from MatTek showed that this RHE was able to correctly classify 5 out of 6 non-irritants and 5 out of 6 irritants (Figure 40) according to the irritancy threshold of 50% viability. Allyl phenoxy-acetate ($134 \pm 6.29\%$; $p < 0.001$), isopropanol, ($69.1 \pm 2.62\%$; $p < 0.001$), 4-methyl-thio-benzaldehyde ($110.4 \pm 5.66\%$; $p < 0.001$), heptyl butyrate ($104.3 \pm 9.57\%$) and hexyl salicylate ($111.3 \pm 4.17\%$; $p < 0.001$) were correctly classified as non-irritants as the viability observed was above 50%, while 1-decanol ($20.5 \pm 0.67\%$; $p < 0.001$), 1-bromohexane ($23.4 \pm 0.85\%$; $p < 0.001$), heptanal ($21.6 \pm 0.82\%$; $p < 0.001$), tetrachloroethylene ($20.38 \pm 0.8\%$; $p < 0.001$) and TX-1% ($19.9 \pm 0.38\%$; $p < 0.001$) were correctly classified as irritants showing viability below the 50% threshold. However, the viability results of 4-methyl-thio-benzaldehyde ($110.4 \pm 5.66\%$; $p < 0.001$), heptyl butyrate ($104.3 \pm 9.57\%$) and hexyl salicylate ($111.3 \pm 4.17\%$; $p < 0.001$) were all above 100% cell viability, meaning that their viability is greater than PBS viability (100%). This discrepancy could be due to technical error during the experiment.

Similar to the results from the 3D epidermal skin models with the Alvetex Strata Scaffold, the viability following exposure to 1-bromo-4-chlorobutane viability was again below the irritancy threshold ($29.7 \pm 0.79\%$; $p < 0.001$), considering this chemical as a false positive irritant. On the contrary, di-n-propyl disulphide was categorised as a false negative since it results showed a viability response of $117.4 \pm 5.11\%$; $p < 0.001$.

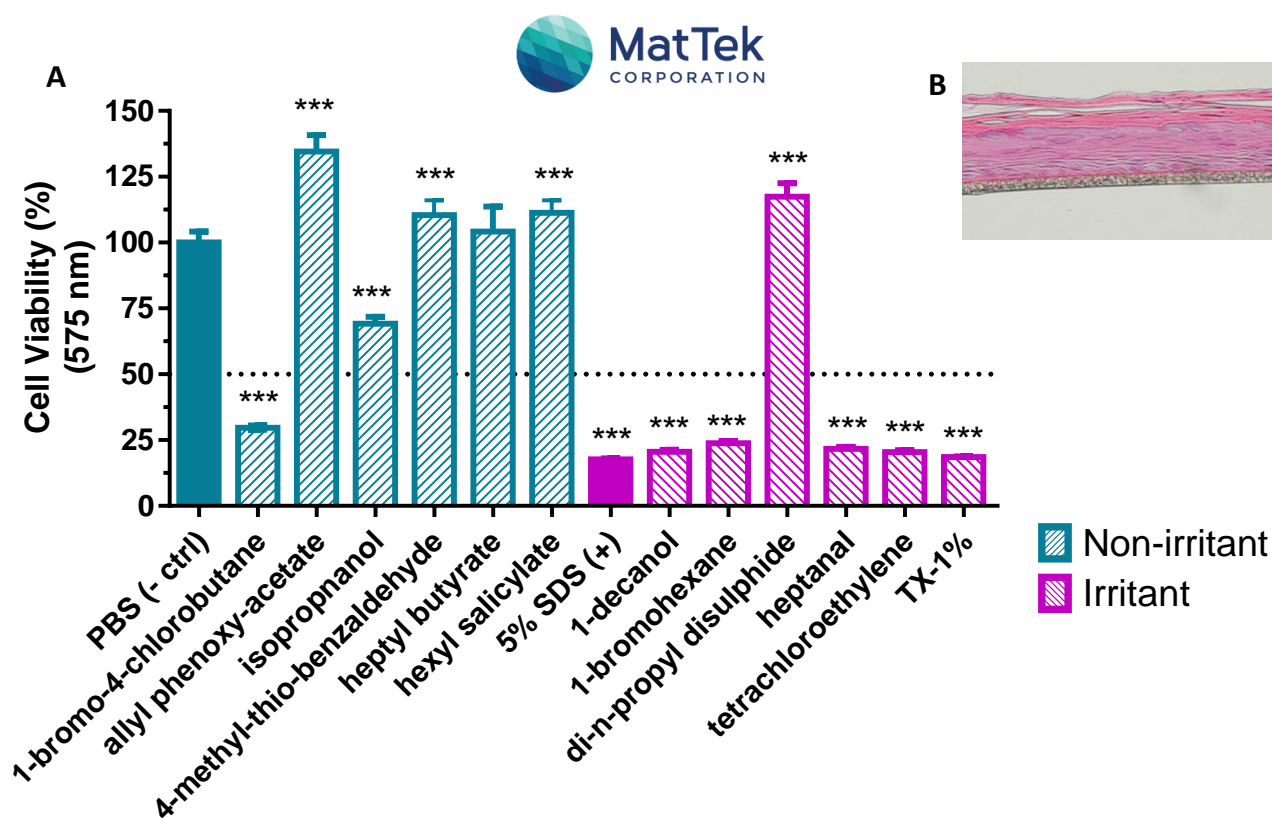


Figure 40. *In vitro* testing of TG 439 skin irritation using the EpiDerm™ RHE model (MatTek). **A.** *In vitro* performance testing of the commercially available RHE model using six non-irritants (blue striped columns) and six irritants (pink striped columns). Results are expressed as mean and standard deviation of 1 experiment. *** $p < 0.001$ when compared to the negative control (- ctrl), PBS (blue filled column). Positive control (+ ctrl) as 5% SDS in aqueous solution (pink filled column). Dotted line represents the 50% viability threshold. **B.** Representative image of the EpiDerm™ RHE model.

Overall, the skin irritation testing results for the EpiDerm™ RHE model were in accordance with the OECD TG 439 standards of irritancy - 50% viability threshold. However, four non-irritant chemicals showed a viability greater than 100% and one non-irritant chemical was classified as false negative. This together with the fact that all 24 RHE models are possibly derived from the same donor could justify the irregularity of the skin irritation testing results. Further repeat of this work would be required, however it would again not be possible to determine if the new EpiDerm™ RHE model would be developed using keratinocytes from the same donor as the previous bought one.

Considering that the epidermal model is a commercially available RHE model and it is widely used for toxicity studies regarding skin irritation, results showed that the 3D epidermal skin culture could correctly classify as many non-irritants from irritants as the EpiDerm™ RHE model. These findings validate the applicability of the 3D epidermal skin culture for skin irritation testing purposes.

4.2.4. Skin irritation testing using a keratinocyte monolayer culture

To better understand the behavioural difference between keratinocytes in a monolayer 2D culture and keratinocytes in a 3D multilayer culture, a monolayer keratinocyte culture of the same 10 donors used for the 3D epidermal skin culture were developed for skin irritation testing.

As expected, keratinocytes in monolayer culture did not show the same outcome as the 3D epidermal skin culture when following the OECD TG 439 guidelines. While the monolayer 2D culture was able to correctly identify the positive controls – 5%SDS ($11.80 \pm 3.63\%$; $p < 0.001$) and TX-1% ($36.50 \pm 8.07\%$; $p < 0.001$), it could only correctly identify 3 out of 6 non-irritants. Allyl phenoxy-acetate ($51.26 \pm 7.91\%$; $p < 0.001$), heptyl butyrate ($68.55 \pm 15.74\%$; $p < 0.001$) and hexyl salicylate ($75.36 \pm 19.55\%$; $p < 0.001$) were correctly classified as non-irritants, by showing a cell viability above 50%. All 6 irritant chemicals were correctly identified by the monolayer 2D culture - 1-decanol ($18.16 \pm 3.46\%$ viability; $p < 0.001$), 1-bromohexane ($24.18 \pm 10.49\%$; $p < 0.001$), di-n-propyl disulphide ($24.64 \pm 5.78\%$; $p < 0.001$), heptanal ($28.96 \pm 6.78\%$; $p < 0.001$) and tetrachloroethylene ($24.94 \pm 4.31\%$; $p < 0.001$) showing a viability below 50% (Table 11 and Figure 41).

Once again, 1-bromo-4-chlorobutane was below the irritancy threshold ($32.67 \pm 22.04\%$; $p < 0.001$), being classified as a false positive. Isopropanol ($26.68 \pm 9.74\%$; $p < 0.001$) and 4-methyl-thio-benzaldehyde ($21.49 \pm 5.77\%$; $p < 0.001$) were also classified as false positives in the keratinocyte monolayer culture.

Ultimately, performance of the keratinocyte monolayer culture was sub-standard compared to the 3D epidermal skin culture and to the EpiDermTM RHE model. Keratinocytes in a monolayer culture are not differentiated, do not present stratified layers and do not grow at ALI conditions (but rather in submersed culture medium). Therefore, these keratinocytes will behave differently from fully stratified keratinocytes that grow at ALI as real human skin. The results from the skin irritation testing have shown that monolayer culture is not suitable for skin irritation testing, since it was not able to correctly identify irritants and non-irritants.

Table 11. Cell viability results for the keratinocyte monolayer culture for skin irritation testing following TG 439. 6 non-irritant (■) and irritant (□) chemicals from TG 439 for skin irritation were tested in a keratinocyte monolayer culture in 10 donors with 30μL of the testing chemical dispensed in the cell culture supernatant. Cell viability is reported as percentage of viability for each chemical is calculated in comparison to the negative control (PBS). For each donor, chemical test was performed in triplicate and viability is reported as average of 10 independent tests with standard deviation (SD).

Chemical	% Cell viability ± Standard Deviation (SD)										
	Donor 1	Donor 2	Donor 3	Donor 4	Donor 5	Donor 6	Donor 7	Donor 8	Donor 9	Donor 10	Total 10 donors
PBS (- ctrl) ■	100.00±1.57	100.00±0.30	100.00±0.40	100.00±11.91	100.00±16.31	100.3±1.20	99.75±0.30	100.30±0.77	103.3±6.15	99.33±5.30	100.30±5.33
1-bromo-4-chlorobutane ■	13.89±0.18	15.20±0.41	15.15±0.44	24.74±2.09	80.79±7.04	29.39±9.78	34.45±4.41	25.15±0.44	34.74±2.91	74.12±6.60	32.67±22.04
allyl phenoxy-acetate ■	49.42±4.20	56.32±0.53	46.51±0.22	55.71±0.92	36.21±1.61	49.42±3.59	62.57±5.07	52.01±4.66	58.71±3.29	42.87±6.20	51.26±7.91
Isopropanol ■	16.32±0.53	16.92±1.16	19.88±4.44	18.13±3.34	20.61±0.51	33.32±4.89	40.92±4.44	35.13±3.66	38.13±2.76	26.61±5.16	26.68±9.74
4-methyl-thio-benzaldehyde ■	16.25±0.97	15.62±0.9	15.67±0.19	14.43±0.42	23.15±0.25	26.25±0.97	26.37±8.08	25.95±0.47	26.10±1.58	26.15±3.7	21.49±5.77
heptyl butyrate ■	66.63±0.51	58.86±0.24	48.71±0.09	100.10±3.10	77.91±13.59	67.63±1.32	58.86±4.24	55.46±5.46	90.11±3.10	79.58±6.00	68.55±15.74
hexyl salicylate ■	68.22±0.10	56.70±0.34	56.84±0.24	108.8±14.15	98.85±17.52	69.22±1.21	75.20±10.02	55.84±3.49	88.77±7.26	98.52±7.56	75.36±19.55
5% SDS (+ ctrl) □	9.71±0.51	12.43±0.09	13.37±1.14	6.078±0.56	11.33±0.04	9.49±0.67	16.68±5.69	15.12±2.44	8.74±2.40	13.00±2.08	11.80±3.63
1-decanol □	18.17±0.52	17.54±0.10	17.59±0.09	12.53±0.42	21.51±0.38	17.67±0.74	16.29±1.40	20.09±3.37	15.19±2.81	25.51±2.37	18.16±3.46
1-bromohexane □	15.67±0.19	17.31±0.09	17.02±0.10	33.40±11.50	35.96±8.79	17.17±1.85	18.81±2.00	19.56±3.40	40.07±7.24	39.63±5.41	24.18±10.49
di-n-propyl disulphide □	16.01±0.24	29.06±0.10	29.64±0.12	18.55±4.64	25.29±3.73	17.26±1.50	27.10±3.07	28.14±3.70	24.55±2.14	30.29±3.06	24.64±5.78
Heptanal □	20.19±0.65	29.50±0.44	29.60±0.18	28.91±3.75	35.14±10.81	21.14±1.89	27.50±2.51	29.10±5.90	35.58±2.26	38.47±8.05	28.96±6.78
Tetrachloro Ethylene □	19.57±0.8	27.38±1.172	26.17±0.19	19.34±1.38	28.16±2.98	21.32±2.16	28.38±2.69	26.42±4.60	23.01±5.00	29.83±1.17	24.94±4.31
TX-1% □	42.77±4.3	39.72±4.54	44.31±3.48	23.73±6.33	43.27±5.12	44.31±3.45	39.22±4.57	39.15±7.08	26.73±0.43	31.27±4.20	36.50±8.07

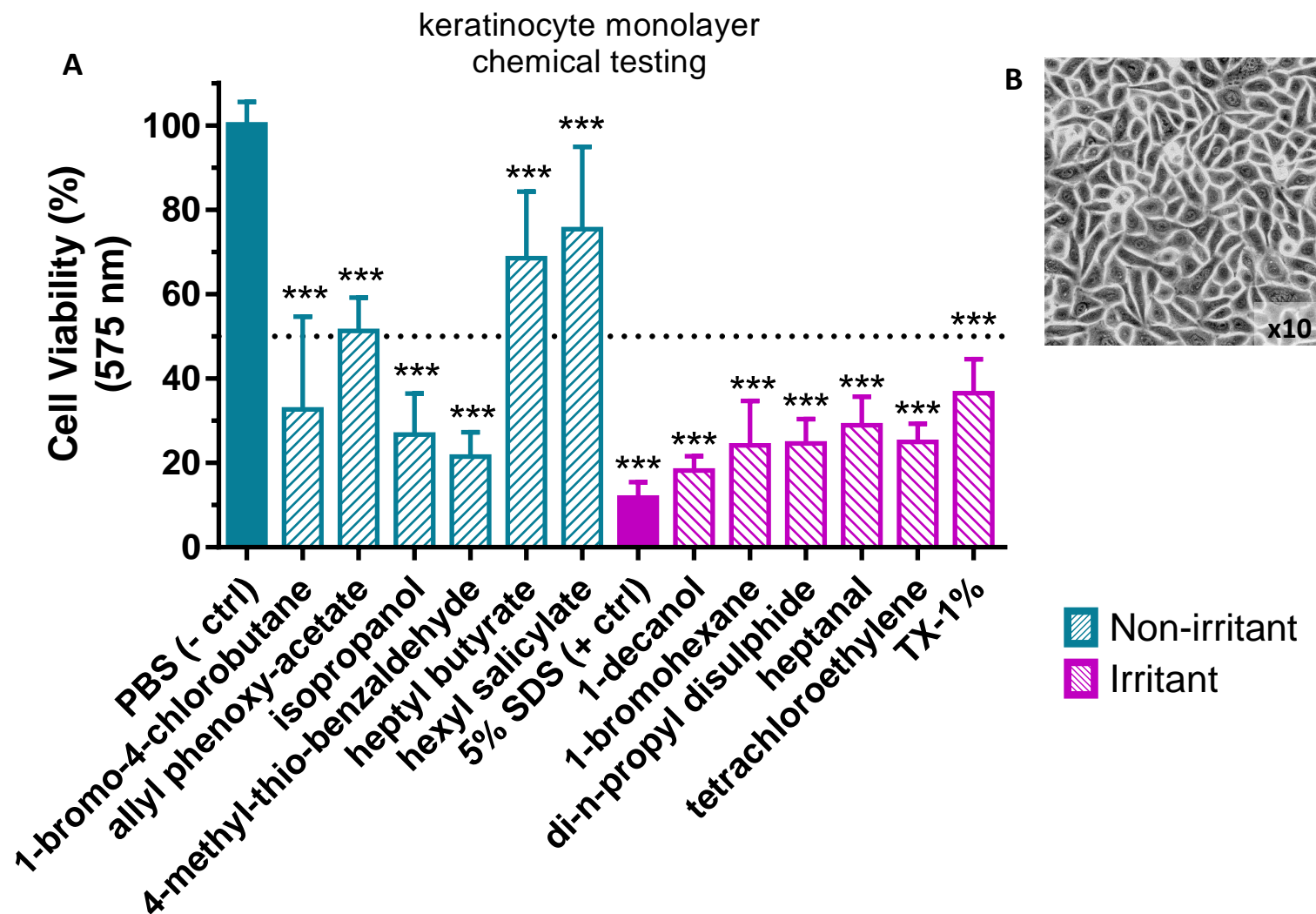


Figure 41. *In vitro* testing of TG 439 skin irritation using a keratinocyte monolayer culture. **A.** *In vitro* performance testing of a keratinocyte monolayer culture seeded at 5×10^3 keratinocytes/well (passage 3) using six non-irritants (blue striped columns) and six irritants (pink striped columns). Results are expressed as mean and standard deviation of ten independent experiments. *** $p < 0.001$ when compared to the negative control (- ctrl), PBS (blue filled column). Positive control (+ ctrl) as 5% SDS in aqueous solution (pink filled column). Dotted line represents the 50% viability threshold. **B.** Representative image of the keratinocyte monolayer culture (donor 5).

4.2.5. Skin irritation testing using a collagen-based scaffold

As mentioned in Chapter 3 section 3.2.4, the Corning® Transwell®-COL collagen scaffold (rat tail collagen-based scaffold) was used as a comparison to the Alvetex Strata. From this parallel study, skin irritation testing was also performed but on a smaller scale – 3D epidermal skin cultures were developed from keratinocytes of five donors and two non-irritants (1-bromo-4-chlorobutane and heptyl butyrate) and two irritants (heptanal and tetrachloroethylene) were tested with the negative and positive controls.

Results from the Corning® Transwell®-COL scaffold showed that this scaffold behaved poorly compared to the 3D epidermal skin culture or the monolayer culture (Table 12 and Figure 42). It failed to correctly identify the two non-irritants: 1-bromo-4-chlorobutane ($48.64 \pm 14.25\%$; $p < 0.001$) and heptyl butyrate ($47.86 \pm 22.58\%$; $p < 0.001$), showing a viability below 50% for both chemicals. However, it did correctly identify the two irritants: heptanal ($40.60 \pm 11.22\%$; $p < 0.001$) and tetrachloroethylene ($33.02 \pm 9.16\%$; $p < 0.001$), as well as the two positive controls: 5% SDS in aqueous solution ($26.47 \pm 8.67\%$; $p < 0.001$) and TX-1% ($31.28 \pm 10.83\%$; $p < 0.001$).

Table 12. Cell viability results for the collagen-coated Transwell scaffold (Corning) for skin irritation testing following TG 439. Two non-irritant (■) and two irritant (□) chemicals from TG 439 for skin irritation were tested in the collagen-coated Transwell scaffold culture in 5 donors with 30µL of the testing chemical dispensed directly on top of the skin model. Cell viability is reported as percentage of viability for each chemical is calculated in comparison to the negative control (PBS). For each donor, chemical test was performed in triplicate and viability is reported as average of 5 independent tests with standard deviation (SD).

Chemical	% Cell viability ± Standard Deviation (SD)					
	Donor 1	Donor 2	Donor 3	Donor 4	Donor 5	Total 5 donors
PBS (- ctrl) ■	99.94±0.56	100.20±0.22	99.86±0.19	100.10±0.11	101.00±1.37	100.20±0.69
1-bromo-4-chlorobutane ■	68.76±0.33	52.31±14.91	40.17±6.28	32.54±0.19	49.43±5.83	48.64±14.25
heptyl butyrate ■	49.02±0.17	38.38±9.38	32.39±1.17	31.17±0.29	88.32±10.44	47.86±22.58
5% SDS (+ ctrl) □	30.05±3.68	23.53±2.92	21.17±1.17	19.20±0.11	42.31±2.26	26.47±8.67
Heptanal □	48.26±0.17	37.01±9.83	31.12±0.72	30.36±0.11	56.27±3.95	40.60±11.22
Tetrachloro Ethylene □	32.52±0.17	30.01±2.03	27.84±2.08	25±0.13	49.72±3.09	33.02±9.16
TX-1% □	34.58±1.22	26.67±7.77	23.23±1.51	22.49±0.76	49.43±0.49	31.28±10.83

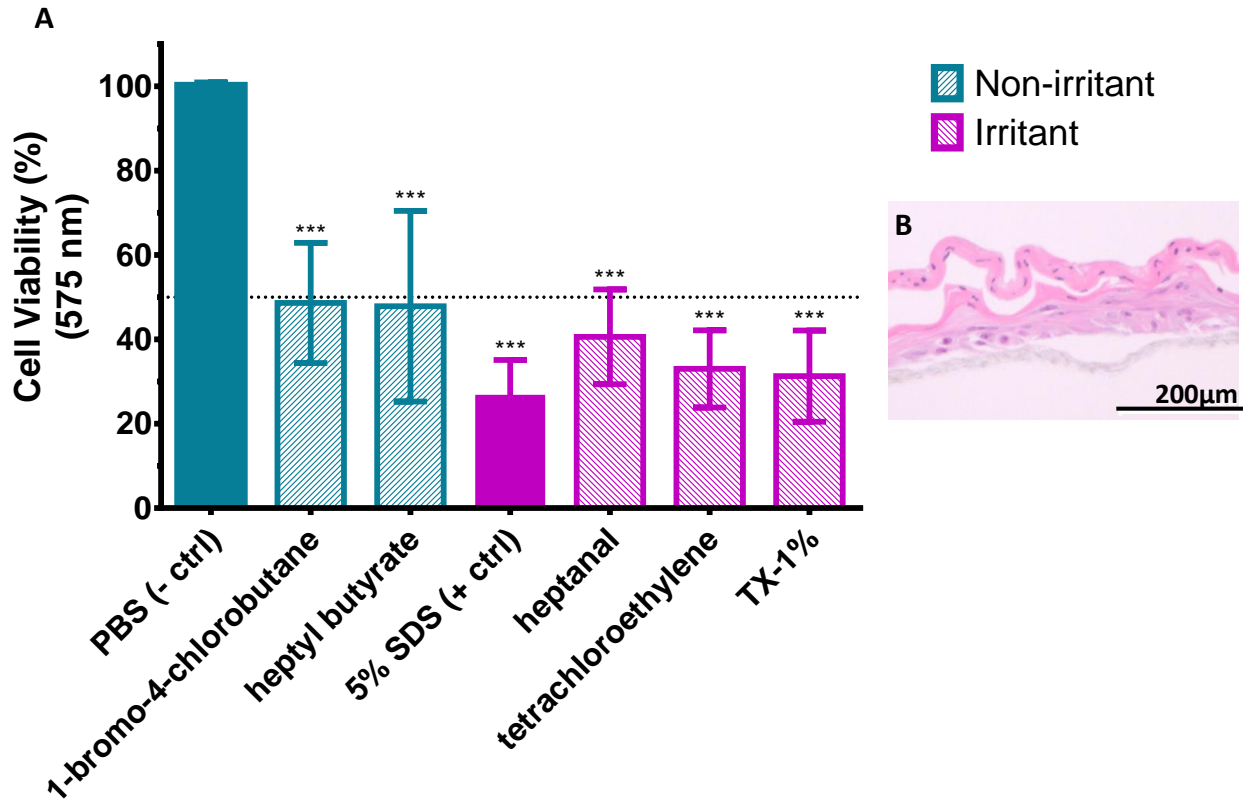


Figure 42. *In vitro* testing of TG 439 skin irritation using a collagen-based Transwell scaffold (Corning). **A.** *In vitro* performance testing of the 3D epidermal model using a scaffold coated with collagen (rat tail) for six non-irritants (blue stripped columns) and six irritants (pink stripped columns). Results are expressed as mean and standard deviation of three independent experiments. *** $p < 0.001$ when compared to the negative control (- ctrl), PBS (blue filled column). Positive control (+ ctrl) as 5% SDS in aqueous solution (pink filled column). Dotted line represents the 50% viability threshold. **B.** Representative image of the collagen-based Transwell 3D skin model (donor 5).

4.3. Performance analysis of the models for TG 439

Overall, performance results showed that the 3D epidermal skin culture could correctly determine irritants from non-irritants, matching the performance results from the commercially available RHE model validated by ECVAM for TG 439, the EpiDerm™ RHE model (Table 13).

Knowing that the keratinocyte monolayer culture was developed using the same donors as in the 3D epidermal skin culture, it would be expected that the performance outcome of both tests would be similar for each chemical. However, the keratinocyte monoculture was not able to correctly classify non-irritants as well as the 3D epidermal skin culture, identifying 3 non-irritants as false positives. These findings highlight the difference between 2D and 3D conditions, where cell differentiation and behaviour are not similar.

Table 13. OECD TG 439 results from different *in vitro* skin models. Predictive capacity of each *in vitro* assay is shown as correct classification of non-irritants or irritants (number of positive classifications from the total number of chemicals).

	Non-irritants	irritants
3D epidermal skin culture	4/6	6/6
EpiDerm™ RHE model	5/6	5/6
Keratinocyte monolayer culture	3/6	6/6
Corning® Transwell®-COL scaffold	0/2	3/3
Total	12/20	20/21

Further statistical analysis was performed to understand if classification of non-irritant and irritant from all models was performed correctly or was instead due to random classification. Null hypothesis was defined as classification between irritants and non-irritants being due to random or aleatory classification. Result from the chi-square (χ^2) test of independence showed that classification of irritants and non-irritants was accurate, as null hypothesis was rejected with $\chi^2(3) = 0.76522$, $p = 0.8578$.

However, Table 13 also shows that the *in vitro* skin models were less able to correctly classify the non-irritants than the irritant chemicals. This could be supported by the p value of each specific category - non-irritant ($p=0.227$) and irritant ($p=0.983$). The fact that classification of non-irritants had a much lower p value indicates that there is a higher probabilistic error for classification of non-irritants being accurate. This could be explained by the fact that the non-irritants tested are lacking relevant *in vivo* GHS data for proper

classification as irritants. Therefore, these results could indicate that the non-irritants tested could in fact be irritants and that the *in vitro* models were able to predict their irritancy.

To compare the predictive capacity of each *in vitro* model, a comparative two-way ANOVA was performed. Null hypothesis was defined as no significant difference between the different *in vitro* models for irritancy. The independent variables were defined as the different chemicals (all 12 tested plus the negative and positive controls) and the different *in vitro* models. The result from the two-way ANOVA showed that there was a significant difference between the irritants and non-irritants ($p=0.0396$) but not between the different *in vitro* models ($p=0.8319$) (Table 14). The statistically significant difference between the chemicals can be explained by the fact that it includes both irritants and non-irritants chemicals, which are quite different in their irritancy profile. The fact that there was no statistically significant difference between the four *in vitro* models indicates that there is not one *in vitro* model which performs better than the others. While this result suggests that the 3D epidermal skin model developed using the Alvetex Strata has an equal predictive capacity to the commercially available EpiDerm™ RHE model, it also suggests that it is similar to the keratinocyte monolayer culture, even though the keratinocyte monolayer culture correctly predicted fewer chemicals than the 3D epidermal skin culture. Further testing in a larger chemical dataset would be required to support the fact that the 3D epidermal skin model has a better predictive capacity when compared to the keratinocyte monolayer culture.

In conclusion, there results suggest that the 3D epidermal skin model developed using the Alvetex Strata could be used for assessment of skin irritation. Moreover, results also suggest that it has a similar predictive capacity to commercially available RHE models. However, further studies should be carried on in a larger cohort of keratinocyte samples to further support this evidence.

Table 14. Comparison of the predictive capacity of each *in vitro* model for prediction of irritancy. A two-way ANOVA analysis was performed including two independent variables – the chemicals (non-irritant and irritant) and the *in vitro* models. Interaction between the two independent variables was also calculated. Results from the two-way ANOVA are described as F value. Statistical significance is reported as p value < 0.05.

Independent variables of variation	Sum of squares	Degrees of freedom	F (ANOVA value)	P value
Irritants versus non-irritants	0.6944444444	1	4.62962963	0.039596819
<i>In vitro</i> models	0.055555556	2	0.185185185	0.831893053
Interaction between chemicals and <i>in vitro</i> models	0.388888889	2	1.296296296	0.288426527

4.4. Discussion of the results

This chapter intended to show the predictive capacity of the 3D epidermal skin culture for skin irritation testing following OECD TG 439.

Performance standards from the OECD TG 439 state that the ability of a 3D skin model to distinguish between irritants and non-irritants can only be possible due to proper barrier function of the stratum corneum. Skin irritation testing results from the 3D epidermal skin culture cultured at different ALI times (Figure 38) perfectly reflects this problem, as the 3D epidermal skin culture at 14 days of ALI was not able to correctly identify the positive controls as irritants. If considering the histology results from Chapter 3, this 3D construct presented a poor epidermal layer, hence no proper epidermal barrier. Consequently, skin irritation testing of this 3D construct failed to predict irritant chemicals.

On the contrary, results from the 3D epidermal skin culture cultured for 30 days at ALI showed that the 3D construct was able to distinguish PBS as a non-irritant and 5% SDS as an irritant, due to its properly formed stratum corneum. Further justification regarding the quality of the stratum corneum of the 3D epidermal skin model was the fact that this model correctly predicted 4 out of 6 non-irritants and 6 out of 6 irritants. These results highlight the quality of the barrier function of the stratum corneum from the 3D epidermal skin culture, as only 2 non-irritants were classified as false positive. Damage to the epidermis was only caused by the irritant chemicals, which were able to penetrate the stratum corneum layer.

While not stated in the OECD Testing Guideline 439 for skin irritation, other complementary studies of barrier function could be performed to further assess its integrity as barrier integrity is vital for the physiological activities of the skin tissue (*in vivo*) and skin models (*in vitro*). For example, Transepithelial/transendothelial electrical resistance (TEER) is a widely accepted method for assessment of the barrier integrity of skin models, as it measures the integrity of the cell's junctions between the different skin layers through electrical resistance (ionic conductance). Strong tight junctions will result in proper barrier integrity for assessment of chemical permeability studies (Alexander Jr, Eggert, & Wiest, 2018). Additionally, this method could be used in combination with the TG 439 skin irritation testing, as TEER is a non-invasive method that can be applied to live cells. Further optimization would be required to adapt TEER for assessment of barrier integrity using the 3D epidermal skin culture developed with the Alvetex Strata, but collection of those results would only strengthen validation of the 3D epidermal skin culture as an *in vitro* RHE model for assessment of human safety.

Alternatively, it could also be combined with a different Testing Guideline, TG 428 for skin absorption studies (OECD, 2004). Briefly, TG 428 describes a diffusion cells mechanism in which the testing chemical is applied to a skin sample in the donor chamber and expected to be absorbed through the receptor chamber. This absorption is measured during a given time and calculated as the difference between the quantity of chemical present in the receptor chamber (percentage recovery of absorbed chemical) and the quantity of chemical in the donor chamber (percentage of not absorbed chemical) (Bartosova & Bajgar, 2012).

While this TG might not be applicable for testing of all irritant and non-irritant chemicals described in TG 439 for skin irritation, it can still be used as an initial qualitative evaluation of skin penetration of these chemicals. Once again, optimization using the 3D epidermal model with the Alvetex Strata would have to be performed to guarantee integrity of the 3D structure of the skin layers throughout the assay since the TG is described using excised skin samples.

Combination of TG 428 for skin absorption with TG 439 for skin irritation could be of special importance to understand the chemical properties of each testing chemical and maybe shed some light on the incorrect identification of 2 non-irritant chemicals - 1-bromo-4-chlorobutane and 4-methyl-thio-benzaldehyde. Overall, all *in vitro* assays were able to correctly classify all irritants, but some non-irritants were classified as false positives. It may be argued that with regards to human safety testing, it would be better to “over” predict rather than “under” predict skin irritation. Therefore, the 3D epidermal skin culture model was able to correctly predict all irritants and could be regarded as a sensitive *in vitro* assay for skin

irritation testing. The fact that two non-irritant chemicals were wrongly classified as false positives, 1-bromo-4-chlorobutane and 4-methyl-thio-benzaldehyde, could be justified by the fact that all chemicals were tested in the same culture plate. As so, volatile fractions from the most hazardous skin irritants (as the case of tetrachloroethylene that releases a strong odour) could negatively influence the outcome of the non-irritant chemicals. This hypothesis could help justify the results, but further analysis should be carried out to better understand the impact of volatile fractions in skin irritation testing.

Regarding within-donor variability, the 3D epidermal skin culture model did not present significant standard deviations to the average percentage of cell viability. However, the keratinocyte monolayer culture using the same donors presented some standard deviation to the average value. Considering that both *in vitro* assays were performed using the same donor cells, the standard deviation results indicate that a monolayer cell culture would not perform as well as a 3D skin model in skin irritation testing. This hypothesis is of crucial importance for quality control standards defined in TG 439, in which states that the *in vitro* test should have physiological resemblance to epidermal skin with proper differentiation of the stratum corneum layer. However, statistical analysis carried on evaluating the predictive capacity of each *in vitro* model showed that the *in vitro* models were able to correctly classified each chemical (as opposed to random classification) and that there was no significant performance difference between the *in vitro* models. It is important to take into consideration that these results are representative of a small chemical range and it is vital to repeat this in a larger cohort of samples with a larger chemical dataset. Only then with the proper statistical power, would the results undoubtedly support the use of the 3D epidermal skin culture for skin irritation purposes. Eventually, this would help promote the performance capacity of the 3D epidermal skin culture over the keratinocyte monolayer culture. Likewise, it would support the high-quality control standard of the 3D epidermal skin culture model, as vital pre-validation data for official EURL-ECVAM validation.

In conclusion, all results presented in this chapter demonstrate that the 3D epidermal skin model is in concordance with OECD TG performance standards for skin irritation and could be used for skin irritation studies. Proper ECVAM validation for skin irritation testing would require intra- and inter-lab cross-reproducibility studies.

CHAPTER 5

**Use of Skimune® for testing the immunotoxicity of aggregated
and non-aggregated monoclonal antibodies**

5. Immunotoxicity by aggregated monoclonal antibodies

5.1. Aim

Skimune® is already established as an *in vitro* assay for assessing skin sensitization potential to chemicals (Ahmed et al., 2016). We have further advanced in this work by using the modified Skimune® assay for monoclonal antibodies, the Skimune® Mab.

In this chapter, we describe the Skimune® assay as possible application for testing the immunotoxicity of aggregated monoclonal antibodies. We investigated the influence of aggregated monoclonal antibodies by observing *in vitro* immune responses using two commercially available monoclonal antibodies. Both antibodies were subjected to heat stress conditions to induce aggregation followed by characterization of protein content as well as comparison of potential immunogenic profiles. Immune activation was assessed by testing the heat stressed mAbs samples in the skin explant assay and determining T cell proliferation responses, observing histopathological damage in the skin, measuring cytokine release and observing for cell death activation.

5.2. Results

5.2.1. Skimune® for assessment of immunotoxicity to mAbs (native form)

Three mAbs and one glycoprotein (provided by FUJI) (Table 15) were used for assessment of immunotoxicity using the Skimune® Mab skin explant assay. The compounds were tested at 1 and 10µg/mL concentration.

Table 15. Technical information of the testing compounds provided by FUJI.

Testing compound	Class and type	Target	Proof for immunogenicity
anti-CD20	IgG1 antibody	Commercially available as Rituximab, is a pharmaceutical drug for the treatment of haematological cancers. It inhibits B cell activation in early stages of cancer development by binding to CD20 protein (thus inducing cell apoptosis) (Smith, 2003);	Very rare cases of cell death (Kimby, 2005) and serum sickness (Guenno, Ruivard, Charra, & Phillipe, 2011)
anti-B72.3	antibody	Is a tumour-associated protein (TAG 72.3) mAb used for diagnosis purposes – tumour cells have a selective reactivity for TAG 72.3, being characteristically over-expressed in breast, gastro-intestinal and gynaecologic cancers. Thus, anti-B72.3 mAb is widely used as a differential diagnosis tool for the diagnosis of neoplasms, especially before surgical resection (by immunohistochemistry) (Guadagni et al., 1996);	None (is used as diagnosis tool)
recombinant Anti-TNF-α	antibody	Is a Tumour necrosis factor- α (TNF) antibody, designed to suppress the action of TNF- α during inflammatory response (Prado, Bendtzen, & Andrade, 2017).	Can lead to formation of anti-drug antibodies (ADA), causing hypersensitivity (Bendtzen, 2012)
Lactoferrin	glycoprotein	large glycoprotein (around 80kD) from the transferrin family that can be found in milk, saliva and nasal secretions. It has antimicrobial properties, especially for infants during breast feeding. Its primary role is to capture free iron, not allowing bacteria to use it as a growth requirement (Almond et al., 2013; Almond, Flanagan, Kimber, & Dearman, 2012).	Wild type lactoferrin elicits IgE response (as in food allergy). Recombinant form is not so aggressive (Almond et al., 2013).

T cell proliferation assay was used to measure the proliferative capacity of the cells in response to exposure to the testing compounds, by thymidine incorporation per cell division for each test condition. Threshold for mAb-induced immune activation was defined as log(2)-fold increase in the T cell proliferation response, as reported elsewhere (Rombach-Riegraf et al., 2014). Supernatants from all test conditions were collected for cytokine release analysis.

OKT3 as a positive control for T cell proliferation caused significant cell activation above the log(2)-fold threshold ($p < 0.05$), with a 3-fold increase response. On the contrary, IgG1 as the isotype control showed no significant T cell proliferation above the log(2)-fold threshold.

No major significant increase of T cell proliferation was observed in response to any of the mAb or glycoprotein concentrations (Figure 43) as all concentrations failed to reach above the log(2)-fold threshold.

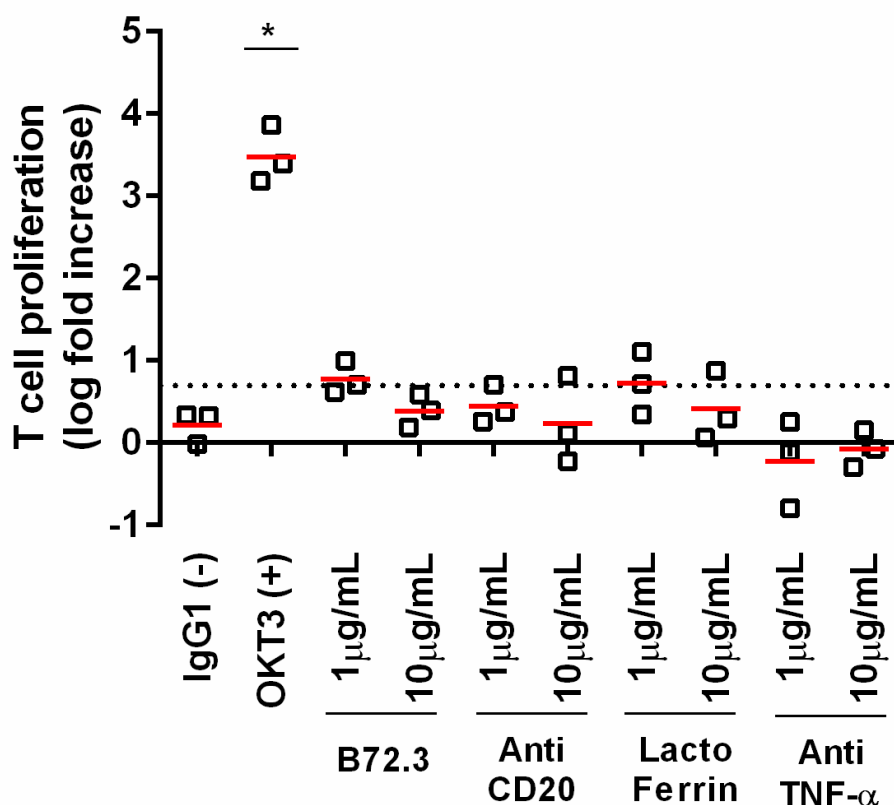


Figure 43. T cell proliferation following exposure to mAb samples. PBMCs were exposed to Anti-B72.3, Anti-CD20 and Anti-TNF- α antibodies and LactoFerrin at 1 and 10 μ g/mL and assessed for cell proliferation by the 3 H-Thymidine uptake assay. Immune activation threshold was positive if it was regarded as log(2)-fold increase in the T cell proliferation results (dotted line) *p < 0.05. Mean values represented by the red line.

The lack of T cell proliferation is not unsurprising considering the function of these compounds. Anti-B72.3 mAb is a diagnostic marker for tumour cells and therefore, would not cause any major reaction of the immune system. Anti-CD20 mAb is a pharmaceutical mAb for haematological cancers, targeting B cells only by binding to their CD20 antigen receptor. However, a recent study has shown that T cells also express CD20 receptor at a low expression level and that anti-CD20 antibodies (such as Rituximab and Ocrelizumab) can effectively eliminate T lymphocytes with CD-20 expression (Palanichamy et al., 2015). Nevertheless, this would only represent a small fraction of the total T cell pool and therefore, no major T cell depletion or activation would be likely upon exposure to the anti-CD20 antibody. Anti-TNF- α mAb is a neutralizing antibody against TNF- α , downregulating its pro-inflammatory effect (Prado et al., 2017). Therefore, this mAb should have a negative effect on the immune cells, and this can be observed from the T cell proliferation results. Regarding Lactoferrin, this glycoprotein is known to modulate the inflammatory response against microbial infections by

direct competition with the lipopolysaccharides (LPS) binding site, preventing activation and proliferation of monocytes (Baveye, Ellass, Mazurier, Spik, & Legrand, 1999). As a key modulator of the immune response, Lactoferrin is not expected to induce any type of cell activation. The T cell proliferation results were in concordance with this aspect, as no significant increase of T cell was observed for Lactoferrin.

In line with the T cell proliferation assay, the skin explant assay was also performed in the same donors for assessment of immunotoxicity by the testing compounds from FUJI. The same four healthy donors from the T cell proliferation assay were tested for each mAb concentration and the histopathological damage was assessed according to Lerner scoring scale (Lerner et al., 1974). This scoring system is based on characterization of skin damage by visual appearance of vacuoles or separation of the skin layers. It ranges from a score I (negative score) to a score IV (maximum score for damage). The complete description for each score is the following: score I for intact upper epidermis layer, score II for minor vacuolisation of the skin, score III for start of separation between epidermis and dermis layers and score IV for complete separation of the skin layers (Figure 44).

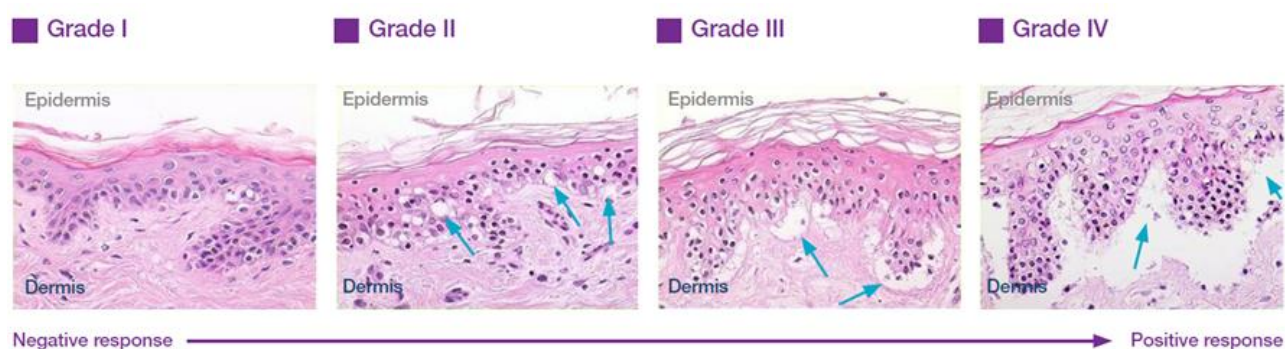


Figure 44. Grading score for assessment of skin damage using the Skimune® skin explant assay. The endpoint is a grading score of histopathological damage: score I (intact upper epidermis layer), score II (minor vacuolisation of the skin), score III (start of separation between epidermis and dermis layers) and score IV (complete separation of the skin layers).

Results from the Skimune® Mab for skin damage showed that OKT3 as a positive control showed significant positive damage, with a consistent grade II response in all 5 donors. For B72.3 and CD20 mAbs, the results from the skin explant assay matched with the results from T cell proliferation assay, as no major histopathological damage was observed (Figure 45). B72.3 only caused a weak grade II damage in 2 out of 5 donors at 1µg/mL and in 1 out of 5 donors at 10µg/mL. All remaining donors presented a negative grade I. Similarly, CD20 only caused a weak grade II damage in 1 out of 5 donors at 1µg/mL. All donors at 10µg/mL presented a negative grade I.

However, in the case of Lactoferrin and Anti-TNF-α significant positive damage was observed at 10µg/mL, with a grade III response in 4 out of 5 donors. Moreover, and while not statistically significant, Lactoferrin and Anti-TNF-α caused a grade II damage in all 5 donors at 1µg/mL. This is considered a weak positive damage response.

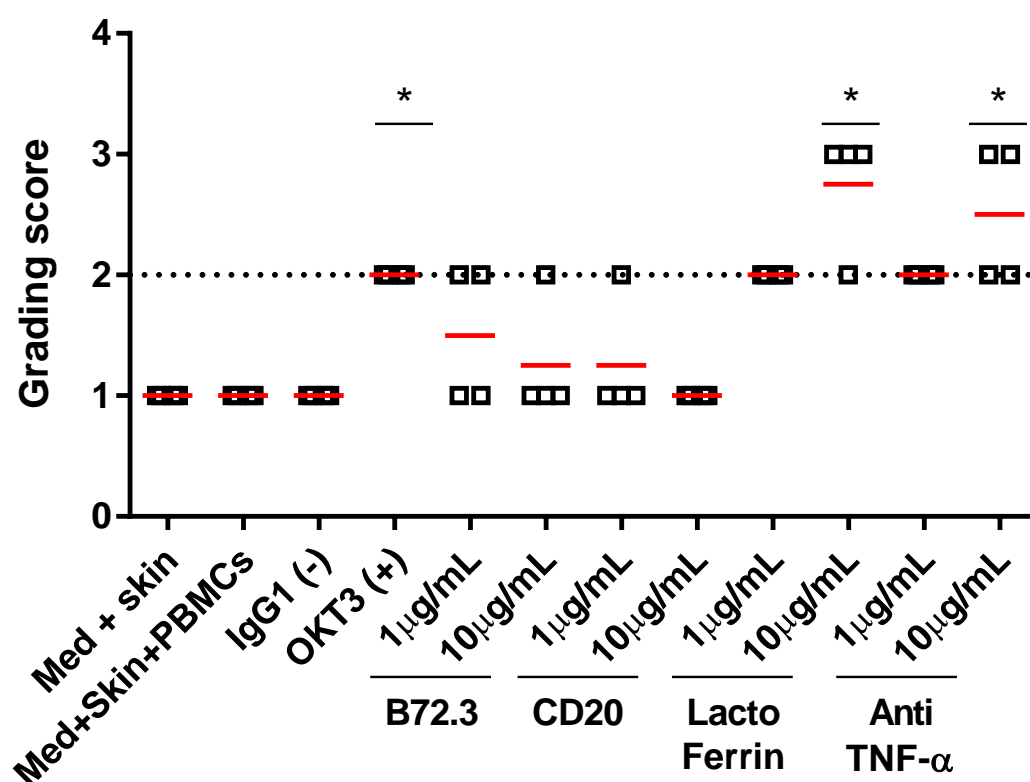


Figure 45. Skimune® Mab result with testing of biopharmaceutical compounds. Three monoclonal antibodies (Anti-B72.3, Anti-CD20 and Anti-TNF-α) and 1 glycoprotein (LactoFerrin) were tested at 1 and 10µg/mL with the Skimune® Mab assay in 5 donors for assessment of immunogenicity. Output of assay is measured as grading score of histopathological damage ranging from I to IV. Mean values represented by the red line.

Overall, B72.3 and CD20 mAbs did not cause any significant T cell proliferation response or histopathological damage in the skin assay at 1µg/mL and 10µg/mL concentration. At

1µg/mL, Lactoferrin and Anti-TNF-α caused a weak positive grade II histopathological damage that escalated to a grade III damage at 10µg/mL in the same donors. However, T cell proliferation responses from Lactoferrin and Anti-TNF-α showed no positive activation of cells.

The fact that weak positive skin damage was observed for both Lactoferrin and Anti-TNF-α testing conditions could be linked to the general storage condition of these testing compounds. These compounds were provided by a consortium partner so no specific storage information was given (i.e. long-term or short-term storage), except that the compounds were kept at -20°C. One could argue that long-term storage could affect the primary structure of the monoclonal antibodies, possibly even inducing aggregation. However, this hypothesis would have to be further tested with protein analysis studies like similar to the ones performed for the heat stressed monoclonal antibodies (section 5.2.2.1). Nevertheless, the fact that the skin explant assay was able to detect histopathological damage, while T cell proliferation response was not increased supports the predictive role of this skin explant assay for assessment of immunotoxicity to novel compounds, showing that it is a more sensitive test.

Ultimately, four biopharmaceutical compounds from FUJI were tested for immunogenicity using the skin explant assay and T cell proliferation assay. Results showed that Anti-B72.3 and Anti-CD20 had little to no immunotoxic profile, at both low (1µg/mL) and high concentrations (10µg/mL). Regarding Anti-TNF-α and Lactoferrin, they also presented a weak immunotoxic profile at 1µg/mL that increased considerably at 10µg/mL, causing significant immune damage. Comparing the two *in vitro* assays, the skin explant assay proved to be a more sensitive and accurate assay for assessing immune damage than the T cell proliferation assay as it was able to predict immunotoxic damage by Anti-TNF-α and Lactoferrin while T cell proliferation assay showed no significant increase.

5.2.2. Skimune® for assessment of immunotoxicity to aggregated mAbs

In this study, two therapeutic antibodies – Rituximab (chimeric IgG1 mAb) and Herceptin (humanized IgG1 mAb), were exposed to a heat stress protocol. The testing temperatures were intended to mimic storage conditions at 4°C, normal physiological temperature (37°C) and elevated body temperature during an infectious episode (40°C). These stress conditions ensured that mAb degradation reflects inadequate storage conditions rather than industrial manufacturing.

5.2.2.1. *Protein analysis of the stressed mAb samples*

To determine the protein content of the heat stressed mAb samples, the aggregated samples were analysed by SV-AUC. Only the extreme testing conditions were analysed, at the following time points: 4°C for 0 hours, 37°C for 48 hours, 40°C for 48 hours and 65°C for 1 hour (positive control for aggregation). Overall, the loss of monomers by heat stress was found to be very low, with up to 4% aggregation of the total protein content (Table 16). This result is in concordance with previously reported studies, where a low level (<3%) of total protein content was reported as aggregated (Ahmadi, Bryson, Cloake, Welch, Filipe, Romeijn, Hawe, Jiskoot, Baker, et al., 2015).

Considering 4°C for 0 hours as the baseline condition, more than 97% of the protein content was found in the monomer form in both heat-stressed Rituximab and Herceptin. For Rituximab, there was no major variation in the monomer content throughout the heat stress protocol, since at 37°C for 48 hours there was 97.38% monomer content and at 40°C for 48 hours there was a 97.73% overall monomer content. Dimer content at baseline was shown to be 1.14% of the overall protein content, with a small increase to 1.61% after 48 hours at 37°C and 1.15% after 48 hours at 40°C. For the larger molecules, e.g. trimers, tetramers and heavier molecules, there was a small increase from 0.93% at baseline to 1.48% after 48 hours at 37°C and 1.44% after 48 hours at 40°C. For Herceptin, the decrease of monomer content was more evident. Starting from 97% monomer content at baseline, the monomer content reduced to 94.8% after 48 hours at 37°C and to 95.51% after 48 hours at 40°C. Correspondingly, the dimer content increased from 1.701% at baseline (0 hours at 4°C) to 2.854% after 48 hours at 37°C and to 2.611% 48 hours at 40°C. There was also an increase in the appearance of larger molecules, ranging from 0.468% at baseline to 2.653% after 48 hours at 37°C and to 1.929% after 48 hours at 40°C.

Size distribution of the sedimentation velocity of the aggregated Rituximab (Figure 46) and Herceptin (Figure 47) showed a good distribution of the monomer, dimer and larger molecule forms across the different temperature ranges. Size-distribution showed most monomeric species sedimented at 6.3S with a molecular weight of 152 kDa when present in solution, alongside some dimeric species. These dimeric species had different stoichiometry with both elongated configuration and sedimentation close to 8S and more globular configuration with sedimentation just below 10 S. At 37°C, even larger species were observed with sedimentation up to 15S. This change in protein size reflected the heat stress causing the mAb to become heavier as it aggregated. As a result, the sedimentation velocity increased when compared to non-aggregated samples.

The internal positive control for aggregation (65°C incubation for one hour in acidic conditions) aggregated very easily, as expected, with 73% content of larger molecules for Rituximab and 69% for Herceptin. Size-distribution of this control showed a lower number of monomer content and an increased number of trimers, tetramers and larger molecules (up to 10-15mers), demonstrating the more aggregated state of this sample.

Overall, the results from the SV-AUC showed that Rituximab was not as susceptible to thermodynamic changes as Herceptin, indicating to be a more stable monoclonal antibody. This was because only Herceptin showed variation in content of monomer, dimer and large structure molecules throughout the heat stress protocol. These results correlate with the outcome predicted by the Bayesian model (red dotted line) calculated by the SEDNTERP software. Standard deviation calculated by the root mean square deviation (RMSD) values showed no major differences between observed and expected results.

Table 16. Quantification of aggregated content of heat-stressed mAb samples by analytical ultra-centrifugation.

Absorbance data										
	Temp (°C)	time (h)	monomer			dimer			Larger molecules	RMSD
			sedimentation (S)	Mass (kDa)	%	sedimentation (S)	Mass (kDa)	%	%	
Rituximab	4	0	6.412	152.1	97.92	9.25	263.653	1.14	0.93	0.015
		48	6.415	138.3	97.72	9.715	257.707	1.7	0.58	0.017
	37	0	6.411	153.4	96.16	9.089	258.781	2.69	1.15	0.014
		3	6.411	149.9	97.41	9.27	274.93	1.68	0.91	0.013
		6	6.408	152.5	96.88	9.19	261.938	2.07	1.05	0.011
		12	6.413	149.3	96.69	9.522	270.064	2.28	1.11	0.010
		24	6.426	146.8	99	-	-	-	1	0.018
		48	6.424	148.3	97.38	8.34	229.272	1.61	1.48	0.014
	40	0	6.415	153	97.26	9.042	262.435	2.23	1.24	0.016
		3	6.407	147.4	98.34	8.997	262.004	1.18	1.3	0.017
		6	6.399	149.5	98.16	8.768	249.582	1.15	1.04	0.017
		12	6.397	155.3	98.40	-	-	-	1.60	0.017
		24	6.425	150.3	97.38	9.461	281.061	1.32	1.42	0.018
		48	6.42	147.6	97.73	9.649	281.75	1.15	1.44	0.016
	65	1	1.587	13.11	0.706	6.503	108.75	2.544	73.01	-
Herceptin	4	0	6.441	149	97.96	9.432	263.977	1.701	0.468	0.010
	37	48	6.427	148.1	94.8	9.109	249.839	2.854	2.653	0.010
	40	48	6.421	148.1	95.51	9.235	255.364	2.611	1.929	0.011
	65	1	6.346	132.6	2.661	9.862	256.928	6.107	69.246	0.010

Quantification of monomers, dimers, and larger molecules in Rituximab and Herceptin monoclonal antibodies (at 1 mg/mL) after exposure to a heat-stress protocol (4, 37 and 40°C for 0, 3, 6, 12, 24 and 48 hours). Quantification by sedimentation velocity (S), mass (kDa) and percentage in overall mAb sample (%). Standard deviation calculated as Root Mean Square Deviation (RMSD). Missing values (-).

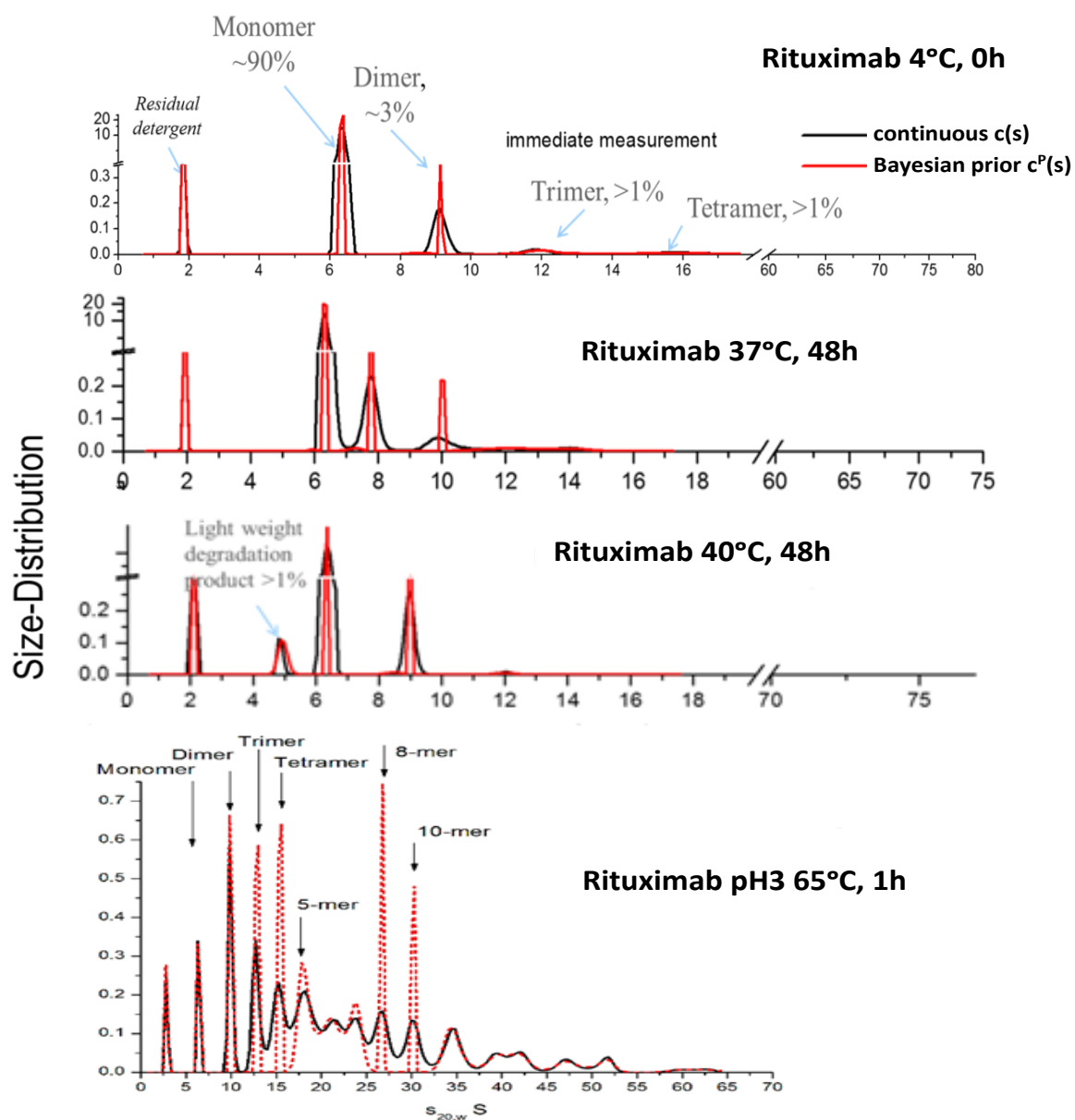


Figure 46. Size distribution of the heat-stressed aggregated samples of Rituximab. Quantification of the aggregation state of heat stressed Rituximab sample by analytical ultra-centrifugation for 4°C for 0 hours; 37°C for 48 hours; 40°C for 48 hours and 65°C for 1 hour (black line). The results fit the Bayesian prediction model (red dotted line). Monomer species at around 6S with elongated dimers appearing at 8S and globular dimers appearing at 10S.

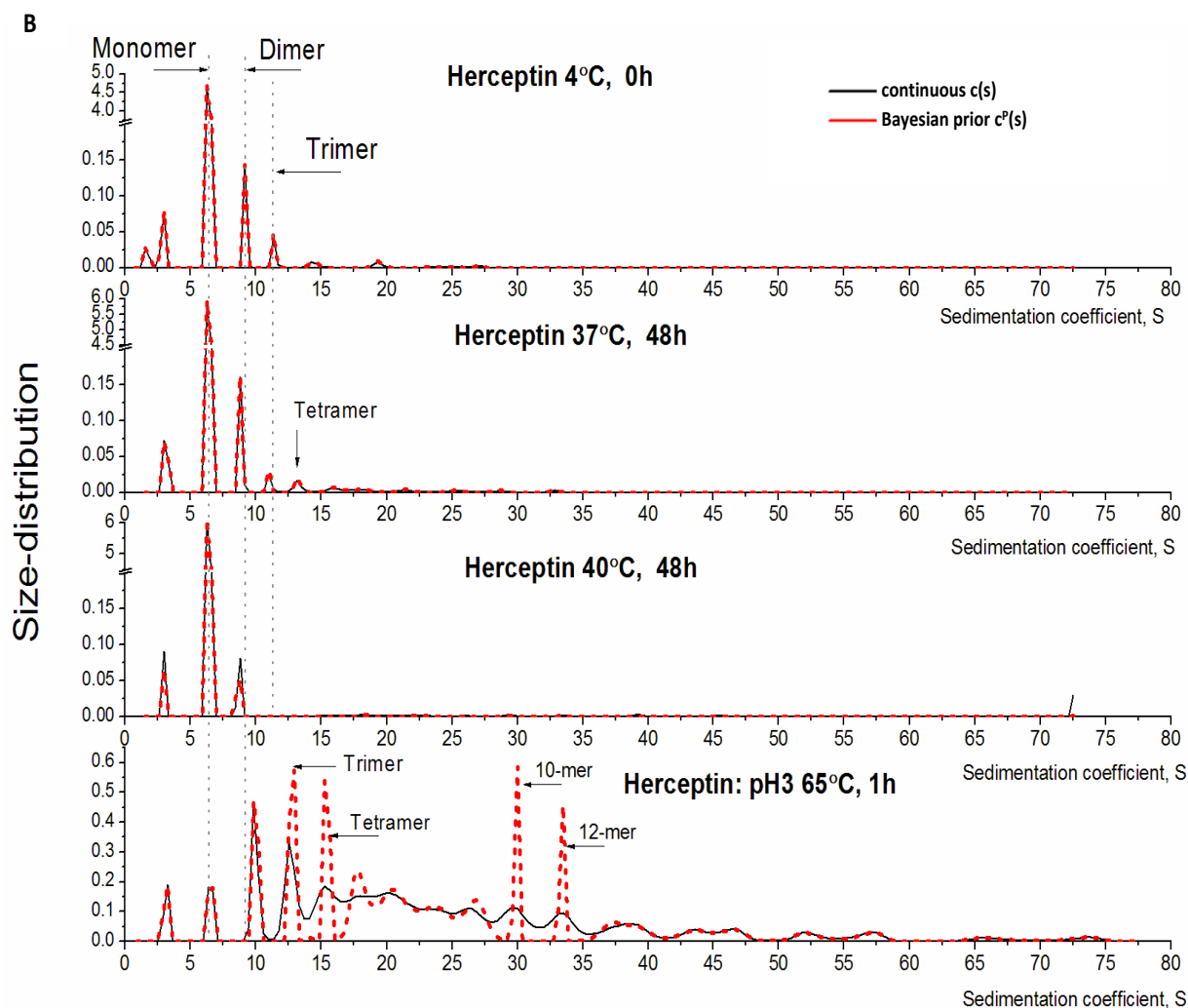


Figure 47. Size distribution of the heat-stressed aggregated samples of Herceptin. Quantification of the aggregation state of heat stressed Herceptin sample by analytical ultra-centrifugation for 4°C for 0 hours; 37°C for 48 hours; 40°C for 48 hours and 65°C for 1 hour (black line). The results fit the Bayesian prediction model (red dotted line). Monomer species at around 6S with elongated dimers appearing at 8S and globular dimers appearing at 10S.

5.2.2.2. *Visual characterization of the aggregates*

Transmission Electron Microscopy (TEM) allows for the visual characterization of the aggregated heat stressed mAb samples and provides a more qualitative analysis of aggregation.

Compared to the blank grid, loading of mAb samples to the grid showed visible microscopic particles that were regarded as small aggregates (Figure 48). TEM results showed that the higher the temperature (from 4°C to 65°C), the more visible are the microscopic aggregates caused by heat stressed mAb samples. The unstressed mAb samples at 4°C contain almost no microscopic particles, whereas the heat stressed samples at 40°C showed small aggregates as black masses scattered through the grid (indicated by white arrows). The amount of detectable aggregates was greater in the positive control for aggregation at 65°C, as confirmed by the previous results of protein analysis.

Together, TEM and SV-AUC indicate that heat stress modified the secondary structure of the mAb and promoted low levels of aggregation. Furthermore, the intensity of the heat stress protocol, as in the case of the positive control at 65°C, exacerbated the level of aggregation.

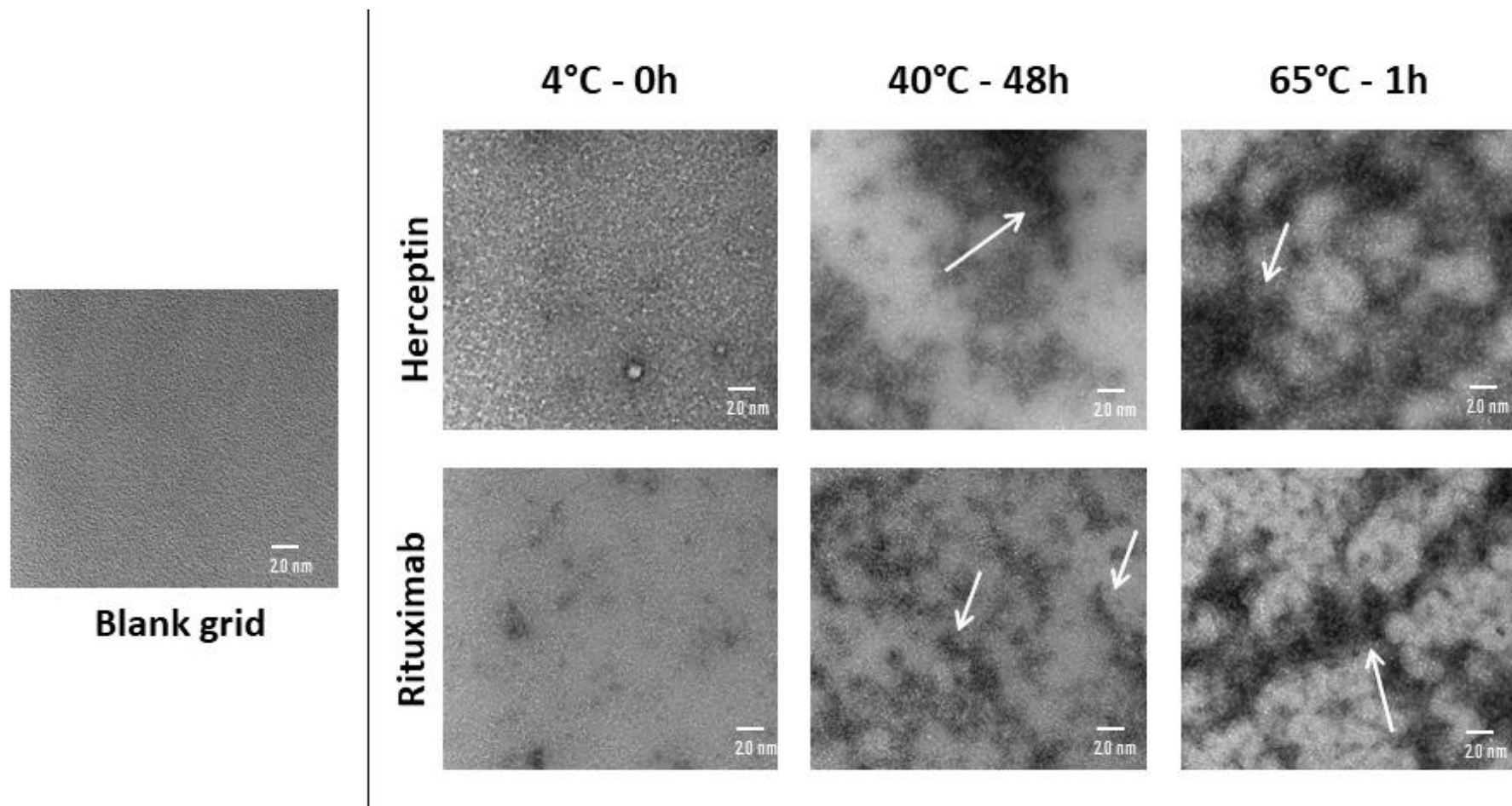


Figure 48. Visual characterization of two heat-stressed mAb samples by TEM. Comparison of aggregation status of two mAbs, Rituximab and Herceptin, after a heat stress protocol (indicated by white arrow). Scale bar of 2.0 nm is similar in all testing conditions.

When comparing the protein content of both heat stressed mAbs, heat stressed Herceptin showed a slightly increased aggregation level compared to Rituximab. Differences in the primary sequence of these mAbs may explain the differences in the degree of aggregation, since Rituximab is a chimeric mAb and Herceptin is a humanized mAb (Obrezanova et al., 2015).

5.2.2.3. *Aggregated mAb samples induce immune activation*

In view of the observations that heat stress can alter mAb structure and induce aggregation, it was important to understand if this aggregation could lead to immunotoxic events during mAb administration to patients. The effect of the heat stressed mAbs on immune activation was assessed by a human skin explant assay, T cell proliferation and cytokine release assays. PBMCs and skin biopsies from five healthy donors were stimulated with heat stressed aggregated samples of Rituximab and Herceptin (at 1 and 10µg/mL) and assessed for increased immune activation.

Responses in the skin explant assay showed tissue damage in response to both aggregated Rituximab and Herceptin samples (Figure 49). Using Lerner's skin damage classification system, positive skin damage is considered a grade II or higher (Figure 50). At a concentration of 1µg/mL, Herceptin caused significant tissue damage ($p<0.05$) with grade III damage in three out of five donors at the 40°C testing condition for 48 hours, when compared to the negative control (Figure 49). Herceptin tested at 4°C and 37°C, caused either a negative grade I or weak positive grade II skin damage, which was not statistically different from the negative control. At a concentration of 10µg/mL, Herceptin caused significant tissue damage when tested at 40°C for 48 hours ($p<0.05$), with grade III skin damage being observed in four out of five donors. OKT3 was the positive control and caused significant grade III skin damage at both 1 and 10µg/mL. The positive control for aggregation (pH=3) caused a grade II damage response in three out of five donors at both 1µg/mL and 10µg/mL and a grade III damage response in one out of five donors at 10µg/mL. While still considered to be positive for skin damage, it fails to be statistically significant from the negative control.

At 1µg/mL, Rituximab did not cause any significant skin damage as all temperature testing conditions caused either a negative grade I or weak positive grade II skin damage response and responses were not significantly different from the negative control. OKT3 caused significant damage ($p<0.05$), with a grade II response in three out of five donors and a grade III response in one donor. At 10µg/mL, Rituximab tested at 40°C for 48 hours caused a positive grade III skin damage response in three out of five donors.

The fact that Herceptin caused significant skin damage at both 1 and 10µg/mL while Rituximab only caused significant damage at 10µg/mL, suggested aggregated Herceptin and Rituximab have different immunotoxic potency profiles due to their aggregation levels. This also links in with the protein analysis results, where the reported monomer content for Herceptin was lower than for Rituximab meaning higher aggregation levels. Consequently, Herceptin caused more histopathological damage than Rituximab.

These results corroborate previous findings done in cell activation assays, where Herceptin was shown to cause higher rates of immune activation than Rituximab by activation of CD4⁺ T cells (Ahmadi, Bryson, Cloake, Welch, Filipe, Romeijn, Hawe, Jiskoot, & Fogg, 2015).

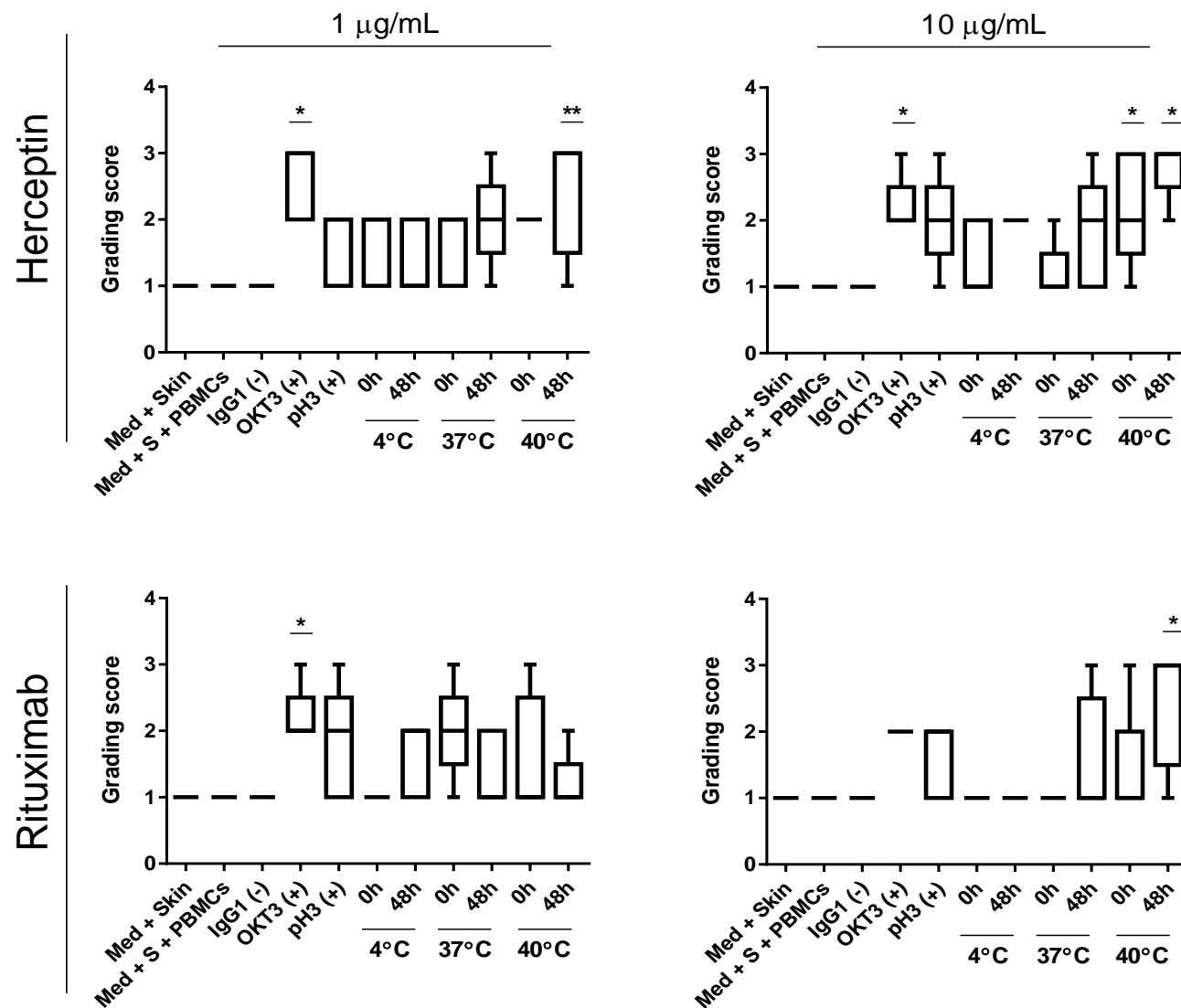


Figure 49. Skin explant assay results from exposure to heat stressed mAb samples. Heat stressed samples of Herceptin and Rituximab (1 and 10µg/mL) were incubated with PBMCs and autologous skin biopsies from 5 healthy donors for the skin explant assay. Score of the histopathological damage ranges from grading score I to IV. *p<0.05; **p<0.01

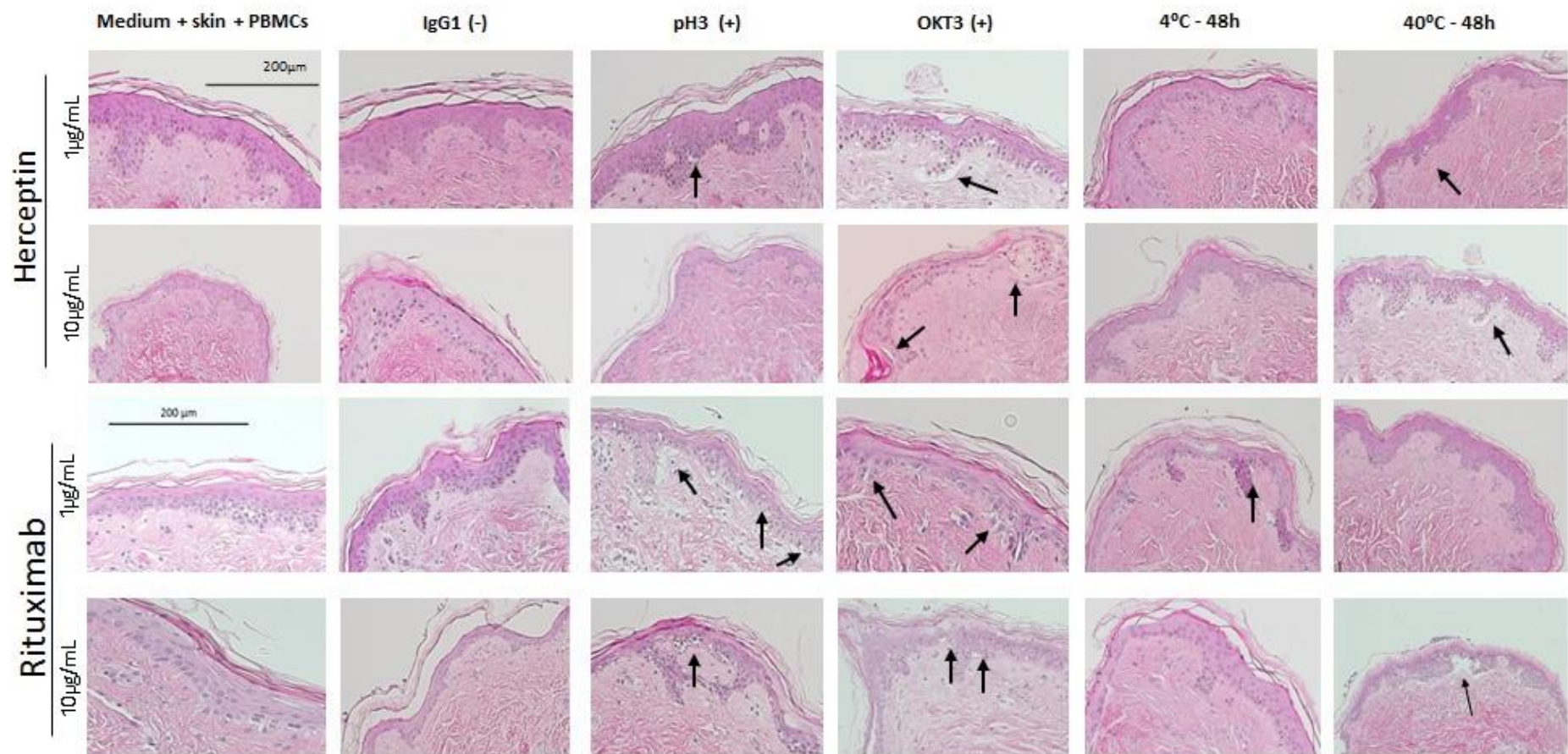


Figure 50. Histopathological damage from exposure to heat stressed mAb samples. H&E staining of the skin explant after incubation with the heat-stressed samples of Herceptin and Rituximab at 1 and 10 µg/mL. Black arrows represent histopathological damage of the skin. Scale bars represent 200 µm. The endpoint is a grading score of histopathological damage: score I (intact upper epidermis layer), score II (minor vacuolisation of the skin), score III (start of separation between epidermis and dermis layers) and score IV (complete separation of the skin layers). Scale bar of 200 µm from negative control is representative and similar in all testing conditions.

The T cell proliferation assay showed no significant increase in T cell proliferation responses upon exposure to aggregated Herceptin and Rituximab (Figure 51) in any of the testing conditions. Only OKT3 elicited positive T cell stimulation indices above the log(2)-fold threshold, in all tests at 1 and 10 $\mu\text{g/mL}$.

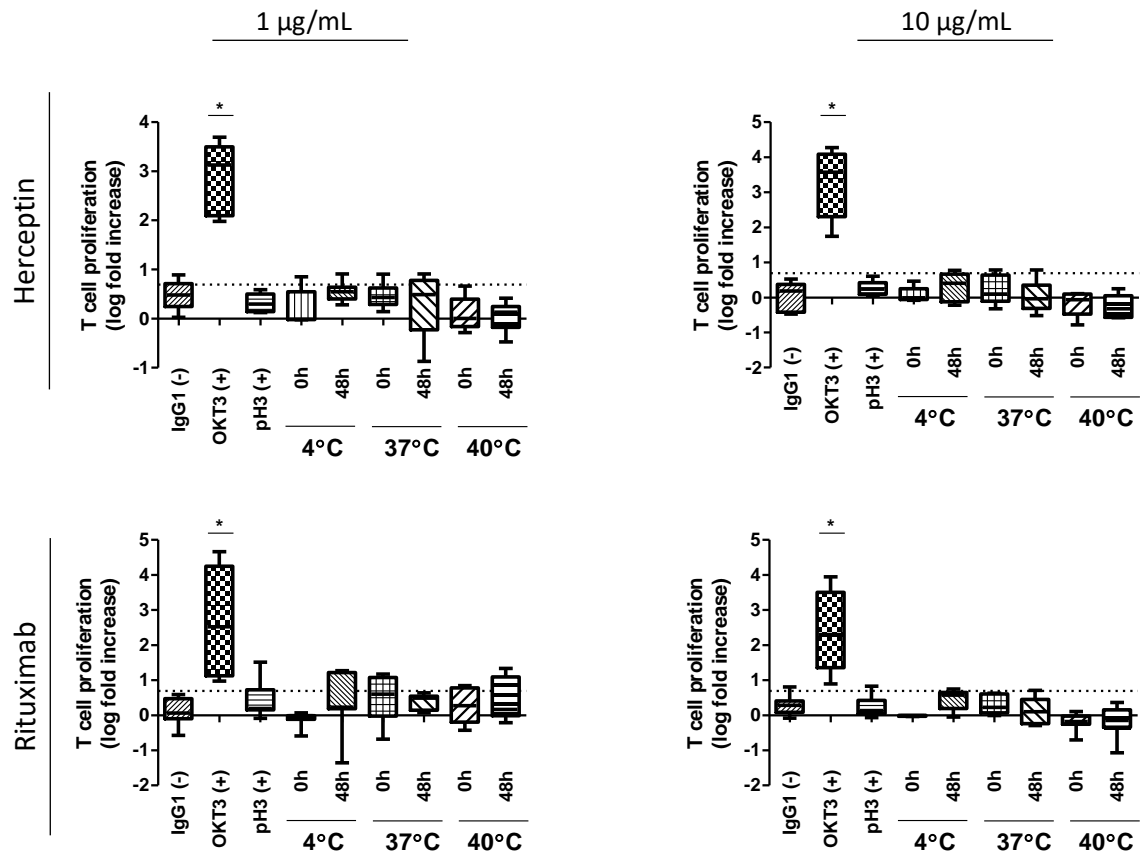


Figure 51. T cell proliferation responses following exposure to heat stressed mAb samples. Herceptin and Rituximab mAbs (1 and 10 $\mu\text{g/mL}$) were exposed to a heat stress protocol (4, 37 and 40°C for 0 and 48 hours). Immune activation threshold was positive if it was regarded as log(2)-fold increase in the T cell proliferation results (dotted line) * $p < 0.05$.

Cytokine levels of IFN- γ , IL-10 and TNF- α were measured from the cell culture supernatants of the skin explant assay for each testing condition. At 1 $\mu\text{g/mL}$, IL-10, IFN- γ and TNF- α levels were only significantly elevated after exposure to OKT3 in both Rituximab and Herceptin (Figure 52). At 10 $\mu\text{g/mL}$, the positive control for aggregation for Rituximab showed a significant increase in IL-10 levels (Figure 53). While not statistically significant, the same trend could be observed for the positive control for aggregation of Herceptin at 10 $\mu\text{g/mL}$, with two out of five donors showing expression of IL-10 above the log(2)-fold threshold.

An overall trend for increased levels of IFN- γ at 10 $\mu\text{g/mL}$ was observed, especially in some donors exposed to aggregated Rituximab. More specifically, expression of IFN- γ was elevated in 3 out of 5 donors for the positive control of aggregation (pH=3) for Rituximab.

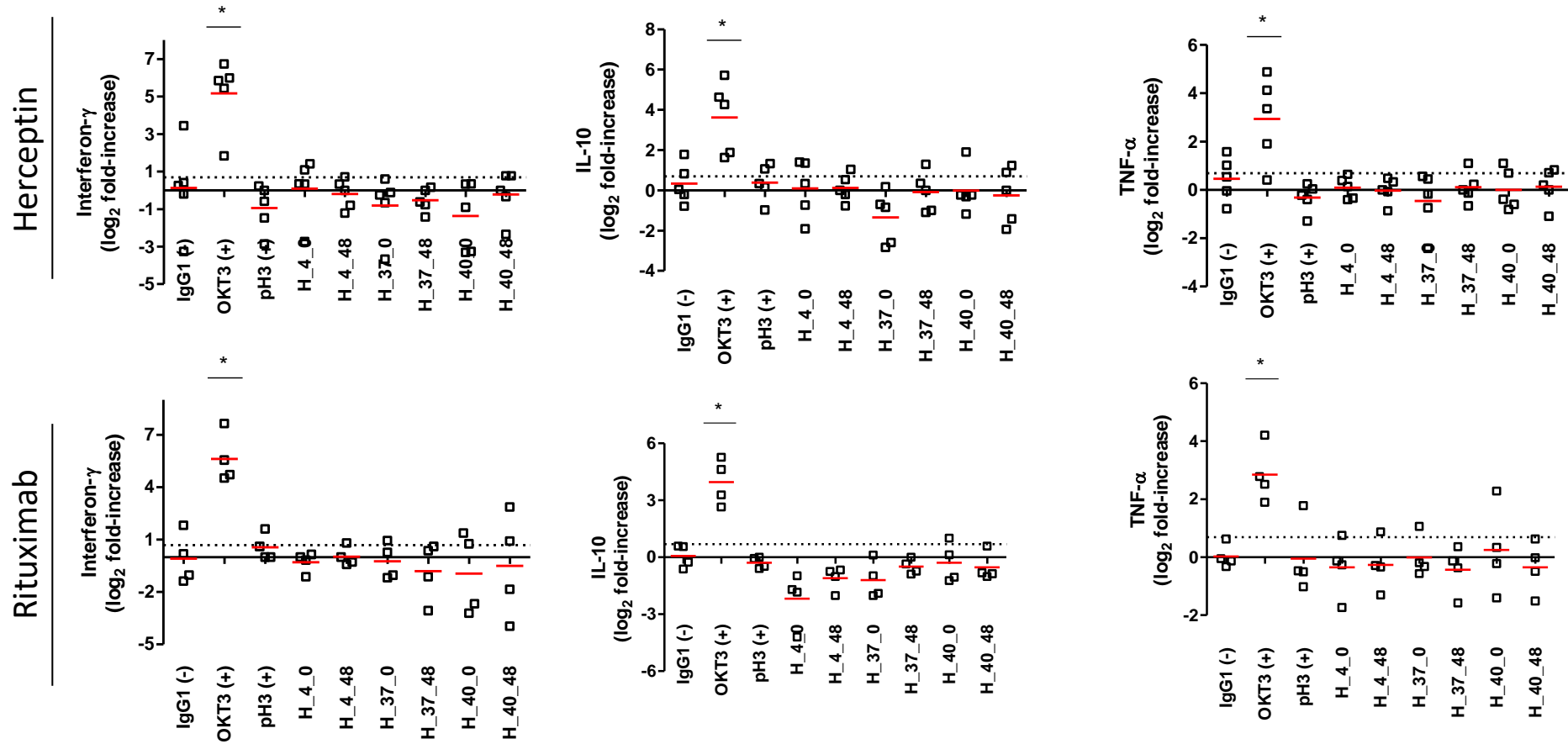


Figure 52. Pro-inflammatory cytokine profile at 1µg/mL. Quantification in log₂-fold-increase of Interferon-γ, IL-10 and TNF-α upon exposure to aggregated Herceptin and Rituximab at 1µg/mL. Dotted line indicates a log₂-fold threshold for immune activation. Mean values represented by the red line. *p<0.05.

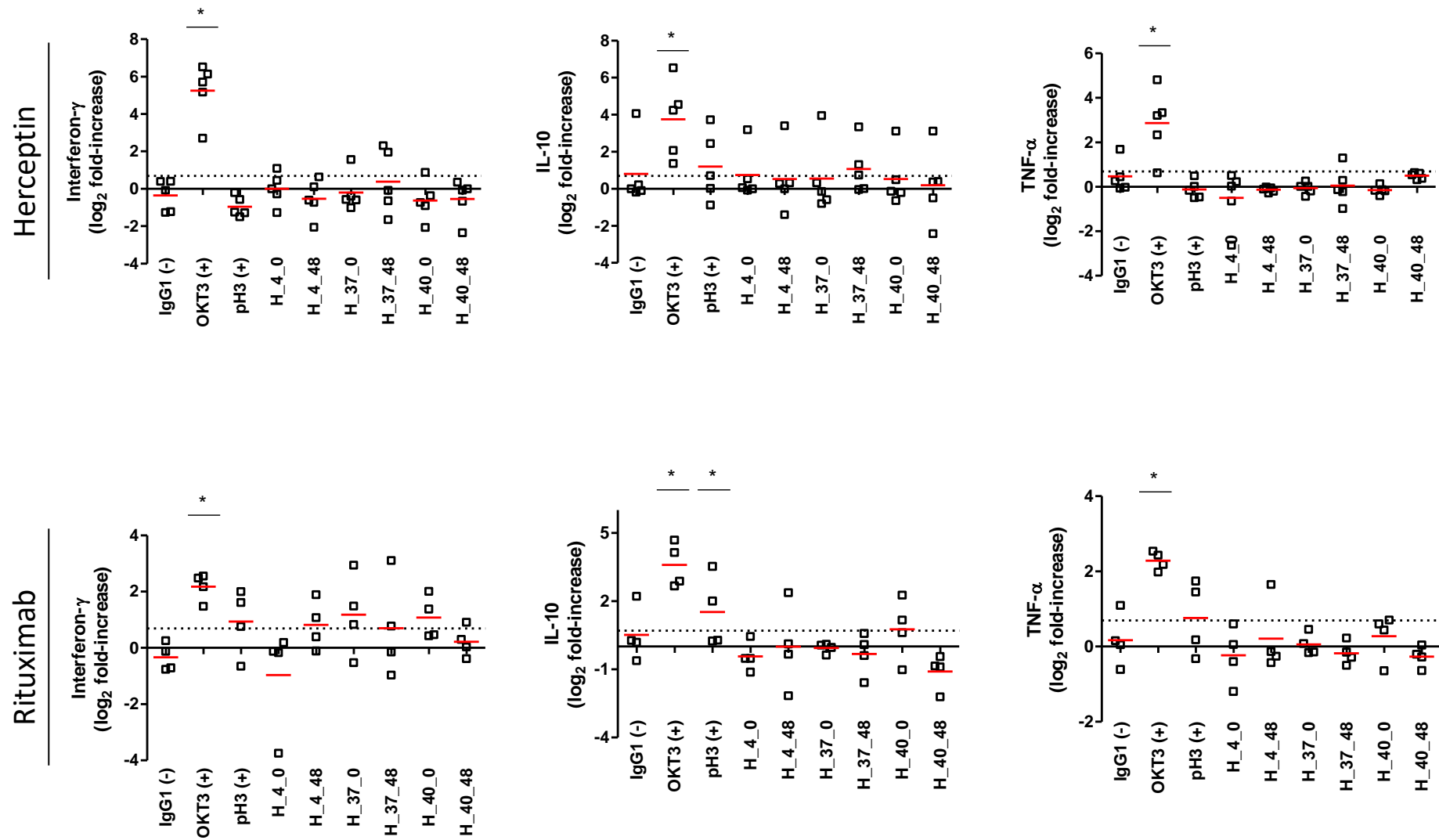


Figure 53. Pro-inflammatory cytokine profile at 10µg/mL. Quantification in log(2)-fold-increase of Interferon- γ , IL-10 and TNF- α upon exposure to aggregated Herceptin and Rituximab at 10µg/mL. Dotted line indicates a log(2)-fold threshold for immune activation. Mean values represented by red line. * $p < 0.05$.

While an increase in T cell proliferation was not observed upon exposure to heat stressed mAbs, significant histopathological damage and IL-10 supernatant expression were reported in the *in vitro* skin explant assay. To further understand these events of immune activation, immunofluorescence staining for cell death was performed. Tissue sections from the *in vitro* skin explant assay containing histopathological damage were stained for Heat Shock Protein (HSP) 70 and Caspase (Casp) 3. Figure 54 shows positive HSP 70 staining (bright green) for the 37°C and 40°C conditions in both Herceptin and Rituximab at 10µg/mL. Positive control for aggregation (pH=3) also showed positive expression of HSP70. No positive expression of Casp3 was observed for any of the temperature conditions. These results suggested that heat stressed Rituximab and Herceptin caused mild apoptotic damage, not strong enough to cause cell death hence lack of positive staining of Casp3.

In summary, results from the heat stressed aggregated mAbs showed that the skin explant assay could be used as a potential *in vitro* assay for assessment of immunotoxicity by mAb aggregation.

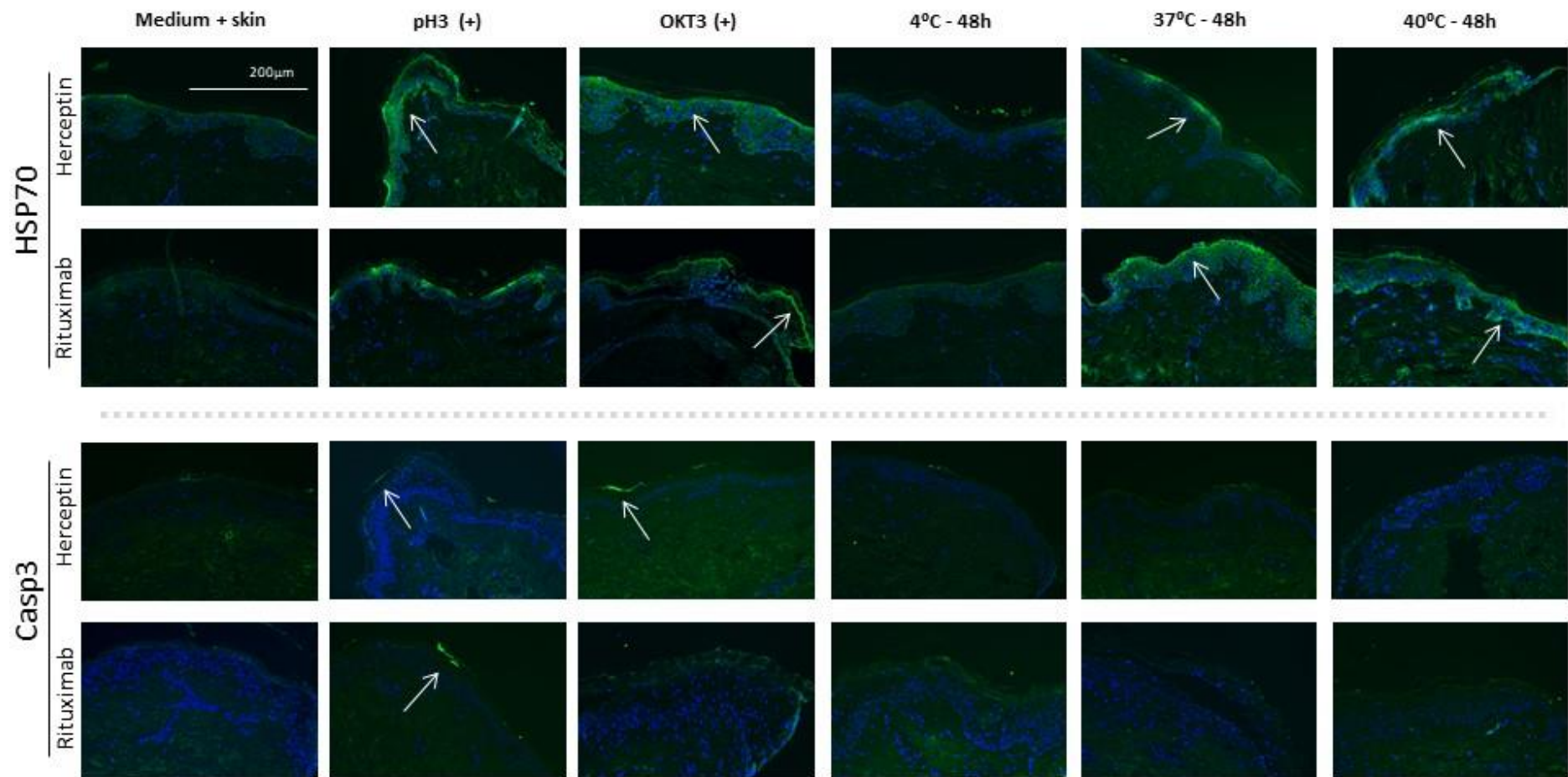


Figure 54. Cell death caused by mAb aggregation. Heat stressed aggregated samples of Herceptin and Rituximab at 10µg/mL were stained for HSP70 and Casp3 (green) by immunofluorescence. DAPI was used as nuclear marker (blue). White arrows indicate positive staining. Scale bar of 200µm from negative control is representative and similar in all testing conditions.

5.3. Discussion of the results

To our knowledge, this study is the first to show the use of a human *in vitro* skin explant assay to determine the potential of aggregated monoclonal antibodies samples to induce an immune response. Developing a method for *in vitro* assessment of immunotoxicity potentially caused by mAb aggregation would be an indispensable downstream service in the pipeline of mAb development.

Previous studies addressing the immunotoxic potential of mAb aggregation used heat stress protocols of temperatures, as high as 65°C (Joubert et al., 2012), 70°C (Ahmadi, Bryson, Cloake, Welch, Filipe, Romeijn, Hawe, Jiskoot, Baker, et al., 2015) or 80°C (Boll et al., 2017; Rombach-Riegraf et al., 2014). In comparison to those protocols, the maximum temperature condition set for this study was 40°C. The temperature test points were chosen for its relevance from a physiological perspective. Our results show that there is some level of protein unfolding and consequent rearrangement of the mAb secondary structure by evidence of the presence of larger molecules in aggregated samples (as demonstrated by SV-AUC results). These thermodynamic changes accounted for less than 4% aggregation of the total protein content, which is in accordance with previous reports of 3% aggregation (Ahmadi, Bryson, Cloake, Welch, Filipe, Romeijn, Hawe, Jiskoot, Baker, et al., 2015) of the total protein content.

There is evidence that protein aggregation can occur at different stages of mAbs production or during further storage, imposing a health risk to patients upon administration of therapeutic mAbs (Kent et al., 2018; Kiese et al., 2008; Peters et al., 2013). We have studied the potential immunotoxic effect of mAb aggregation by investigating T cell proliferation, cytokine release and histopathological assessment of cell damage in a novel *in vitro* skin explant assay. Overall, the heat stressed Herceptin and Rituximab samples did not enhance the immune activation (by T cell proliferation) but rather triggered a cascade of cell death events, by activating apoptosis pathways that ultimately led to histopathological damage of the skin. Cytokine release analysis of skin culture supernatants showed increased levels of anti-inflammatory IL-10 cytokine in 4 out of 5 donors. IL-10 is an immunosuppressive cytokine that inhibits expression of pro-inflammatory cytokines (Murray, 2005). Elevated expression of IL-10 in the positive control for aggregation (pH=3) could suggest that cells are actively forming a protection mechanism from the damage caused by the aggregated mAbs. It could also help explain why the positive control for aggregation did not cause evident histopathological damage.

A trend for elevated expression of IFN- γ was observed at 10 μ g/mL for Herceptin and Rituximab. This could be related to the significant increase of IL-10 for this same condition, as a counter-acting anti-inflammatory defence mechanism (Joubert et al., 2012).

The combination of increased levels of cytokine expression combined with the histopathological damage caused could suggest that heat stressed Rituximab and Herceptin do cause some degree of immune activation. These results do not fully corroborate previously published studies, where it was shown that mAb aggregation by heat stress elicits *in vitro* innate and late-stage T cell responses (Joubert et al., 2012), activates dendritic cells to stimulate T cells (Rombach-Riegraf et al., 2014) and induces CD4⁺ T cell proliferation from pro-inflammatory cytokine release (Ahmadi, Bryson, Cloake, Welch, Filipe, Romeijn, Hawe, Jiskoot, Baker, et al., 2015) as results from the T cell proliferation assay did not show any cell activation. However, it is important to notice that this characterization was not done using the same method as described in published studies. Therefore, assessment of T cell activation by flow cytometry using cell activation markers might be more sensitive for determination of cell activation. Also, these studies were performed in larger cohorts (more than 50 donors) so it would be important to test both the *in vitro* skin explant assay and the T cell activation assay in a larger cohort than the one described in this study.

Further examination of the results from the immune activation experiments indicates that aggregated Herceptin and Rituximab cause mild apoptotic damage shown by the positive staining for HSP70. This heat shock protein serves as a molecular chaperone in cases of cell stress (as heat shock or oxidative stress). HSP70 is crucial for cell survival after apoptotic stimuli (Mosser, Caron, Bourget, Denis-larose, & Massie, 1997; Qi et al., 2011), as shown by Klein *et al.* (2002) in which macrophages heat-stressed for two hours at 42°C showed overexpression of HSP70 (Klein & Brune, 2002). Upregulation of HSP70 can suppress heat-shock damage, by inactivating the upstream action of caspase 3, preventing cell death by apoptosis (Klein & Brune, 2002; Mosser et al., 1997). For the apoptotic stimuli to be severe (and thus irreparable), Caspase 3 would be positively stained due to upregulation of the caspase pathway. Since this was not the case, the results could be attributable to HSP70 actively protecting the cell from apoptotic stimuli caused by the aggregated mAb by inhibiting the apoptotic pathway, hence no positive staining for Caspase 3 (Klein & Brune, 2002; Li, Lee, Ko, Kim, & Seo, 2000). HSP70 is most likely involved in the protein refolding after exposure to the aggregated Herceptin and Rituximab and its overexpression could be rescuing the cells from apoptotic death, hence the mild histopathological damage.

A recent study regarding HSP70 impurities has shown that a recombinant mouse-derived HSP70 bonded to aggregates of different IgG2 mAbs but not to the monomer forms of the same IgG mAbs (Rane et al., 2019). Moreover, it also reported increased IFN- γ production from dendritic cells stimulated with the aggregated IgG mAbs. Overall, this novel work suggests that HSP70 can selectively adhere to mAb aggregates, influencing the immunogenic responses to therapeutic proteins. These findings could help corroborate the results from our study, as immunofluorescence staining showed an increased in HSP70 expression for the heat-stressed Herceptin and Rituximab samples, and not in Caspase 3.

Regarding the different heat-stressed samples, only the highest testing temperature (40°C) caused significant histopathological damage in comparison to the baseline condition. Grade III skin damage was observed in most of the donors, while at 4°C and 37°C an overall weak positive grade II was observed. While the outcome is not a severe grade, these results still show a weak positive skin damage response caused by heat stressed aggregated mAbs. Therefore, it is probable that heat stress alters the structural conformation of the monoclonal antibody, which then elicits an adverse immune effect. Considering that the positive control for aggregation (pH=3) contained a higher level of aggregation (more than 70% aggregation), it was surprising that it did not cause an immune activation response. However, it did elicit increased expression of IL-10 – an anti-inflammatory cytokine. The higher condition of heat stress (40°C) did cause more severe histopathological damage than the positive control. Highly aggregated mAbs (as in the case of the positive control) can affect the normal binding of these proteins to the antigen-presenting cells (Rombach-Riegraf et al., 2014). It has been shown that the structural mAb rearrangements that result from exposure to temperature shock can lead to neo-epitopes (Boll et al., 2017) (new epitopes formed during aggregation), glycosylation/pegylation changes (Hermeling, Crommelin, Schellekens, & Jiskoot, 2004) and other post-translational modifications that break tolerance towards these mAbs, thus causing immunotoxicity. Furthermore, it has been shown that only covalently modified aggregates can induce immunogenicity (Bessa et al., 2015).

However, in order for aggregated mAbs to cause an immunogenic response, it is vital that conformation of the protein's active site remains preserved regardless of aggregation (Boll et al., 2017). Thus, we can speculate that the internal positive control denatured to such an extent that protein conformation was lost by denaturation during the heat stress. The consequential aggregation occurring after denaturation impeded preservation of the protein's active site. These results also highlight the fact that protein aggregation does not always results in immunogenicity. While structural changes might occur due to aggregation, it does not mean

that protein functionality is compromised. Previous studies showed that immunogenicity is only achieved if the primary structure of the mAb protein is deeply modified after aggregation stress (Bessa et al., 2015). Therefore, it can be argued that the internal positive control did not cause a great level of immune activation/cell death due to the new structural rearrangement of the protein, hiding its active site.

Further work is required to better understand the potential use of the skin explant assay in assessment of immunogenicity. Nevertheless, it should still be emphasized that this novel skin explant assay could detect immune activation as accurately as previous studies with much larger sample sizes. For example, Ahmadi *et al.* reported a significant increase in CD4⁺ T cell proliferation upon stimulation with heat stressed Herceptin in only four out of 25 donors (Ahmadi, Bryson, Cloake, Welch, Filipe, Romeijn, Hawe, Jiskoot, Baker, et al., 2015). The skin explant assay results are comparable with these results, highlighting the sensitivity level of skin explant assay. Ultimately, this *in vitro* skin explant assay proved to be a potentially valid assay to assess immunogenicity by aggregation of monoclonal antibodies.

CHAPTER 6

Concluding remarks

6. Concluding remarks and future work

As mentioned previously in section 1.10, the main research hypothesis of this project was: How can we improve assessment of sensitization using *in vitro* test methods, in a more accurate and human relevant manner? This hypothesis was then broke down into two parallel hypotheses:

- Is it possible to develop an open source *in vitro* epidermal model that can compete with the commercially available ones for assessment of skin irritation? Can this optimized *in vitro* epidermal model be free of animal components, reproducible and demonstrate accurate identification of irritants vs non-irritant chemicals in the context of safety testing regulations?
- Considering immunotoxicity as a form of sensitization, is it possible to assess immunotoxicity using a human-based *in vitro* assay for the effect of aggregated monoclonal antibodies?

To answer the first question, results from chapter 3 and 4 indicated that, yes, it is possible to develop an open source *in vitro* epidermal model for assessment of skin irritation, with correct identification of irritants vs non-irritant chemicals. Optimization of cell culture, nutrients and scaffold specifications was performed, and results suggested that the optimal conditions for development of a 3D epidermal skin model was seeding of 1×10^6 keratinocytes/scaffold in a collagen-coated Alvetex Strata membrane for 14 days at ALI enriched with 1.5mM vitamin C and calcium for proper development of stratum corneum and stratum basale layers (confirmed by immunofluorescence staining). It could be argued that coating of the scaffold with human collagen is an expensive step but since this step allows to shorten the ALI culture time to 14 days, it might compensate for all the culturing medium and supplements required for 30 days at ALI.

Furthermore, the 3D epidermal skin model was able to correctly identify all 6 irritant chemicals and 4 out of 6 non-irritant chemicals. Most importantly, performance of the 3D epidermal skin model was comparable with EpiDerm™ (commercially available from MatTek) as no statistical significance was found in their capability to assess irritancy. All together, these results validate the initial research hypothesis and strongly indicate that the 3D epidermal skin model could be a valuable *in vitro* tool for assessment of irritancy. Future work on the development of the 3D epidermal skin model would focus on its reproducibility and improvement of its manufacturing with advanced technologies like 3D bioprinting.

Regarding the second hypothesis, results from chapter 5 showed that the aggregated samples of Rituximab and Herceptin at 40°C for 48 hours caused significant grade III skin damage with positive expression of cell death marker HSP70. These results indicate that Skimune® could be used as a valid tool for assessment of aggregated monoclonal antibodies but further studies need to be conducted to validate if skin damage as output of the Skimune® assay is immune-related or not. Current results seem to indicate that the damage provided by the aggregated monoclonal antibodies might happen at the cellular level, by death of the keratinocytes. The lack of T cell activation of cytokine involvement might suggest that this cell death event is unrelated to unwanted immune activation, i.e. immunotoxicity. Therefore, further studies using a larger cohort of donor samples and different aggregated monoclonal antibodies would have to be tested. Nevertheless, the Skimune® assay was able to detect damage by the aggregated monoclonal antibodies.

From a commercial perspective, there are multiple applications for 3D skin models, either for research or commercial studies of skin toxicity, skin metabolism and skin absorption. Skin toxicity is a common regulatory concern as allergic contact dermatitis is estimated to be one of the main reported causes of occupational illness (Duarte, Lazzarini, & Rotter, 2010; Thyssen, Linneberg, Menné, & Johansen, 2007). In fact, it is estimated that 15 to 20% of the general population will develop an allergic reaction to any chemical in their lifetime (Thyssen et al., 2007), leading to a negative impact on the quality of life.

Governmental bodies like the European Union and OECD have given the first step to recognise skin toxicity as an important occupational health issue, by implementing laws and directives to reduce animal experimentation in safety testing of commercial products intended for human consumption. One of the most important bans was the Cosmetic Directive, implemented in 2013 by the European Union, to stop testing of cosmetic products on animals models in Europe (European Commission, 2009). One other effort to improve cosmetic safety for human health is the implementation of Cosmetovigilance, a health surveillance concept.

Cosmetovigilance is defined as the ongoing monitoring of all human health related safety issues regarding cosmetics, aiming to detect and compile adverse effects to cosmetic products in the form of official reports. This way, it is possible to collect genuine information of marketed cosmetic products that caused adverse effects impacting human health and have a quantitative measurement of cosmetic safety on human health. Regulatory organizations can also take advantage of the outcome feedback of Cosmetovigilance to evaluate current directives

or the necessity of tougher legislations for potentially hazardous cosmetic products (Vigan & Castelain, 2014).

Despite the efforts made from these entities to reduce animal experimentation by giving preference to alternative *in vitro* models, there are currently no gold standard alternative methods to assess skin toxicity. However, different *in vitro* and *in silico* tools are available to improve prediction of skin toxicity without using animal models. From the use of AOPs for risk assessments to QSAR tools for prediction of toxicity, there are a plenitude of decision-making tools working as a framework for better prediction of toxicity.

Some *in vitro* cell-based and 3D RHE models have received formal EURL-ECVAM validation for assessment of skin toxicity in its different dimensions – irritation, corrosion, sensitization. For the last 10 to 15 years, the 3D RHE models have been widely accepted as the more suitable alternative method for skin toxicity studies, as their physiologically much more similar to human skin than *in vitro* cell-based assays. The commercially available EpiDerm™, EpiSkin™ and SkinEthic™ models are the most used models worldwide as they are currently validated by EURL-ECVAM for skin irritation, corrosion, UV exposure, among other toxicity studies. In fact, many of the Testing Guidelines from OECD for standardized skin toxicity studies have been defined resourcing to these RHE models.

For example, TG 439 for skin irritation testing provides a standardized protocol for skin irritation using the RHE mentioned above by quantification of cell viability by MTT (OECD, 2013). The MTT assay is a sensitive, affordable and fast method used in TG 439 to evaluate tissue viability of RHE models after chemical exposure, determining GHS category 2 irritants from non-irritant chemicals. EURL-ECVAM guidelines state that this protocol can actually be used as a replacement of the *in vivo* Draize test (rabbit skin sensitization) for hazard identification of irritant chemicals (ECVAM, 2009d).

Many newly developed 3D RHE models seeking formal EURL-ECVAM validation follow TG 439 for comparative performance analysis with the commercially available 3D RHE models. The first objective of this study was to develop an animal-free 3D epidermal skin culture model for assessment of skin irritation following TG 439. Therefore, a comparative analysis was performed between the 3D epidermal skin model, the EpiDerm™ model, a 3D RHE model using collagen-based scaffold and a keratinocyte monolayer culture.

The results presented in this work showed that the 3D epidermal skin culture model was able to correctly classify 4 out of 6 non-irritants and 6 out of 6 irritants in a total of 10 keratinocyte donor samples. Moreover, the same 10 keratinocyte donor samples were used to develop a keratinocyte monolayer culture and performance results from TG 439 showed that

the keratinocyte monolayer culture was only able to correctly predict 3 out of 6 non-irritants and 6 out of 6 irritants with big standard variations. Additionally, the 3D epidermal skin model “overpredicted” the irritancy of two non-irritants. As these two non-irritants currently have no GHS category, it could be argued that they do in fact have an irritancy potential but lack of irreputable *in vivo* data makes it impossible to determine their irritancy potential so far. Thus, these results could highlight the predictive capacity of the 3D epidermal skin culture model and its sensitivity to assess hazardous irritant chemicals.

Ultimately, the results presented in this work indicate that the 3D epidermal skin culture developed could be employed as a relevant *in vitro* test method for evaluation of skin irritation. Direct comparison of the predictive capacity of the different *in vitro* test methods used for this study showed no statistically significant difference between the 3D epidermal skin culture and the commercially available 3D RHE model. These findings are vital to support the establishment of the 3D epidermal skin model as an *in vitro* test method for skin irritation purposes and could also be used as preliminary data for validation.

Commercialization of the 3D epidermal model would broaden Alcyomics service pipeline. Currently, Alcyomics focus on pre-clinical screening of novel drugs and biopharmaceuticals and has already patented an *in vitro* skin explant assay for assessment of adverse immune events to chemicals, the Skimune® assay. Further modifications were made to the Skimune® to use it for detection of adverse events to monoclonal antibodies.

In this study, the Skimune® assay was used to assess adverse immune events to aggregated monoclonal antibodies. It is still unclear the direct consequences of administration of aggregated monoclonal antibodies to the human immune system. Previous reports from cell-based studies indicate that low levels of aggregated monoclonal antibodies caused unwanted activation of the immune system (Ahmadi, Bryson, Cloake, Welch, Filipe, Romeijn, Hawe, Jiskoot, Baker, et al., 2015; Joubert et al., 2012; Rombach-Riegraf et al., 2014). One of the big limitations of these reports is the fact that only a small percentage of the overall cohort presented significant cell activation, meaning that large cohorts are necessary to study immune activation by aggregated mAbs. As mentioned before, this can be complex to achieve during drug development phase, as it can be necessary to screen several drug compounds in a time and a cost-efficient manner. Therefore, development of a faster, but still accurate, *in vitro* method for assessment of adverse events by mAb aggregation is needed.

Novel approaches like “immunoprofiling” are now emerging as assessment tools for the study of immunogenicity by mAb aggregation in a clinical setting. This tool allows to compare antibody responses from both the monomer and the aggregate form of clinically used IgG

mAbs, by peptide microarray analysis to identify patterns of antibody recognition against libraries of peptide antigens (Legutki et al., 2014). Immunoprofiling has been used in vaccine studies to improve their efficacy, by studying abnormal antibody elevated responses to particular epitopes in certain individuals (Legutki & Johnston, 2013). Moreover, immunoprofiling of epitope mapping has been used to identify aggregate-specific “immunosignatures”. As mentioned previously in section 5.3, misfolding of therapeutic proteins is a risk factor for immunogenicity, as neo-epitopes are formed or exposed during protein unfolding, which can increase the aggregated mAb response (Maas, Hermeling, Bouma, Jiskoot, & Gebbink, 2007). Homann et al. have characterized immunogenic epitopes to the TNF- α targeted MAbs Infliximab and Adalimumab, which are known to cause immunogenicity. Screening of serum samples from patients treated with Infliximab showed six relevant B cell epitopes in the variable region of Infliximab with an N-glycosylation sequence (Homann, Röckendorf, Kromminga, Frey, & Jappe, 2015). Individual IgG epitopes of anti-drug antibodies against adalimumab were also identified by epitope mapping via peptide microarray (Homann et al., 2017). Further studies in animal models have also identified aggregate-specific B cell epitopes upon protein unfolding. Peptide microarray analysis of an IgG2 mAb showed partial unfolding of the variable domain region of the mAb, with a critical replacement of tryptophan with alanine (Eyes et al., 2019). Overall, these findings can help identify aggregation-specific “immunosignatures” from anti-drug antibody serum responses of clinical patients, improve the existing methods for detection of immunogenicity and ultimately enhance the design of the therapeutic mAbs.

This study aimed to also contribute with a possible *in vitro* approach for detection of immunogenicity by mAb aggregation. A skin explant assay was used in combination with T cell proliferation and cytokine quantification methods to assess the immunotoxicity caused by heat-stressed Herceptin and Rituximab. The fact that Skimune® could predict the same outcome as the previously reported studies but in a much smaller cohort, can only highlight the specificity of this *in vitro* method, which was the ultimate goal of this study.

Ultimately, this project has provided new insights for animal-free *in vitro* test methods with reliable predictive capacity to improve the hazardous classification of any compound designed for human use.

6.1. Future work

This project was designed to develop novel *in vitro* test methods for assessment of skin irritation and adverse immune events relevant to human safety. Results from chapter 3 showed that a new 3D epidermal skin model using the Alvetex Strata membrane was optimized and could, additionally, be used for skin irritation testing (chapter 4). Likewise, results from chapter 5 indicate that Skimune® could be modified to assess immunotoxicity by aggregated monoclonal antibodies. But while results are promising, there are still several questions or issues that need to be addressed regarding these novel *in vitro* test methods, like:

- how reproducible is the 3D epidermal skin model?
- is the 3D epidermal skin model ready for commercialization – quality control, storage, shipping?
- can the 3D epidermal skin model be used for different form of skin toxicity?

Regarding the Skimune® test for immunotoxicity:

- can it be used for different monoclonal antibodies?
- will it be able to detect different levels of aggregated monoclonal antibodies?

Therefore, further experiments would be required to address these questions. In order to achieve official EURL-ECVAM validation, the 3D epidermal skin culture model would have to show intra- and inter-laboratorial reproducibility for all 20 reference chemicals, meeting all the quality standards defined in TG 439. However, considering that formal EURL-ECVAM validation can be a long process, Alcyomics short-term pipeline development strategies could include the 3D epidermal skin culture as an in-house service assay for skin toxicity studies or as a commercial RHE model. The in-house service assay strategy would require quality control evaluation by intra-laboratorial review and possibly a new product development phase to assess applicability of the 3D epidermal skin culture for skin corrosion, phototoxicity or absorption studies. The commercialization of the 3D epidermal skin culture model would also require quality control studies, as well as reproducibility, long term stability and shipment stability validation. Nevertheless, all these validation studies would be relevant as pre-validation data for formal EURL-ECVAM validation.

Regarding Skimune®, the *in vitro* skin explant assay for assessment of immunotoxicity, further validation with a larger range of aggregated mAbs would robust the data already

collected in this work. From testing Skimune® in monoclonal antibodies with different IgG subclasses (i.e. IgG1 or IgG2) to monoclonal antibodies with different levels of aggregation, further testing would be crucial to strengthen the use of Skimune® as a valid platform for assessment of aggregated monoclonal antibodies.

Furthermore, it would be crucial to understand if the skin damage readout from Skimune® assay is immune-related or not. Different testing conditions in the presence and absence of immune cells would help clarify the role of immune cells (more specifically T cells) in the assessment of immunotoxicity by aggregated monoclonal antibodies using the Skimune®.

CHAPTER 7

Appendices

7. Appendices

Appendix A – Publications

Published abstracts:

- **Ana Ribeiro**, Shaheda Ahmed, Anne Dickinson. *Skimune® - a novel in vitro tool for detection of immunogenicity by mAb aggregation*. ESBES 12th edition 2018 (Lisbon, Portugal) Oral Presentation
- **Ana Ribeiro**, Shaheda Ahmed, Anne Dickinson. *Skimune® - a novel in vitro tool for detection of immunogenicity by mAb aggregation*. PEGS 14th edition 2018 (Boston, USA) Oral Presentation and poster
- **Ana Ribeiro**, Shaheda Ahmed, Anne Dickinson. *Skimune® - a novel in vitro tool for detection of immunogenicity and adverse immune reactions to novel compounds*. MCAA General Assembly and Annual Conference 2018 (Leuven, Belgium) Poster Presentation
- **Ana Ribeiro**, Shaheda Ahmed, Anne Dickinson. *Skimune® - a novel in vitro tool for detection of immunogenicity and adverse immune reactions to novel compounds*. EUSAAT, 2016 (Linz, Austria) Oral Presentation
- **Ana Ribeiro**, Shaheda Ahmed, Anne Dickinson. *Skimune® - a novel in vitro tool for detection of immunogenicity and adverse immune reactions to novel compounds*. ICM Postgrad poster session, 2017 (Newcastle, UK) Poster Presentation (award 2nd best poster)
- **Ana Ribeiro**, Shaheda Ahmed, Anne Dickinson. *Skimune® - a novel in vitro tool for detection of immunogenicity and adverse immune reactions to novel compounds*. ESBES 10th edition, 2016 (Dublin, Ireland) Poster Presentation
- **Ana Ribeiro**, Shaheda Ahmed, Anne Dickinson. *Skimune® - predicting adverse immune reactions to biologics*. WPC 15th edition, 2016 (Boston, USA) Poster Presentation
- **Ana Ribeiro**, Shaheda Ahmed, Anne Dickinson. *Skimune® - a novel in vitro tool for detection of immunogenicity by mAb aggregation*. ICM research Seminar, 11th January 2018 (NCL, UK) Oral Presentation

Manuscripts:

- **Martins-Ribeiro A**, Kizhedath A, Ahmed SS, Glassey J, Dickinson AM. A human skin explant test as a novel *in vitro* assay for the detection of adverse immune reactions to aggregated monoclonal antibodies. mABs (2019) – in preparation

Appendix B – Personal development

Training weeks (TW) from BIORAPID

- TW1 and 2 – 24th August 2015 to 04th September 2015 - Experimental procedures & Entrepreneurship, organized by Newcastle University and Alcyomics (NCL, UK)
- TW3 – 05th December 2015 to 09th December 2015 - Modelling/data interpretation & QbD training, organized by Technical University of Denmark (Ghent, Belgium)
- TW4 – 03rd April 2016 to 08th April 2016 - Microscale and small-scale reactors for process development training, organized by Technische Universität Berlin (Berlin, Germany)
- TW5 – 29th May 2017 to 02nd June 2017 - Sensor technology & Innovative product design, organized by Linköping University and ACREO (Linköping, Sweden)
- Biorapid Mid-Term project meeting: project update meeting, January 2017 (NCL, UK)

Secondment trainings:

- Toxicology Department – March 2016 (with Prof. Simon Wilkinson group) – to gain knowledge of *in vitro* toxicology testing to later apply this knowledge in the Skimune® technology for toxicity testing
- FUJIFILM (Billingham) – March 2017 (with Prof. Graham McCreath) – to gain knowledge of biopharma manufacture of monoclonal antibodies; industrial process of mAb degradation (aggregation, fragmentation,...)

Courses/workshops attended:

- Flow Cytometry training
- ePortfolio and Personal Development training
- Managing your PhD, MD or MPhil
- Introduction to Statistical Considerations in Experimental Research
- Learning Agreement
- Endnote
- Chemical Safety training

- Basic fire training induction
- ICM induction morning
- Public speaking
- Risk assessment
- Biological Agents and GMO
- Insights from industry, Good manufacturing practice
- Recording your research (Lab books, research diaries, etc)
- Robust research methodologies for Literature Review
- Very basic Stats
- Haematology department sample tracking system training
- Academic writing
- Convincing CVs and Covering Letters
- Research ethics
- Thesis writing
- Human Tissue Act training
- ISIS database training
- Database training
- Basic Rad protection workshop
- Second year annual review: your research outputs
- Communication and presentation skills
- ILTHE – Introduction to Learning and Teaching

Additional activities:

- BIORAPID newsletter issue 1 and 2 – article on Paris internship and experience
- BIORAPID promotional video
<https://www.youtube.com/watch?v=HSXyvEoaXXM&t=2s>
- Engineering Futures - Outreach activity in Hotspur Primary School for STEM awareness (May 2017)
- Travel grant writing – awarded 2 travel grants from Newcastle university and WPC



National Research Ethics Service
Newcastle & North Tyneside 1 Research Ethics Committee

TEDCO Business Centre
Room 002
Rolling Mill Road
Jarrow
NE32 3DT

Telephone: 0191 428 3564
Facsimile: 0191 428 3432

05 November 2010

Professor Anne Dickinson
Haematological Sciences
Institute of Cellular Medicine
Newcastle University
NE2 4HH

Dear Professor Dickinson

Study Title: Development of an in vitro human skin explant safety assay for the detection of immunogenicity and hypersensitivity reactions to novel compounds and drugs
REC reference number: 10/H0906/58
Protocol number: 2/8/10 Version 1

Thank you for your letter of 25 October 2010, responding to the Committee's request for further information on the above research and submitting revised documentation.

The further information has been considered on behalf of the Committee by the Chair.

Confirmation of ethical opinion

On behalf of the Committee, I am pleased to confirm a favourable ethical opinion for the above research on the basis described in the application form, protocol and supporting documentation as revised, subject to the conditions specified below.

Ethical review of research sites

The favourable opinion applies to all NHS sites taking part in the study, subject to management permission being obtained from the NHS/HSC R&D office prior to the start of the study (see "Conditions of the favourable opinion" below).

Conditions of the favourable opinion

The favourable opinion is subject to the following conditions being met prior to the start of the study.

Management permission or approval must be obtained from each host organisation prior to the start of the study at the site concerned.

Management permission ("R&D approval") should be sought from all NHS organisation(s) involved in the study in accordance with NHS research governance arrangements. Guidance on applying for NHS permission for research is available in the Integrated Research Application System (IRAS) or at <http://www.rdforum.nhs.uk>.

This Research Ethics Committee is an advisory committee to the North East Strategic Health Authority
The National Research Ethics Service (NRES) represents the NRES Directorate within
the National Patient Safety Agency and Research Ethics Committees in England

Now that you have completed the application process please visit the National Research Ethics Service website > After Review

You are invited to give your view of the service that you have received from the National Research Ethics Service and the application procedure. If you wish to make your views known please use the feedback form available on the website.

The attached document "*After ethical review – guidance for researchers*" gives detailed guidance on reporting requirements for studies with a favourable opinion, including:

- Notifying substantial amendments
- Adding new sites and investigators
- Progress and safety reports
- Notifying the end of the study

The NRES website also provides guidance on these topics, which is updated in the light of changes in reporting requirements or procedures.

We would also like to inform you that we consult regularly with stakeholders to improve our service. If you would like to join our Reference Group please email referencegroup@nres.npsa.nhs.uk.

10/H0906/58

Please quote this number on all correspondence

Yours sincerely

pp. J. Kirkbride

Mr Chris Turnock
Chair

Email: laura.kirkbride@sotw.nhs.uk

Enclosures: "After ethical review – guidance for researchers"

Copy to: Newcastle upon Tyne Hospitals NHS Foundation Trust

Now that you have completed the application process please visit the National Research Ethics Service website > After Review

You are invited to give your view of the service that you have received from the National Research Ethics Service and the application procedure. If you wish to make your views known please use the feedback form available on the website.

The attached document "*After ethical review – guidance for researchers*" gives detailed guidance on reporting requirements for studies with a favourable opinion, including:

- Notifying substantial amendments
- Adding new sites and investigators
- Progress and safety reports
- Notifying the end of the study

The NRES website also provides guidance on these topics, which is updated in the light of changes in reporting requirements or procedures.

We would also like to inform you that we consult regularly with stakeholders to improve our service. If you would like to join our Reference Group please email referencegroup@nres.npsa.nhs.uk.

10/H0906/58

Please quote this number on all correspondence

Yours sincerely

pp. *L. Kirkbride*

Mr Chris Turnock
Chair

Email: laura.kirkbride@sotw.nhs.uk

Enclosures: "After ethical review – guidance for researchers"

Copy to: Newcastle upon Tyne Hospitals NHS Foundation Trust

CHAPTER 8

References

8. References

- Abaci, H. E., Guo, Z., Doucet, Y., Jackow, J., & Christiano, A. (2017). Next generation human skin constructs as advanced tools for drug development. *Experimental Biology and Medicine*, 242, 1657–1668. <http://doi.org/10.1177/1535370217712690>
- Ade, N., Martinozzi-teissier, S., Pallardy, M., & Rousset, F. (2006). Activation of U937 Cells by Contact Sensitizers: CD86 Expression is Independent of Apoptosis Activation. *Journal of Immunology*, 3, 189–197. <http://doi.org/10.1080/15476910600978038>
- Ahmadi, M., Bryson, C. J., Cloake, E. A., Welch, K., Filipe, V., Romeijn, S., Hawe, A., Jiskoot, W., Baker, MP., Fogg, M. H. (2015). Small amounts of sub-visible aggregates enhance the immunogenic potential of monoclonal antibody therapeutics. *Pharmaceutical Research*, 32(4), 1383–1394. <http://doi.org/10.1007/s11095-014-1541-x>
- Ahmed, S. S., Wang, X. N., Fielding, M., Kerry, A., Dickinson, I., Munuswamy, R., Kimber, I., Dickinson, A. M. (2016). An in vitro human skin test for assessing sensitization potential. *Journal of Applied Toxicology*, 36(5), 669–684. <http://doi.org/10.1002/jat.3197>
- Ahmed, S. S., Whritenour, J., Ahmed, M. M., Bibby, L., Darby, L., Wang, X. N., Watson, J., Dickinson, A. M. (2019). Evaluation of a human in vitro skin test for predicting drug hypersensitivity reactions. *Toxicology and Applied Pharmacology*, 369, 39–48. <http://doi.org/10.1016/j.taap.2019.02.005>
- Alexander Jr, F. A., Eggert, S., & Wiest, J. (2018). Skin-on-a-Chip: Transepithelial Electrical Resistance and Extracellular Acidification Measurements through an Automated Air-Liquid Interface. *Genes*, 9(114), 1–10. <http://doi.org/10.3390/genes9020114>
- Almond, R. J., Flanagan, B. F., Antonopoulos, A., Haslam, S. M., Dell, A., Kimber, I., & Dearman, R. J. (2013). Differential immunogenicity and allergenicity of native and recombinant human lactoferrins: Role of glycosylation. *European Journal of Immunology*, 43, 170–181. <http://doi.org/10.1002/eji.201142345>
- Almond, R. J., Flanagan, B. F., Kimber, I., & Dearman, R. J. (2012). Influence of protein expression system on elicitation of IgE antibody responses: Experience with lactoferrin. *Toxicology*, 301, 50–57. <http://doi.org/10.1016/j.tox.2012.06.018>
- Aptula, A. O., Patlewicz, G., & Roberts, D. W. (2005). Skin Sensitization: Reaction Mechanistic Applicability Domains for Structure–Activity Relationships. *Chemical Research in Toxicology*, 18, 1420–1426.
- Attarwala, H. (2010). TGN1412: From Discovery to Disaster. *Journal of Young Pharmacists*, 2(3), 332–336. <http://doi.org/10.4103/0975-1483.66810>
- Baert, F., Noman, M., Vermeire, S., Assche, G. Van, Haens, G. D., Carbonez, A., & Rutgeerts, P. (2003). Influence of Immunogenicity on the Long-Term Efficacy of Infliximab in Crohn's Disease. *The New England Journal of Medicine*, 348(7), 601–608.
- Balls, M. (2005). Alternatives to Animal Experiments: Serving in the Middle Ground. *AATEX*, 11(1), 4–14.
- Balls, M., Blaauboer, B., Brusick, D., Frazier, J., Lamb, D., Pemberton, M., Reinhardt, C., Roberfroid, M., Rosenkranz, H., Schimd, B., Spielmann, H., Stamatii, A., Walum, E.

- (1990). Report and Recommendations of the Caat Ergatt Workshop on the Validation of Toxicity Test Procedures. *ATLA*, 18, 313–337.
- Balls, M., Blaauboer, B. J., Fentem, J. H., Bruner, L., Combes, R. D., Ekwall, B., Zucco, F. (1995). Practical aspects of the validation of toxicity test procedures - The report and Recommendations of ECVAM Workshop 5. *ATLA*. Retrieved from <http://scholar.google.com/scholar?hl=en&btnG=Search&q=intitle:Practical+aspects+of+the+validation+of+toxicity+test+procedures#0>
- Balls, M., & Fentem, J. H. (1999). The validation and acceptance of alternatives to animal testing. *Toxicology in Vitro*, 13(4–5), 837–846. [http://doi.org/10.1016/S0887-2333\(99\)00067-3](http://doi.org/10.1016/S0887-2333(99)00067-3)
- Bartosova, L., & Bajgar, J. (2012). Transdermal Drug Delivery In Vitro Using Diffusion Cells. *Current Medicinal Chemistry*, 19, 4671–4677.
- Basketter, D. A., Blaikie, L., Dearman, R. J., Kimber, I., Ryan, C. A., Gerberick, G. F., Harvey, P., White, I. R., Rycroft, R. J. G. (2000). Use of the local lymph node assay for the estimation of relative contact allergenic potency. *Contact Dermatitis*, 42, 344–348.
- Basketter, D. A., Clapp, C., Jefferies, D., Safford, B., Ryan, C. A., Gerberick, F. G., Dearman, R.J., Kimber, I. (2005). Predictive identification of human skin sensitization thresholds. *Contact Dermatitis*, 53, 260–267.
- Basketter, D. A., Roberts, D. W., Cronin, M., & Scholes, E. W. (1992). The value of the local lymph node assay in quantitative structure-activity investigations. *Contact Dermatitis*, 27, 137–142.
- Baveye, S., Ellass, E., Mazurier, J., Spik, G., & Legrand, D. (1999). Lactoferrin: A Multifunctional Glycoprotein Involved in the Modulation of the Inflammatory Process. *Clin Chem Lab Med*, 37(3), 281–286.
- Belot, N., Sim, B., Longmore, C., Roscoe, L., & Treasure, C. (2017). Adaptation of the KeratinoSensTM Skin Sensitization Test to Animal-Product-Free Cell Culture. *ALTEx*, 34(4), 560–564. <http://doi.org/10.14573/altex.1701311>
- Bendtzen, K. (2012). Anti-TNF- α biotherapies: perspectives for evidence-based personalized medicine. *Immunotherapy*, 4(11), 1–2. <http://doi.org/doi.org/10.2217/imt.12.114>
- Berkowitz, S. A. (2006). Role of Analytical Ultracentrifugation in Assessing the Aggregation of Protein Biopharmaceuticals. *The AAPS Journal*, 8(3), 590–605.
- Bessa, J., Boeckle, S., Beck, H., Buckel, T., Schlicht, S., Ebeling, M., Kiialainen, A., Koulov, A., Boll, B., Weiser, T., Singer, T., Rolink, A.G., Iglesias, A. (2015). The Immunogenicity of Antibody Aggregates in a Novel Transgenic Mouse Model. *Pharmaceutical Research*, 32, 2344–2359. <http://doi.org/10.1007/s11095-015-1627-0>
- Bhhatarai, B., Wilson, D. M., Parks, A. K., Carney, E. W., & Spencer, P. J. (2016). Evaluation of TOPKAT, TOXTREE and DEREK Nexus in silico models for ocular irritation and development of a knowledge-based framework to improve the prediction of severe irritation. *Chemical Research in Toxicology*, 29(5), 810–822. <http://doi.org/10.1021/acs.chemrestox.5b00531>
- Boll, B., Bessa, J., Folzer, E., Quiroz, A. R., Schmidt, R., Bulau, P., Finkler, C., Huwyler, J.,

- Iglesias, A., Koulov, A. V. (2017). Extensive Chemical Modifications in the Primary Protein Structure of IgG1 Subvisible Particles Are Necessary for Breaking Immune Tolerance. *Molecular Pharmaceutics*, 14, 1292–1299. <http://doi.org/10.1021/acs.molpharmaceut.6b00816>
- Bouwstra, J. A., & Ponc, M. (2006). The skin barrier in healthy and diseased state. *Biochimica et Biophysica Acta - Biomembranes*, 1758(12), 2080–2095. <http://doi.org/10.1016/j.bbmem.2006.06.021>
- Buchner, J., Renner, M., Lilie, H., Hinz, H.-J., & Jaenicke, R. (1991). Alternatively folded states of an immunoglobulin. *Biochemistry*, 30(28), 6922–6929. <http://doi.org/10.1021/bi00242a016>
- Carter, P. (2001). Improving the efficacy of antibody-based cancer therapies. *Nature Reviews. Cancer*, 1(2), 118–129. <http://doi.org/10.1038/35101072>
- Chase, M. W. (1941). Inheritance in guinea pigs of the susceptibility to skin sensitization with simple chemical compounds. *Journal of Experimental Medicine*, 73(6), 711–726.
- Cole, J. L., Lary, J. W., Moody, T., & Laue, T. M. (2008). Analytical Ultracentrifugation: Sedimentation Velocity and Sedimentation Equilibrium. *Methods in Cell Biology*, 84(07), 143–179. [http://doi.org/10.1016/S0091-679X\(07\)84006-4](http://doi.org/10.1016/S0091-679X(07)84006-4). Analytical
- CPMP. (1997). *Replacement of Animal studies by in-vitro models (CPMP/SWP/728/95)*. Committee for Proprietary Medicinal Products. London. Retrieved from http://www.ema.europa.eu/ema/index.jsp?curl=pages/regulation/general/general_content_000397.jsp&mid=WC0b01ac058002956f
- Dean, J. H., Twerdok, L. E., Tice, R. R., Sailstad, D. M., Hattan, D. G., & Stokes, W. S. (2001a). ICCVAM Evaluation of the Murine Local Lymph Node Assay - II. Conclusions and recommendations of an independent scientific peer review panel. *Regulatory Toxicology and Pharmacology*, 34(3), 258–273. <http://doi.org/10.1006/rtp.2001.1498>
- Dean, J. H., Twerdok, L. E., Tice, R. R., Sailstad, D. M., Hattan, D. G., & Stokes, W. S. (2001b). ICCVAM Evaluation of the Murine Local Lymph Node Assay - III. Data analysis completed by the national toxicology program interagency center for the evaluation of alternative toxicological methods. *Regulatory Toxicology and Pharmacology*, 34(3), 274–286. <http://doi.org/10.1006/rtp.2001.1498>
- Dickinson, A. M., Sviland, L., Wang, X. N., Jackson, G., Taylor, P., Dunn, A., & Proctor, S. J. (1998). Predicting Graft-versus-Host Disease in HLA-identical Bone Marrow Transplants: A Comparison of T-Cell Frequency Analysis and a Human Skin Explant Model. *Transplantation*, 66(7), 857–863.
- Draize, J. H., Woodard, G., & Calvery, H. O. (1944). Methods for the study of irritation and toxicity of substances applied topically to the skin and mucous membranes. *Journal of Pharmacology and Experimental Therapy*, 82, 377–390.
- Drozdroff, V., & Pledger, W. J. (1993). Commitment to Differentiation and Expression of Early Differentiation Markers in Murine Keratinocytes In Vitro Are Regulated Independently of Extracellular Calcium Concentrations. *Journal of Cell Biology*, 123(4), 909–919.
- Duarte, I., Lazzarini, R., & Rotter, A. (2010). Frequency of occupational contact dermatitis in

- a ambulatory of dermatologic allergy. *Anais Brasileiros de Dermatologia*, 85(4), 455–459. <http://doi.org/10.1590/S0365-05962010000400006>
- Eckert, R. L., & Rorke, E. A. (1989). Molecular biology of keratinocyte differentiation. *Environmental Health Perspectives*, 80, 109–116. <http://doi.org/10.1289/ehp.8980109>
- ECVAM. (1998). *ESAC statement on the scientific validity of the EpiSkin™ test (an in vitro test for skin corrosivity)*. Retrieved from https://ntp.niehs.nih.gov/iccvm/methods/dermal/epiderm/epiddocs/episkin_statement.pdf
- ECVAM. (2000). *ESAC statement on the application of the EpiDerm™ human skin model for skin corrosivity testing*.
- ECVAM. (2009a). *ESAC statement on the scientific validity of an in vitro test method for skin corrosivity testing*.
- ECVAM. (2009b). *Performance Standards for in vitro Skin Irritation Test Methods based on Reconstructed Human Epidermis (RHE) (No. ESAC31). Official Journal of the European Union*. Retrieved from https://eurl-ecvam.jrc.ec.europa.eu/validation-regulatory-acceptance/docs-skin-irritation-1/DOC8-updated_ECVAM_PS_2009.pdf
- ECVAM. (2009c). *Statement on the performance under UN GHS of three in vitro assays for skin irritation testing and the adaptation of the reference chemicals and defined accuracy values of the ECVAM skin irritation performance standards*. Retrieved from <http://oxfordhandbooks.com/view/10.1093/oxfordhb/9780199546282.001.0001/oxfordhb-9780199546282-e-24>
- ECVAM. (2009d). *Statement on the performance under UN GHS of three in vitro assays for skin irritation testing and the adaptation of the reference chemicals and defined accuracy values of the ECVAM skin irritation performance standards*.
- Elsholz, F., Harteneck, C., Muller, W., & Friedland, K. (2014). Calcium - a central regulator of keratinocyte Keratinocyte differentiation in health. *European Journal of Dermatology*, 24(6), 650–661. <http://doi.org/10.1684/ejd.2014.2452>
- Emter, R., Ellis, G., & Natsch, A. (2010). Performance of a novel keratinocyte-based reporter cell line to screen skin sensitizers in vitro. *Toxicology and Applied Pharmacology*, 245(3), 281–290. <http://doi.org/10.1016/j.taap.2010.03.009>
- EpiCS. (2012). *Standard Operating Procedure in vitro Skin Corrosion: Human Skin Model Test epiCS*.
- EpiSkin. (2009). *Validation of EpiSkin Test Method for the prediction of acute skin irritation of chemicals*.
- EPISKIN. (2013). *INVITTOX Protocol No . 118 EPISKIN™ Skin Corrosivity Test Index*.
- European Commission (1986). Council Directive 86/609/EEC of 24 November 1986 on the approximation of laws, regulations and administrative provisions of the Member States regarding the protection of animals used for experimental and other scientific purposes. Official Journal of the European Union, 1-28. Retrieved from <https://publications.europa.eu/en/publication-detail/-/publication/cc3a8ccb-5a30-4b6e-8da8-b13348caeb0c/language-en>

- European Commission (2006). Regulation (EC) 1907/2006 of the European Parliament and of the Council of 18 December 2006 concerning the Registration, Evaluation, Authorization and Restriction of Chemicals (REACH), establishing a European Chemicals Agency, amending Directive 1999/45/E, Official Journal of the European Union 396–849. Retrieved from <http://doi.org/http://eur-lex.europa.eu/LexUriServ/LexUriServ.do?uri=OJ:L:2006:396:0001:0849:EN:PDF>
- European Commission. (2007). *Fifth Report from the Commission to the Council and the European Parliament on the Statistics on the Number of Animals used for Experimental and Other Scientific Purposes in the Member States of the European Union*. Brussels. Official Journal of the European Union, 1–40. Retrieved from https://eurlex.europa.eu/resource.html?uri=cellar:e99d2a56-32fc-4f60-ad69-61ead7e377e8.0001.03/DOC_1&format=PDF
- European Commission (2008). European Regulation (EC) No 1272/2008 on classification, labelling and packaging of substances, Pub. L. No. 1272/2008 (2008). Official Journal of the European Union. Retrieved from <https://eur-lex.europa.eu/legalcontent/EN/TXT/HTML/?uri=CELEX:32008R1272&from=EN>
- European Commission (2009). Regulation (EC) No 1223/2009 of the European Parliament and of the Council of 30 November 2009 on cosmetic products, Official Journal of the European Union 59–209. Retrieved from <https://eur-lex.europa.eu/legalcontent/EN/TXT/HTML/?uri=CELEX:32009R1223&from=EN>
- European Commission (2010). Directive 2010/63/EU of the European Parliament and of the Council of 22 September 2010 on the protection of animals used for scientific purposes, Official Journal of the European Union 33–79. Retrieved from <https://eurlex.europa.eu/legal-content/EN/TXT/HTML/?uri=CELEX:32010L0063&from=EN>
- European Commission (2012). The Adverse Outcome Pathway for Skin Sensitisation Initiated by Covalent Binding to Proteins - Part 1: Scientific Evidence. Official Journal of the European Union: Series on Testing and Assessment. Retrieved from [http://olisweb.oecd.org/vgn-ext-templating/auth.jsp?docId=JT03321047&documentId=602493&original=/ENV-JM-MONO\(2012\)10-PART1-ENG.pdf&date=1336140602027&fileName=JT03321047.pdf&organisationId=1&originalURI=/vgn-ext-templating/auth.jsp](http://olisweb.oecd.org/vgn-ext-templating/auth.jsp?docId=JT03321047&documentId=602493&original=/ENV-JM-MONO(2012)10-PART1-ENG.pdf&date=1336140602027&fileName=JT03321047.pdf&organisationId=1&originalURI=/vgn-ext-templating/auth.jsp)
- European Commission. (2013). *Seventh Report on the Statistics on the Number of Animals used for Experimental and other Scientific Purposes in the Member States of the European Union*. Official Journal of the European Union, 1–40. Retrieved from https://eurlex.europa.eu/resource.html?uri=cellar:e99d2a56-32fc-4f60-ad69-61ead7e377e8.0001.03/DOC_1&format=PDF
- EvaluatePharma. (2014). *World Preview 2018, Outlook to 2024: in-depth forecast models of medtech market. EvaluatePharma's World Preview* (11th ed.).
- Evans, W. (2015). Removing Aggregates in Monoclonal Antibody Purification. *Pharmaceutical Technology*, 39(3), 72–74.
- Eyes, T. J., Austerberry, J. I., Dearman, R. J., Johannissen, L. O., Kimber, I., Smith, N., Thistlethwaite, A., Derrick, J. P. (2019). Identification of B cell epitopes enhanced by

- protein unfolding and aggregation. *Molecular Immunology*, 105, 181–189. <http://doi.org/10.1016/j.molimm.2018.11.020>
- Felter, S. P., Robinson, M. K., Basketter, D. A., & Gerberick, G. F. (2002). A review of the scientific basis for uncertainty factors for use in quantitative risk assessment for the induction of allergic contact dermatitis. *Contact Dermatitis*, 47, 257–266.
- Felter, S. P., Ryan, C. A., Basketter, D. A., Gilmour, N. J., & Gerberick, F. G. (2003). Application of the risk assessment paradigm to the induction of allergic contact dermatitis. *Regulatory Toxicology and Pharmacology*, 37(1), 1–10.
- Filipe, V., Poole, R., Kutscher, M., Forier, K., Braeckmans, K., & Jiskoot, W. (2011). Fluorescence Single Particle Tracking for the Characterization of Submicron Protein Aggregates in Biological Fluids and Complex Formulations. *Pharmaceutical Research*, 28, 1112–1120. <http://doi.org/10.1007/s11095-011-0374-0>
- Filipe, V., Poole, R., Oladunjoye, O., Braeckmans, K., & Jiskoot, W. (2012). Detection and Characterization of Subvisible Aggregates of Monoclonal IgG in Serum. *Pharmaceutical Research*, 29, 2202–2212. <http://doi.org/10.1007/s11095-012-0749-x>
- Frank Gerberick, G., Ryan, C. A., Dearman, R. J., & Kimber, I. (2007). Local lymph node assay (LLNA) for detection of sensitization capacity of chemicals. *Methods*, 41(1), 54–60. <http://doi.org/10.1016/j.ymeth.2006.07.006>
- Frankild, S., Volund, A., Wahlberg, J. E., & Andersen, K. E. (2000). Comparison of the sensitivities of the Buehler test and the guinea pig maximization test for predictive testing of contact allergy. *Acta Dermato-Venereologica*, 80(4), 256–262. <http://doi.org/10.1080/000155500750012126>
- Franz, T. J., Lehman, P. A., & Raney, S. G. (2009). Use of Excised Human Skin to Assess the Bioequivalence of Topical Products. *Skin Pharmacology and Physiology*, 22, 276–286. <http://doi.org/10.1159/000235828>
- Fraunhofer, W., & Winter, G. (2004). The use of asymmetrical flow field-flow fractionation in pharmaceuticals and biopharmaceuticals. *European Journal of Pharmaceutics and Biopharmaceutics*, 58, 369–383. <http://doi.org/10.1016/j.ejpb.2004.03.034>
- Freeman, A. E., Igel, H. J., Herrman, B. J., & Kleinfeld, K. L. (1976). Growth and Characterization of Human Skin Epithelial Cell Cultures. *Society for in Vitro Biology*, 12(5), 352–362.
- Groeber, F., Schober, L., Schmid, F. F., Traube, A., Kolbus-hernandez, S., Daton, K., ... Mewes, K. R. (2016). Catch-up validation study of an in vitro skin irritation test method based on an open source reconstructed epidermis (phase II). *Toxicology in Vitro*, 36, 254–261. <http://doi.org/10.1016/j.tiv.2016.07.008>
- Guadagni, F., Roselli, M., Cosimelli, M., Ferroni, P., Spila, A., Cavaliere, F., Arcuri, R., Carlini, S., Mariotti, S., Gandolfo, G. M., Casciani, C. U., Greiner, J. W., Schlom, J. (1996). TAG - 72 expression and its role in the biological evaluation of human colorectal cancer. *Anticancer Research*, 16(4B), 2141–2148
- Guenno, G. Le, Ruivard, M., Charra, L., & Phillippe, P. (2011). Rituximab-induced serum sickness in refractory immune thrombocytopenic purpura. *Internal Medicine Journal*,

202–205. <http://doi.org/10.1111/j.1445-5994.2010.02384.x>

- Hartung, T. (2007). *Statement on the validity of in vitro tests for skin irritation*. ECVAM
- Hartung, T., Bremer, S., Casati, S., Coecke, S., Corvi, R., Fortaner, S., Gribaldo, L., Halder, M., Hoffmann, S., Roi, A. J., Prieto, P., Sabbioni, E., Scott, L., Worth, A., Zuang, V. 186 (2004). A modular approach to the ECVAM principles on test validity. *ATLA*, 32(5), 467–472. <http://doi.org/10.1177/026119290403200503>
- Hennings, H., Michael, D., Cheng, C., Steinert, P., Holbrook, K., & Yuspa, S. H. (1980). Calcium Regulation of Growth and Differentiation of Mouse Epidermal Cells in Culture. *Cell*, 19(January), 245–254.
- Hermeling, S., Crommelin, D., Schellekens, H., & Jiskoot, W. (2004). Structure-immunogenicity relationships of therapeutic proteins. *Pharmaceutical Research*, 21(6), 897–903.
- Hewitt, N. J., Edwards, R. J., Fritsche, E., Goebel, C., Aeby, P., Scheel, J., Reisinger, K., Ouédraogo, G., Duché, D., Eilstein, J., Latil, A., Kenny, J., Moore, C., Kuehn, J., Barroso, J., Fautz, R., Pfuhler, S. (2013). Use of human *in vitro* skin models for accurate and ethical risk assessment: metabolic considerations. *Toxicological Sciences*, 133(2), 209–217. <http://doi.org/10.1093/toxsci/kft080>
- Hodivala, K. J., & Watt, F. M. (1994). Evidence that cadherins play a role in the downregulation of integrin expression that occurs during keratinocyte terminal differentiation. *Journal of Cell Biology*, 124(4), 589–600. <http://doi.org/10.1083/jcb.124.4.589>
- Homann, A., Röckendorf, N., Kromminga, A., Frey, A., & Jappe, U. (2015). B cell epitopes on infliximab identified by oligopeptide microarray with unprocessed patient sera. *Journal of Translational Medicine*, 13(339), 1–10. <http://doi.org/10.1186/s12967-015-0706-7>
- Homann, A., Röckendorf, N., Kromminga, A., Frey, A., Platts-mills, T. A., & Jappe, U. (2017). Glycan and Peptide IgE Epitopes of the TNF-alpha Blockers Infliximab and Adalimumab – Precision Diagnostics by Cross-Reactivity Immune Profiling of Patient Sera. *Theranostics*, 7(19), 4699–4709. <http://doi.org/10.7150/thno.20654>
- Imokawa, G., Kuno, H., & Kawai, M. (1991). Stratum corneum lipids serve as a bound-water modulator. *The Journal of Investigative Dermatology*, 96, 845–851. <http://doi.org/10.1111/1523-1747.ep12474562>
- Janeway, C. A., Travers, P., Walport, M., & Shlomchik, M. J. (2001). *Immunobiology: The immune system in health and disease*. (G. Science, Ed.) (5th ed.). New York.
- Joubert, M. K., Deshpande, M., Yang, J., Reynolds, H., Bryson, C., Fogg, M., Baker, M. P., Herskovitz, J., Goletz, T. J., Zhou, L., Moxness, M., Flynn, G. C., Narhi, L. O., Jawa, V. (2016). Use of *in vitro* assays to assess immunogenicity risk of antibody-based biotherapeutics. *PLoS ONE*, 11(8), 1–22. <http://doi.org/10.1371/journal.pone.0159328>
- Joubert, M. K., Hokom, M., Eakin, C., Zhou, L., Deshpande, M., Baker, M. P., Goletz, T. J., Kerwin, B. A., Chirmule, N., Narhi, L. O., Jawa, V. (2012). Highly aggregated antibody therapeutics can enhance the *in vitro* innate and late-stage T-cell immune responses. *Journal of Biological Chemistry*, 287(30), 25266–25279.

- <http://doi.org/10.1074/jbc.M111.330902> Joubert, M. K., Luo, Q., Nashed-Samuel, Y., Wypych, J., & Narhi, L. O. (2011). Classification and characterization of therapeutic antibody aggregates. *Journal of Biological Chemistry*, 286(28), 25118–25133. <http://doi.org/10.1074/jbc.M110.160457>
- Jung, K., Lee, S., Jang, W., Jung, H., Heo, Y., Park, Y., Bae, S., Lim, K. M., Seok, S. H. (2014). 187
KeraSkin™-VM: A novel reconstructed human epidermis model for skin irritation tests. *Toxicology in Vitro*, 28(5), 742–750. <http://doi.org/10.1016/j.tiv.2014.02.014>
- Kandárová, H., Liebsch, M., Spielmann, H., Genschow, E., Schmidt, E., Traue, D., Guest, R., Whittingham, A., Warren, N., Gamer, A. O., Remmele, M., Kaufmann, T., Wittmer, E., De Wever, B., Rosdy, M. (2006). Assessment of the human epidermis model SkinEthic RHE for *in vitro* skin corrosion testing of chemicals according to new OECD TG 431. *Toxicology in Vitro*, 20, 547–559. <http://doi.org/10.1016/j.tiv.2005.11.008>
- Kent, K. P., Schroeder, C. E., & Sharma, C. (2018). Solution pH jump during antibody and Fc-fusion protein thaw leads to increased aggregation. *Journal of Pharmaceutical Analysis*, 8, 302–306. <http://doi.org/10.1016/j.jpha.2017.09.002>
- Kiese, S., Papppenberger, A., Freiss, W., & Mahler, H.-C. (2008). Shaken, not stirred: Mechanical stress testing of an IgG1 antibody. *Journal of Pharmaceutical Sciences*, 97(10), 26–33. <http://doi.org/10.1002/jps>
- Kimber, I., & Basketter, D. A. (1997). Contact sensitization: A new approach to risk assessment. *Human and Ecological Risk Assessment: An International Journal*, 3(3), 385–395. <http://doi.org/10.1080/10807039709383695>
- Kimber, I., & Dearman, R. J. (2010). The local Lymph Node Assay and Skin Sensitization Testing. In R. R. Dietert (Ed.), *Immunotoxicity Testing: Methods and Protocols* (Vol. 598, pp. 221–231). Humana Press. <http://doi.org/10.1007/978-1-60761-401-2>
- Kimber, I., Mitchell, J. A., & Griffin, A. C. (1986). Development of a murine local lymph node assay for the determination of sensitization potential. *Food and Chemical Toxicology*, 24(6), 585–586.
- Kimber, I., & Weisenberger, C. (1989). A murine local lymph node assay for the identification of contact allergens - assay development and results of an initial validation study. *Archives of Toxicology*, 63, 274–282.
- Kimby, E. (2005). Tolerability and safety of rituximab (MabThera). *Cancer Treatment Reviews*, 31, 456–473. <http://doi.org/10.1016/j.ctrv.2005.05.007>
- Klein, S. D., & Brune, B. (2002). Heat-shock protein 70 attenuates nitric oxide-induced apoptosis in RAW macrophages by preventing cytochrome c release. *Biochemical Journal*, 362, 635–641.
- Klicks, J., Molitor, E. Von, Ertongur-fauth, T., & Hafner, M. (2017). In vitro skin three-dimensional models and their applications. *Journal of Cellular Biotechnology*, 3, 21–39. <http://doi.org/10.3233/JCB-179004>
- Kolle, S. N., Hill, E., Raabe, H., Landsiedel, R., & Curren, R. (2019). Regarding the references for reference chemicals of alternative methods. *Toxicology in Vitro*, 57(January), 48–53.

<http://doi.org/10.1016/j.tiv.2019.02.007>

- Kolly, C., Suter, M. M., & Mu, E. J. (2005). Proliferation, Cell Cycle Exit, and Onset of Terminal Differentiation in Cultured Keratinocytes: Pre-Programmed Pathways in Control of C-Myc and Notch1 Prevail Over Extracellular Calcium Signals. *Journal of Investigative Dermatology*, 124, 1014–1025. <http://doi.org/10.1111/j.0022-202X.2005.23655.x>
- Kumar, L. S., Tangadpalliwar, S. R., Desai, A., Singh, V. K., & Jere, A. (2016). Integrated Computational Solution for Predicting Skin Sensitization Potential of Molecules. *PloS One*, 1–22. <http://doi.org/10.1371/journal.pone.0155419>
- Landsteiner, K., & Chase, M. W. (1939). Studies on the sensitization of animals with simple chemical compounds. *Journal of Experimental Medicine*, (12).
- Landsteiner, K., & Chase, M. W. (1941). Studies on the sensitization of animals with simple chemical compounds. *Journal of Experimental Medicine*, 73(3), 431–438.
- Legutki, J. B., & Johnston, S. A. (2013). Immunosignatures can predict vaccine efficacy. *Proceedings of the National Academy of Sciences*, 110(46), 18614–18619. <http://doi.org/10.1073/pnas.1309390110>
- Legutki, J. B., Zhao, Z., Greving, M., Woodbury, N., Johnston, S. A., & Stafford, P. (2014). Scalable high-density peptide arrays for comprehensive health monitoring. *Nature Communications*, 5, 1–7. <http://doi.org/10.1038/ncomms5785>
- Lerner, K., Kao, G., Storb, R., Buckner, C., Clift, R., & Thomas, E. (1974). Histopathology of graft-vs.-host reaction (GvHR) in human recipients of marrow from HL-A-matched sibling donors. *Transplantation Proceedings*, 6(4), 367–371.
- Li, C., Lee, J., Ko, Y., Kim, J., & Seo, J. (2000). Heat Shock Protein 70 Inhibits Apoptosis Downstream of Cytochrome c Release and Upstream of Caspase-3 Activation *. *The Journal of Biological Chemistry*, 275(33), 25665–25671. <http://doi.org/10.1074/jbc.M906383199>
- Liebsch, M., & Spielmann, H. (2002). Currently available in vitro methods used in the regulatory toxicology. *Toxicology Letters*, 127(1–3), 127–134. [http://doi.org/10.1016/S0378-4274\(01\)00492-1](http://doi.org/10.1016/S0378-4274(01)00492-1)
- Lillie, J. H., MacCallum, D. K., & Jepsen, A. (1980). Fine structure of subcultivated stratified squamous epithelium grown on collagen rafts. *Experimental Cell Research*, 125, 153–165.
- Louis-Dit-Sully, C., Blumenthal, B., Duchniewicz, M., Beck-Garcia, K., Fiala, G. J., BeckGarcia, E., Mukenhirn, M., minguet, S., Schamel, W. W. (2014). Activation of the TCR Complex by Peptide-MHC and Superantigens. In S. F. Martin (Ed.), *T Lymphocytes as Tools in Diagnostics and Immunotoxicology* (pp. 9–24). <http://doi.org/10.1007/978-3-0348-0726-5>
- Luo, Q., Joubert, M. K., Stevenson, R., Ketchem, R. R., Narhi, L. O., & Wypych, J. (2011). Chemical modifications in therapeutic protein aggregates generated under different stress conditions. *Journal of Biological Chemistry*, 286(28), 25134–25144. <http://doi.org/10.1074/jbc.M110.160440>
- Maas, C., Hermeling, S., Bouma, B., Jiskoot, W., & Gebbink, M. F. B. G. (2007). A Role for

- Protein Misfolding in Immunogenicity of Biopharmaceuticals. *The Journal of Biological Chemistry*, 282(4), 2229–2236. <http://doi.org/10.1074/jbc.M605984200>
- Manaves, V., Qin, W., Bauer, A. L., Rossie, S., Kobayashi, M., & Rane, S. G. (2004). Calcium and vitamin D increase mRNA levels for the growth control hIK1 channel in human epidermal keratinocytes but functional channels are not observed. *BMC Dermatology*, 4(7), 1–12. <http://doi.org/10.1186/1471-5945-4-7>
- Marionnet, C., Vioux-Chagnoleau, C., Pierrard, C., Sok, J., Asselineau, D., & Bernerd, F. (2006). Morphogenesis of dermal – epidermal junction in a model of reconstructed skin: beneficial effects of vitamin C. *Experimental Dermatology*, 15, 625–633. <http://doi.org/10.1111/j.0906-6705.2006.00454.x>
- Marzulli, F. N., & Maibach, H. I. (1975). The rabbit as a model for evaluating skin irritants: A comparison of results obtained on animals and man using repeated skin exposures. *Food and Cosmetics Toxicology*, 13(5), 533–540. [http://doi.org/10.1016/0015-6264\(75\)90008-5](http://doi.org/10.1016/0015-6264(75)90008-5)
- Marzulli, F. N., & Mamach, H. I. (1974). The use of graded concentrations in studying skin sensitizers: experimental contact sensitization in man. *Food and Cosmetics Toxicology*, 12, 219–227.
- MatTek. (2004). *In vitro skin irritation test: Human skin model - Model: EpiDerm™ -200*.
- MatTek. (2008). *Validation of EpiDerm Test Method for the prediction of acute skin irritation of chemicals*.
- MatTek. (2012). *SOP for: in vitro EpiDerm skin corrosion test (EPI-200-SCT)*.
- Mayer, R. L. (1954). *Group Sensitization to Compounds of Quinone Structure and its Biochemical Basis. Role of these Substances in Cancer*. (S. Karger, Ed.) *Progress in Allergy*. Basel-New Yorl.
- Mcnamee, P. M., Marie, A., Basketter, D. A., Gerberick, G. F., Gilpin, D. A., Hall, B. M., Jowsey, I., Robinson, M. K. (2008). A review of critical factors in the conduct and interpretation of the human repeat insult patch test. *Regulatory Toxicology and Pharmacology*, 52(1), 24–34. <http://doi.org/10.1016/j.yrtph.2007.10.019>
- Menzen, T., & Friess, W. (2014). Temperature-ramped studies on the aggregation, unfolding, and interaction of a therapeutic monoclonal antibody. *Journal of Pharmaceutical Sciences*, 103(2), 445–455. <http://doi.org/10.1002/jps.23827>
- Mewes, K. R., Fischer, A., Zöller, N. N., Laubach, V., Bernd, A., Jacobs, A., van Rompay, A., Liebsch, M., Pirow, R., Petersohn, D. (2016). Catch-up validation study of an *in vitro* skin irritation test method based on an open source reconstructed epidermis (phase I). *Toxicology in Vitro*, 36, 238–253. <http://doi.org/10.1016/j.tiv.2016.07.007>
- Mosser, D. D., Caron, A. W., Bourget, L., Denis-larose, C., & Massie, B. (1997). Role of the Human Heat Shock Protein hsp70 in Protection against Stress-Induced Apoptosis. *Molecular and Cellular Biology*, 17(9), 5317–5327.
- Murray, P. J. (2005). The primary mechanism of the IL-10-regulated antiinflammatory response is to selectively inhibit transcription. *Proceedings of the National Academy of Sciences*, 102(24), 8686–8691.

- Naish, J., & Syndercombe Court, D. (2014). Pathology and Immunology. In J. Naish & D. Syndercombe Court (Eds.), *Medical Sciences* (2nd ed., p. 840). Saunders.
- National Research Council. (2007). *Toxicity Testing in the 21st Century: A Vision and a Strategy*. Washington: The National Academies Press.
- Natsch, A., Emter, R., Gfeller, H., Haupt, T., & Ellis, G. (2015). Predicting Skin Sensitizer Potency Based on In Vitro Data from KeratinoSens and Kinetic Peptide Binding: Global Versus Domain-Based Assessment. *Toxicological Sciences*, 143(2), 319–332. <http://doi.org/10.1093/toxsci/kfu229>
- Natsch, A., Ryan, C. A., Foertsch, L., Emter, R., Jaworska, J., Gerberick, F., & Kern, P. (2013). A dataset on 145 chemicals tested in alternative assays for skin sensitization undergoing prevalidation. *Journal of Applied Toxicology*, Epub(January). <http://doi.org/10.1002/jat.2868>
- Nixon, G. A., Tyson, C. A., & Wertz, W. C. (1975). Interspecies comparisons of skin irritancy. *Toxicology and Applied Pharmacology*, 31(3), 481–490. [http://doi.org/10.1016/0041-008X\(75\)90272-0](http://doi.org/10.1016/0041-008X(75)90272-0)
- Obrezanova, O., Arnell, A., Cuesta, R. G., Berthelot, M., Gallagher, T. R., Zurdo, J., & Stallwood, Y. (2015). Aggregation risk prediction for antibodies and its application to biotherapeutic development. *MAbs*, 7(2), 352–363.
- OECD. (2004). *OECD Testing Guideline No. 428: Skin Absorption: in vitro Method* (OECD Guidelines for the testing of chemicals No. 428). Paris: OECD Publishing.
- OECD. (2005). Guidance document on the validation and international acceptance of new or updated test methods for hazard assessment. *Series on Testing and Assessment* (Vol. No. 34). Paris: OECD Publishing
- OECD. (2010). OECD Test Guideline No. 429: Skin Sensitization - Local Lymph Node Assay. *OECD Guidelines for the testing of chemicals* (No. 429). Paris: OECD Publishing.
- OECD. (2012a). OECD Test Guideline No. 405: Acute Eye Irritation/Corrosion. *OECD Guidelines for the testing of chemicals* (No. 405). Paris: OECD Publishing.
- OECD. (2012b). *Proposal for a template, and guidance on developing and assessing the completeness of adverse outcome pathways*. Paris: OECD Publishing
- OECD. (2013). OECD Testing Guideline No. 439: *in vitro* skin irritation - Reconstructed Human Epidermis (RHE) Test Method. *OECD Guidelines for the testing of chemicals* (No. 439). Paris: OECD Publishing.
- OECD. (2014). OECD Test Guideline No. 431: *in vitro* skin corrosion - Reconstructed Human Epidermis (RHE) Test Method. *OECD Guidelines for the testing of chemicals* (No. 431). Paris: OECD Publishing.

- OECD. (2015a). OECD Test Guideline No. 404: Acute Dermal Irritation/Corrosion. *OECD Guidelines for the testing of chemicals (No. 404)*. Paris: OECD Publishing.
- OECD. (2015b). OECD Testing Guideline No. 442D: *in vitro* skin sensitisation - ARE-Nrf2 Luciferase. *OECD Guidelines for the testing of chemicals (No. 442D)*. Paris: OECD Publishing.
- OECD. (2018). OECD Testing Guideline No. 442E: *in vitro* skin sensitisation assays addressing the key event on activation of dendritic cells on the adverse outcome pathways for skin sensitization. *OECD Guidelines for the testing of chemicals (No. 442E)*. Paris: OECD Publishing
- Palanichamy, A., Jahn, S., Nickles, D., Derstine, M., Abounasr, A., Hauser, S., Baranzini, S. E., Leppert, D., von Büdingen, H. C. (2015). Rituximab efficiently depletes increased CD20 expressing T cells in multiple sclerosis patients. *Journal of Immunology*, 193(2), 580–586. <http://doi.org/10.4049/jimmunol.1400118>. Rituximab
- Pasonen-Seppanen, S., Suhonen, T. M., Kirjavainen, M., Suihko, E., Urtti, A., Miettinen, M., Hyttinen, M., Tammi, M., Tammi, R. (2001). Vitamin C enhances differentiation of a continuous keratinocyte cell line (REK) into epidermis with normal stratum corneum ultrastructure and functional permeability barrier. *Histochem Cell Biol*, 116, 287–297. <http://doi.org/10.1007/s004180100312>
- Pedrosa, T. N., Catarino, C. M., Pennacchi, P. C., Assis, S. R., Gimenes, F., Consolaro, M., Barros S. B. M., Maria-Engler, S. S. (2017). A new reconstructed human epidermis for *in vitro* skin irritation testing. *Toxicology in Vitro*, 42, 31–37. <http://doi.org/10.1016/j.tiv.2017.03.010>
- Peters, B. J. M., Capelle, M. A. H., Arvinte, T., & van de Garde, E. M. W. (2013). Validation of an automated method for compounding monoclonal antibody patient doses: case studies of Avastin (bevacizumab), Remicade (infliximab) and Herceptin (trastuzumab). *MAbs*, 5(1), 162–170. <http://doi.org/10.4161/mabs.22873>
- Phillips, L., Steinberg, M., Maibach, H. I., & Akers, W. A. (1972). A comparison of Rabbit and Human Certain Skin Response to certain irritants. *Toxicology and Applied Pharmacology*, 21, 369–382.
- Pillai, S., Bikle, D. D., Mancianti, M., Cline, P., & Hincenbergs, M. (1990). Calcium Regulation of Growth and Differentiation of Normal Human Keratinocytes: Modulation of Differentiation Competence by Stages of Growth and Extracellular Calcium. *Journal of Cellular Physiology*, 143, 294–302.
- Piroid, C., Ovigne, J., Rousset, F., Martinozzi-teissier, S., Gomes, C., Cotovio, J., & Alépée, N. (2015). The Myeloid U937 Skin Sensitization Test (U-SENS) addresses the activation of dendritic cell event in the adverse outcome pathway for skin sensitization. *Toxicology in Vitro*, 29, 901–916.
- Poumay, Y., & Coquette, A. (2007). Modelling the human epidermis in vitro: tools for basic and applied research. *Archives of Dermatology Research*, 298, 361–369.

<http://doi.org/10.1007/s00403-006-0709-6>

- Poumay, Y., Dupont, F., Marcoux, S., Leclercq-Smekens, M., Herin, M., & Coquette, A. (2004). A simple reconstructed human epidermis: preparation of the culture model and utilization in in vitro studies. *Archives of Dermatology Research*, 296, 203–211. <http://doi.org/10.1007/s00403-004-0507-y>
- Poumay, Y., & Pittelkow, M. R. (1995). Cell Density and Culture Factors Regulate Keratinocyte Commitment to Differentiation Expression of Suprabasal K1/ K10 Keratins. *Journal of Investigative Dermatology*, 104(2), 271–276. <http://doi.org/10.1111/1523-1747.ep12612810>
- Prado, M., Bendtzen, K., & Andrade, L. C. (2017). Biological anti-TNF drugs: immunogenicity underlying treatment failure and adverse events. *Expert Opin Drug Metab Toxicol*, 13(9), 985–995. <http://doi.org/10.1080/17425255.2017.1360280>
- Presland, R. B., & Dale, B. A. (2000). Epithelial Structural Proteins of the Skin and Oral Cavity: Function in Health and Disease. *Critical Reviews in Oral Biology & Medicine*, 11(4), 383–408. <http://doi.org/10.1177/10454411000110040101>
- Pruniéras, M., Régnier, M., & Woodley, D. (1983). Methods for cultivation of keratinocytes with an air liquid interface. *The Journal of Investigative Dermatology*. <http://doi.org/10.1111/1523-1747.ep12540324>
- Qi, Y., Wang, H., Zou, Y., Liu, C., Liu, Y., Wang, Y., & Zhang, W. (2011). Over-expression of mitochondrial heat shock protein 70 suppresses programmed cell death in rice. *FEBS Letters*, 585(1), 231–239. <http://doi.org/10.1016/j.febslet.2010.11.051>
- Rane, S. S., Dearman, R. J., Kimber, I., Uddin, S., Bishop, S., Shah, M., Podmore, A., Pluen, A., Derrick, J. P. (2019). Impact of a Heat Shock Protein Impurity on the Immunogenicity of Biotherapeutic Monoclonal Antibodies. *Pharmaceutical Research*, 36(51), 1–14.
- Reichert, J. M., & Valge-Archer, V. E. (2007). Development trends for monoclonal antibody cancer therapeutics. *Nature Reviews Drug Discovery*, 6(5), 349–56. <http://doi.org/10.1038/nrd2241>
- Rheinwatd, J. G., & Green, H. (1975). Serial cultivation of strains of human epidermal keratinocytes: the formation of keratinizin colonies from single cell. *Cell*, 6(3), 331–343. [http://doi.org/10.1016/S0092-8674\(75\)80001-8](http://doi.org/10.1016/S0092-8674(75)80001-8)
- Roberts, D. W., Aptula, A. O., & Patlewicz, G. (2006). Mechanistic Applicability Domains for Non-Animal Based Prediction of Toxicological Endpoints. QSAR Analysis of the Schiff Base Applicability Domain for Skin Sensitization. *Chemical Research in Toxicology*, 19, 1228–1233.
- Roberts, D. W., & Williams, D. L. (1982). The Derivation of Quantitative Correlations between Skin Sensitisation and Physio-chemical Parameters for Alkylating Agents, and their Application to Experimental Data for Sultones. *Journal of Theoretical Biology*, 99, 807–825.
- Roger, M., Fullard, N., Costello, L., Bradbury, S., Markiewicz, E., O'Reilly, S., Darling, N., Ritchie, P., Määttä, A., Karakesisoglou, I., Nelson, G., von Zglinicki, T., Dicolandrea, T., isfort, R., Bascom, C., Przyborski, S. (2019). Bioengineering the microanatomy of human

- skin. *Journal of Anatomy*, 234, 438–455. <http://doi.org/10.1111/joa.12942>
- Roitt, I., & Delves, P. (1998). *Encyclopedia of Immunology*. (P. J. Delves & I. Roitt, Eds.) (2nd ed., Vol. volume 1). ACADEMIC PRESS, INC.
- Rombach-Riegraf, V., Karle, A. C., Wolf, B., Sordé, L., Koepke, S., Gottlieb, S., ... Kiessling, A. (2014). Aggregation of human recombinant monoclonal antibodies influences the capacity of dendritic cells to stimulate adaptive T-cell responses in vitro. *PLoS ONE*, 9(1), e86322. <http://doi.org/10.1371/journal.pone.0086322>
- Russel, W. M. S., & Burch, R. L. (1959). *The principles of humane experimental technique*. London: Methuen.
- Sakaguchi, H., Ashikaga, T., Miyazawa, M., Yoshida, Y., Ito, Y., Yoneyama, K., Hirota, M., Itagaki, H., Toyoda, H., Suzuki, H. (2006). Development of an *in vitro* skin sensitization test using human cell lines; human Cell Line Activation Test (h-CLAT) II . An interlaboratory study of the h-CLAT. *Toxicology in Vitro*, 20, 774–784. <http://doi.org/10.1016/j.tiv.2005.10.014>
- SCCS - Scientific Committee on Consumer Safety. (2010). Basic criteria for the *in vitro* 193 assessment of dermal absorption of cosmetic ingredients, SCCS/1358/10. European Commission 1–14. <http://doi.org/10.2772/25843>
- Schäfer-korting, M., Bock, U., Diembeck, W., Düsing, H., Gamer, A., Haltner-Ukomadu, E., Hoffmann, C., Kaca, M., Kamp, H., Kersen, S., Kietzmann, M., Korting, H. C., Krächter, H. U., Lehr, C. M., Liebsch, M., Mehling, A., Müller-Goymann, C., Netzlauff, F., Niedorf, F., Rübbelke, M. K., Schäfer, U., Schmidt, E., Schreiber, S., Spielmann, H., Vuia, A., Weimer, M. (2008). The use of reconstructed human epidermis for skin absorption testing: results of the validation study. *Alternatives to Laboratory Animals*, 36, 161–167.
- Schmook, F. P., Meingassner, J. G., & Billich, A. (2001). Comparison of human skin or epidermis models with human and animal skin in in vitro percutaneous absorption. *International Journal of Pharmaceutics*, 215, 51–56.
- Schneider, K., & Akkan, Z. (2004). Quantitative relationship between the local lymph node assay and human skin sensitization assays. *Regulatory Toxicology and Pharmacology*, 39(3), 245–255. <http://doi.org/10.1016/j.yrtph.2004.02.002>
- Schreiber, S., Mahmoud, A., Vuia, A., Rübbelke, M. K., Schmidt, E., Schaller, M., Kandarova, H., Haberland, A., Schäfer, U. F., Bock, U., Korting, H. C., Liebsch, M., Schäfer-Korting, M. (2005). Reconstructed epidermis versus human and animal skin in skin absorption studies. *Toxicology in Vitro*, 19(6), 813–822. <http://doi.org/10.1016/j.tiv.2005.04.004>
- Schurer, N. Y., & Elias, P. M. (1991). The biochemistry and function of stratum corneum lipids. *Advances in Lipid Research*, 24(1971), 27–56. <http://doi.org/10.1016/B978-0-12-024924-4.50006-7>
- Settivari, R. S., Gehen, S. C., Acosta, R., Visconti, N. R., Boverhof, D. R., & Carney, E. W. (2015). Application of the KeratinoSensTM assay for assessing the skin sensitization potential of agrochemical active ingredients and formulations. *Regulatory Toxicology and Pharmacology*, 72, 350–360.

- SkinEthic. (2012). *INVITTOX Protocol SKINETHIC™ Skin Corrosivity Test Index*.
- SkinEthics. (2009). *Validation of SkinEthic Test Method for the prediction of acute skin irritation of chemicals*.
- Smith, M. R. (2003). Rituximab (monoclonal anti-CD20 antibody): mechanisms of action and resistance. *Oncogene*, 22(47), 7359–7368. <http://doi.org/10.1038/sj.onc.1206939>
- St. Clair, J. B., Detanico, T., Aviszus, K., Kirchenbaum, G. A., Christie, M., Carpenter, J. F., & Wysocki, L. J. (2017). Immunogenicity of Isogenic IgG in Aggregates and Immune Complexes. *Plos One*, 12(1), e0170556. <http://doi.org/10.1371/journal.pone.0170556>
- Starzl, T. E., & Fung, J. J. (1986). Orthoclone OKT3 in Treatment of Allografts Rejected Under Cyclosporine-Steroid Therapy. *Transplantation Proceedings*, 18(4), 937–941. Retrieved from <http://www.pubmedcentral.nih.gov/articlerender.fcgi?artid=3000128&tool=pmcentrez&rendertype=abstract>
- Stebbing, R., Eastwood, D., Poole, S., & Thorpe, R. (2013). After TGN1412: recent developments in cytokine release assays. *Journal of Immunotoxicology*, 10(1), 75–82. <http://doi.org/10.3109/1547691X.2012.711783>
- Stotts, J. (1980). Planning, conduct, and interpretation of human predictive sensitization patch tests. In V. A. Drill & P. Lazar (Eds.), *Current Concepts in Cutaneous Toxicity* (pp. 41–53). New York: Academic Press.
- Sviland, L., & Dickinson, a M. (1999). A human skin explant model for predicting graft-versus-host disease following bone marrow transplantation. *Journal of Clinical Pathology*, 52(12), 910–913. <http://doi.org/10.1136/jcp.52.12.910>
- Talley, K., & Alexov, E. (2010). On the pH-optimum of activity and stability of proteins. *Proteins*, 78(12), 2699–2706. <http://doi.org/10.1016/j.immuni.2010.12.017>.Two-stage
- Thyssen, J. P., Linneberg, A., Menné, T., & Johansen, J. D. (2007). The epidemiology of contact allergy in the general population-prevalence and main findings. *Contact Dermatitis*, 57(5), 287–299. <http://doi.org/10.1111/j.1600-0536.2007.01220.x>
- UN. (2009). *Globally Harmonized System of Classification and Labelling of Chemicals (GHS)* (ST/SG/AC.10/30/Rev.3). New York and Geneva. Retrieved from http://www.unece.org/trans/danger/publi/ghs/ghs_rev03/03files_e.html
- Vermeer, A. W. P., Bremer, M. G. E. G., & Norde, W. (1998). Structural changes of IgG induced by heat treatment and by adsorption onto a hydrophobic Teflon surface studied by circular dichroism spectroscopy. *Biochimica et Biophysica Acta - General Subjects*, 1425(1), 1–12. [http://doi.org/10.1016/S0304-4165\(98\)00048-8](http://doi.org/10.1016/S0304-4165(98)00048-8)
- Vermeer, A. W. P., & Norde, W. (2000). The thermal stability of immunoglobulin: unfolding and aggregation of a multi-domain protein. *Biophysical Journal*, 78(1), 394–404. [http://doi.org/10.1016/S0006-3495\(00\)76602-1](http://doi.org/10.1016/S0006-3495(00)76602-1)
- Vigan, M., & Castelain, F. (2014). Cosmetovigilance: definition, regulation and use “in practice.” *European Journal of Dermatology*, 24(6), 643–649. <http://doi.org/10.1684/ejd.2014.2493>

- Vinken, M. (2013). The adverse outcome pathway concept: A pragmatic tool in toxicology. *Toxicology*, 312, 158–165. <http://doi.org/10.1016/j.tox.2013.08.011>
- Vogelsang, G. A., Hess, A. D., Berkman, A. W., Tutschka, P. J., Farmer, E. R., Converse, P. J., & Santos, G. W. (1985). An in vitro predictive test for graft versus host disease in patients with genotypic HLA-identical bone marrow transplants. *The New England Journal of Medicine*, 313(11), 645–650.
- Vollmers, A., Wallace, L., Fullard, N., Höher, T., Alexander, M. D., & Reichelt, J. (2012). Two- and Three-Dimensional Culture of Keratinocyte Stem and Precursor Cells Derived from Primary Murine Epidermal Cultures. *Stem Cell Reviews and Reports*, 8, 402–413. <http://doi.org/10.1007/s12015-011-9314-y>
- Wafer, L., Kloczewiak, M., & Luo, Y. (2016). Quantifying Trace Amounts of Aggregates in Biopharmaceuticals Using Analytical Ultracentrifugation Sedimentation Velocity: Bayesian Analyses and F Statistics. *The AAPS Journal*, 18(4), 849–860. <http://doi.org/10.1208/s12248-016-9925-y>
- West, R. L., Zelinkova, Z., Wolbink, G. J., Kuipers, E. J., Stokkers, P. C., van der Woude, C. J. (2008). Immunogenicity negatively influences the outcome of adalimumab treatment in Crohn's disease. *Alimentary Pharmacology & Therapeutics*, 28(9), 1122–1126. <http://doi.org/10.1111/j.1365-2036.2008.03828.x>
- Wille, J. J., Pittelkow, M. R., Shipley, G. D., & Scott, R. E. (1984). Integrated control of growth and differentiation of normal human prokeratinocytes cultured in serum-free medium: Clonal analyses, growth kinetics, and cell cycle studies. *Journal of Cellular Physiology*, 121, 31–44.
- Worth, A. P., & Balls, M. (2001). The importance of the prediction model in the validation of alternative tests. *ATLA*, 29(2), 135–144. Retrieved from <http://europepmc.org/abstract/MED/11262759>
- Ye, H. (2006). Simultaneous determination of protein aggregation , degradation , and absolute molecular weight by size exclusion chromatography – multiangle laser light scattering. *Analytical Biochemistry*, 356, 76–85. <http://doi.org/10.1016/j.ab.2006.05.025>
- Zucco, F., De Angelis, I., Testai, E., & Stamatii, A. (2004). Toxicology investigations with cell culture systems: 20 Years after. *Toxicology in Vitro*, 18(2), 153–163. [http://doi.org/10.1016/S0887-2333\(03\)00147-4](http://doi.org/10.1016/S0887-2333(03)00147-4)